Stony Brook University

Biarsenic Based Receptor for Cysteine Peptides

A Dissertation Presented

by

Xiaofei Liang

to

The Graduate School

in Partial Fulfillment of the

Requirements

for the Degree of

Doctor of Philosophy

in

Chemistry

Stony Brook University

May 2016

Stony Brook University

The Graduate School

Xiaofei Liang

We, the dissertation committee for the above candidate for the

Doctor of Philosophy degree, hereby recommend

acceptance of this dissertation.

Dr. Dale G. Drueckhammer – Dissertation Advisor
Professor, Department of Chemistry

Dr. Daniel P. Raleigh - Chairperson of Defense
Professor, Department of Chemistry

Dr. Stephen A. Koch – Third Member of Defense
Professor, Department of Chemistry

Dr. Haidong Huang – Outside Member of Defense
Professor, Department of Chemistry, New Jersey Institute of Technology

This dissertation is accepted by the Graduate School

Charles Taber
Dean of the Graduate School

Abstract of the Dissertation

Biarsenic Based Receptors for Cysteine Peptides

By

Xiaofei Liang

Doctor of Philosophy

in

Chemistry

Stony Brook University

2016

As(III) compounds have high affinity for thiol groups and this affinity has been used in the prior development of FlAsH and related tags for cysteine peptides. We aimed to develop a series of arsenic-based receptors designed to bind to different arrangements of cysteines within native alpha-helical protein structures. Computer modeling was used to define the proper arrangement of arsenic functionality for binding to each targeted sequence. The computer program HostDesigner was then used to discover scaffold structures on which to display the arsenic functionality at the proper distance and relative orientation to bind the targeted sequence. Designed structures were then targeted for synthesis. The synthetic approach to initial probes was based on reaction of a dihaloalkyl-arsenic (III) or related reagent with one equivalent of an organolithium or Grignard reagent. This approach failed due to lack of selectivity for displacement of a single leaving group from arsenic and also due to the instability of products having arsenic attached to a benzylic carbon, as in most of the design targets. A second generation design relied on introduction of arsenic functionality ortho to the hydroxyl group of a phenol via a Pd-catalyzed coupling with an

organomercury intermediate. While the ensuing synthetic work resulted in the development of a new method for the synthesis of arsinous acids, the synthesis of designed target molecules ultimately failed due to difficulties in synthesis and isolation of ortho mercuration intermediate in complex systems. The third generation approach relied on Pd-catalyzed coupling between an arylboronic acid and a dihaloalkylarsenic reagent. In contrast to the second generation approach, this approach does not require a phenolic hydroxyl group on the benzene ring. Further computational studies including new scaffold design using HostDesigner and further computational evaluation of selected scaffolds were conducted. Selected designs were then targeted for synthesis. The synthetic work resulted in development of a second new method for arsinous acid synthesis based on Pd-catalyzed coupling between an arylboronic acid and an arsenic dihalide. This reaction showed high selectivity for substitution of one halide group, leaving the second halide group for displacement by thiol substituents in forming an arsenic-thiol complex.

Contents

Figures

Scheme

Tables

List of Abbreviations

APL	acute promyelocytic leukemia
GSH	glutathione
DMSA	dimercaptosuccinic acid
DHLA	dihydrolipoic acid
DTT	dithiothreitol
QDs	quantum dots
GFP	green fluorescence protein
FRET	fluorescence resonance energy transfer
FlAsH	a fluorescein based probe with As (III) substituents at the 4'- and 5'- positions
ReAsH	a resorufin based probe with As (III) substituents at the 4'- and 5'- positions
EDT	ethanedithiol
BAL	British anti-lewisite
GCN4	transcription factor
DMF	dimethylformamide
AIBN	azobisisobutyronitrile
NBS	n-bromosuccinimide
TLC	thin layer chromatography
NMR	nuclear magnetic resonance spectroscopy
R_f	retardation factor
TMEDA	tetramethylethylenediamine
DCM	dichloromethane
DEA	diethylamine
CAVEAT	computer-assisted vector evaluation and target design
CAAC	a peptide sequence of cysteine alanine alanine cysteine
CGGGC	a peptide sequence of cysteine glycine glycine glycine cysteine
ITC	isothermal titration calorimetry
DCC	dicyclohexylcarbodiimide
DMAP	dimethylaminopyridine
iAsIII	inorganic arsenic III
DMA ($DMAs^V$)	dimethylarsinic acid
MMA	monomethylarsonic acid
$DMAs^{III}$	dimethylarsinous acid

GST	glutathione S-transferase
PNP	purine nucleoside phosphorylase
AS3MT	arsenic (+ 3 oxidation state) methyltransferase
SAM	S-adenosylmethionine
dppf	1,1′-Ferrocenediyl-bis(diphenylphosphine)
-OTf	Trifluoromethanesulfonate

Acknowledgement

I really appreciate the opportunities my dissertation advisor, Professor Dale Drueckhammer, giving me to join in his research group and guiding me into the PhD program. You have provided me with the skills of a synthetic organic and analytical chemist that I intend on carrying with me in my future endeavors. I am so lucky working in our excellent lab for more than five years, and your patient training of a scientist.

I would also like to thank my dissertation committee members, Professor Stephen A. Koch, and Professor Daniel P. Raleigh, and the substitute for my third meeting Professor Joseph W. Lauher for their participation in qualify presentations and discussions, and sharing their experiences and a passion for chemistry with me throughout my doctoral career. I would also like to express my appreciation with Professor Haidong Huang for his willingness to serve as my outside committee member on my dissertation committee.

Thus, I would like to thank Drueckhammer group members, James Liao, my only group member for five and half years, we talk about research every day and work together on maintenance of the whole lab, for former co-worker, Jack, Jesse Poganik, and Xin Cheng, we have worked together on my project. For the colloeagues, Xiuzhu from Professor Goroff's group, Pengju Feng from Professor Ngai's group, and Kongzhen Hu from Professor Ojima's group, thank you all for the chemicals and suggestions on my project. It was a great pleasure working with you all. I wish you all good luck and success in your future journey.

I would like to acknowledge and thank many members of the Chemistry Department for their great contributions to the completion of this dissertation. Dr. Bela Ruzsicska, for teaching me nearly everything about mass spectrometry. Dr. Jim Marecek, for his patience in helping me with NMR spectrometry every day. In addition, I would like to thank my colleagues, both students and faculty, in the Department of Chemistry at Stony Brook University, especially Katherine Hughes, you help me with everything I am confused at school. And for my teaching experiences for more than three years, my supervisor Dr. Rong Cheng, Dr. Susan Oatis, and Dr. Mohammad Akhtar, all trained me with professional skills dealing with students in organic lab, general lab, and lecture.

Most importantly, I would like to thank my friends and family for all their precious love and support

best friends, Wenyuan Li, Yan Ji, Shuang Shi, Zhu Li, Yue Yin, Mengran Yu, Naisheng Jiang, Xiaoqian Jin, and others you always brought me fresh air into my everyday living. To Zhenyu, my listener, my best friend, and my love, you have given me the best support through my living and career life, and you have stood by me both good and bad times. To both of my parents, Bin and Yafeng, you have always believed in my choice both of my career dream and my living style. You have given me everything I need and I cherish all your investments on me.

1 Introduction

1.1 Arsenic compounds and arsenic-thiol complexes

Arsenic is among the most hazardous elements, and it has been found widely in nature, in drinking water,[1] in soil and rice,[2] and in fish oil.[3] Both geochemical and numerous anthropogenic activities generate inorganic arsenic compounds, including mining, combustion of fossil fuels, the use of arsenical pesticides, crop desiccants, and herbicides.[4] Inorganic arsenic normally exists in the oxidation number 3 or 5, both of which are associated with some toxic effects. The transformation between arsenic III and arsenic V occurs readily by oxidation and reduction reactions (Figure 1). Different kinds of inorganic arsenic compounds, arsenic hydrides, arsenic halides, arsenic oxides and acids, and arsenic sulfides cause a serious public health problem with a low chronic exposure all over the world, even though nearly all living things contain arsenic at very low concentrations.

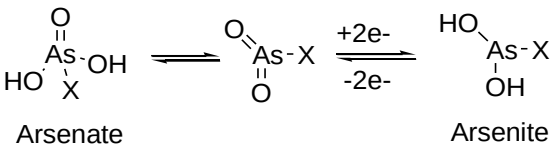

Figure 1. The transformation from As (V) to As (III)

There is evidence showing that exposure to inorganic arsenic compounds is associated with lung and skin cancer, as well as with disorders of the nervous system.[5] The thiols contained in vital cellular enzymes of biomolecules have a high affinity with the +3 oxidation state of arsenic through the formation of a covalent arsenic sulfur bond, which may be the toxic mechanism or chemical basis for

the cytotoxicity of arsenic compounds (Figure 2).

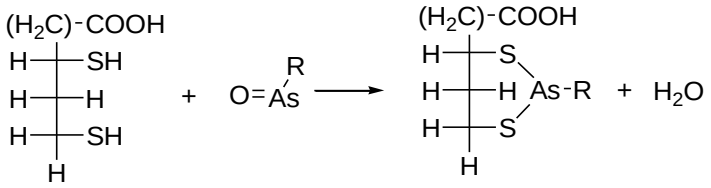

Figure 2. The affinity of the +3 oxidation state of arsenic for thiol groups with the formation of covalent bonds. Adapted from reference [5]

Based on arsenic's chemical properties, arsenic reagents can be applied in medical therapy. Arsenic has been widely used as a chemical therapy of cancer. $As(OH)_3$ (trisenox) was discovered as a chemotherapeutic agent for acute promyelocytic leukemia (APL) in 2000,[6] as arsenic trioxide can kill APL cells. Arsenic has been shown to inhibit the activity of glutathione reductase, thioredoxin reductase, and pyruvate dehydrogenase,[7] which is due to the covalent bonding between arsenic and thiol groups. Arsenic has been used as a pharmaceutical reagent for many years, such as Chinese traditional medicine, such as Xionghuang (As_2S_3).

Arsenic binding to proteins can be performed by covalent bond formation between arsenic and thiol groups, as in E. *coli* ArsA ATPase (Figure 3). Arsenic (III) has a high affinity for thiols, which exist in cysteine-containing peptides. The three coordinated trigonal pyramidal complex formation between arsenite and thiols of cysteine peptides inhibit certain biological activities of the enzyme. Binding of iAs^{III} (inorganic arsenic III) to the ArsR repressor from *E. coli* plasmid R773 results in conformational change of the repressor. Figure 3 also shows the crystal structure of the binding between iAs^{III} and Cys32, Cys34, and Cys37.[9]

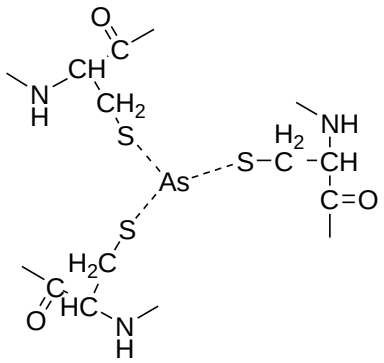

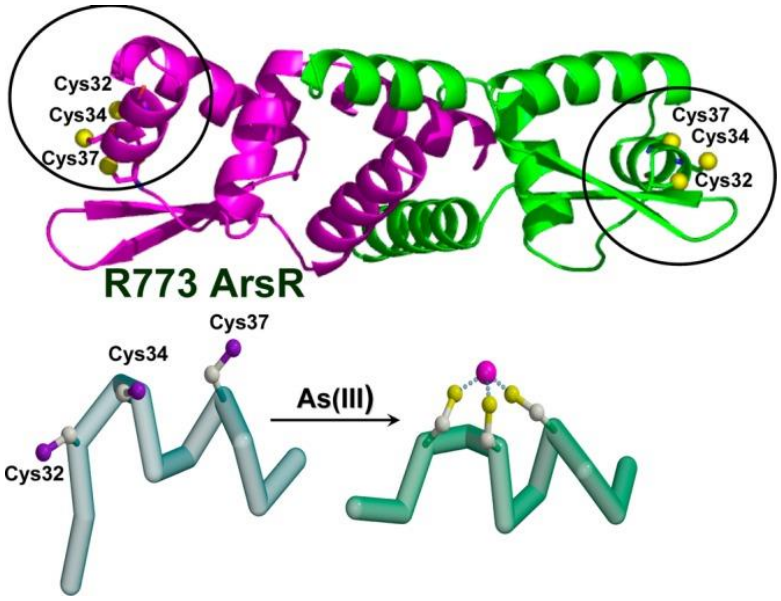

Figure 3. Arsenic coordination with cysteines in E. coli ArsA ATPase, and the crystal model of iAsIII binding to the Escherichia coli repressor protein ArsR. Reprinted from reference [9]

Efforts have been made for removing inorganic arsenic from covalent complexes with cysteine-containing proteins and other biological thiols. For instance, some dithiols have been used to combat the toxicity of arsenic (III) compounds by removing arsenic from its protein complexes (Figure 4).

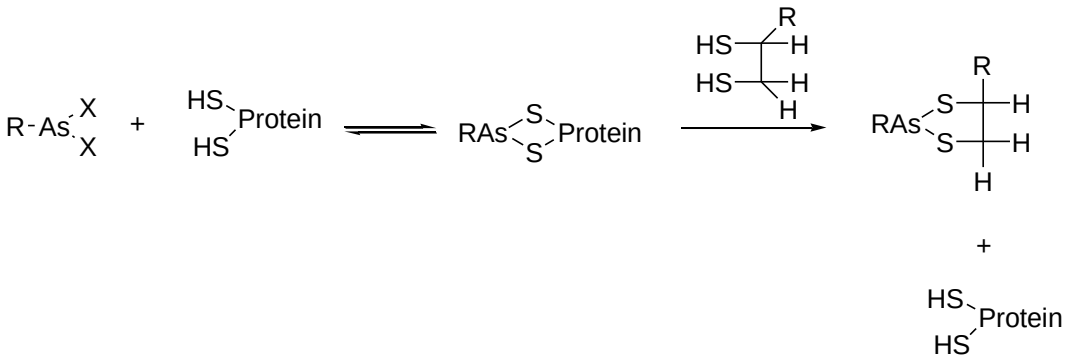

Figure 4. Dithiols combat the toxicity of arsenic compounds. Adapted from reference [9]

Through the methods of UV absorption spectroscopy and isothermal titration calorimetry, the equilibrium and thermodynamics of thiol groups binding to arsenic compounds have been determined, and the affinity to glutathione (GSH) and the dithiols dimercaptosuccinic acid (DMSA), dihydrolipoic acid (DHLA), and dithiothreitol (DTT) (Figure 5) have been compared (Table 1).[10] MMA refers to

monomethylarsonic acid, which shows higher affinities with thiols compared with $As(OH)_3$. And the equilibrium constants of the same arsenic functionality differ with different thiol groups. Both GSH and phytochelation (PCs) are considered as the detoxification agents of arsenic in plants, and again the detoxification mechanism is the chelation between arsenic components and the available thiol groups.[4]

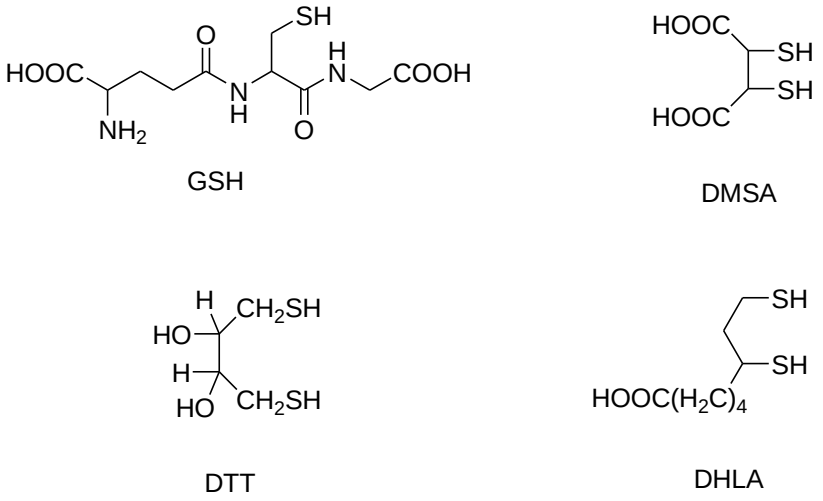

Figure 5. Common thiols which form covalent complexes with arsenic (III). Adapted from reference [4]

	$As(OH)_3$ (M^{-1})	MMA (M^{-1})
GSH	$K_1 = 20$ $K_2 = 430$ $K_3 = 1.2 \times 10^7$	$K_1 = 1.6 \times 10^4$ $K_2 = 1.9 \times 10^3$ $K_3 = 2.3(\pm 0.5) \times 10^7$
DMSA	$K_1 = 3.0 \times 10^4$ $K_2 = 1.6 \times 10^5$	$K = 2.7(\pm 0.2) \times 10^5$
DHLA		$K = 3.2(\pm 0.3) \times 10^6$
DTT	$K = 1.1(\pm 0.5) \times 10^6$	$K = 2.0(\pm 0.8) \times 10^6$

Table 1. Comparison of equilibrium constants of thiols with arsenic compounds. Adapted from reference [4]

Arsenic can also form bonds to carbon to form a wide variety of organic arsenic compounds. Biomethylation has long been considered as an effective procedure for the detoxification of inorganic arsenicals, but recent studies on cell culture and animal toxicity suggest that some specific methylated arsenic species are also toxic.[11] Figure 6 shows the methylation and demethylation of arsenic reagent.

Arsenic oxide can be ionized by base, arsenic (+ 3 oxidation state) methyltransferase (AS3MT) catalyze the methylation of arsenite. Both glutathione S-transferase (GSTO) and purine nucleoside phosphorylase (PNP) can be used as arsenate reductases, which catalyze the reduction of arsenate species. S-adenosylmethionine (SAM) is used as the methyl donor in the biomethylation pathways.

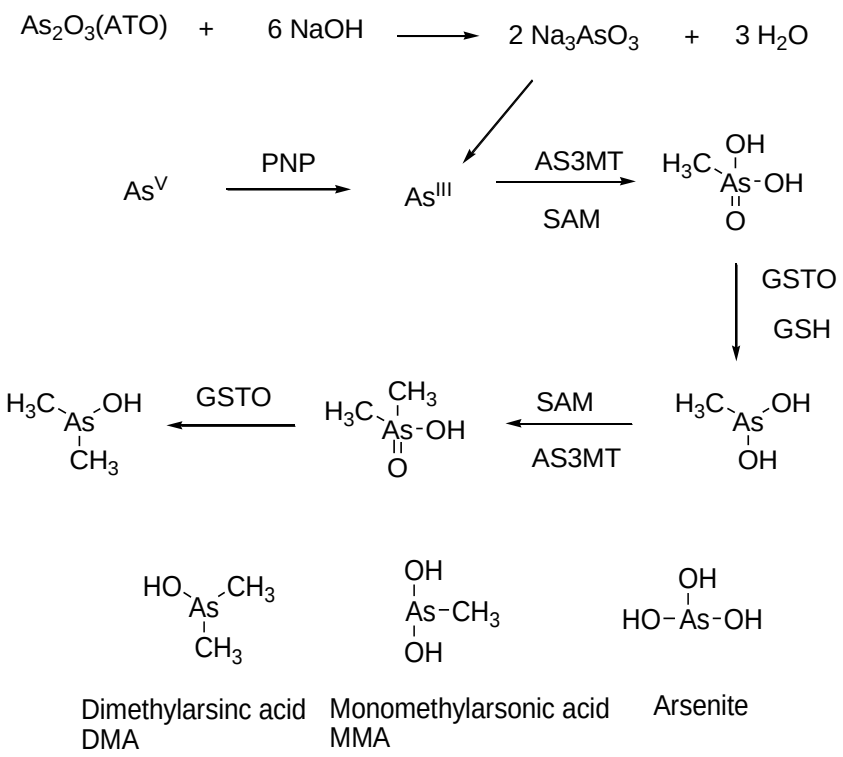

Figure 6. Pathway of biotransformation of arsenic (III) methylation and demethylation in mammalian system. Adapted from reference [11]

1.2 Fluorescent labeling of proteins

Fluorescent labeling methods play an important role in the study of proteins, and have been used to study protein structure, dynamics, and protein-protein interactions.[12] The biological activities of certain proteins, including conformational dynamics and molecular interaction or tracking the movements of proteins, are monitored by fluorescence created by single molecule experimental techniques. Labeling is also used to monitor, control, and modify protein function, and to study protein expression, location

and activity in living cells.[13]

In a recent method, site-specific mutations assist in protein identification and manipulation in both *in vitro* and *in vivo* contexts.[14] The applications of fluorescent labeling of proteins in biology, drug discovery, and medical research have been well studied after the discovery of its effects *in vivo*. Fluorescent labeling techniques have helped overcome challenges in cell biology. For instance, Roger Tsien developed a pulse-chase approach to label newly synthesized connexin 43 protein, which made it possible to assess the life cycle of protein levels and functions in cells.[12] In order to purify a fluorescently labeled protein from a crude reaction mixture with affinity matrix,[15] and to incorporate non-natural amino acids with suppressor-codon mutagenesis, fluorophore assisted light inactivation has been developed.[16]

1.2.1 Fluorophore-Based Tags

Fluorophores can be used to tag other, non-fluorescent molecules for fluorescence-based detection. Small organic dyes perform better in wave-length range, brightness, photostability, and reduction in self-quenching, compared with fluorescent macromolecules.[17] The early fluorescent labels were based on the xanthene dyes rhodamine and fluorescein and a cyanine structure (Figure 7).[18]

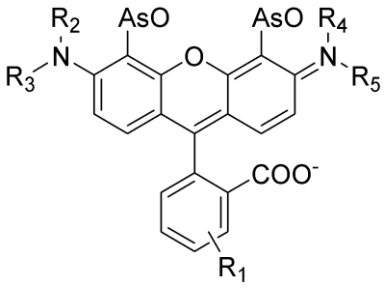

bis-arsine oxide derivative of rhodamine

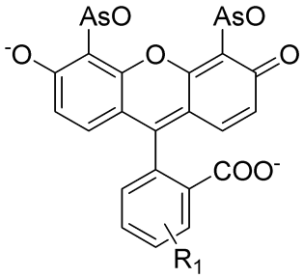

labeled FlAsH

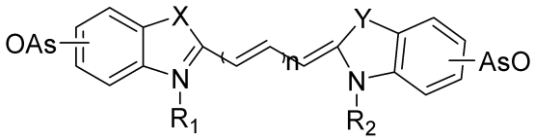

n = 2, 3, 5 and 7

X, Y refer to CO, or NH

bis-arsine oxide derivative of cyanine

Figure 7. The early fluorescent labels. Adapted from reference [18]

Different types of fluorophores have been applied to detect connexin 43 in Hela cells, and alpha tubulin in fibroblasts.[19] Enzyme-linked immunosorbent assay facilitates antibody conjugation with relatively larger size fluorophores. Photoswitchable fluorophores have been developed to turn from dark to bright or from one color to another, which is useful for monitoring protein diffusion, trafficking, and age determination.[20] Fluorophores generate relatively little reactive oxygen species upon illumination, which can be mutated based on chromophore formation. Additionally, QDs (quantum dots) act as semiconductors with electronic characteristics closely related to the size and shape of the individual crystal, with high extinction coefficients, and with good quantum yields.

The energy difference between the highest valence band and the lowest conduction band can be absorbed and released as photons, associated with color shifts. Color switchable fluorophore-based tags can be used in tracking biomolecules, including receptors, antigens, antibodies, enzymes, proteins, and nucleic acids.[21] Enzyme labeling requires DNA construct with the fluorescent protein, chemical tags facilitate chemical labeling with fluorescence turn on or turn off, and the target protein folding and function normally cannot be disrupted with protein labeling.

1.2.2 Fluorescent proteins

Fluorescent proteins are associated with different colors, due to variations in the chromophore covalent structure and the noncovalent environment.[22]

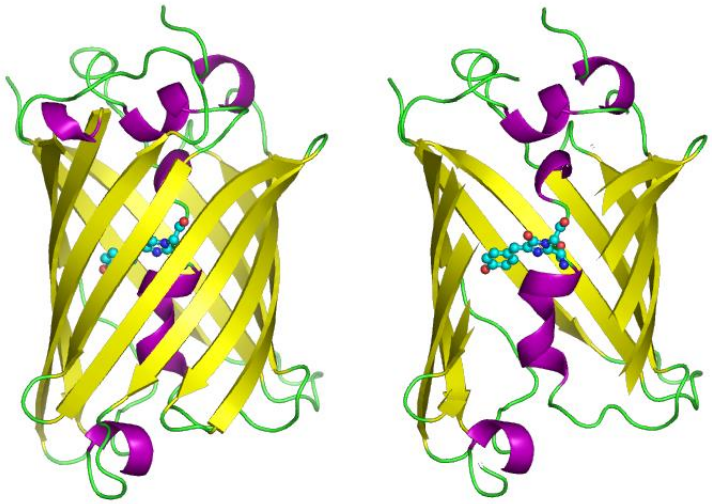

Figure 8. GFP molecules drawn in cartoon style, one fully and one with the side of the beta barrel cut away to reveal the chromophore. Reprinted from reference [22]

Different kinds of fluorescent proteins have been used in biological imaging, especially green fluorescent protein from the jellyfish *Aequorea victoria*, which has specific covalent conformation, and environmental sensitivity. The Ser 65 promotes chromophore ionization through hydrogen bonding with Glu 222 to maintain the stereostructure, and the sensitive effects of pH, temperature, protein concentration, and prior illumination, are consistent with its generation of a highly visible, effectively emitting internal fluorophore (Figure 8).

Green fluorescent proteins have been biologically applied as a tag and an indicator. For instance, as a reporter gene or a cell maker, green fluorescent protein is able to detect gene expression *in vivo*.[23] Additionally, as a fusion tag, it reacts as a genetic fusion partner in host proteins to monitor their localization and fate. The structure of a rigid shell surrounding the chromophore enables it to be fluorescent, with resistance to photobleaching, and reduced environmental sensitivity. In cell biology, green fluorescent proteins exhibit absolute specificity in living cells labeling, as they are genetically encoded. In addition to this specificity, green fluorescent proteins resist proteolysis with its stable structure having the chromophore sheltered by the structure barrel. Mutants of the green fluorescent protein form different colors of fusion proteins, making it possible to detect the localization and movement of fused proteins in cells.[24]

1.2.3 Fluorescence resonance energy transfer

The quantum-mechanical phenomenon fluorescence resonance energy transfer (FRET) describes the energy transfer between two chromophores, when two fluorophores are in a specific spatial proximity. FRET requires overlap between the emission spectrum of one fluorophore, as the donor, with the excitation spectrum of the second fluorophore, as the acceptor. The efficiency of FRET is determined by the distance between the two fluorophores and the relative orientation of their transition dipoles.[25] Fluorescence resonance energy transfer based on small-molecular fluorescent dyes enables the monitoring of interaction between two distinct proteins, or different domains inside one protein structure.[26]

FRET may detect protein dynamic conformational changes and resulting change in distance and orientation between two attached fluorophores. FRET based indicators have been used to measure both small G proteins and histone acetylases, the balance between protein kinase and phosphatase activities, and activities of proteases. Fret based indicators have also been used to detect and quantify several ions, cyclic nucleotides, metabolites, and neurotransmitters.[27]

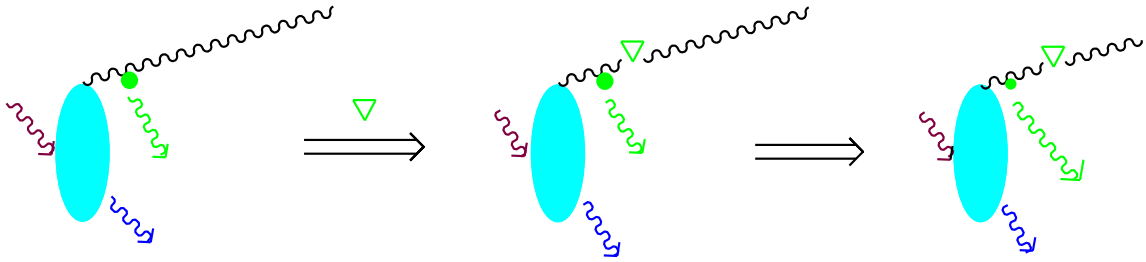

Figure 9. The example of FRET reporter. Conformational change happens within the structure of receptor and fluorescence is turn on. Reprinted from reference [27]

The interaction between distinct proteins can be analyzed by fluorescence resonance energy transfer, such as that in the figure of FRET reporter (Figure 9). The modified probe can be imaged directly with the increased intensity of fluorescence after the addition of genetic tag, as the thickness of arrow represents the intensity of fluorescence.[27b]

1.2.4 Biarsenical labeling of tetracysteine-tagged proteins

Recent biochemical and cell biological studies suggest undesirable effects associated with the fluorescent labeling technology of green fluorescent proteins.[28] First, the relatively large structure of about 235 amino acid interferes with the structure, localization, and activity of the fusion proteins. Second, the barrel structure around the chromophore restricts accessibility to the cellular environment, which is necessary for the specific sensitivity to the environment, such as calcium concentration. The current technology on chemical labeling has been greatly advanced by the biarsenical labeling of tetracysteine-tagged proteins.[29] The structure of biarsenic probes are shown in Figure 10. When these biarsenical sensors bind to their target, the fluorescence intensity increased resulting in decreased background noise associated with green fluorescence protein. Additionally, compared with the relatively large molecular weight of green fluorescence proteins, the tetracysteine tag fused to the biarsenical probes is small enough to maintain the biological function of the cellular proteins,[30] as the tetracysteine tag can be stably associated to the terminus structure or some secondary structure of the target protein. Figure 10 shows different protein secondary structures with tetracysteine motifs that have been targeted with biarsenical probes.

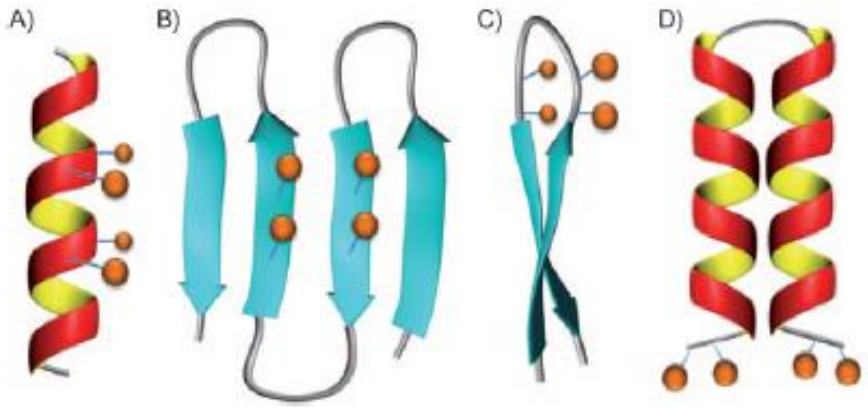

Figure 10. Different protein secondary structures with a linear tetracysteine motif. Reprinted from reference [30]

Finally, the detection of fluorescence can be confirmed by electron microscopy for the biarsenical labeling system.[31]

The structure Cys-Cys-Xaa-Xaa-Cys-Cys is the most optimal for binding to FlAsH and ReAsH, in which Xaa refers to any amino acid. FlAsH or ReAsH itself has limited fluorescence, but fluorescence is turned on when the probe is bound to its tetracysteine target (Figure 11).

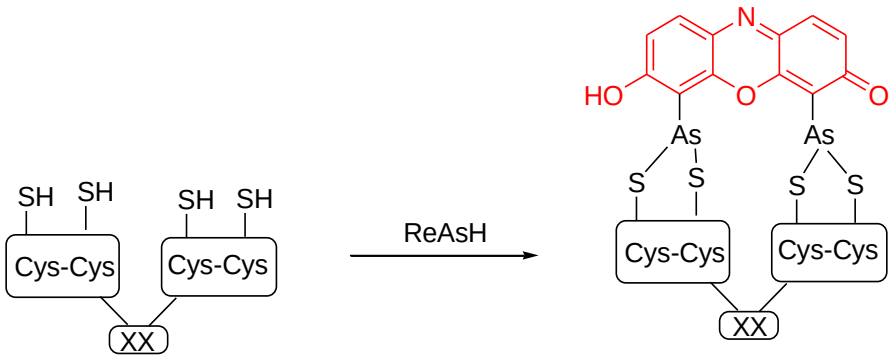

Figure 11. ReAsH bond with linear tetracysteine peptides. Adapted from reference [31]

The phenolic oxygen facilitates ortho-mercuration in the first step of the synthesis of FlAsH and ReAsH, which is followed by Pd-catalyzed transfer of the mercury intermediate to arsenic (Figure 12, 13). FlAsH is usually introduced as adducts with dithiol antidotes, such as ethanedithiol (EDT) and 2, 3-dimercaptopropanol (British anti-Lewisite BAL), but BAL performance is limited due to the low membrane permeability of the complex.[32]

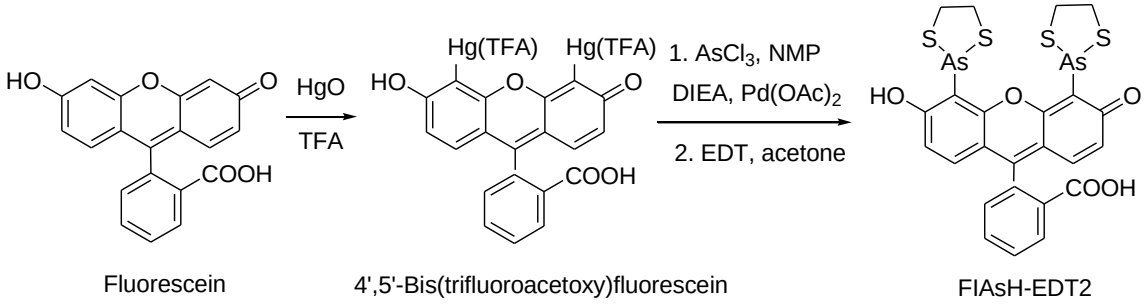

Figure 12. The synthesis of FlAsH-EDT2 and ReAsH-EDT2. Adapted from reference [32]

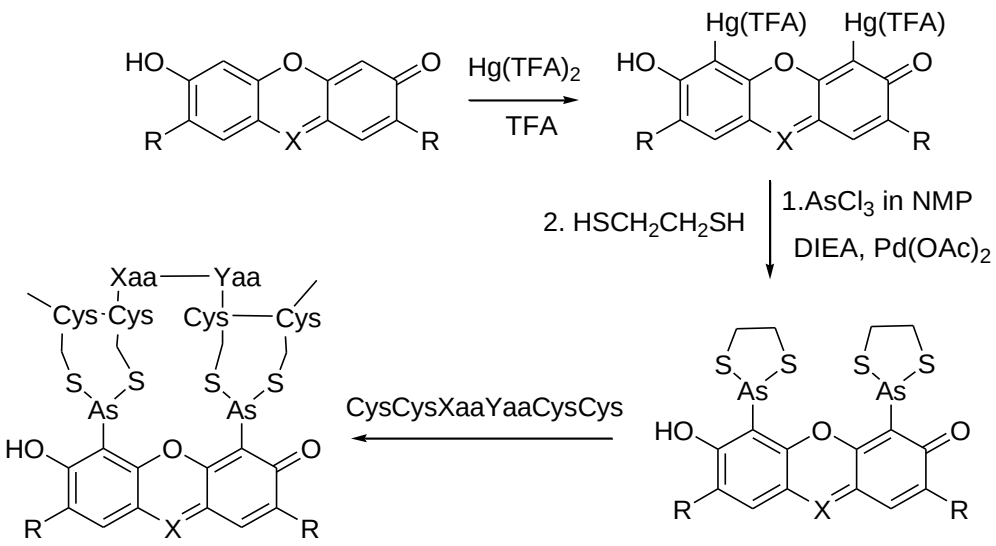

Figure 13. The synthesis of typical biarsenical probes and their binding to tetracysteine peptide sequence. Adapted from reference [32]

Two pairs of Cys-Cys separated by residues Pro-Gly form the brightest and highest affinity complexes. FlAsH binds to a β hairpin structure of the tetracysteine peptide. Structures containing the Pro-Gly residues are optimized for the spacing and relative orientation between the two Cys-Cys pairs, as the increase in effective molarity contributes to the high affinity, and a minimized geometry results in better brightness. Some mutants of the Pro-Gly sequence, with similar distance and orientation between the two Cys-Cys pairs in space, are promising for detection of protein tertiary and quaternary structures.[33]

In addition to its applications in intact cell visualization, there are other reported biological applications of FlAsH. First, the tetracysteine target is able to monitor protein conformational changes when bonded with the biarsenical motif, inducing changes in fluorescent intensity or properties, which indicate the associated conformational change. For example, the application to cellular retinoic acid binding protein 1, when containing a linear tetracysteine tag inside one internal loop, facilitated monitoring of the protein denatured states. As shown in figure 14, the properly folded retinoic acid binding protein 1 is recognized by the biarsenical motif, but only when it is denatured to a specific unfolded linear structure can the associated fluorescence be detected. Additionally, the study of the mechanism and kinetics of aggregation can be performed on some specific mutants of the cellular retinoic acid binding protein 1. The different oligomerization states of various aggregating proteins show sharply distinct fluorescent properties, for the monomers form a fluorescent complex with the biarsenical motif, but in the higher

oligomerizated aggregate almost no fluorescence can be detected as the tetracysteine tag is buried inside the larger aggregated structure.

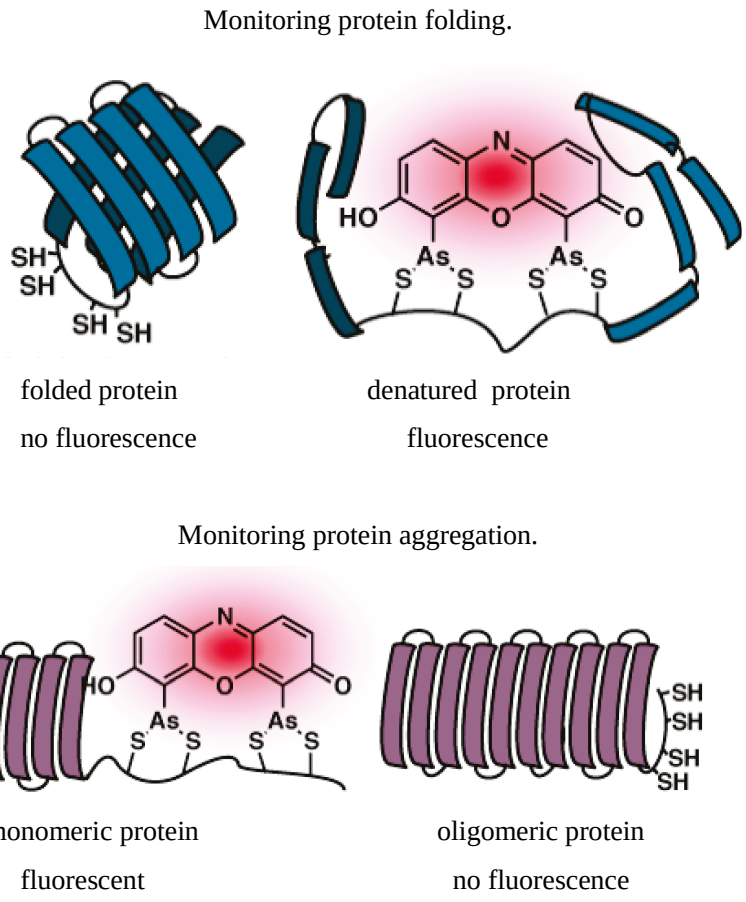

Figure 14. The first biological application associated with FlAsH. Reprinted from reference [33]

Second, the ability of FlAsH to monitor or control specific protein activities is highlighted by an encodable sensor for the Src family kinases. Even though the linear tetracysteine tag exists in the unphosphorylated tryosine kinase, fluorescence can only be detected after the tryosine kinase is phosphorylated (Figure 15).

Figure 15. Monitoring tyrosine kinase activity using ReAsH. Reprinted from reference [33]

Third, complex-edited electron microscopy based on ReAsH facilitates the detection of protein-protein interactions. The intermolecular tetracysteine motif in the GCN4 leucine zipper dimer is readily recognized by ReAsH, forming a fluorescent GCN4 dimer (Figure 16). Only the parallel assembled dimer emits signal after labeling with ReAsH in complex-edited electron microscopy (EM). Diaminobenzidine (DAB) would polymerize around each protein dimer complex, turning off the fluorescence of the GCN4 dimer. After treatment with OsO_4, only those dimers that are closely interacting can show a resulting visible EM signal.[34]

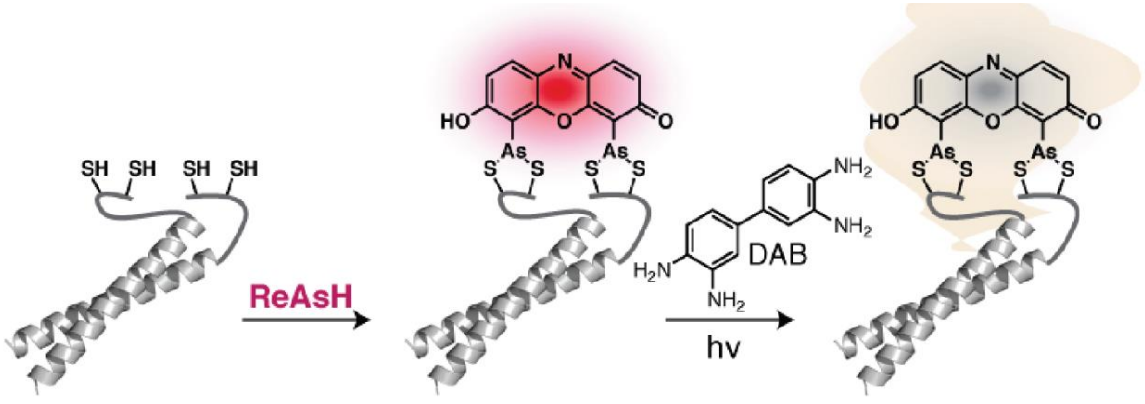

Figure 16. ReAsH detection of GCN4 dimer. Reprinted from reference [34]

Last, biarsenical labeling technology has been used in biotechnology and analytical biochemistry applications, such as electrophoresis, affinity purification of protein,[35] fluorescent reporters, protein-protein interaction indicators, etc. Most of the applications are based on the affinity of arsenic functionalities with thiols inside protein structure, and the molecular weight or polarity changes after covalent bonding with thiols.

An unavoidable limitation of FlAsH, is the cytotoxicity of the arsenic. Additionally, FlAsH only recognizes the tetracysteine motif with the four reduced thiols, which is not available in a cellular oxidizing environment. Furthermore, different protein targets can only be labeled simultaneously by one color biarsenical probe, and for cysteine rich proteins non-specific labeling by FlAsH induces relatively high background fluorescence.

2 The design of initial biarsenic probes

Based on the limitation of earlier biarsenic probes, the initial biarsenic probes were designed for the bonding with cysteine peptides within the same alpha helix structure.

2.1 Receptors for dicysteine-containing peptides/proteins

Previous receptors for cysteine-containing peptides are based on arsinous acids and arsine oxides, in which each arsenic atom bonds to two thiol groups, as in the reaction with a simple dithiol in Figure 17a. We aim to target cysteine thiols in proteins using arsinous acids, which form a reversible covalent bond with a single thiol group (Figure 17b). Computer modeling indicates that an arsinous acid cannot bind a pair of cysteine thiol groups in any relative position in an α-helical peptide without significant distortion of the α-helix (Figure 17c). Alpha helical peptides having specific distances and orientation between cysteines will be selectively recognized by receptors having a pair of arsenous acid groups positioned on an appropriate scaffold (Figure 17d). A pair of arsinous acid groups will be positioned on an appropriate scaffold for selective recognition of alpha helical peptides having specific distances between cysteines.

a.

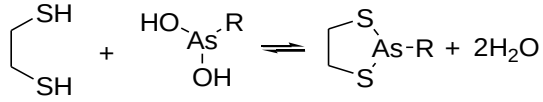

b.

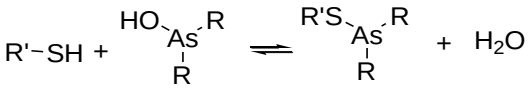

c.

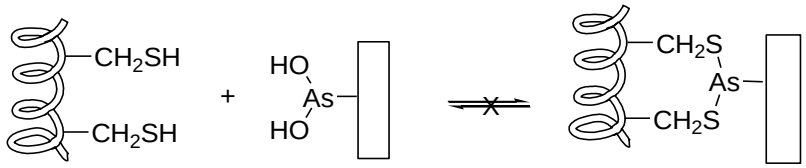

d.

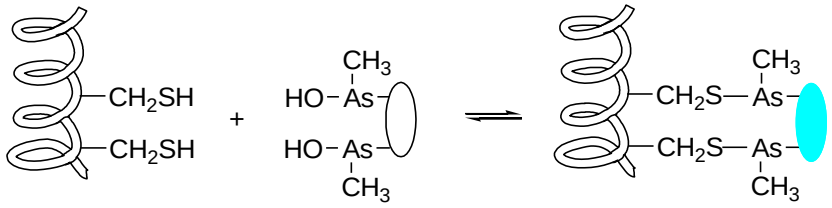

Figure 17. Complex formation between an α-helical dicysteine peptide and a bis-arsinous acid based receptor

2.2 General approach of initial receptor design.

Figure 10 shows the general process of receptor design using the computer program HostDesigner. The design goal is to display functional groups on a scaffold structure that bind to complementary functionality on the target structure. Standard computational modeling is used to minimize the structure of a related complex in which the scaffold is replaced by a pair of methyl groups or other simple groups attached to each functional group of the intended receptor. A vector pair is defined based on the bond connecting the functional groups of the receptor to the methyl substituents, which represent the specific distance and relative orientation of the attachment points to the scaffold. Through a virtual library search, using the computer program HostDesigner, scaffold structures with the specific distance and dihedral angle are identified. Finally, the potential receptor is arrived at by grafting the binding groups onto the scaffold structure. Other

modifications may be made, such as replacing an alkene with an isosteric amide in order to improve synthetic accessibility or other attributes. Further computational modeling of the designed receptor and the receptor target complex is generally performed to further validate the design before initiating synthesis.

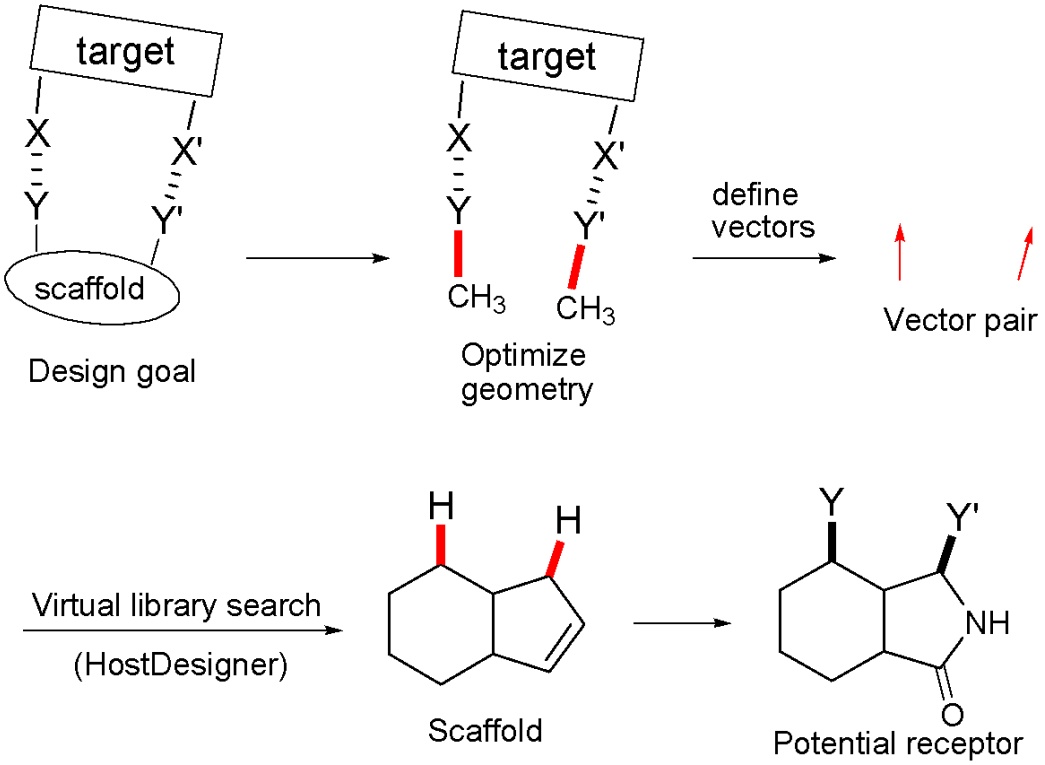

Figure 18. The general approach to receptor design using HostDesigner

2.3 Synthetic approach to initial probes

Based on the structure of the early fluorescent labels and the potential dicysteine peptide receptors from HostDesigner three molecules were chosen for synthesis (Figure 19). Compound **1**, designed to bind to an α-helical i, i+3 dicysteine sequence (having two amino acids between the cysteine pair) is a naphthalene ring substituted at positions 1 and 6 with two arsenical groups, and a methoxy group at position 2. Compound **2**, designed to bind to an i, i+4 dicysteine sequence is a diphenyl ether with the para position of one ring and a meta position of the other substituted by arsenic groups. Compound **3** is an alternative i, i+3 probe, equivalent to compound **1** but lacking the methoxy group.

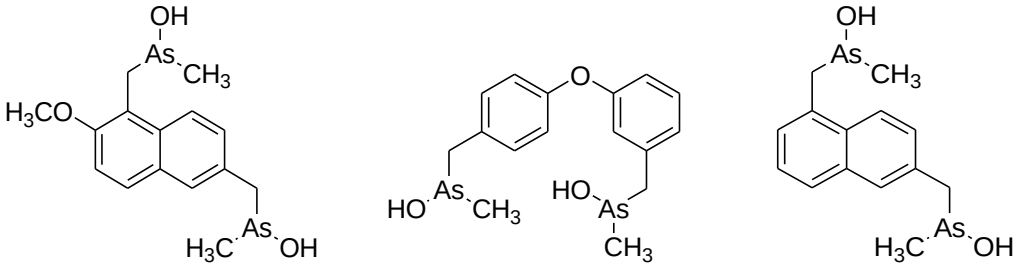

1 **2** **3**

i, i+3 i, i+4 Alternative i, i+3

Figure 19. Compounds designed by HostDesigner for synthesis

The synthesis requires access to both the scaffold moiety and the arsenic functionality. Either a Grignard reagent as shown or the equivalent lithium reagent of the scaffold structure might serve as the reactant for incorporation of electrophilic arsenic functionality (Figure 20).

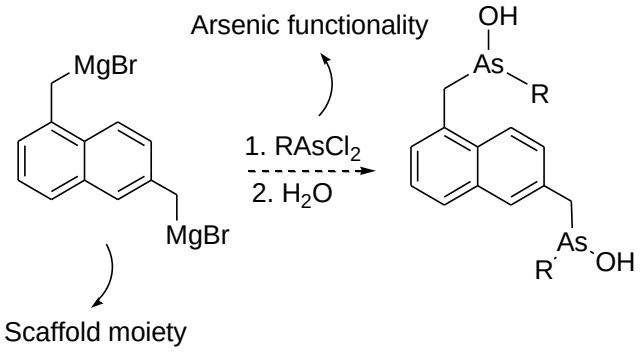

Figure 20. Final assembly from the scaffold and arsenic moieties

2.3.1 Synthesis of the scaffold moiety of 1

The synthesis of the scaffold moiety of compound **1** was undertaken as shown in Scheme 1 starting from the commercially available 1,6-dibromo-2-naphthol **4**. First the hydroxyl at position 2 was protected by methylation to form **5**.[36] The next step was to convert the two bromine atoms to aryl-lithium groups by reaction with *n*-butyl lithium followed by introduction of aldehyde groups by reaction with DMF followed by hydrolysis to form **6**.[37] The aldehyde groups would then be reduced to alcohol groups by $NaBH_4$.[38]

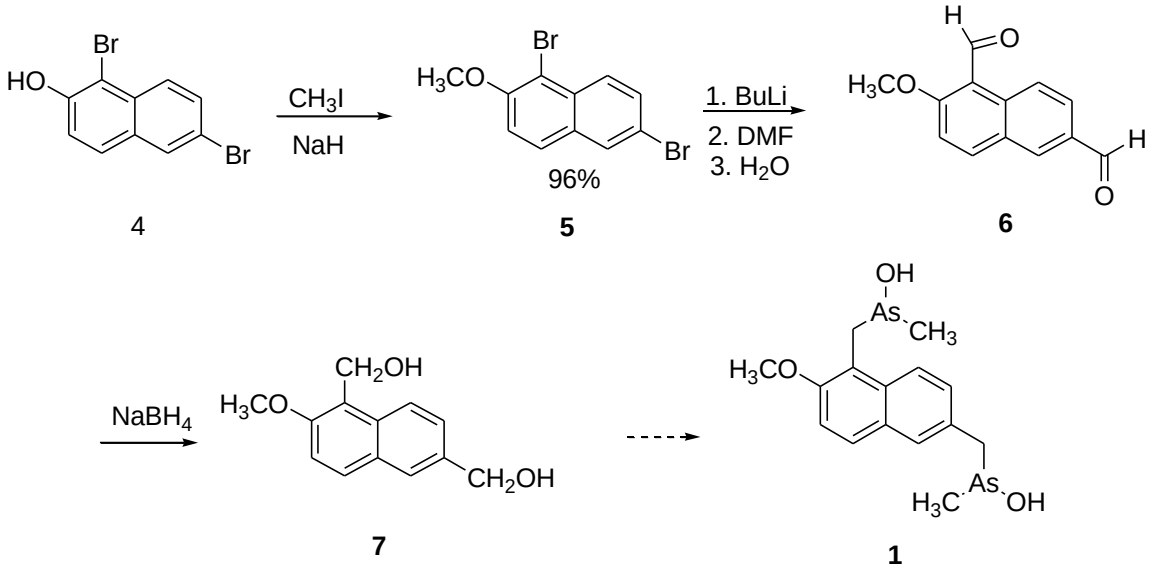

Scheme 1. Synthetic approach to compound **1** starting from 1,6-dibromo-2-naphthol

However, the second step gave a product mixture consisting of reactant **5**, the desired dialdehyde **6**, and both mono-aldehydes resulting from replacement of only one of the two bromine atoms (Figure 21).

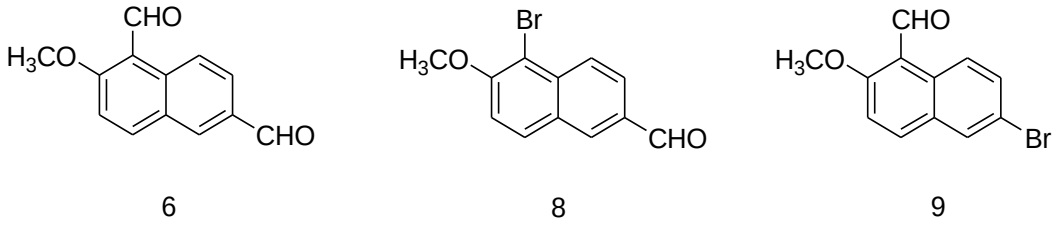

Figure 21. Product mixture of the attempted bis-formylation reaction

As an alternative approach, the aldehyde was introduced at position 1 first, instead of forming two aldehyde groups on the naphthalene ring simultaneously, to form **9** (Scheme 2).

Thus reaction of **5** with only 1 eq. of *n*BuLi followed by addition of DMF and hydrolysis formed **9**. Reduction of the aldehyde with $NaBH_4$ formed **10**. Reaction of **10** with 2 eq. of *n*BuLi to form the intermediate **11** was followed by addition of DMF and subsequent hydrolysis. However, the crude ^{1}H-

NMR showed a complex mixture of products. The synthesis of compound **1** was later abandoned due to problems described in section 2.3.1.

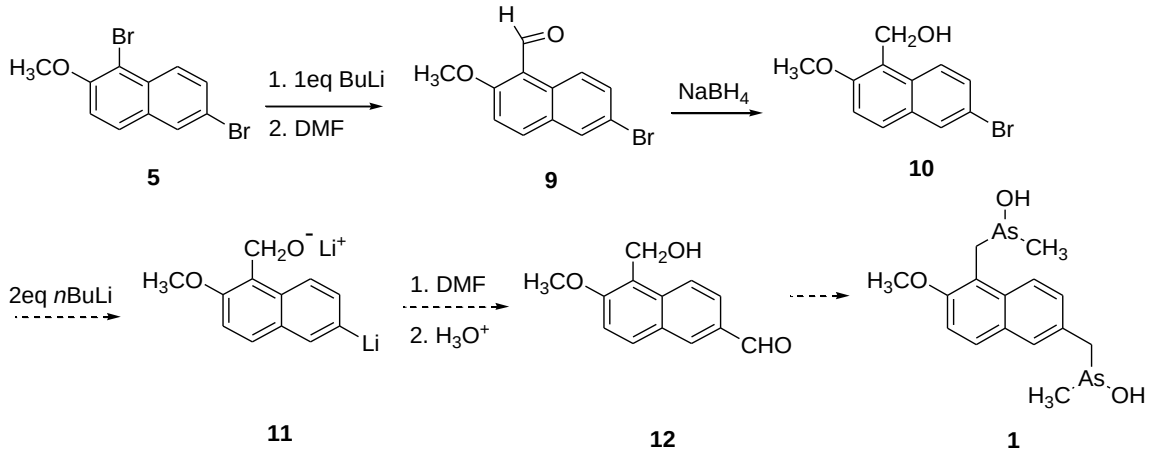

Scheme 2. Alternative synthetic procedure of compound **1** starting from 1,6-dibromo-2-methoxy-naphthalene

2.3.2 Synthetic approach to scaffold structure of compound 2

2.3.2.1 Radical bromination approach to the scaffold structure of compound 2

For the synthetic approach to the scaffold structure of compound **2**, a radical bromination reaction of **13** to form **14** was performed first with AIBN as the radical initiator, and NBS as the bromine source. Initial heating at 70°C for 8 h showed a complicated mixture of spots on TLC, and the desired product peaks could not be identified in the ^{1}H-NMR spectrum of the crude product. Photochemical reaction conditions were then attempted by irritation of the reaction mixture by bright UV light. The reaction was monitored by TLC starting at 0.5 hour reaction time, in reactions using 1.0 eq. and 0.5 eq. NBS (starting material R_f = 0.72, monobromine substituent R_f = 0.64, ethyl acetate : hexane = 1:3). After about 3 hours, a spot apparently corresponding to the desired product **14** was detected on TLC (R_f = 0.53, ethyl acetate: hexane = 1:3), which was confirmed in the ^{1}H-NMR spectrum. However, just a tiny amount of the desired product was recovered from the reaction crude (Scheme 3).

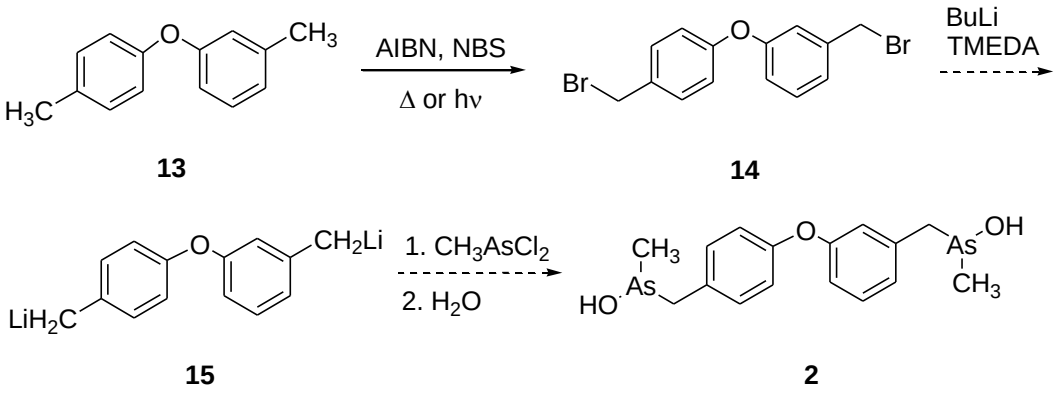

Scheme 3. Radical bromination approach to **2**

2.3.2.2 Phenolic coupling approach to the scaffold structure of compound 2

Marcoux and coworkers published the diphenyl ether synthesis shown in Figure 22.[39] Their results included examples of selective coupling to phenolic oxygen in the presence of an alcohol group.

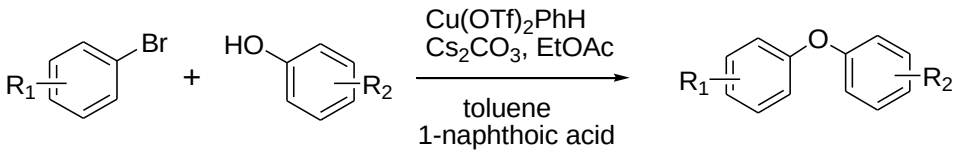

Figure 22. Cu-catalyzed biphenyl ether synthesis. Adapted from reference [39]

As an approach to the synthesis of receptor **2**, the published reaction conditions were followed with reactants **16** and **17** to form **18** (Scheme 4). However, the reaction was not selective for coupling to phenolic oxygen as the product mixtures contained the alcohol coupling product **20** in addition to the desired product **18** (R_f = 0.72, starting material R_f = 0.2, 0.24, ethyl acetate : hexane = 1:3) (Figure 23).

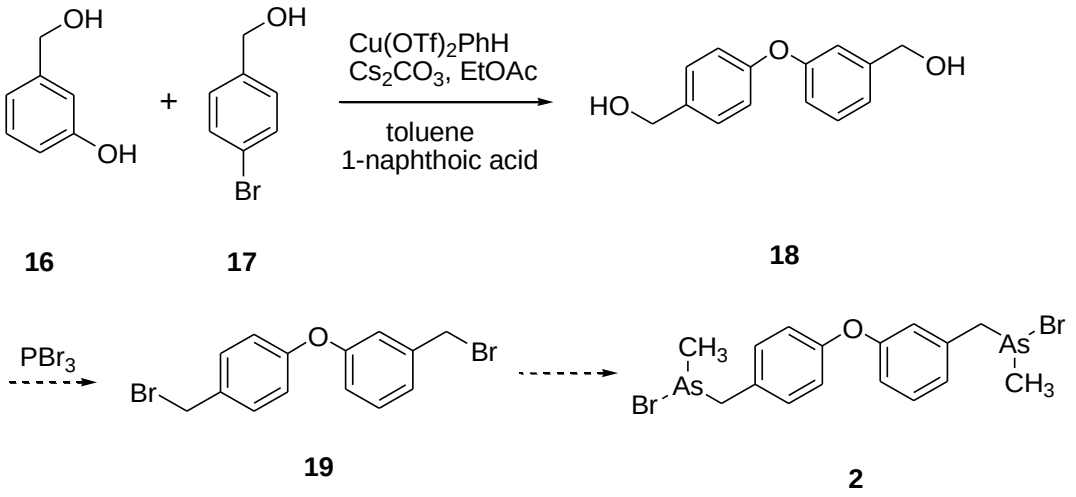

Scheme 4. Phenolic coupling reaction

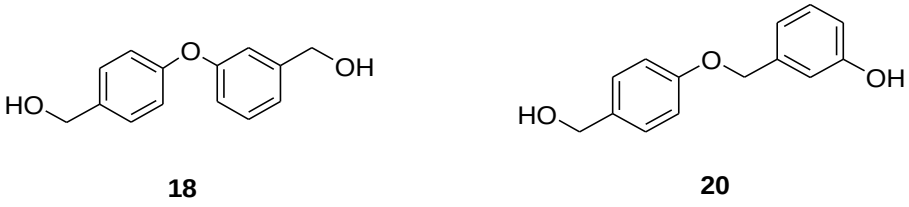

Figure 23. The coupling reaction product mixture

As an alternative approach, 4-bromobenzoic acid **21** was used in place of the alcohol **17** in the coupling reaction (Scheme 5).

However, this reaction also formed the alcohol coupling product **23** in addition to the desired product **22**. As with the previous receptor target, efforts toward the synthesis of **2** were ultimately abandoned due to problems in formation and stability of benzylic arsenic compounds.

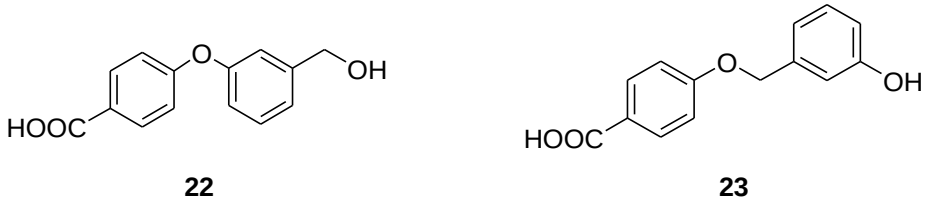

Figure 24. The product mixture for the modified coupling reaction

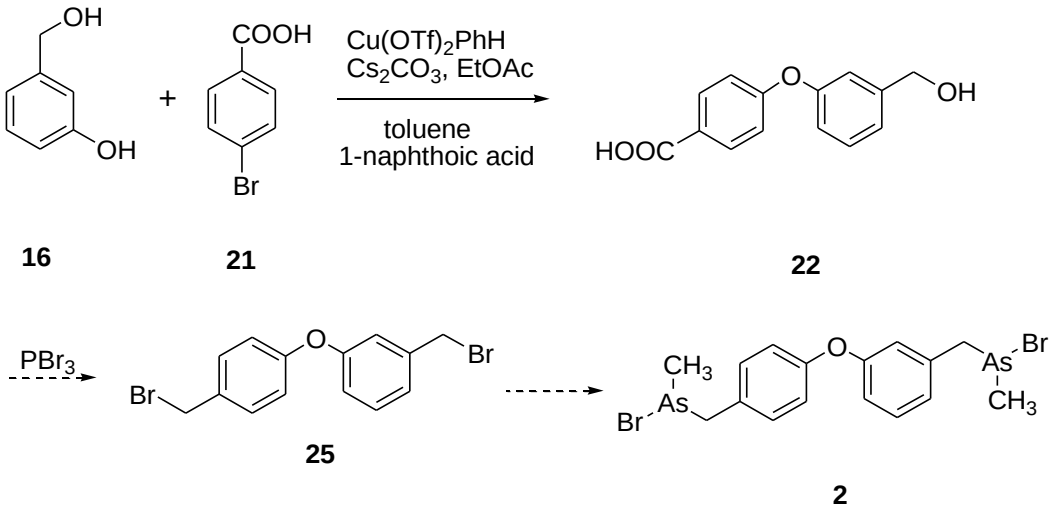

Scheme 5. Modified coupling reaction

2.3.3 The synthetic approach to scaffold structure of compound 3

The synthesis of the desired receptor **3** was undertaken starting from the commercially available 1,6-dihydroxylnaphthalene **26** following the same general approach as described in section 2.3.1 for target compound **1** (Scheme 6).[40] First the two hydroxyls at positions 1 and 6 were to be converted to bromides to obtain **27** following a published procedure.[41] Conversion of bromides to hydroxymethyl groups to form **28** and reaction with PBr_3 to replace the two hydroxyl groups with bromide would form **29**. Again lithium halogen exchange would form the reactive intermediate **30** for reaction with the arsenic reagent. However, the first step gave only the recovered reactant **26**. While the published procedure for this step used microwave heating, we heated with a sand bath at 240 ° C instead and may have not reached the necessary temperature for the reaction to occur. Due to the failure of this reaction, an alternate approach was developed as described in the next section.

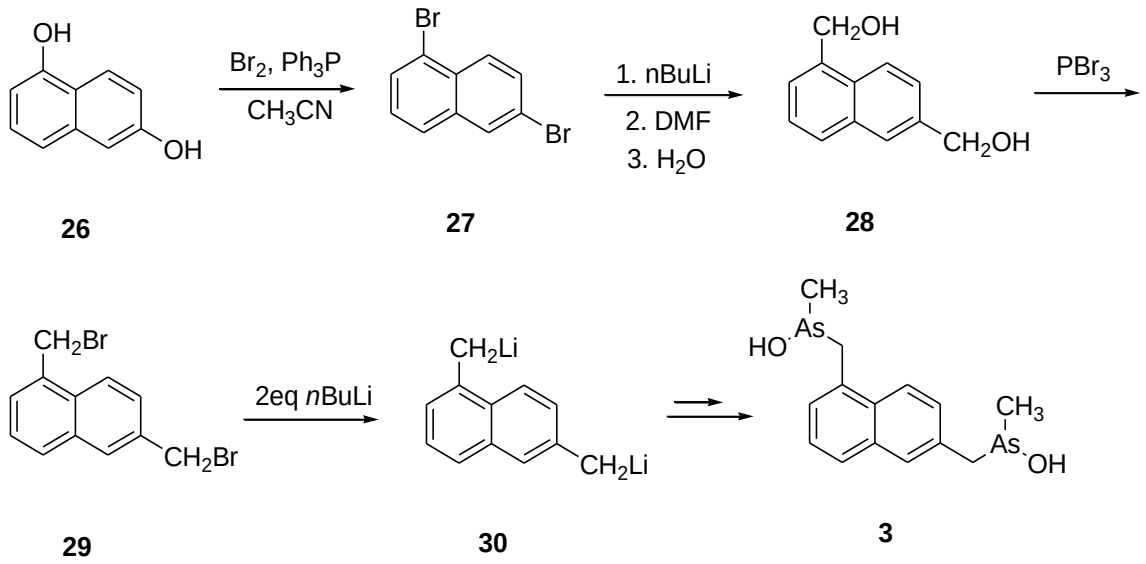

Scheme 6. Synthetic approach to compound **3** starting from 1,6-dihydroxylnaphthalene. Adapted from reference [42]

2.3.4 Alternative synthetic approach to scaffold structure of compound 3

For alternative synthetic approach to scaffold structure of compound **3**, the hydroxyl groups at positions 1 and 6 of the naphthalene ring were converted to the triflates to form **35** (Scheme 7).[42] TMEDA was used to facilitate the introduction of two triflate groups. It is well known that triflate groups are good leaving groups, MeMgBr catalyzed by a nickel complex was used to introduce two methyl groups at the positions of the two triflate groups to form **36**.[43] The remaining steps were to deprotonate the two methyl groups with two equivalents of *n*-butyl lithium to form the reactive lithium intermediate **37**, which would be reacted with dihaloalkyl arsenic reagent to form the desired diarsenical probe **3**.

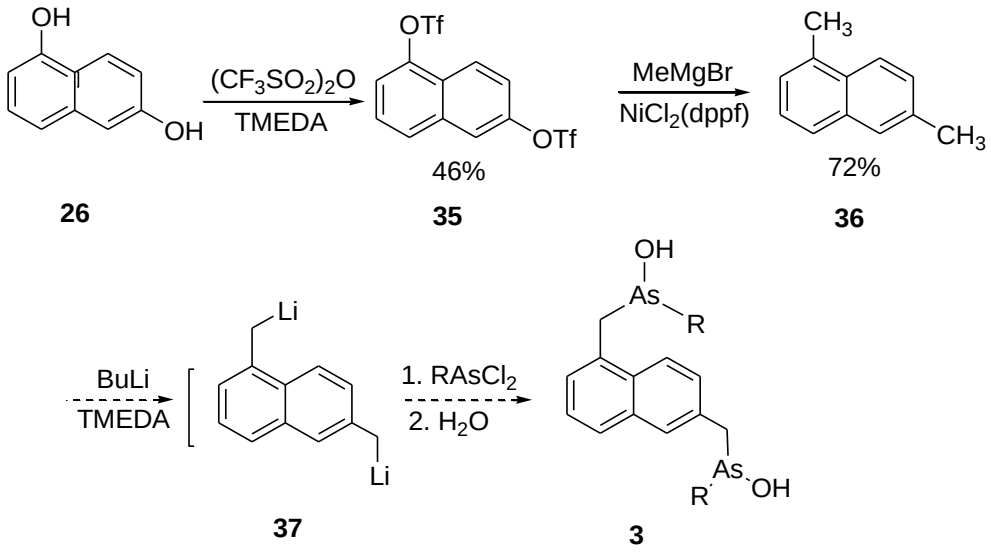

Scheme 7. Synthetic approach to compound **3**

The final steps toward the product **3** are shown in more detail in Scheme 8. **36** was reacted with two equivalents of *n*-butyl lithium in the presence of TMEDA in an effort to form **37**. Methylarsenic dibromide (see section 2.4.1) was added to the reaction mixture to form **3**, followed by addition of mercaptoethanol to form the more stable and isolable product **39** (Scheme 8). The ^{1}H-NMR spectrum of the crude product showed peaks corresponding to the starting material **36**, and the byproduct $CH_3As(SCH_2CH_2OH)_2$ formed by reaction of methylarsenic dibromide with mercaptoethanol. This indicates that deprotonation of **36** by *n*-butyl lithium in the first step did not occur, or possibly that water or another proton source was introduced in the second step. Efforts to solve this problem were ultimately not further pursued due to problems in formation and stability of benzylic arsenic compounds.

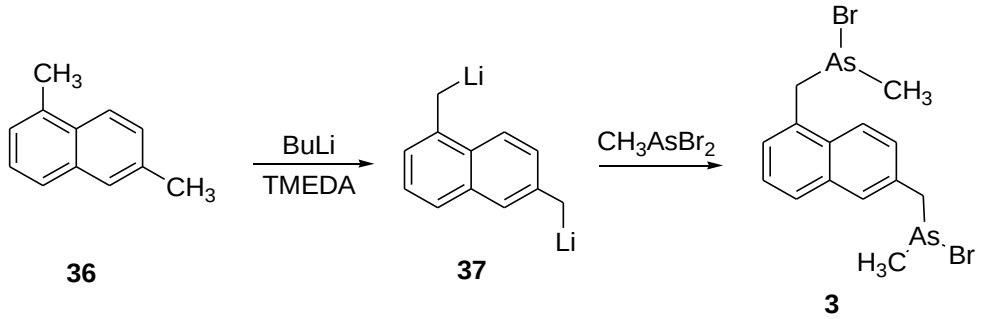

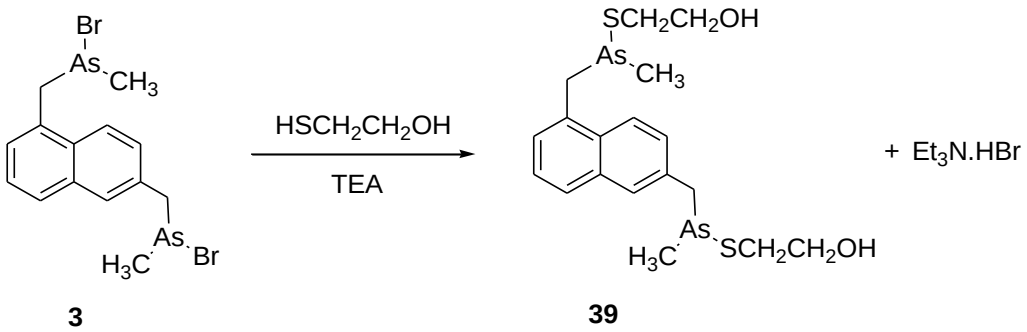

3 **39**

Scheme 8. The proposed formation of the arsenic carbon bond in the final steps of the synthesis of **3**

2.4 Synthesis and model reactions of dihalo-organoarsenic reagents

2.4.1 Synthesis of organoarsenic dihalide compounds

Most available arsenic compounds have the As(V) oxidation state, thus formation of an As(III) organoarsenic dihalide requires a reduction reaction. Thus for the synthesis of phenylarsenic dichloride **41** (Scheme 9), commercially available phenylarsonic acid **40** was dissolved in concentrated aq. HCl. Sodium bisulfite was reacted with aq. HCl in a separate flask to form SO_2 gas, which was bubbled through the solution and along with a catalytic amount of iodine was used to facilitate the reduction reaction. This reaction required a rather long reaction time of bubbling SO_2 for about 6 h at 45° C followed by further reaction at room temperature overnight. Then cacodylic acid **42** was used as the starting material to increase the reaction rate to form **43**. A more convenient procedure was later found using aq. H_3PO_2 added directly to the reaction mixture as the reducing agent, which gave product in two hr at 40-45° C. Commercially available cacodylic acid **42** was used as the starting material for the synthesis of methylarsenic (III) halide compounds. Cacodylic acid was dissolved in concentrated aq. HCl and aq. H_3PO_2 was added as the reductant, 2h reaction time at 40-45 °C gave the product **43**, which was isolated by extraction into dichloromethane.

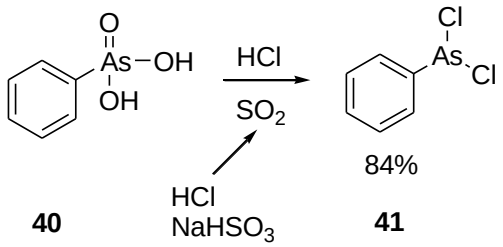

40 **41**

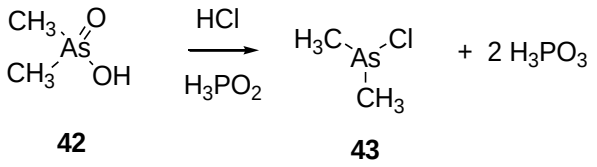

42 **43**

Scheme 9. Synthesis of alkyl arsenic dichloride

2.4.2 Arsenic carbon bond formation of phenyl arsenic dichloride and Grignard reagent

Phenylarsenic dichloride was reacted with simple Grignard reagents as model reactions for C-As bond formation (Scheme 10).[44] As the receptor structures **1, 2, 3** all have arsenic attached benzylic carbon, benzyl magnesium chloride **44** was used, as well as methyl magnesium chloride **47**. However, reactions with Grignard reagents **44** and **47** showed no selectivity for the replacement of only one chloride atom, and a mixture of reactant **41** and dialkyl substituted products **46** (or **49**) were identified in the ^{1}H-NMR spectrum of the crude product, with only a very small amount of the desired monodisplacement products **45** (or **48)** observed.

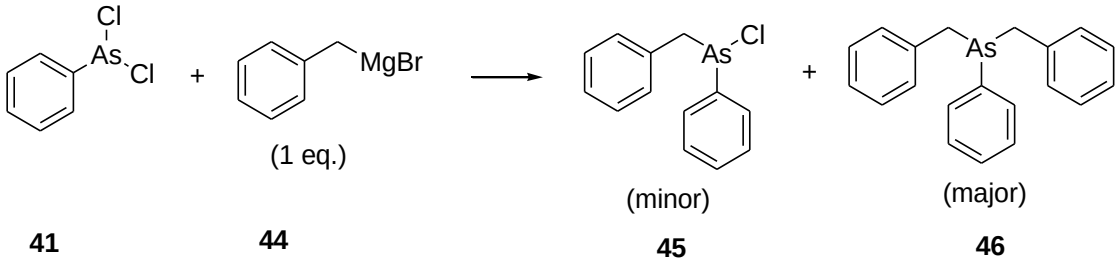

41 **44** **45** **46**

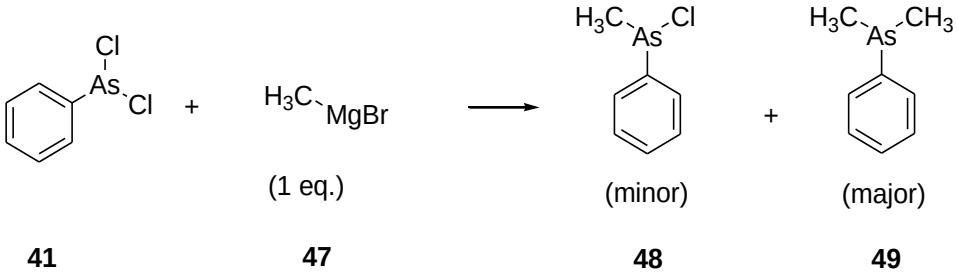

41 **47** **48** **49**

Scheme 10. Phenyl arsenic dichloride reacts directly with Grignard reagent

2.4.3 Conversion of phenyl arsenic dichloride to less reactive derivatives.

Phenyl arsenic dichloride has been successfully modified by ethanethiol, 2-aminoethanethiol, 2-mercaptoethanol, and 2-mercaptoacetic acid to form **50, 51, 52,** and **53** (Scheme 11). **53** was not stable during the purification, and thus the crude product was used in subsequent reaction. Arsenic sulfur bonds should be much more stable than an arsenic chloride bonds, which might increase the selectivity in the reaction with a Grignard reagent.

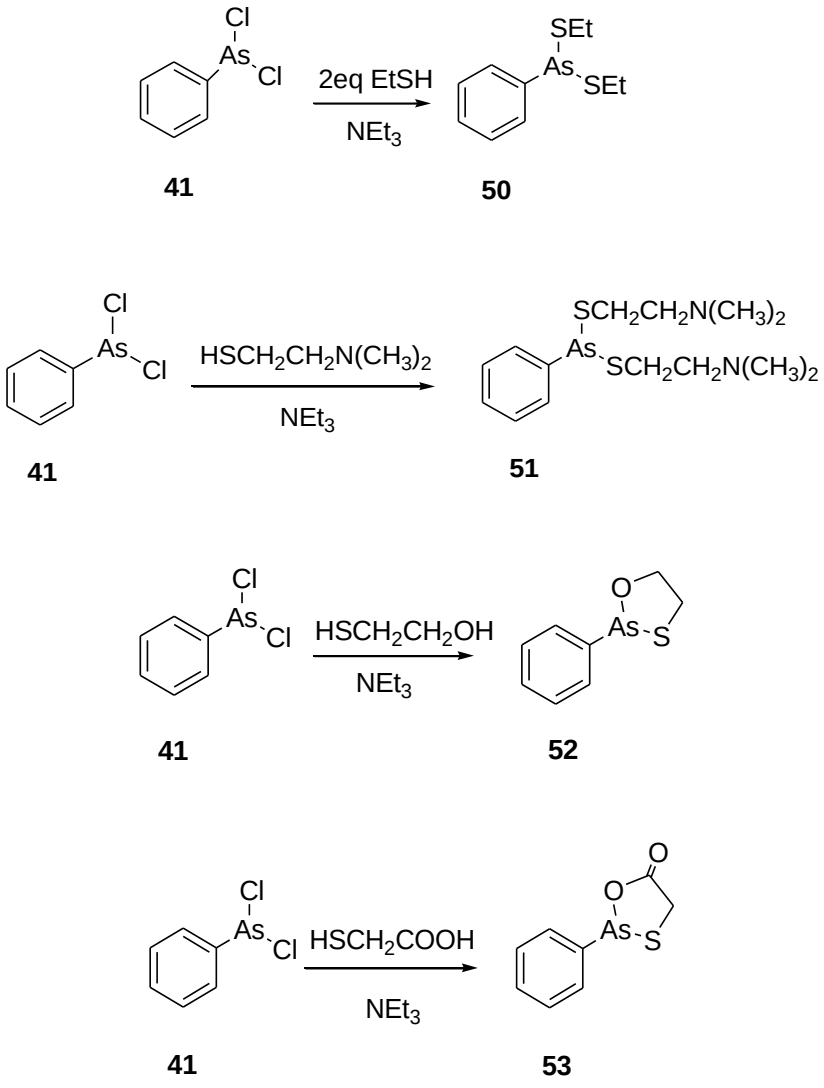

Scheme 11. Modification of phenyl arsenic dichloride

2.4.4 Reaction of modified Arsenic derivatives with Grignard reagents

While the displacement of the sulfur groups by alkyl magnesium chloride did occur (Scheme 12), the reaction was still not selective and as the ^{1}H-NMR spectrum showed a mixture of reactant and primarily dimethyl substituted products in the reaction crude. Purification of the desired product from the product mixture was also difficult, as all the products showed similar polarity, even with the substituents of high polarity. Lower temperature reaction conditions (including butyl lithium reagent) were used, but the selectivity was not increased. Finally, the five-member ring compound **52** was used, with the expectation that As-O bond might be more easily to be broken than the As-S bond. However, both ^{1}H-NMR spectrum and TLC results showed that the product mixture contained primarily the dialkyl substituted product, indicating that the reaction with the Grignard reagent was still non-selective.

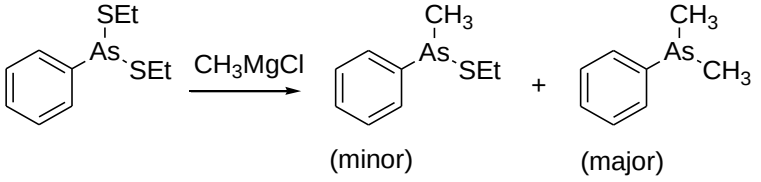

(minor) (major)

50 **54** **49**

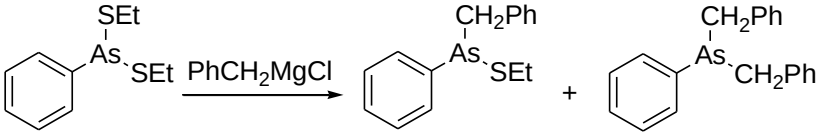

(minor) (major)

50 **55** **46**

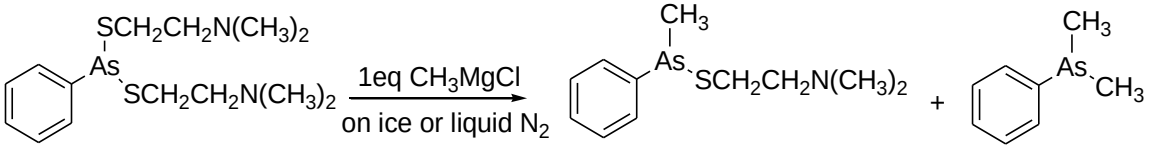

(minor) (major)

51 **56** **49**

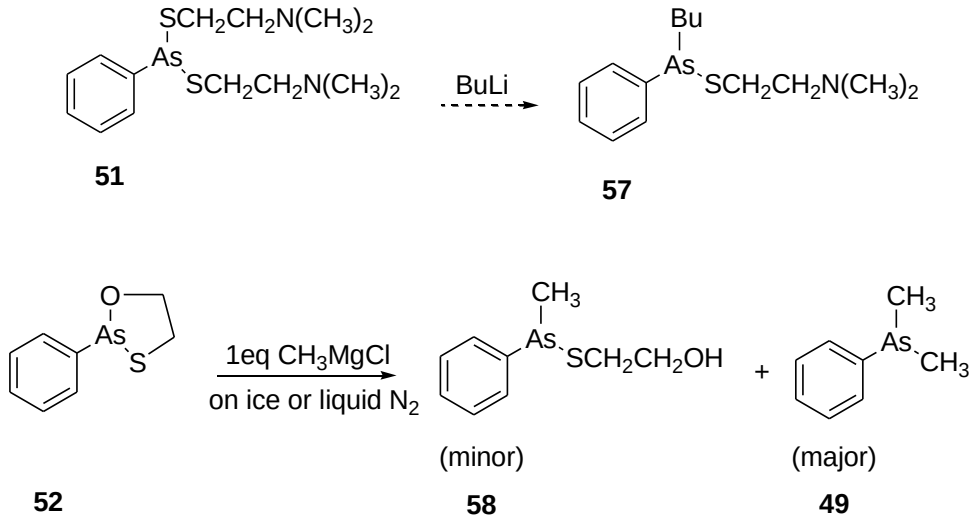

Scheme 12. Modified reaction with Grignard reagent

2.4.5 Further efforts to increase selectivity of substitution on the arsenic atom

2.4.5.1 Conversion of phenyl arsenic dichloride to two different derivatives

The modification of phenyl arsenic dichloride was undertaken as shown in Scheme 13. First ionization of thiol groups by sodium hydride to form the intermediate **59** and **62** was followed by coupling with one equivalent of phenyl arsenic dichloride **41**. The next step was to convert the less stable arsenic chloride bond to arsenic carbon bond by reaction with simple Grignard reagent under low temperature conditions. However, the ^{1}H-NMR spectrum showed a complex mixture of products, both the desired mono-arsenic carbon substituent **54** and **63** resulting from replacement of only one arsenic chloride bond of the two arsenic substituents, and the intermediate. This indicates that the intermediate with sulfur and chloride substituted arsenic atom **60** and **62** showed rather similar polarity with the sulfur and carbon substituted arsenic compounds **54** and **63**. Due to the failure of the purification, an alternate modification approach was developed as described in the next section.

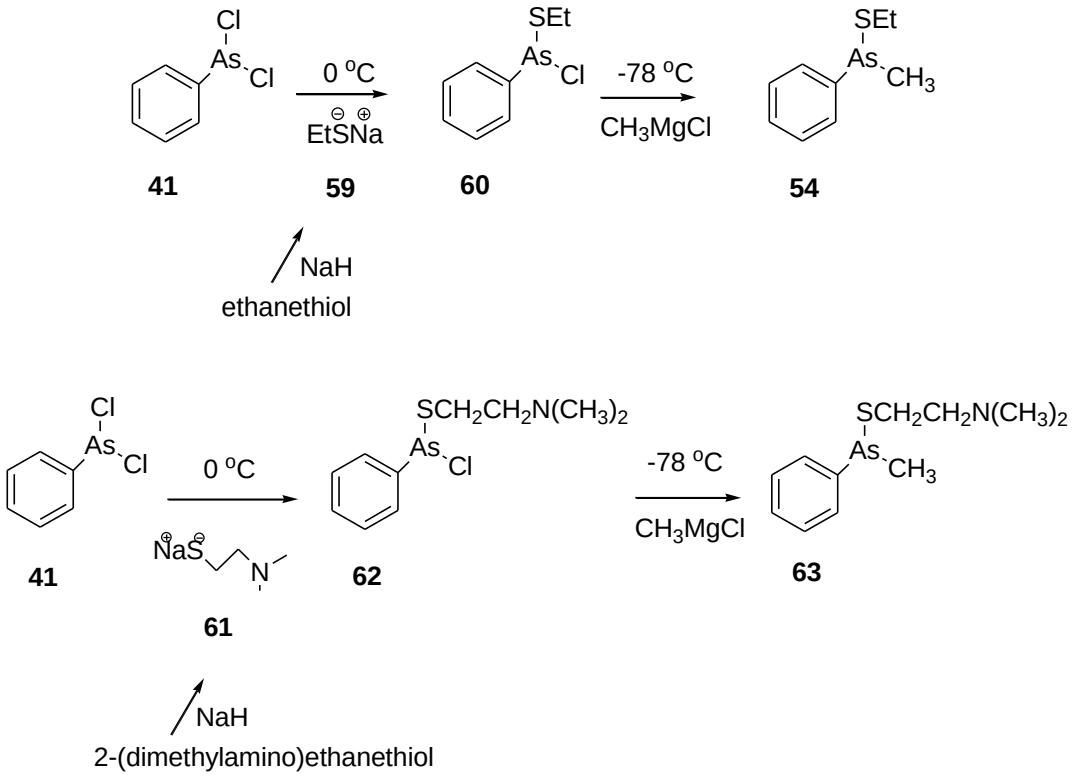

Scheme 13. Further modification of phenyl arsenic dichloride

2.4.5.2 An alternative conversion of phenyl arsenic dichloride to nitrogen atom derivatives

The modification of phenyl arsenic dichloride was undertaken as shown in Scheme 14. First ionization of amine by *n*-butyl lithium to form the intermediate **67** was followed by coupling with one equivalent of phenyl arsenic dichloride **41**. Reaction of the intermediate with one equivalent of methyl magnesium chloride to convert the less stable arsenic chloride bond to arsenic carbon bond was the next step. However, the ^{1}H-NMR spectrum showed a complex mixture of products, the intermediate, and both the desired products **65** and **69** resulting from selective replacement of arsenic chloride bond and the byproduct with both arsenic nitrogen and arsenic chloride bonds removed. This indicates that the intermediate with nitrogen and chloride atoms substituted arsenic atom **64** and **68** showed rather similar polarity with the nitrogen and carbon atoms substituted arsenic compounds **65** and **69**, and the reaction

with Grignard reagent was still not selective for replacement of arsenic chloride bond instead of arsenic nitrogen bond.

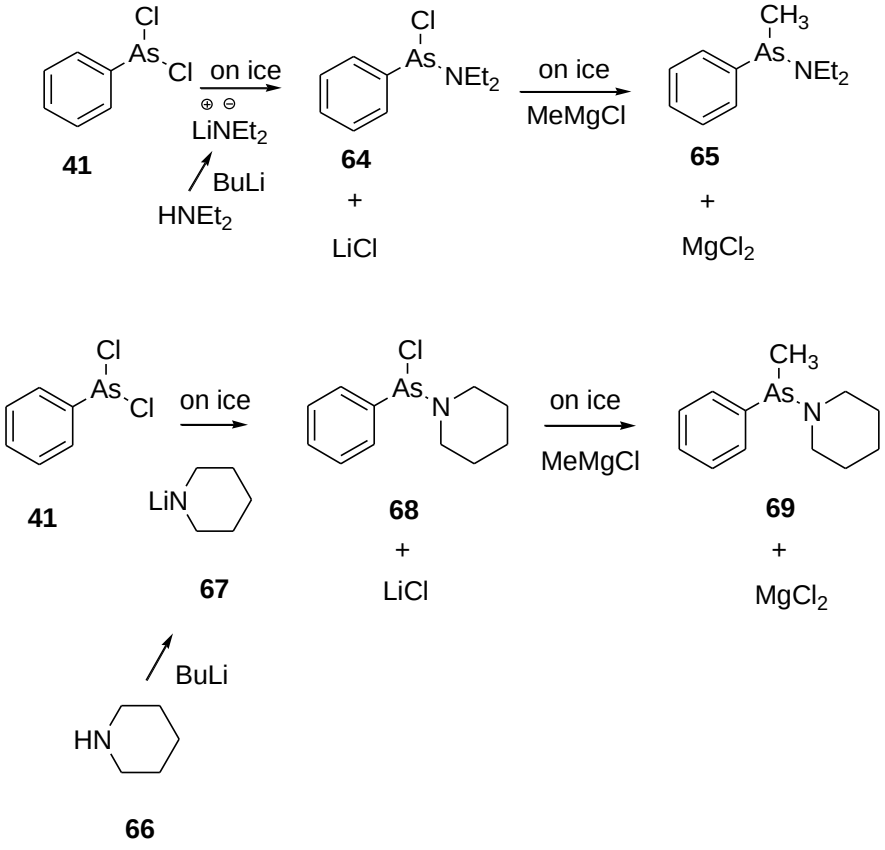

Scheme 14. Further modification of phenyl arsenic dichloride

2.4.6 Further efforts to convert arsenic halide compounds to amine derivatives

Irgolic and coworkers reported the arsenic nitrogen bond formation as shown in Scheme 15. Their results included examples of selective displacement of one or two chlorides from $AsCl_3$ in the presence of diethylamine.

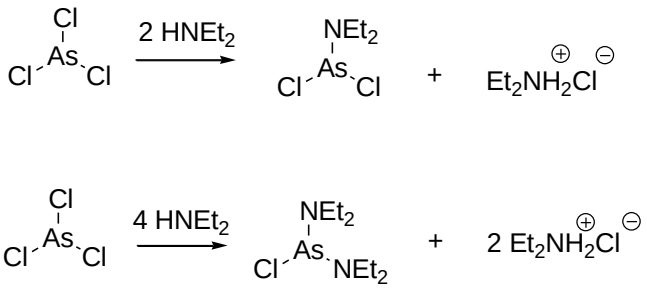

Scheme 15. Conversion of arsenic chloride bonds to arsenic nitrogen bonds

2.4.6.1 Reaction of $PhAsCl_2$ with diethylamine

Thus reaction of $PhAsCl_2$ **41** was conducted with various equivalents of amine as shown in Scheme 16. Reaction with four equivalents of diethylamine formed the derivative **70**, having both chlorides replaced with amines. To displace a single chloride, the reaction was performed with two equivalents of diethylamine, or with one equivalent of diethylamine as the nucleophile and one equivalent of triethylamine as the base. Both the desired product **64** resulting from selective replacement of one arsenic chloride bond and the byproduct **70** were identified in the ^{1}H-NMR spectrum. One equivalent of diethylamine was added into the phenylarsenic dichloride crude to increase the selectivity of the breakage of arsenic dihalide bonds **41** with 0.5 equivalent of diethylamine as the nucleophile and the other 0.5 equivalent as the base (Scheme 16).

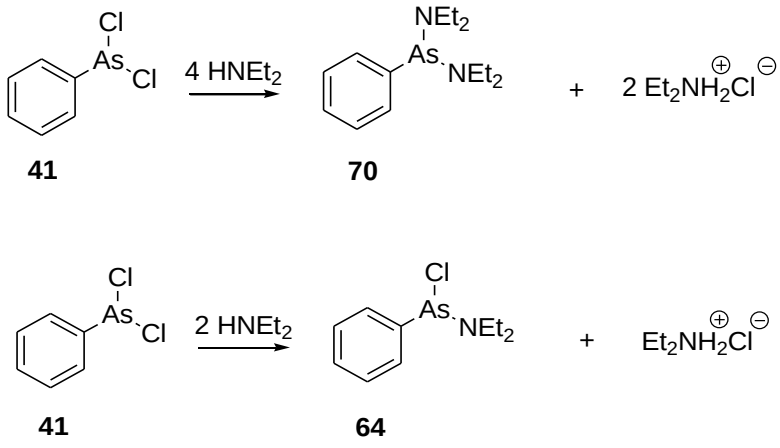

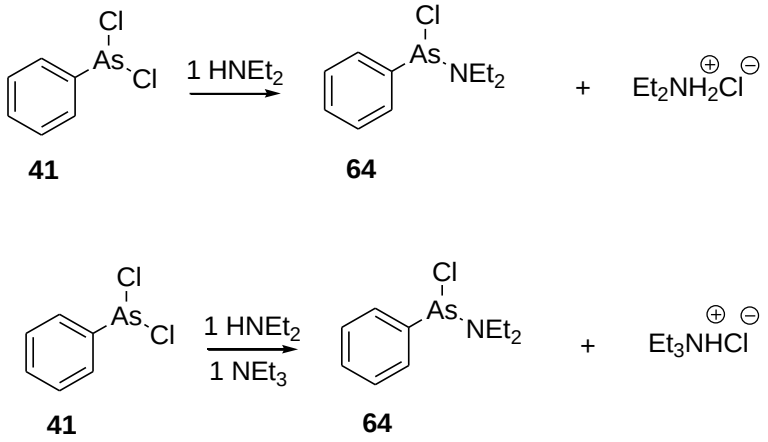

Scheme 16. Conversion of arsenic chloride bonds to arsenic nitrogen bond by diethylamine

2.4.6.2 Reactions of $(CH_3)_2AsCl$ with diethylamine

Reaction of $(CH_3)_2AsCl$ **71** with two equivalents of diethylamine was performed to form **72**, with one equivalent of diethylamine acting as the base and the other equivalent as the nucleophile (Scheme 17). . The purified desired product **72** was identified by ^{1}H-NMR.

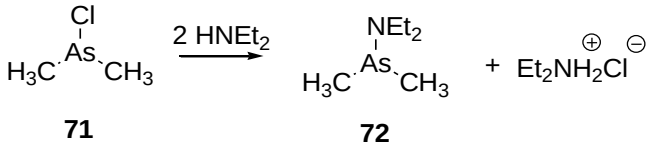

Scheme 17. Conversion of $(CH_3)_2AsCl$ by $HNEt_2$

2.4.6.3 Reactions of CH_3AsBr_2 with diethylamine

Most available arsenic compounds have the As(V) oxidation state, thus formation of an As(III) organoarsenic dihalide requires a reduction reaction. Thus for the synthesis of methylarsenic dibromide **73** (Scheme 18), commercially available methylarsonic acid **42** was dissolved in conc. aq. HBr and aq. hypophosphorous acid, heated at 120 ℃ for about 7 h, then allowed to stay at room temperature overnight, which was isolated by extraction into dichloromethane. The introduction of bromide

compound was because of the volatility properties of the arsenic chloride compounds, the bromide would be relatively heavy atom to make the arsenic compounds less volatile. Reactions of methylarsenic dibromide **73** were performed with two equivalents of dimethylamine or diethylamine with one equivalent of amine acting as the base, and the other equivalent as the nucleophile. The purified desired products **75** and **76** resulting from replacement of one arsenic bromide bond were identified by ^{1}H-NMR.

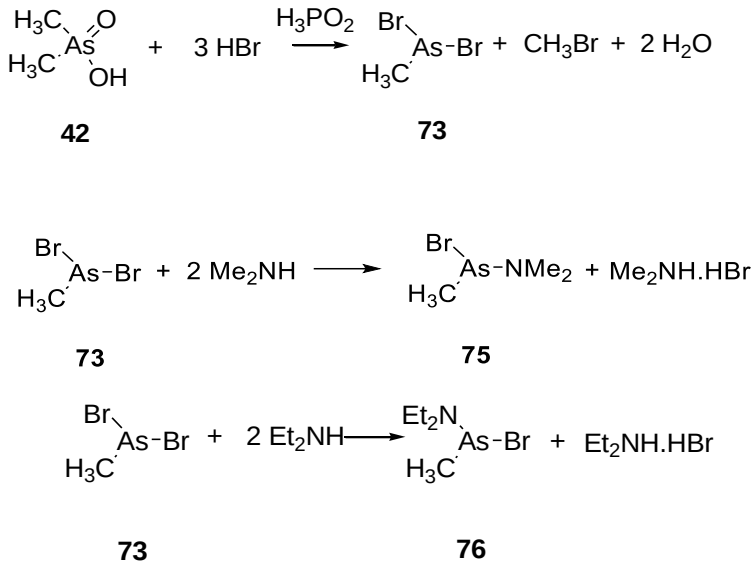

Scheme 18. Reactions of methyl arsenic dibromide with amines

2.4.7 Reactions of Arsenic-Amine Adducts with Grignard reagents

2.4.7.1 Reaction with phenyl magnesium chloride

The Grignard reagent phenyl magnesium chloride was initially used in model reactions for arsenic carbon bond formation. **76** was formed in section 2.4.6.3, with the expectation that the arsenic bromine bond might be more easily broken than the arsenic nitrogen bond. However, upon reaction with one equivalent of phenyl magnesium chloride, both ^{1}H-NMR and TLC results showed that the product mixture contained primarily the disubstituted product, indicating that the reaction was still nonselective (Scheme 19).

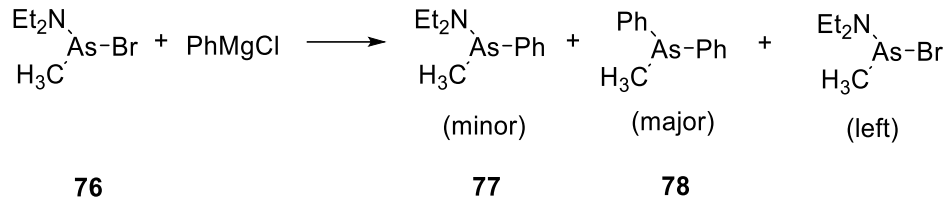

Scheme 19. Reaction with phenyl magnesium chloride

2.4.7.2 Reaction with *n*-butyl magnesium chloride

Butyl magnesium chloride was also used in a model reaction for arsenic carbon bond formation. **76** was formed in Scheme 20 with potassium carbonate as the base (solid base was tried to increase the yield of the arsenic nitrogen bond formation) and diethylamine as the nucleophile, again with the expectation that the arsenic bromine bond might be more easily broken than the arsenic nitrogen bond. Purification of the desired product **79** was facilitated by reaction of the crude product with mercaptoethanol to introduce a more polar thiol substituent to form **80**. However, both ^{1}H-NMR and TLC results showed that the product mixture contained primarily the disubstituted product **80**, indicating that the reaction with methyl magnesium chloride was still nonselective.

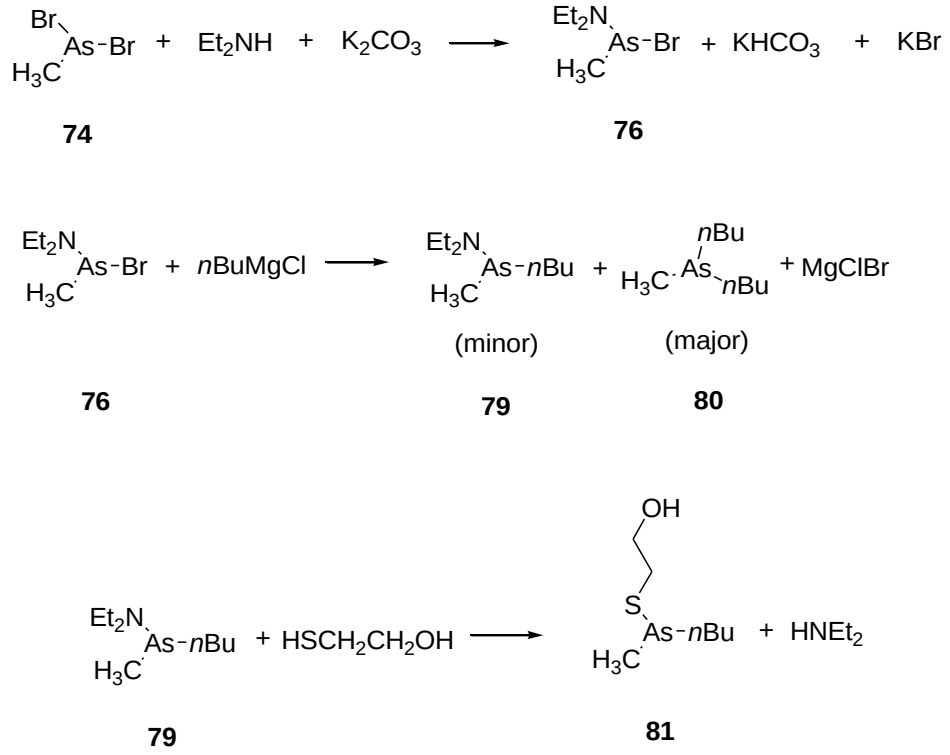

Scheme 20. Reactions using butyl magnesium chloride as a model reaction for C-As bond formation

2.4.8 Reaction of a modified arsenic derivatives with benzyl lithium

An alternative approach of arsenic carbon bond formation was by the lithium reagent **37**, followed by reaction with modified arsenic derivatives to form **3**. Toluene **82** was reacted with one equivalent of *n*-butyl lithium to form **83** under low temperature -78 ℃ conditions. **83** was not isolated but the resulting solution was used directly in the subsequent reactions. However, reactions with the lithium reagent showed no selectivity for replacement of only the bromine atom, and a mixture of starting material and dialkyl product were identified in the ^{1}H-NMR spectrum of the crude product, with only a very small amount of the desired mono displacement product **84** observed. This indicates that the reaction of the lithium reagent was still not selective (Scheme 21).

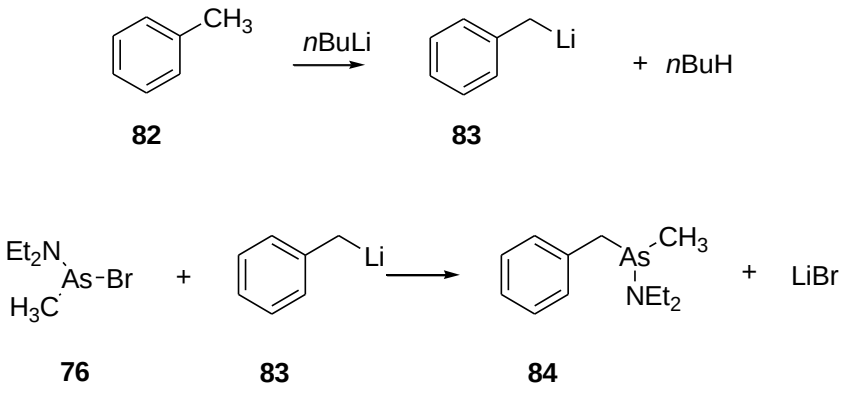

Scheme 21. The reaction with lithium reagent

2.4.9 Attempted arsenic carbon bond formation by metal mediated coupling

$Zn/CdCl_2$ has been found by Cunliu Zhou and Zhiyong Wang to be effective in the reductive coupling of benzyl halides **86** with various aldehydes and ketones **85**, affording the corresponding alcohols **87**. [45] Theses reaction conditions were duplicated but substituting electrophilic arsenic species for the aldehyde to determine if a carbon arsenic bond could be formed under these conditions. Reactions were undertaken as shown in Scheme 22, reacting the commercially available benzylic halide with zinc or magnesium as the reducing reagent, and **88** or **73** as the arsenic reactant. However, ^{1}H-NMR spectrum of the crude reaction mixtures showed only the starting material, indicating that no reaction occurred.

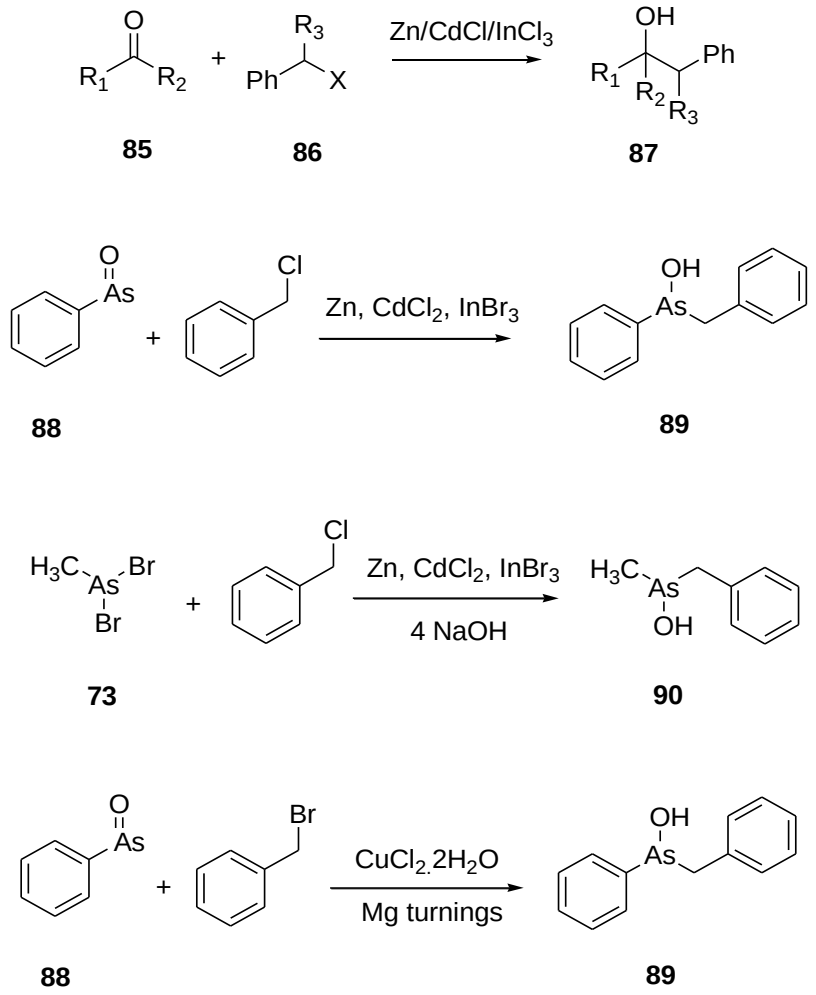

Scheme 22. Unsuccessful metal mediated coupling reactions

2.4.10 An alternative arsenic carbon bond formation of methyl arsenic dibromide with Grignard reagents

Methyl arsenic dibromide **73** was reacted with simple Grignard reagents as model reactions for carbon arsenic bond formation, benzyl magnesium chloride was used, as well as phenyl magnesium chloride. Arsenic bromine intermediate **89** was protected by thiol with TEA as base, and with the expectation that arsenic thiol substituents would show much higher polarity and molecular weight difference facilitating purification. However, reactions with Grignard reagents showed no selectivity for the replacement of only one bromide atom, and a mixture of reactant **73** and dialkyl product **80** were identified in the ^{1}H-

NMR spectrum of the reaction crude, with only a very small amount of the desired mono displacement product **89** or **91** observed (Scheme 23).

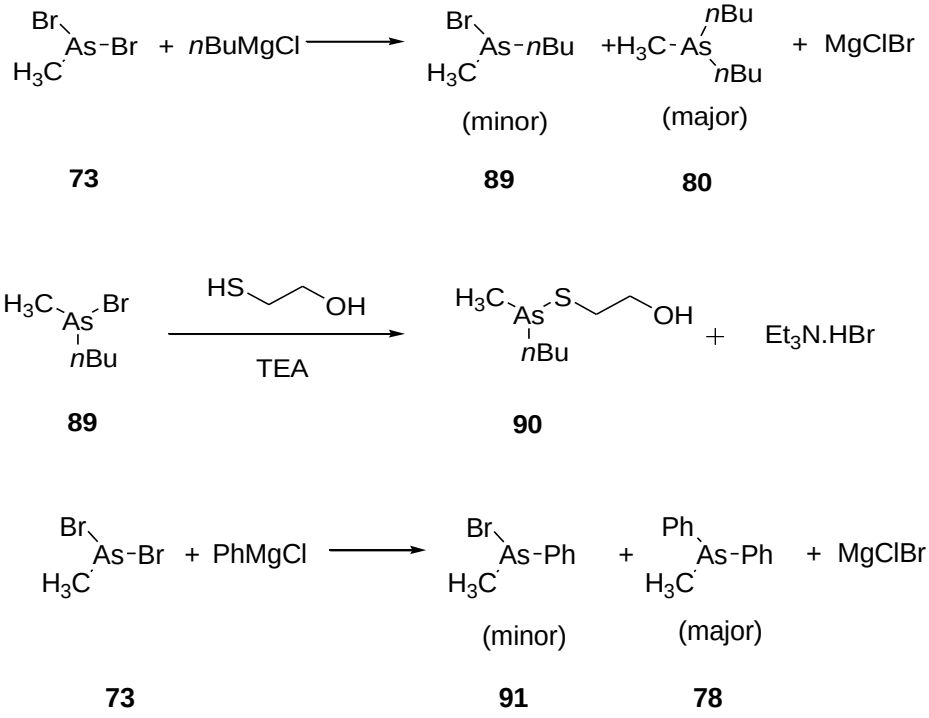

Scheme 23. The reaction with Grignard reagents

Due to the failure in the synthetic approach of the scaffold structure, the synthesis of compound **1**-**3** was abandoned due to the instability of the benzylic group connected with arsenic atom.

3 New methods in the synthesis of aryl-arsenic compounds

The published synthesis of FlAsH was performed through mercuration ortho to phenolic OH followed by Pd-catalyzed C-As bond formation, forming an arsenic dichloride intermediate. A revised approach to receptor design and synthesis was thus pursued that would use similar chemistry for introduction of arsenic functionality onto the receptor scaffold. (Scheme 24)

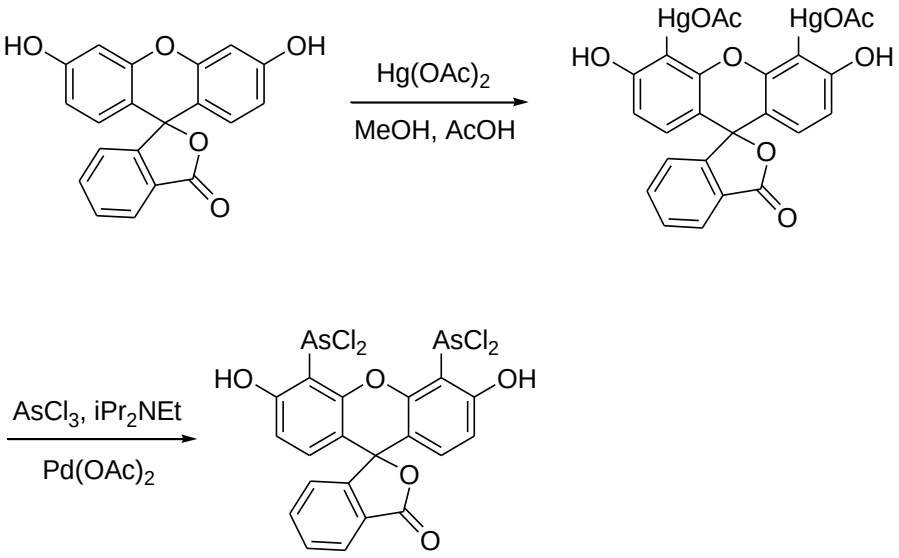

Scheme 24. The published synthetic approach of FlAsH

3.1 Synthesis of an o-hydroxyphenyl arsenic model compound

The chemistry for incorporation of arsenic functionality at the ortho position of a phenol was developed starting from 4-methylphenol **92**. Reaction with mercuric acetate formed the ortho mercuration product **93**, with the methyl group serving to prevent mercuration at the para position. The crude product **93** was reacted directly in the next step with methylarsenic dibromine with palladium catalyzed to form **94**. The crude product was reacted directly with β-mercaptoethanol to form the more stable thiol adduct **95**, which was purified and fully characterized. The success of this reaction scheme indicated that methyarsenic dibromide can successfully replace arsenic trichloride in the Pd-catalyzed replacement of mercury. The free arsinous acid product **96** was formed by reaction with silver nitrate in methanol. Followed by addition of lithium chloride to precipitate any excess silver ion, filtration to remove the precipitated silver salts, and finally hydrolysis of resulting methanol adduct (Scheme 25). The applications of the incorporation of arsenic at the ortho position to phenolic OH will be discussed in sections 3.2 and 3.3.

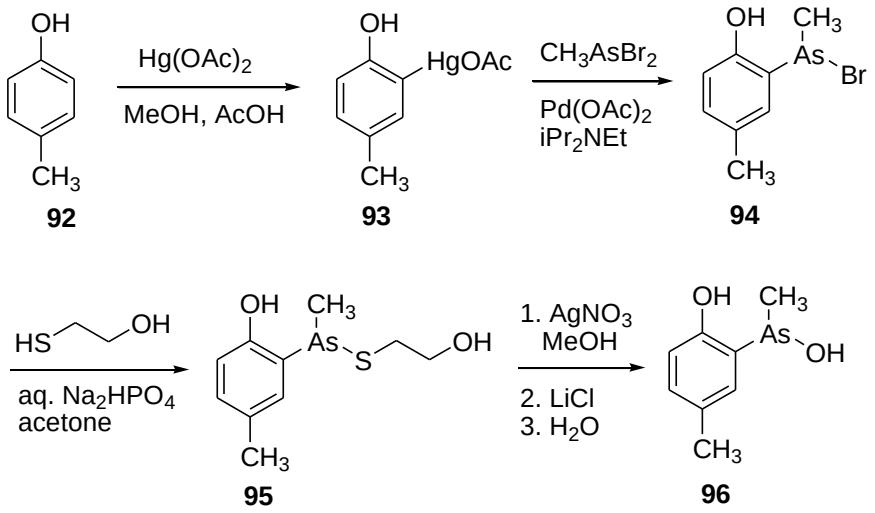

Scheme 25. Synthesis of an o-hydroxyphenyl arsinous acid model compound

3.1.1 Binding constant measured by ITC

The binding constant has been measured by breaking the As-S reversible single bond, which has been published by our group. [47] ITC experiments were performed on a Model CSC 4200 microcalorimeter (Calorimetry Sciences Corp.) at 25° C with stirring at 297 rpm. The cell (1.3 mL) contained a 0.5 mM solution of **97** in 5 mM potassium phosphate buffer pH 7.0 containing 2% DMSO, and was injected with 2–mercaptoethanol (6.0 mM). Cline et al. have shown that $CH_3As(OH)_2$ binds to i,i+1; i,i+2; i,i+3; and i,i+4 dicysteine pairs with almost equal affinity. [46] Formation of the complex **96** between **97** and mercaptoethanol was studied by Isothermal Titration Calorimetry. An association constant of 6×10^4 M^{-1} was determined. This represents approximately 4-fold and 30-fold greater affinity than the values of 1.6×10^4 M^{-1} and 1.9×10^3 M^{-1} for the first and second association constants for binding of methylarsonous acid [$CH_3As(OH)_2$] to two equivalents of thiol (Scheme 26).[47]

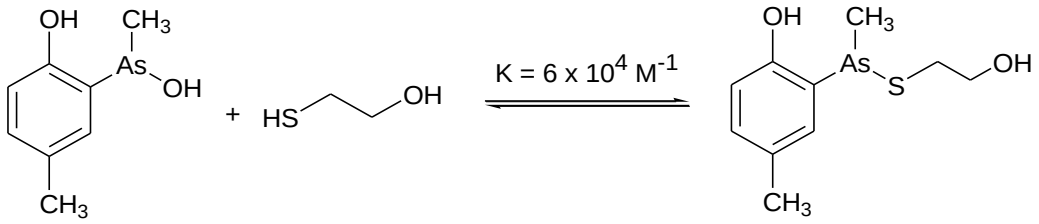

Scheme 26. The binding constant measured by ITC

3.1.2 Displacement of mercury by iodine atom

The displacement of mercury was detected by iodine mercury exchange with iodide and potassium iodide as the source of iodine,[48] which facilitated the identification of the intermediate **93** in the ^{1}H-NMR spectrum. Peaks were corresponding to the iodine substituted compounds **98** in the ^{1}H-NMR spectrum of the reaction crude (Scheme 27).

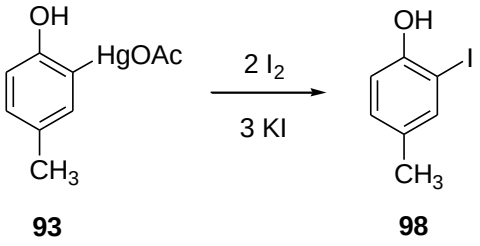

Scheme 27. Replacement of the mercury substituent by iodine atom

3.1.3 Probes designed based on the ortho mercuration model

The ortho mercuration synthetic method provides products having the arsenic group attached directly to an aromatic ring with an o-hydroxyl group. As the initial series of probe designs all had arsenic attached to benzylic carbon, a new series of probes was designed using HostDesigner that are amenable to this alternative synthetic method (Figure 26).

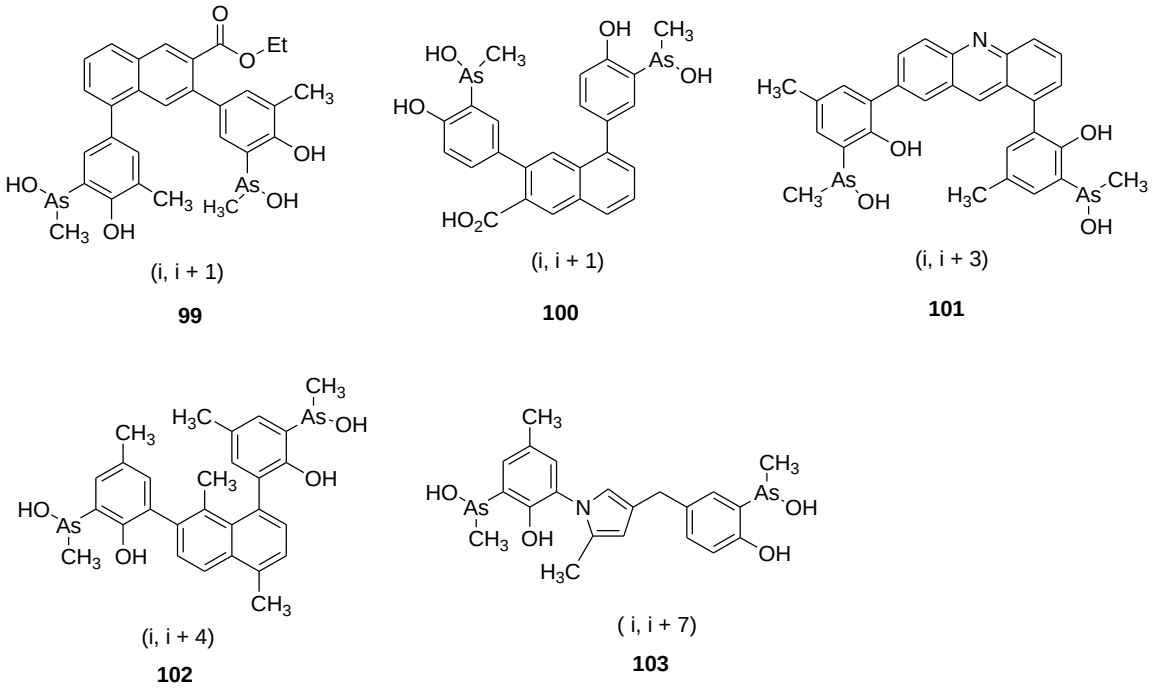

Figure 26. Designed dicysteine peptide receptors based on o-hydroxyphenyl arsenic functionality

3.2 The synthetic approach to 99.

The synthetic approach to **99** is shown in Scheme 28. The commercially available carboxylic acid **104** was converted to the ethyl ester **105**. The two hydroxyl groups were then converted to the triflate esters to form **106** followed by Suzuki coupling at both triflates to form **107**. The methyl substitutes ortho to methoxyl groups will later block one ortho position of each benzene ring from mercuration. Demethylation of **107** was performed by iodocyclohexane to form **108**. The remaining steps follow the chemistry developed in the synthesis of the simple model compound for ortho mercuration to form **109**, followed by conversion to the arsenic compound, and its thiol adduct.

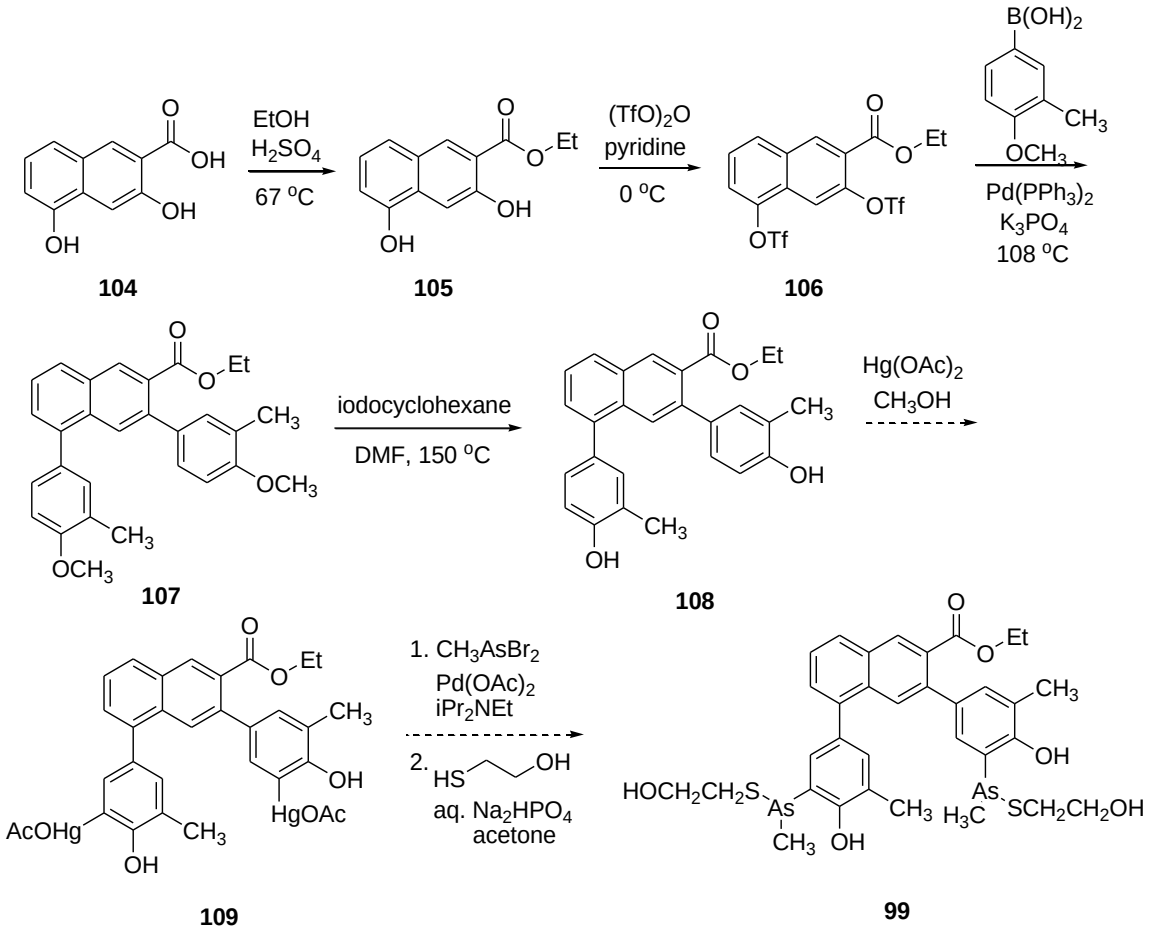

Scheme 28. The synthetic approach to **99**

The esterification of the carboxylic acid at position 2 was performed under different conditions, both DCC coupling and the sulfuric acid catalyzed esterification gave similar yield to form **105**, and sulfuric acid catalyzed esterification required less reaction time (Scheme 28a).

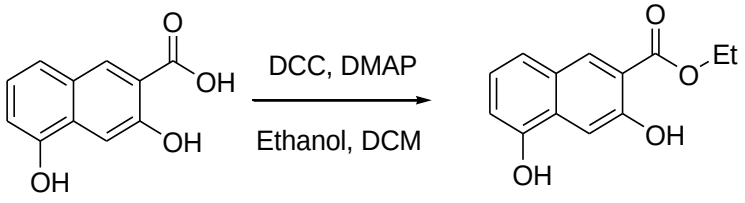

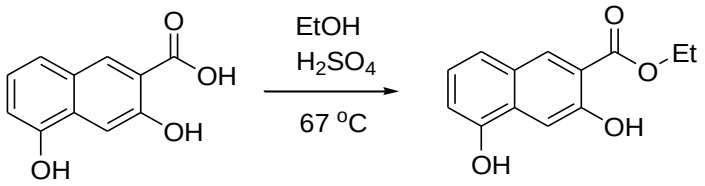

104 **105**

Scheme 28a. Esterification conditions

The Suzuki coupling reaction was performed by different boronic acids with different steric hindrance and different electronic effects. The Suzuki coupling product **110** showed higher yield with less sterically hindered substituents on the benzene ring.

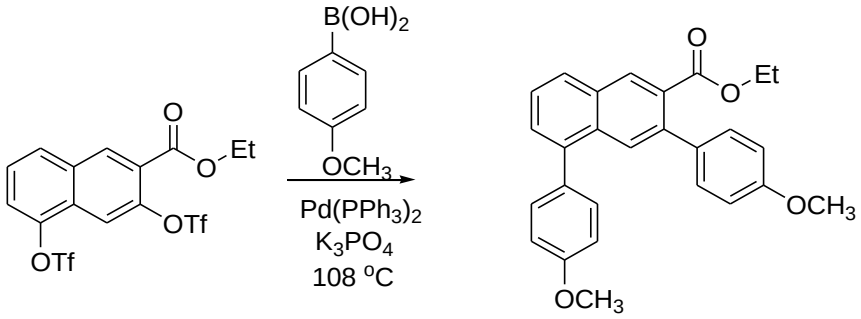

106 **110**

Scheme 28b. Suzuki coupling with boronic acid

The o-demethylation reaction using BBr_3 was accompanied by hydrolysis of the ester group. The alternative method was using iodocyclohexane to remove the methyl substituent shown in Scheme 28 (Scheme 28c).

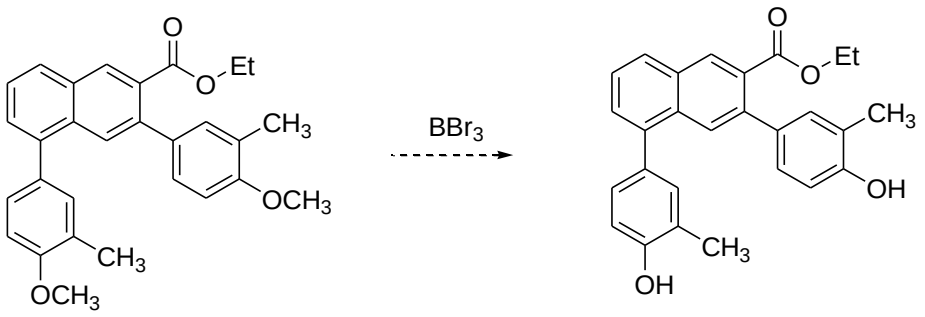

107 **108**

Scheme 28c. Demethylation by BBr_3

The recovered monocoupling product **111** was performed twice Suzuki coupling to form **107** under similar conditions as in Scheme 28 (Scheme 28d).

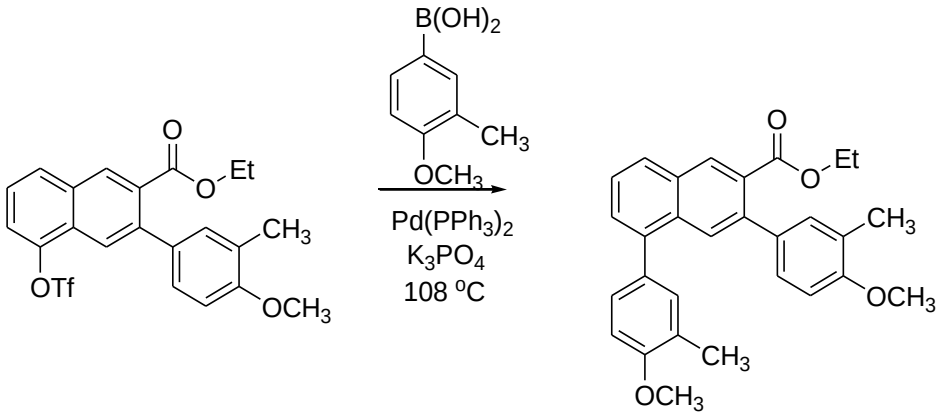

111 **107**

Scheme 28d. Further Suzuki coupling with boronic acid

Further esterification of acid at position 2 was performed by DCC coupling or esterification catalyzed by sulfuric acid to form **107**. However, no desired product has been identified in the ^{1}H-NMR spectrum of the reaction crude (Scheme 29).

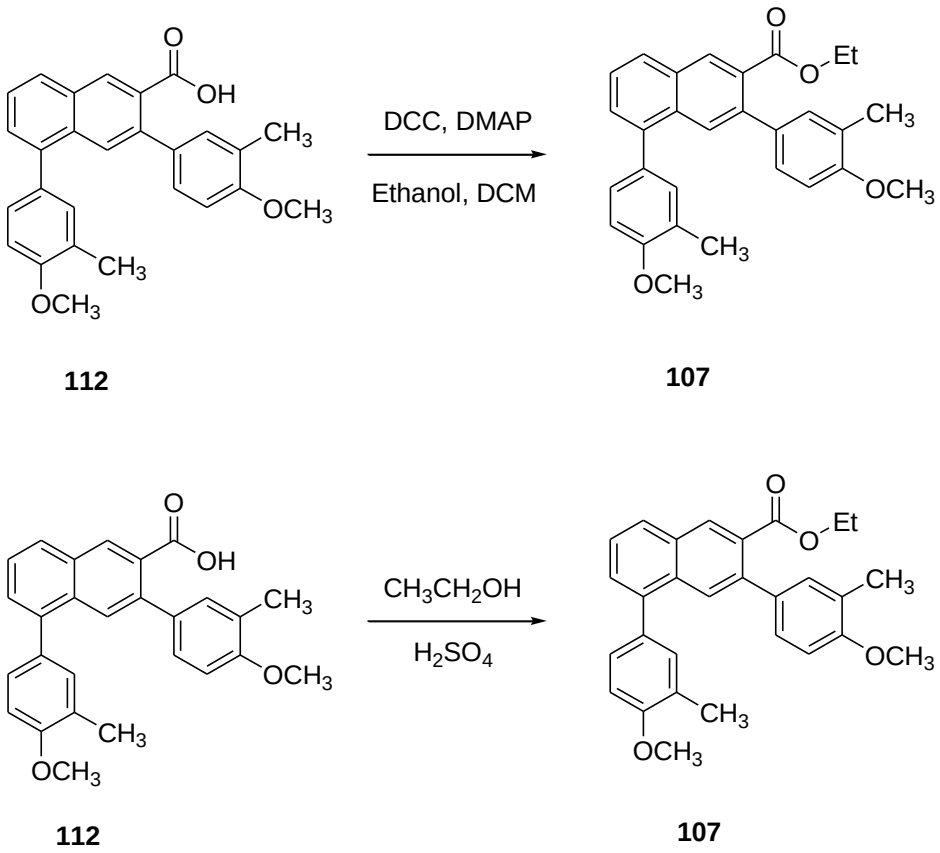

Scheme 29. Further esterification of intermediate **112**

3.3 Displacement of mercury by iodine of 109

The conversion of mercury compound to iodine substituents compound **113** was undertaken as shown in Scheme 30, which would facilitate the identification of the mercury intermediate **109** in the ^{1}H-NMR spectrum of the reaction crude.

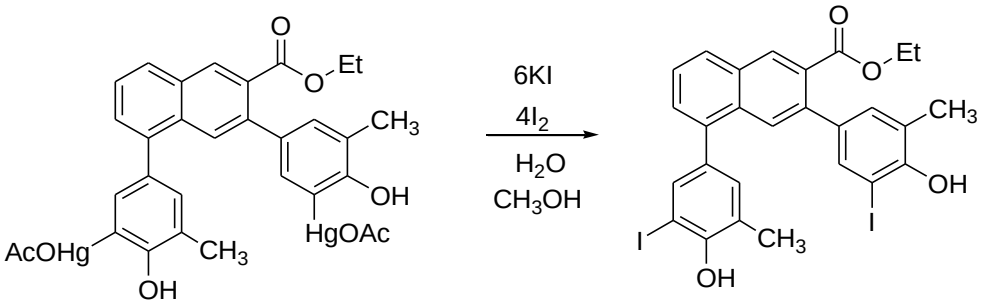

109 **113**

Scheme 30. Displacement of mercury by iodine atoms

3.4 The synthetic approach to 102

The synthetic approach to **102** was undertaken as shown in Scheme 31. First the hydroxyl groups at positions 1 and 7 were protected by methylation to form **115**, with the expectation to block the reaction on the two hydroxyl groups, followed by Vilsmeier–Haack reaction to form an aldehyde group at position 4 of the benzene ring to form **116**. The next step was to convert the aldehyde group to a methyl group by Wolff–Kishner reduction to form **117**, followed by the similar procedure of Vilsmeier–Haack reaction to form the second aldehyde group to form **118**, then the aldehyde group was reduced to methyl group by Wolff–Kishner reduction to form **119**. Demethylation was performed by BBr_3 to form **120**, followed by conversion to triflate groups to form **121** at room temperature and the Suzuki coupling with boronic acid to form **122**, as the triflate group is a very good leaving group.

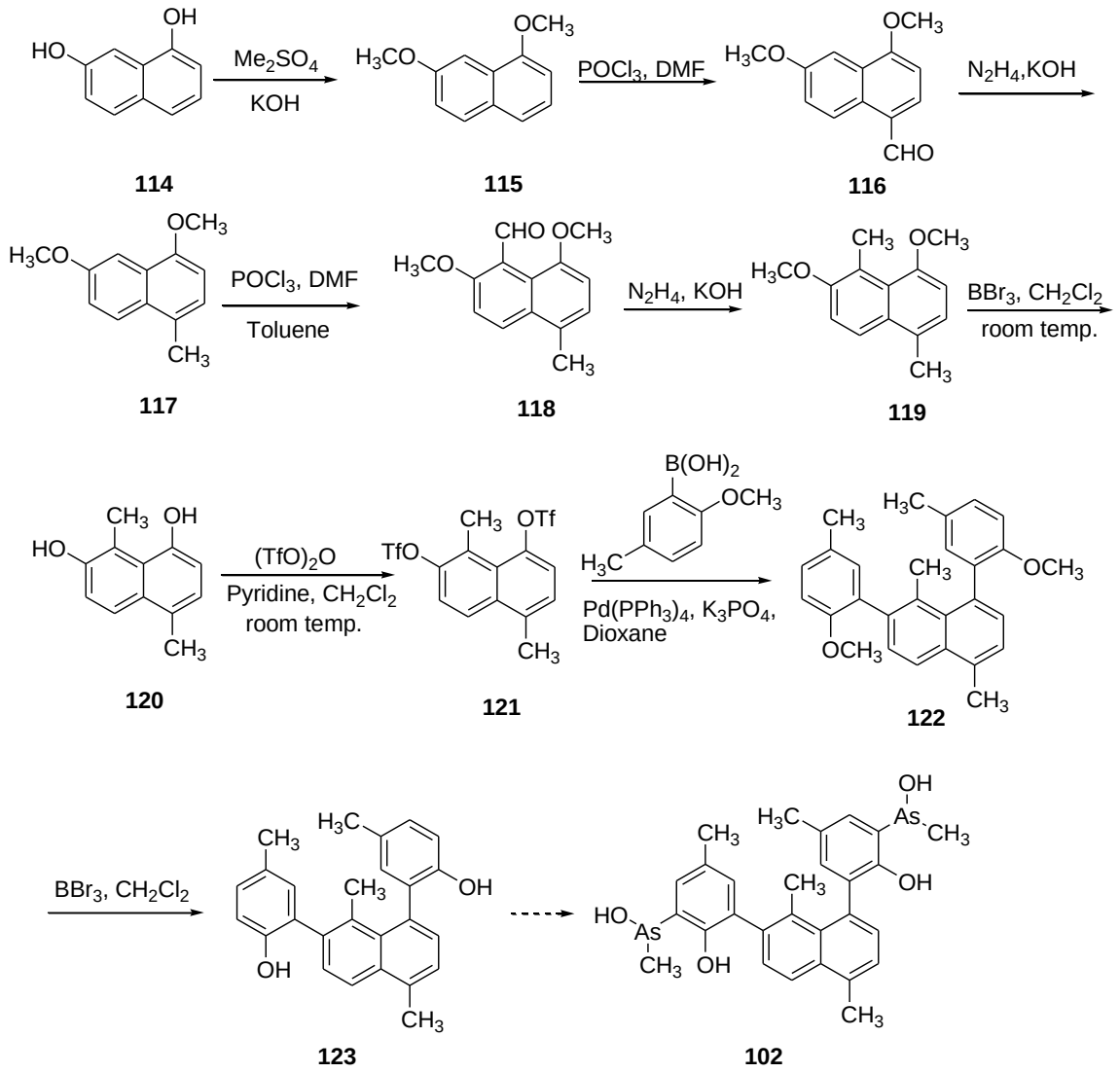

Scheme 31. The synthetic approach to **102**

Due to the failure in the synthesis of earlier compounds **1**, **2**, **3**, **99**, and **102**, as the mercury intermediate cannot be fully purified and recovered from the reaction crude, the final product has never been identified in the ^{1}H-NMR spectrum, other procedures were developed as described in the following section.

3.5 The coupling reaction of boronic acid.

The synthetic approach of aromatic ketones and related compounds was undertaken as

shown in Scheme 32 with palladium or nickel as the catalyst starting from boronic acids.[49]

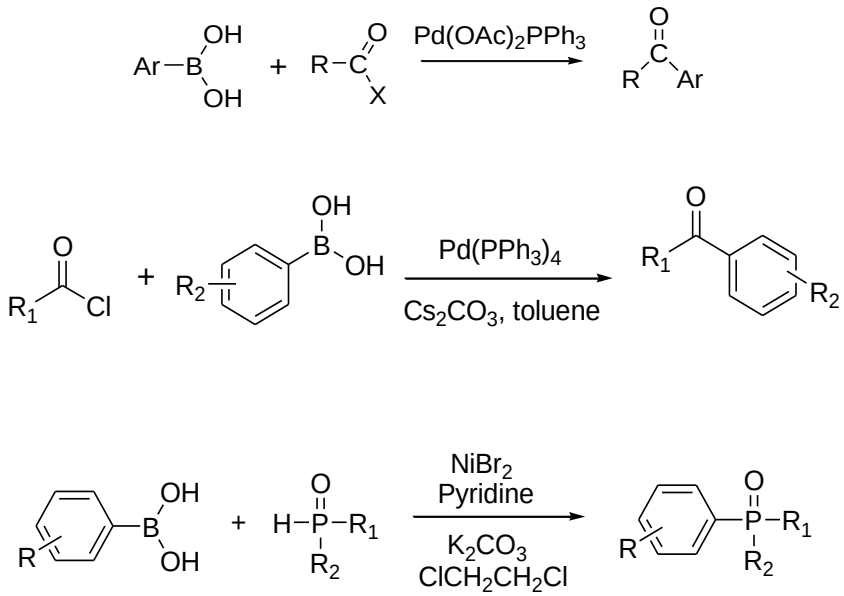

Scheme 32. The coupling reaction of boronic acid

3.5.1 The As-C bond formation of boronic acid and arsenic atoms.

The coupling reaction was performed starting from the commercially available boronic acid **124** and dibromomethylarsenic compound **73** with Tetrakis(triphenylphosphine)palladium(0) as the catalyst, potassium phosphate or cesium carbonate as the base, and dimethylchloride or toluene as the solvent, and stirred at room temperature or heated at 110° C. Based on the ^{1}H-NMR spectrum of the reaction crude, potassium phosphate turned out to be the best base for the coupling, and the solvent toluene was associated with the highest yield (Scheme 33).

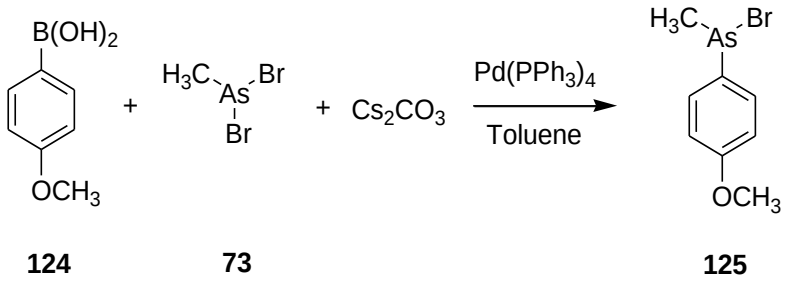

124 **73** **125**

Scheme 33. The As-C bond formation starting from boronic acid

	Solvent	Temperature (° C)	Base	Yield (%)
1	**CH_2Cl_2**	**r.t.**	**K_3PO_4**	**0**
2	**CH_2Cl_2**	**r.t.**	**Cs_2CO_3**	**10**
3	**Toluene**	**110**	**Cs_2CO_3**	**45**
4	**Toluene**	**110**	**K_3PO_4**	**75**

Table 2. The coupling conditions

3.5.2 Modifications on the boronic acids of the Suzuki coupling

The modifications on the boronic acid affected the coupling reaction not too much, the coupling reactions were performed under similar reaction conditions as in section 3.5.1 starting from substituents with different electronic effects and various steric hindrance. All the purified coupling products **127**, **129**, **131**, **133**, **135**, and **137** have been identified in the ^{1}H-NMR spectrum (Scheme 34).

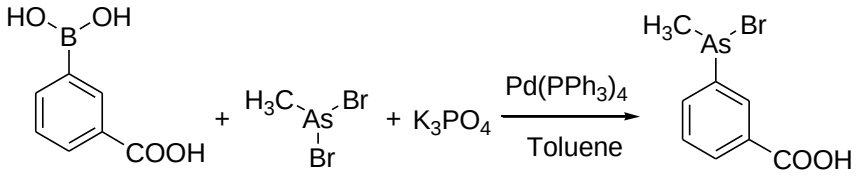

126 **73** **127**

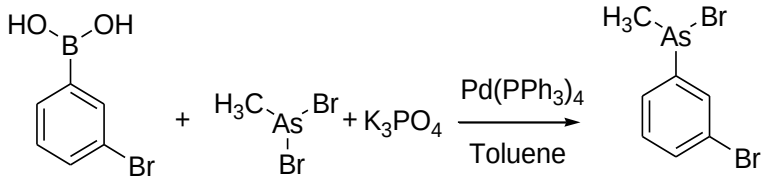

128 **73** **129**

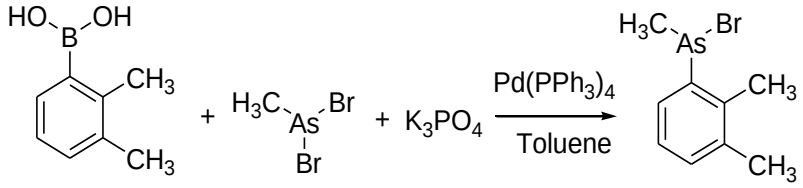

130 **73** **131**

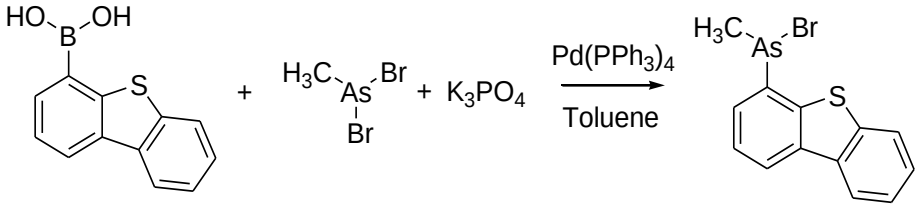

132 **73** **133**

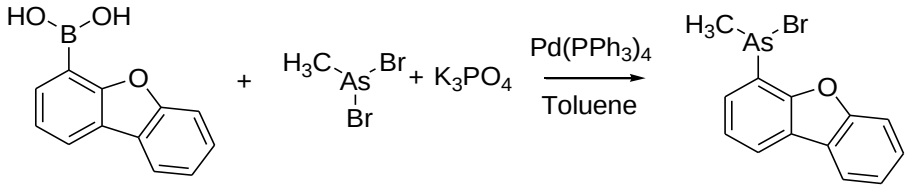

134 **73** **135**

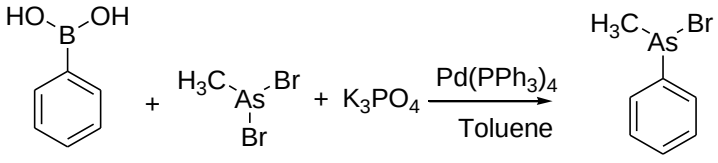

136 **73** **137**

Scheme 34. The As-C bond formation of other boronic acids

3.5.3 The formation to three aromatic groups substituted arsenic center

The synthetic approach to the three aromatic groups substituted arsenic center was undertaken as shown in Scheme 35b starting from boronic acid. The next step was to convert the two bromine atoms to Grignard reagent **139** with iodine as the catalyst, and with the activation of magnesium metal under inert nitrogen gas. However, no desired product **148** was identified in the ^{1}H-NMR spectrum of the reaction crude. Displacement of bromine atom to lithium group was performed by one equivalent of *n*BuLi to form **140**, the peaks of the desired product **141** were identified in the ^{1}H-NMR spectrum after the reaction of acetone (Scheme 35a and c). The synthetic approach of another three aromatic substituted arsenic center was undertaken starting from diethylamine substituted benzene ring to form **146** following the same approach as described above in this section (Scheme 35d). Ethanethiol was used to stabilize the lithium intermediate **147** followed by arsenic carbon bond formation with Grignard reagent **144** to form **148** (Scheme 35e).

(a)

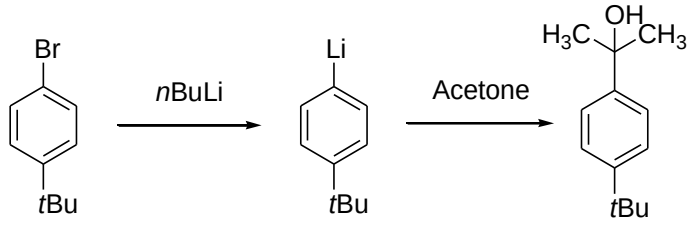

138 **140** **141**

(b)

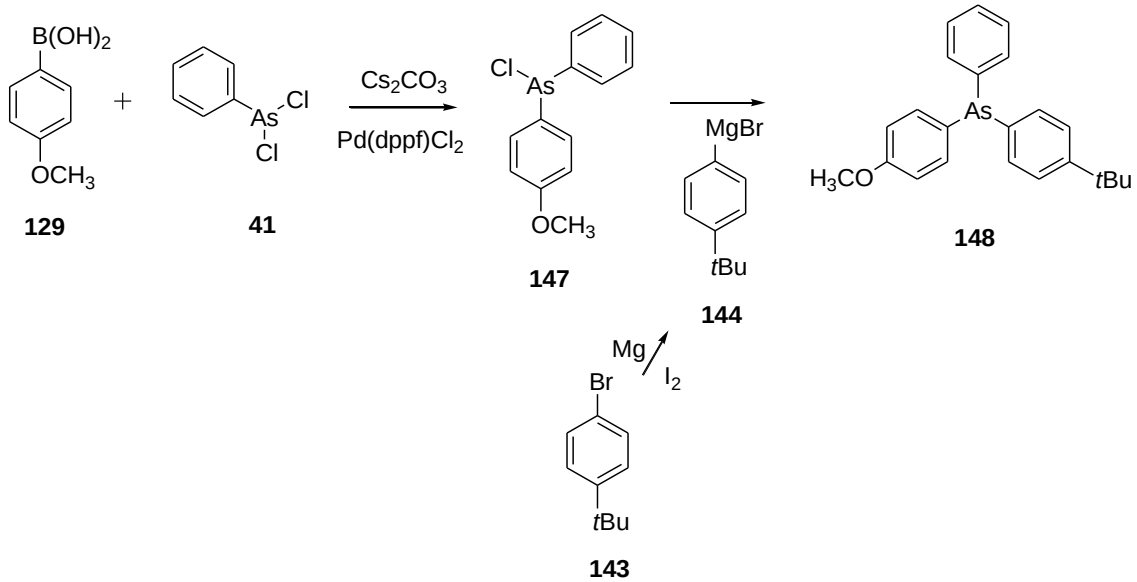

129 **41** **147** **144** **148** **143**

(c)

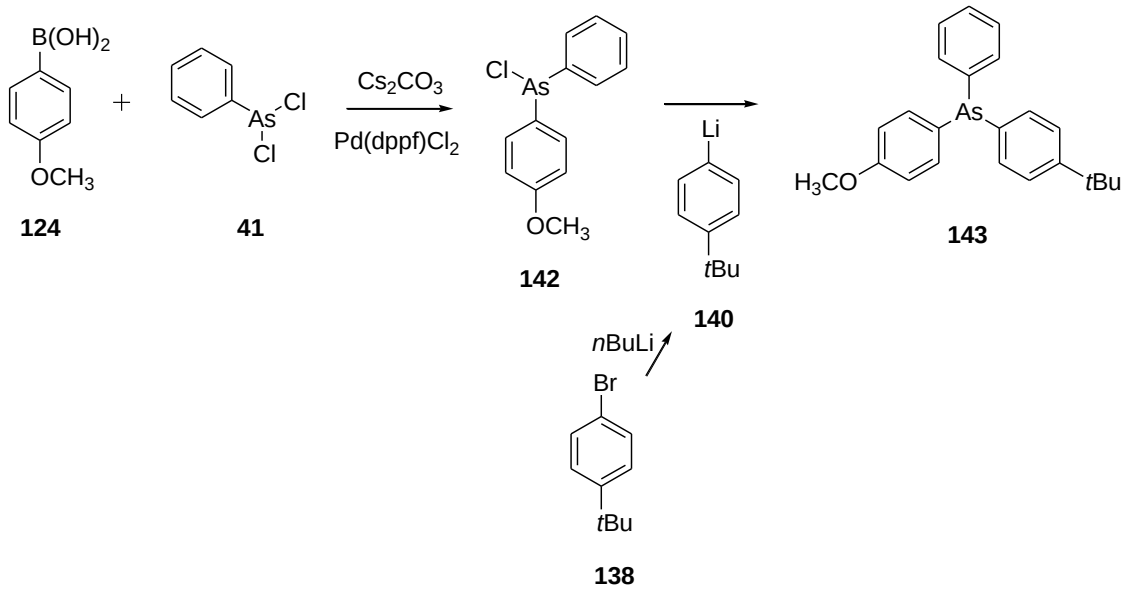

124 **41** **142** **140** **143** **138**

(d)

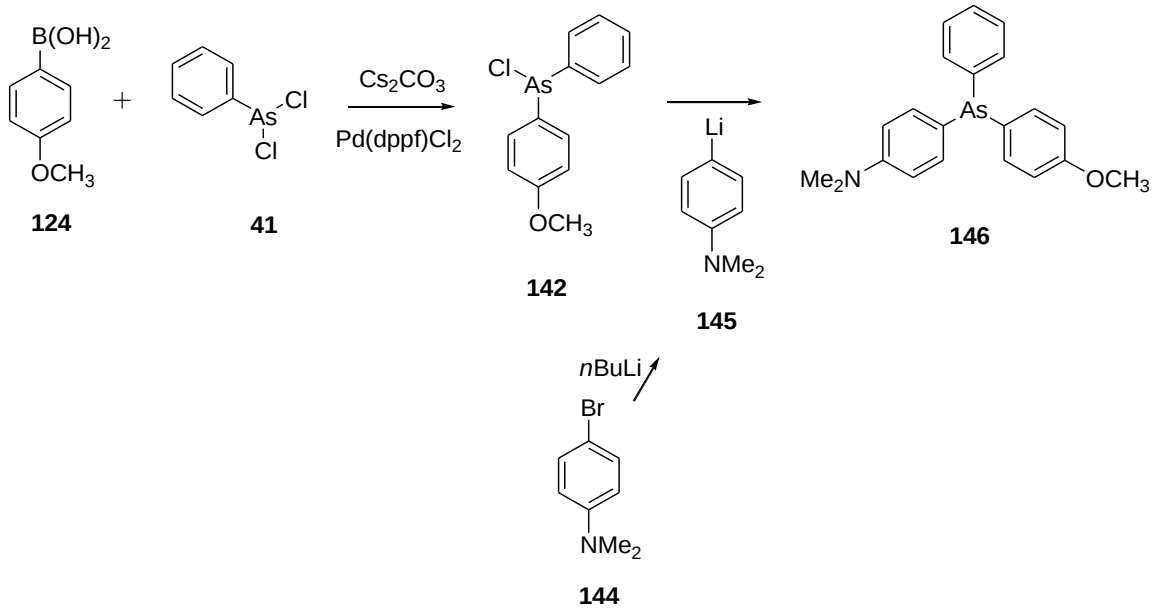

124 **41** **142** **145** **146** **144**

(e)

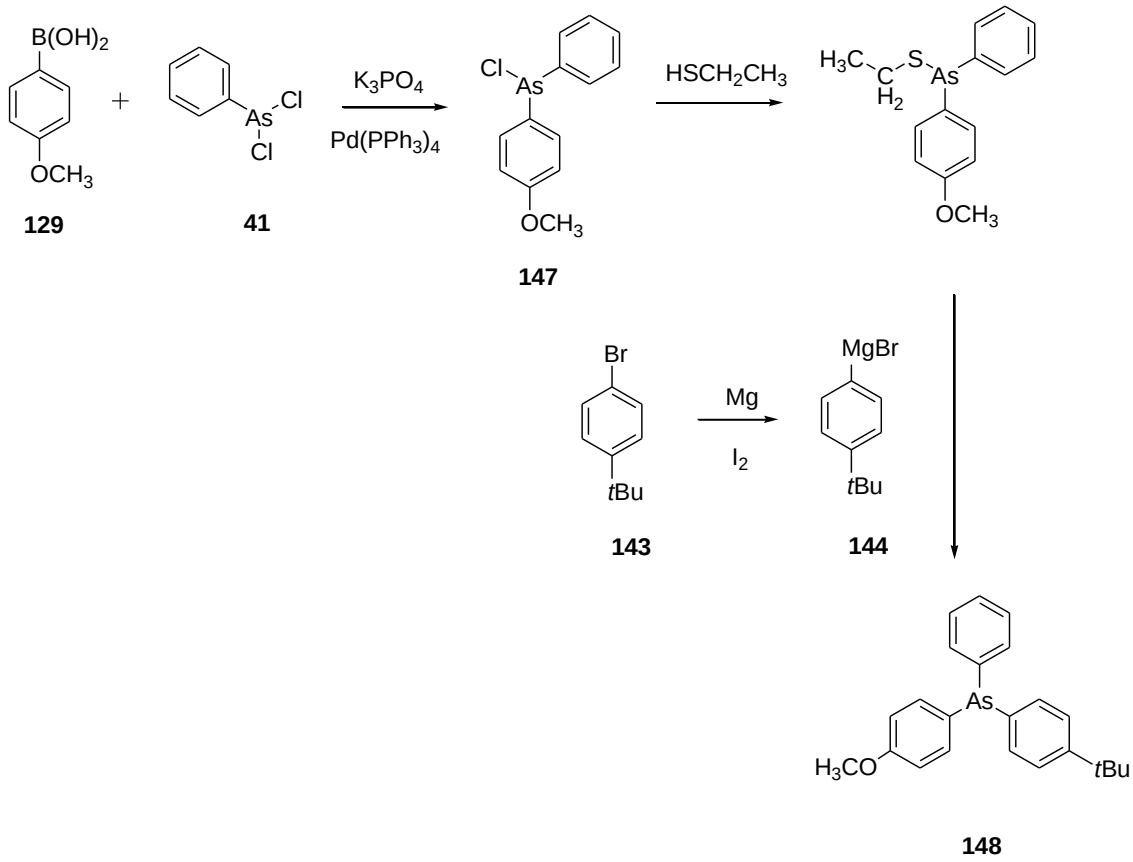

Scheme 35. The synthetic approach to the three aromatic groups substituted arsenic center

4 Third generation probe design using HostDesigner

Based on the coupling reaction of boronic acids and arsenic compounds, the phenolic OH was no longer needed to facilitate the introduction of arsenic group (via mercury). The two thiols from i, i+7 cysteines of the alpha helical peptides was connected with two arsenic atoms, which was bindeded with methyl and phenyl groups separately (Scheme 36).

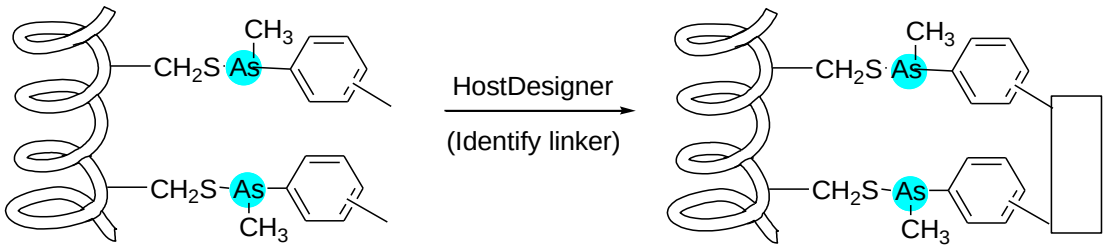

Scheme 36. The process of probe design using HostDesigner

4.1.1 HostDesigner software used for molecular design.

HostDesigner[50] is a molecular design program, which was created for the discovery of metal ion receptors. It is similar to an older program CAVEAT, used in previous work in Drueckhammer group. In both programs, the functional groups and the relative positions of a scaffold structure are defined in one molecule to bind to another guest molecule. A library of potential linker structures are searched to identify a suitable molecular structure for connecting the receptor functionality in the desired orientation. There are millions of candidate structures in HostDesigner, but the identification of three dimensional architectures that position binding sites to provide an optimal interaction with the metal ion just requires several minutes. First the molecular structure is set up as the guest, next the complement binding site structure is searched as the host. The library is developed through the optimization of the 3-D structures by molecular mechanics calculations. The potential energy surfaces for bond rotations are also calculated for each linker structure, and the candidate host structures will be evaluated by HostDesigner. HostDesigner deals with the following problems, first the presence of multiple binding sites, second the host exists as the conformation in which all binding sites are positioned to complement the metal ion structurally, and finally, the conformational freedom of the host can be limited. The potential binding sites can be calculated through the complementary connection with the three dimensional arrays (Figure 27).

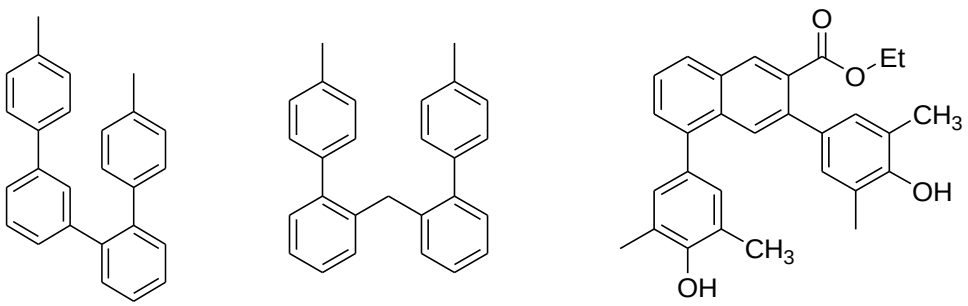

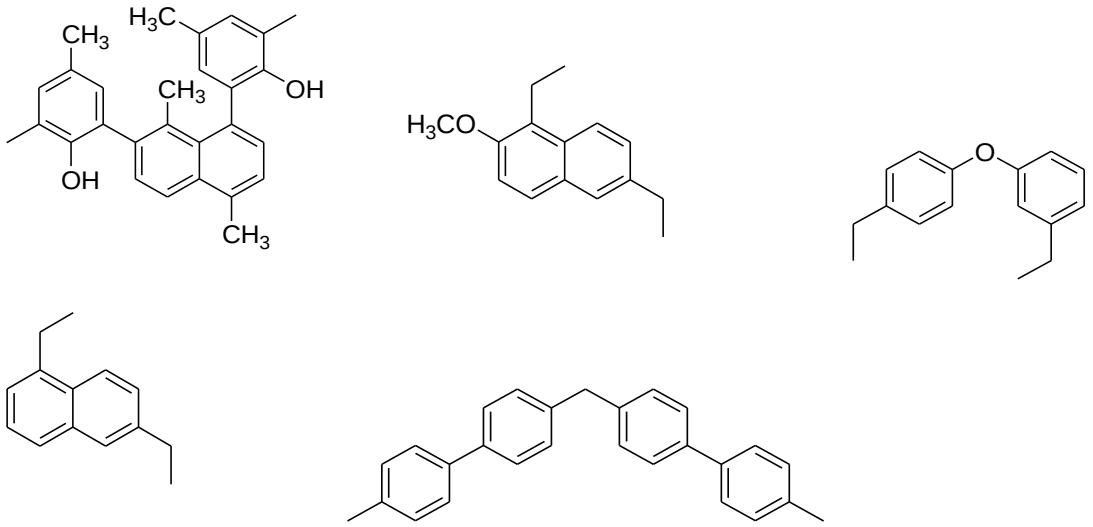

Figure 27. The linking fragment library.

HostDesigner requires efficient computational methods for ranking proposed host structures in terms of their complementarity for specific metal ion guests on a case-by-case basis. New host candidates are generated on the basis of the nature of metal ion and binding site interactions, and the screening of candidate structures. The linkage structures are calculated to connect the binding sites to obtain a host cavity that complements a targeted metal ion guest. The guest molecule structures are calculated to physically interact with an assigned protein structure from pieces that are either atoms, or larger, chemically reasonable fragments. The binding free energy is estimated by summing free energy increments for hydrogen bond interactions, ionic interactions, lipophilic interactions, and the number of rotatable bonds in the guest molecules. Through the computationally demanding evaluations of the host guest complex, the best candidates would be calculated after an initial prioritization.

Some computer programs just address protein organic interactions with a protein binding site, which would not address metal ligand interactions. Based on the field of coordination chemistry, HostDesigner came up as the computer algorithms for building structures from host components and rapid methods for scoring the resulting structures with respect to their complementarity for the targeted guest.

4.1.2 Geometry of complex fragments input structure in HostDesigner and its linker

(a)

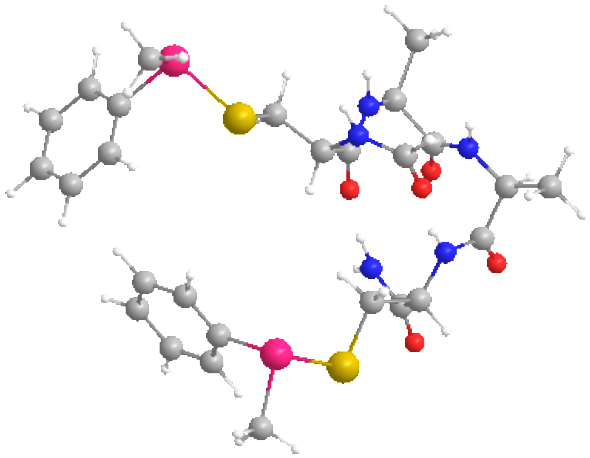

CAACAsPhMe

(b)

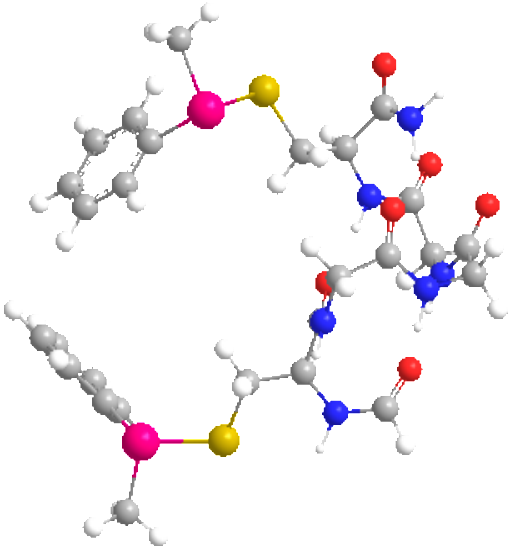

CG3CAsPhMe3a

(c)

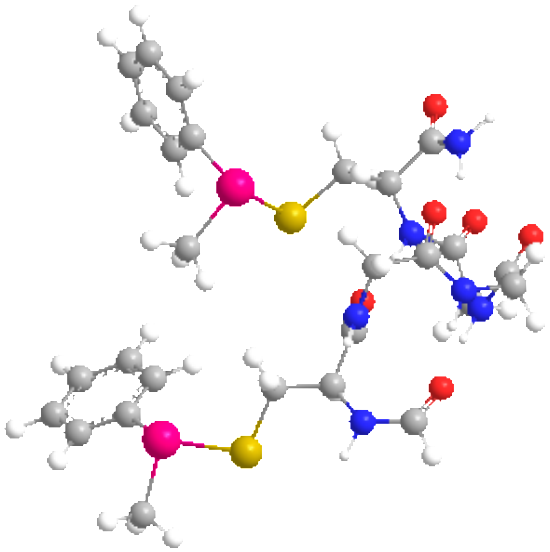

CG3CAsPhMe4a

(d)

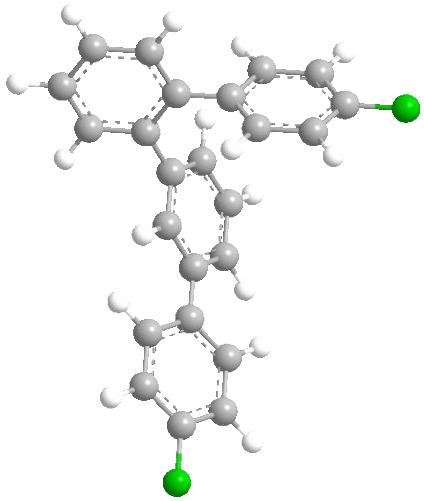

(e)

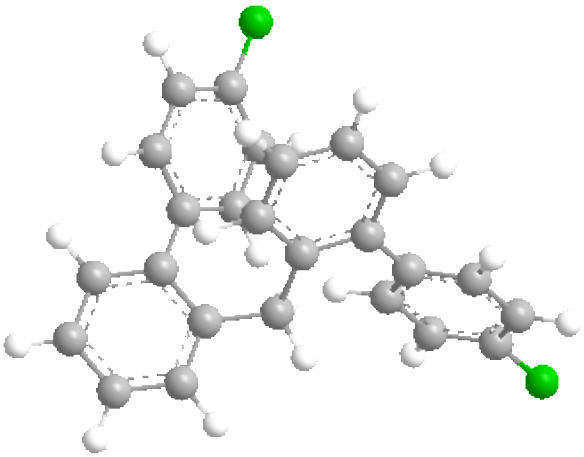

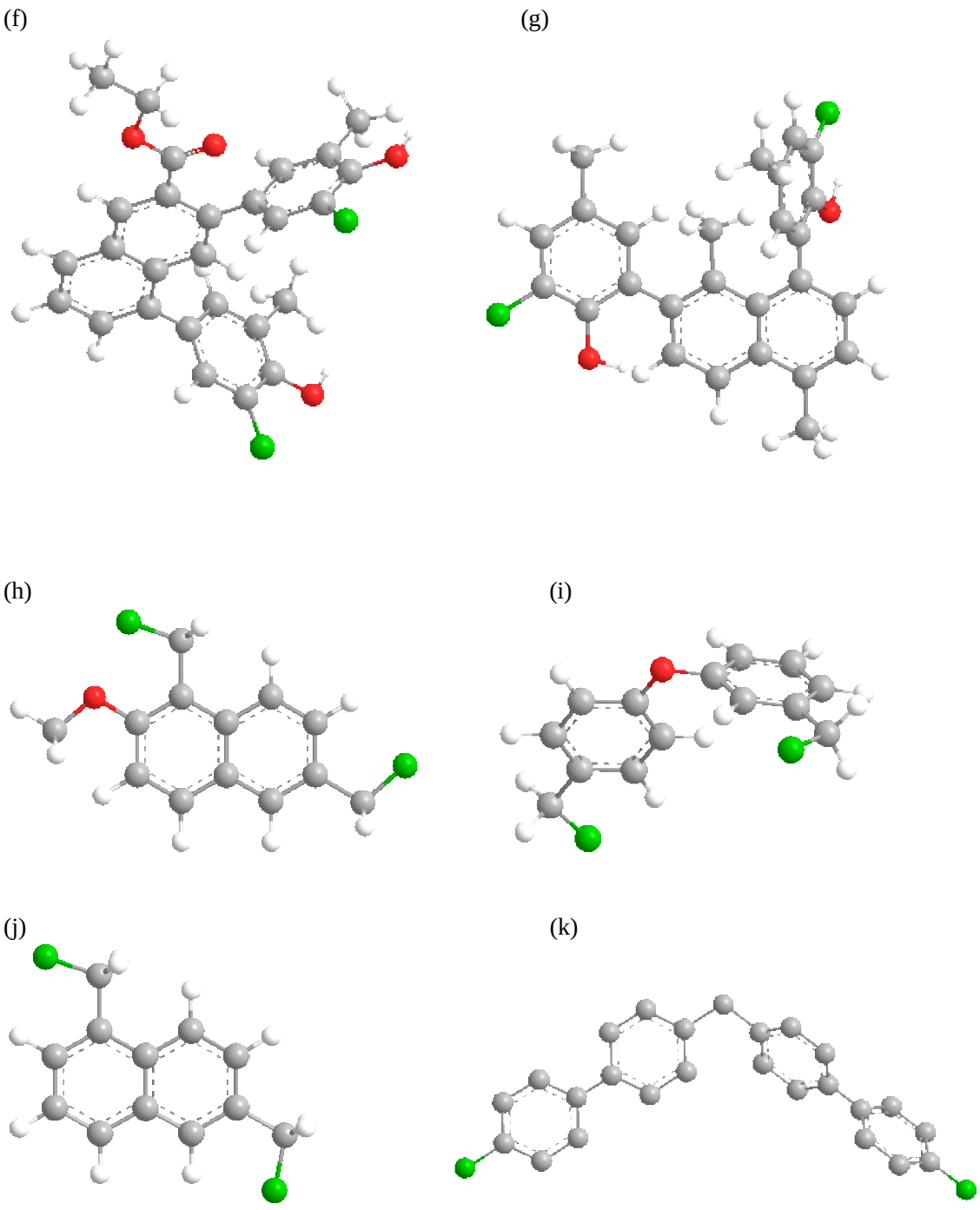

Figure 28. The input structure of complex fragments in HostDesigner were shown as (a) to (c), the linker structures were shown as (d) to (k), the green spheres represent the metal ion guests, the red spheres represent oxygen atom, the blue spheres represent nitrogen atom, the yellow spheres represent sulfur atom, the pink spheres represent the arsenic atom, and the methyl represents the guest structure

4.1.3 The structure based design of molecular receptors

The complex fragment is defined by combining a host component with a guest metal atom, which would be positioned relative to the host component to define a complementary geometry with the strongest interaction between the binding sites of the host component and the metal ion in an actual complex (Figure 29).

(a)

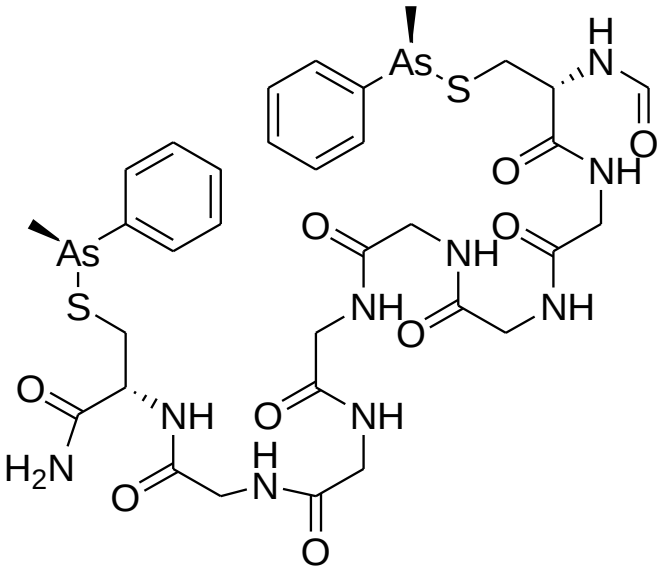

(b)

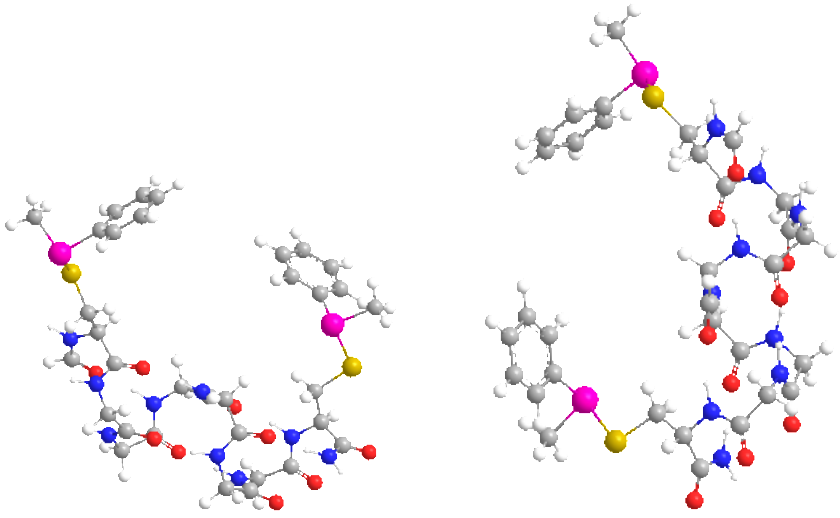

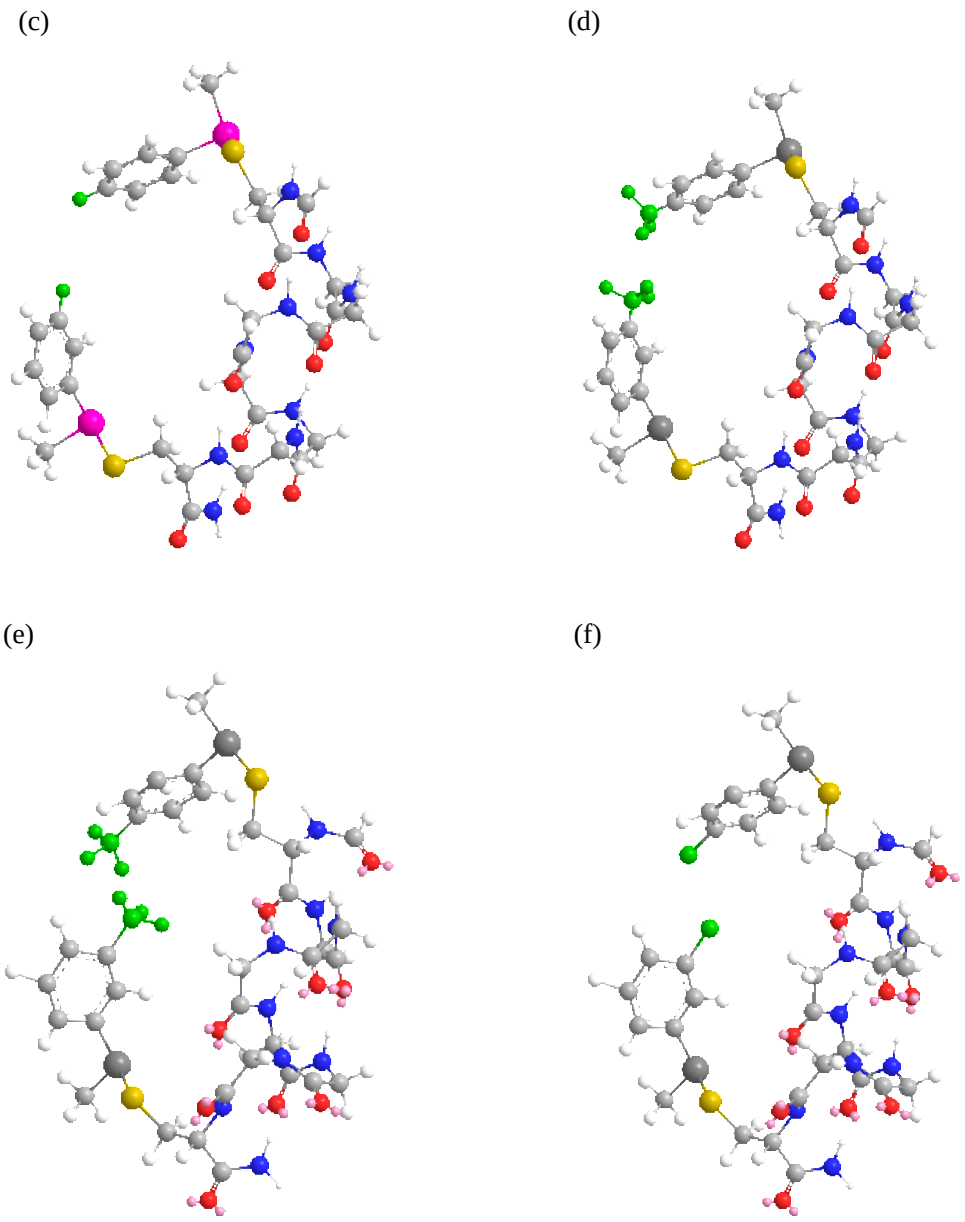

Figure 29. The process of construction of a linking fragment. (a) to (f) show the structure of the calculation process. The steps are as follows: (a) select a connective structure, (b) search to locate stable conformers using the MM2 program, (c) choose one conformer and remove a pair of hydrogen atoms to generate a bonding vector pair, (d) place methyl groups at the ends of the bonding vectors, (e) optimize the structure with the MM2 program, and (f) remove the methyl groups to obtain the final linking fragment with two bonding vectors

The potential probe bonded to biarsenic based receptor was calculated by HostDesigner. The complex

fragment is selected in the first step. Second a bonding vector is left by removing the hydrogens. Third a linking fragment containing two bonding vectors is selected from the library. Fourth based on the hybridization of the carbon atoms a bond between the first complex fragment and the linking fragment is formed by aligning the bonding vectors and the C-C distance is set to an appropriate value. Fifth based on the hybridization and degree of substitution of the carbon atom the dihedral angle is adjusted around the new bond. Sixth a second fragment is selected. Seventh another bonding vector is left by removing the hydrogens. Eighth based on the hybridization of the carbon atoms a bond is formed between the second complex fragment and the remaining bonding vector on the linking fragment by aligning the bonding vectors and the C-C distance is set to an appropriate value. Finally based on the hybridization and degree of substitution of the carbon atoms the dihedral angle is adjust around the new bond to a specific value.

4.1.4 LINKER used in HostDesigner

LINKER (a program within HostDesigner) is used to test the connectivity between the two complex fragments with the given linking fragment, and on the other hand, LINKER is used to examine the conformation of the rotation of the linking fragments and the complex fragments. This example shows that the structure and the distance of the linker fragment clearly. (a) represents the structure with metal distance 0.05 Å, (b) represents dimetal distance 3.42 Å, (c) represents the structure of dimetal distance 4.5 Å, (d) represents the structure of metal distance 6.35 Å (Figure 30).

(a) (b)

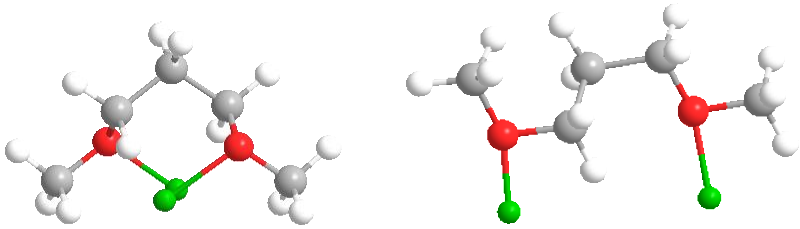

0.05Å 3.42 Å

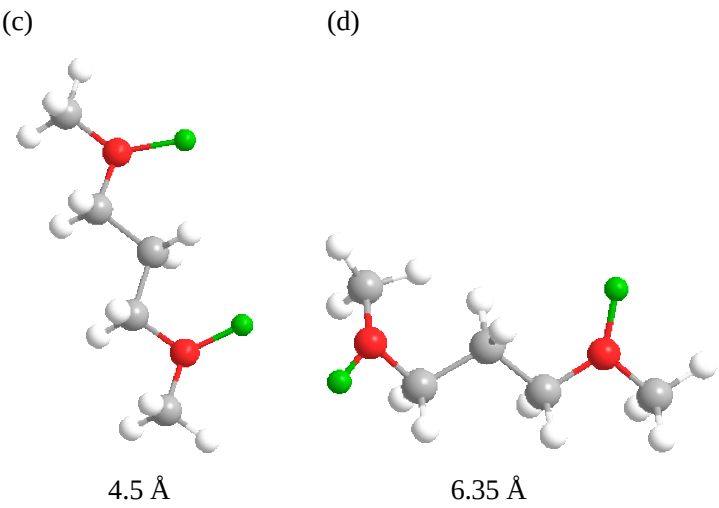

Figure 30. Four unique structures that are generated by combination of two lithium-dimethyl ether complex fragments with the methylene linking fragment. The metal-metal distance is given for each structure. [51]

4.2 The input structure of the software HostDesigner

4.2.1 HostDesigner input structure of peptide CAAC sequence

An alpha-helical peptide (defined by PDB) containing two cysteines was utilized in the calculation. The methyl phenyl arsenic functionality were then grafted onto the sulfur atoms of the cysteine peptides. Bond lengths, angles, and dihedrals were set to match a calculated structure (phenyl methyl arsenic bonded to ethanethiol). Figure 31 shows the input structure for HostDesigner in our project. The yellow atoms represented the sulfur atoms bonded with one carbon group and one arsenic atom on each side, and the two arsenic groups showed the specific scaffold structure of the peptide structure of CAAC sequence (CA2CAsPhMe2b). The arsenic group was connected with one sulfur group and two carbon groups, one was methyl, and the other was phenyl with the para position being substituted. The vector pair was defined by the para substituted benzene ring. Based on the scaffold structure of the vector pair, the desired structure of the potential receptor was searched in the virtual library.

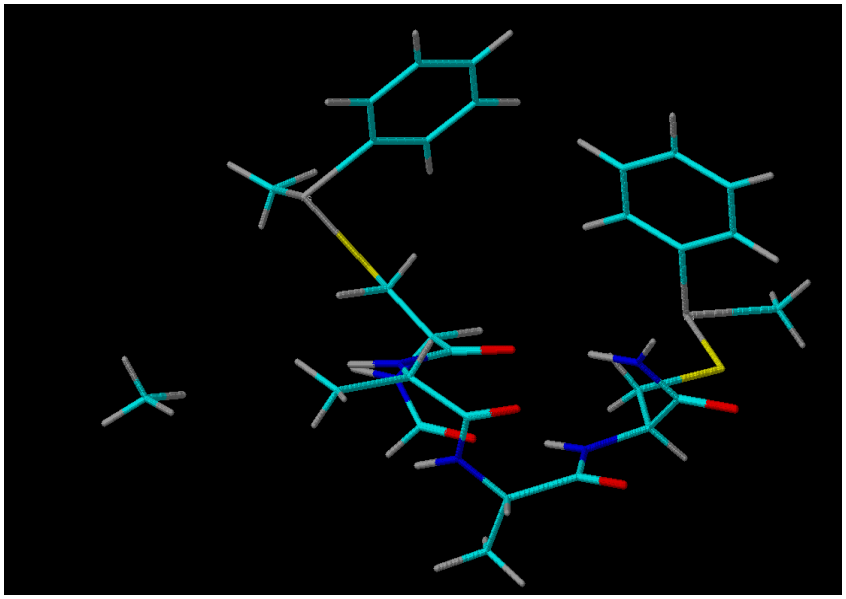

Figure 31. The input structure of the HostDesigner for target peptide structure of CAAC sequence

4.2.2 HostDesigner input structure of peptide CGGGC sequence

Figure 32 shows the input structure of the peptides CGGGC (given the file name CG3CAsPhMe3a) in HostDesigner, which is similar to the structure of Figure 31 shown in Section 4.2.1, except for different distances between the two cysteines in the peptide.

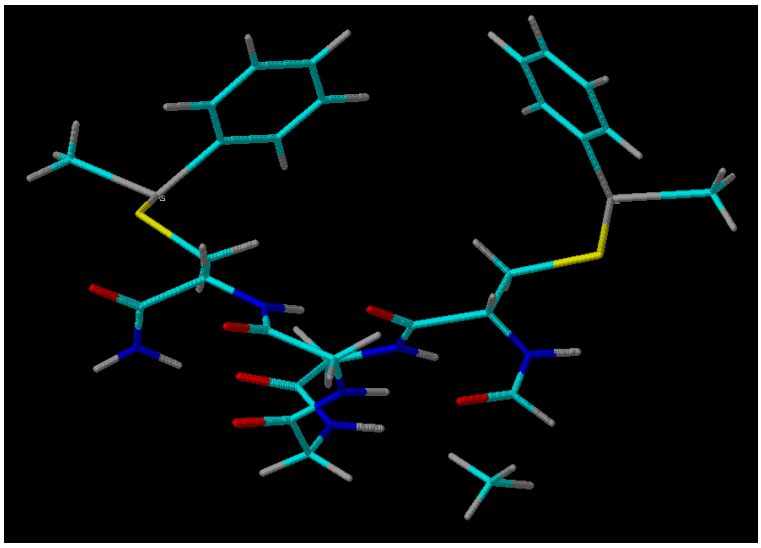

Figure 32. The input structure of HostDesigner for target peptide sequence CGGGC

4.3 The output structure of the software HostDesigner

4.3.1 Output structure of peptides CAAC

The output structure of peptides CAAC by HostDesigner is shown in Figure 33 and 34. Figure 34 is the structure of peptide complex searched in HostDesigner, and Figure 33 shows the chemical structure of the corresponding receptor. The arsenic atom is connected with one sulfur atom (in yellow) and two carbon groups, one is a methyl group, and the other is a phenyl group with the para position being substituted. The desired scaffold structure is the 2-3'-diphenyl biphenyl system, which fits the distance, bond angles, and dihedral angle of the input structure.

CA2C2o1-96

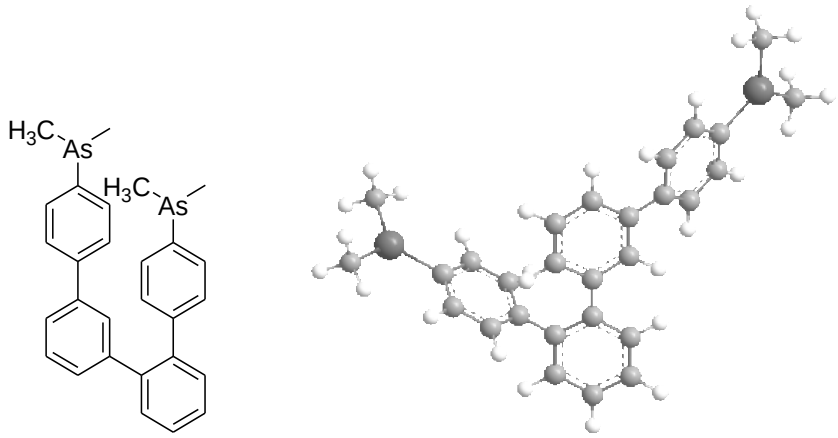

Figure 33. The molecular structure of the output structure for target peptide CA2C2o1-96 in HostDesigner

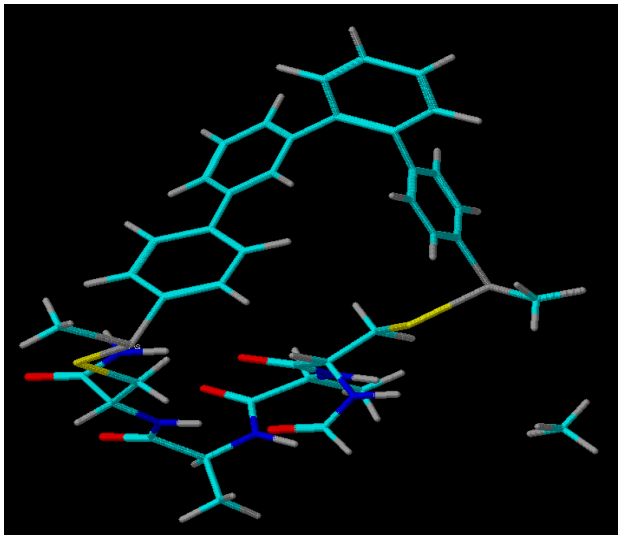

Figure 34. The output structure of HostDesigner for target peptide CA2C2o1-96

5. Energy calculations using Gaussian Software

Gaussian software is based on the fundamental laws of quantum mechanics, it predicts the energies, molecular structures, vibrational frequencies and molecular properties, and the reaction progress in a wide variety of chemical conditions. Gaussian 03 software is used for the energy calculation of different electronic structures. The potential probes with possible energy difference are calculated by Gaussian software using method B3LYP/6-31G(d). The method B3LYP/6-31G(d) is used for the calculation of the ground state geometry optimization. It is the basis set, and adequate for the elements from the first and second row.

5.1 Energy calculation of CAAC2o1-96 by Gaussian Software

The input file of CAAC2o1-96 searched by HostDesigner was from section 4.3.1 (Figure 36a) with the CAAC peptides structure deleted, and two carbon atoms (represented by green sphere) left on two end sides. The next step was to freeze the peptide structure with the two bonds on both sides of the peptides CAAC sequence frozen, the dihedral angle of the left four carbon atoms (represented by green spheres) frozen, and the two angles of the left two carbon atoms frozen, which contributed to the maintenance of the dihedral angle and distance of the left two carbons (Figure 36b). The chemical structure of peptides CA2C2o1-96 is shown in Figure 36c. The energy difference was between the constrained structure that represents the structure of the peptides complex vs. the energy minimized unconstrained structure (table

3). A small energy difference (perhaps ≤ 10 kJ/mol) would indicate that the potential probe could form stable bonds with the peptides structure. Figures 37 and 39 show the calculation results of CA2C2o1-96 and CA2C1o1-62 by the method B3LYP/6-31G(d). Based on the calculated energy differences within 10 kJ/mol, the two potential probes are predicted to form stable covalent bonds with the two assigned peptides sequences (Figure 37, 38, 39, 40).

(a)

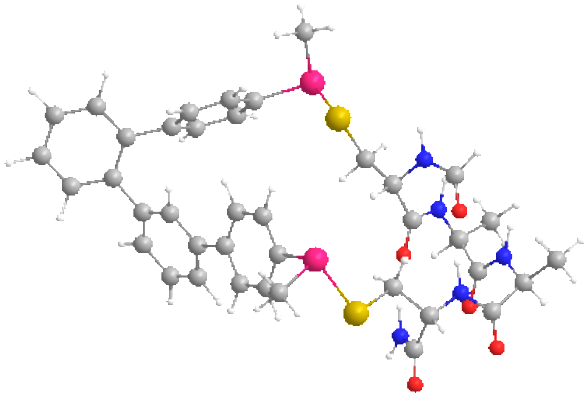

(b)

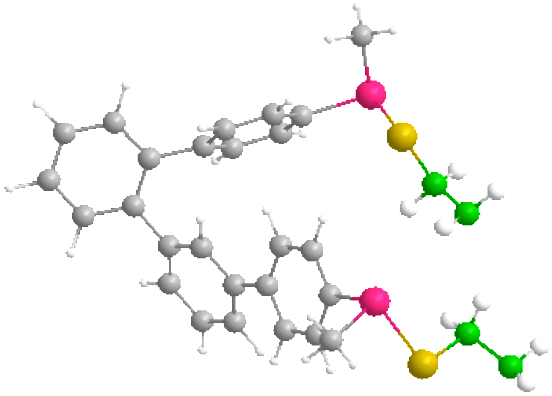

(c)

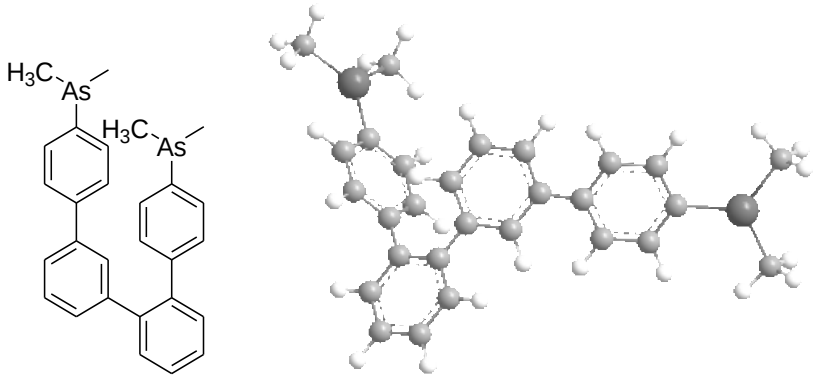

Figure 36. The input structure of Gaussian for target peptides CA2C2o1-96

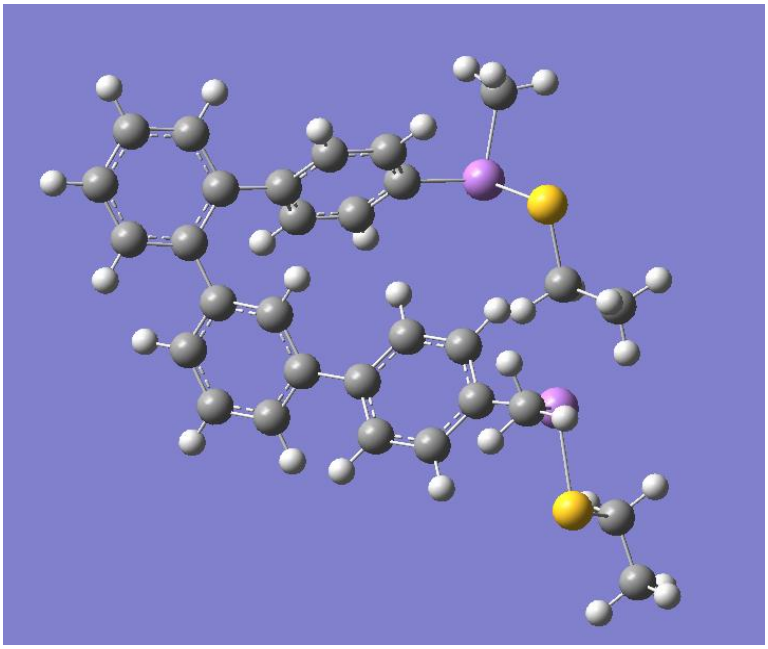

Figure 37. The output structure of Gaussian for target peptide CA2C2o1-96

Constrained Energy	-1971.10230191 au
Unconstrained Energy	-1971.10349936 au
Energy Difference	3.1 kJ/mol

Table 3. Energy calculation of CA2C2o1-96

CA2C1o1-62

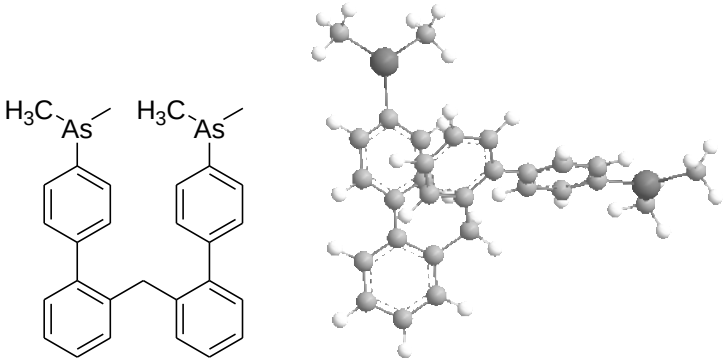

Figure 38. The output structure of HostDesigner for target peptide CA2C1o1-62

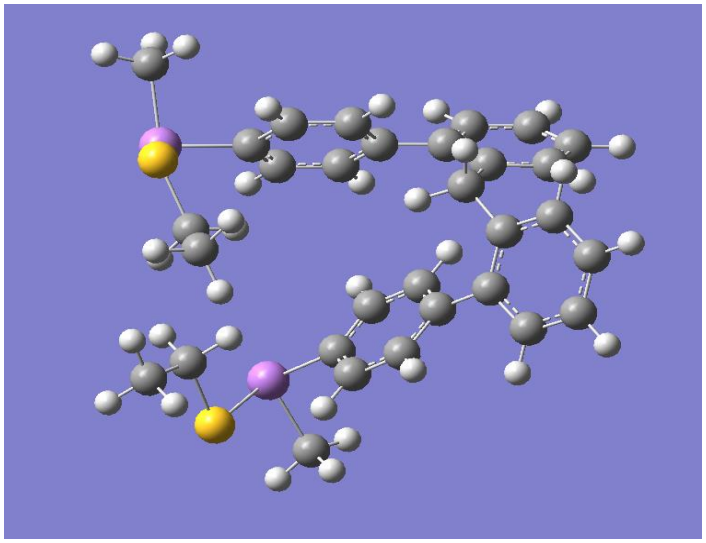

Figure 39. The output structure of Gaussian for target peptide CA2C1o1-62

Constrained Energy	-2010.40664514 au
Unconstrained Energy	-2010.40777187 au
Energy Difference	3.0 kJ/mol

Table 4. Energy calculation of target peptide CA2C1o1-62

5.2 Design of a potential i, i+3 probe.

Figure 40 shows the potential probe in the virtual library search of HostDesigner for the target peptide CGGGC sequence. The chemical structure of the output probe is a 2,3'-diphenyl biphenyl structure with two benzene rings connected at ortho positions and the other two benzene rings connected at para positions. Table 5 shows the results of the calculation by the Gaussian Software, and the energy difference between the constrained structure that represents the structure of the peptides complex vs. the energy minimized unconstrained structure. The strain energy was much larger than 10 kJ/mol, which indicates that the complex of the probe and the target peptide CGGGC would not be stable.

CG3C1o1-63

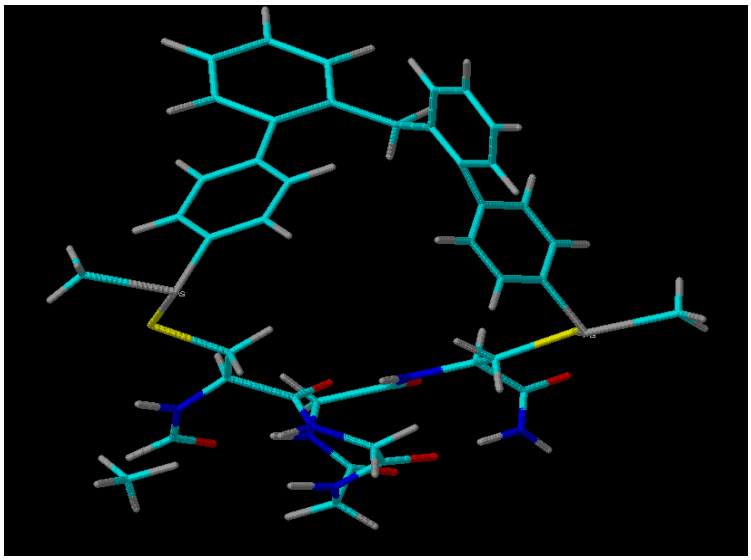

Figure 40a. Output structure of HostDesigner for target peptide CG3C1o1-63=

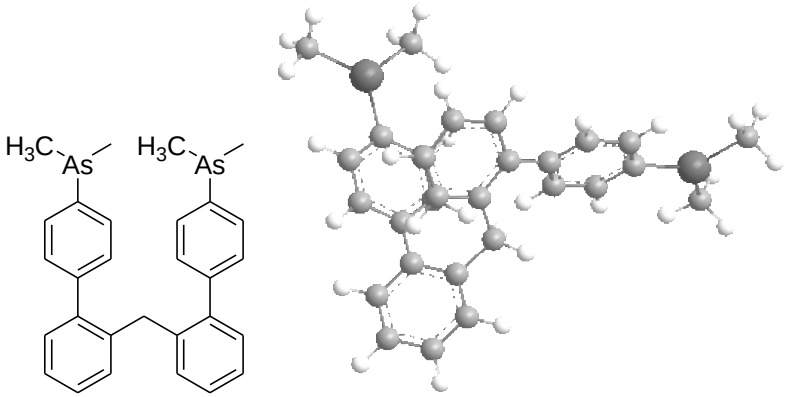

Figure 40b. Chemical structure of target peptide CG3C1o1-63

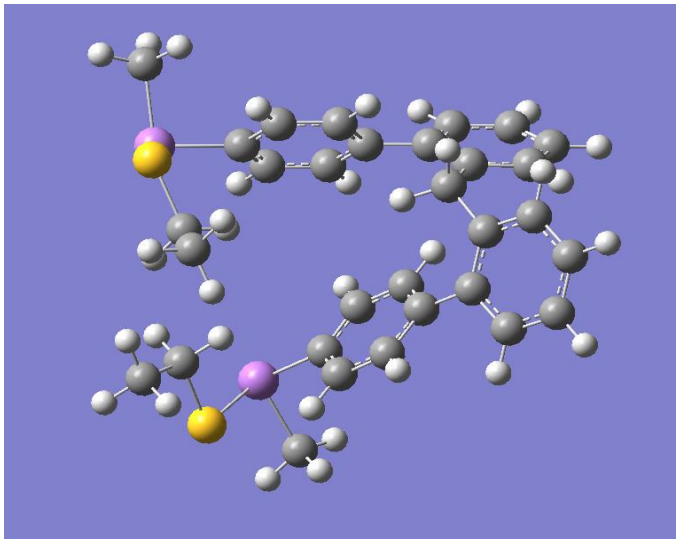

Figure 40c. The output structure of target peptide CG3C1o1-63

Constrained Energy	-2001.56492301 au
Unconstrained Energy	-2001.57340083 au
Energy Difference	22.2542775 kJ/mol

Table 5. Gaussian calculation of target peptide CG3C1o1-63

Based on the structure obtained from HostDesigner and energy calculations by Gaussian, receptor CA2C1o1-62 was chosen as a good target for synthesis. The synthesis of probe CAAC1o1-62 is shown in the following section.

6.1 Synthetic approach to probe CAAC1o1-62

The initial synthetic approach to the designed i, i+3 receptor is shown in Scheme 37. First the ketone group of benzophenone was reduced by Wolff-Kishner reduction to form **148**. Second the para positions of both benzene rings were nitrated to form **149**, followed by halogenation at the ortho positions to form **150**. If the halogenation were successful, Suzuki coupling with p-bromophenyl boronic acid would have been performed to form **151**, followed by conversion of the bromine substituents to arsenic groups in the final step to form **152** (Scheme 37).

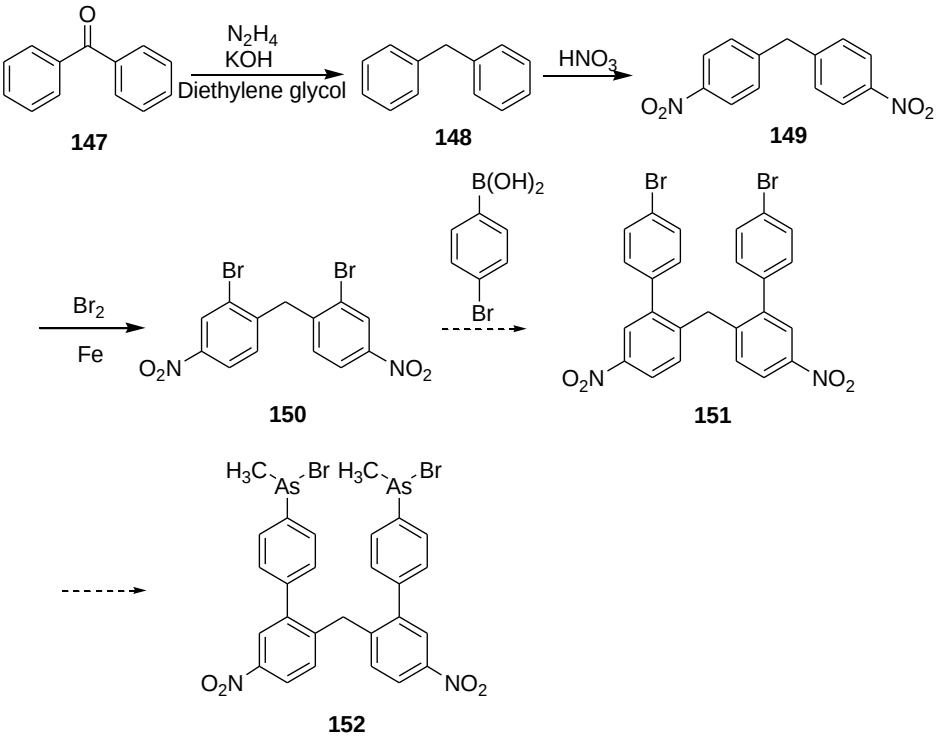

Scheme 37. The synthetic approach to **152**

6.1.1 Three reduction conditions of benzophenone.

The zinc mercury reduction[52] was performed as shown in Scheme 38 starting from the commercially available benzophenone to form **148**, but no desired product was identified in the ^{1}H-NMR spectrum of the reaction crude. Another reduction condition with hypophosphorous acid as the reductant and acetic acid as the catalyst[53] was used to reduce the benzophenone **147** to form **148**, but no desired product was identified in the ^{1}H-NMR spectrum of the reaction crude. Of all three reduction conditions, the Wolff-Kisher reduction[54] showed the highest yield under the mildest reduction conditions (Scheme 38).

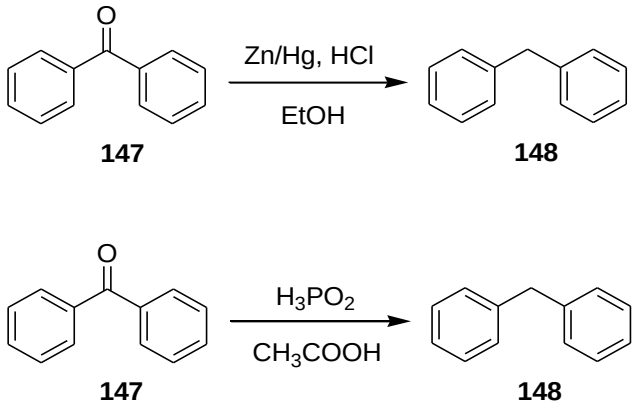

Scheme 38. Two reduction conditions of benzophenone **147**

6.1.2 Nitro group introduction on the two benzene rings

The introduction of nitro groups at the para positions of **148** to form **149** was performed with nitric acid as both the reagent and the catalyst. The purification of the desired product from the starting material was quite straightforward, as a big difference existed in their polarities (Scheme 39).

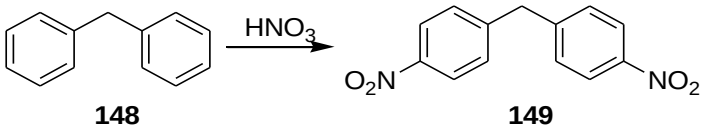

Scheme 39. The introduction of the nitro groups

The side reaction of the introduction of the nitro groups is shown in Scheme 40. The mononitro, trinitro, and tetranitro byproducts **153**, **154,** and **155** can be separated from the crude product easily.

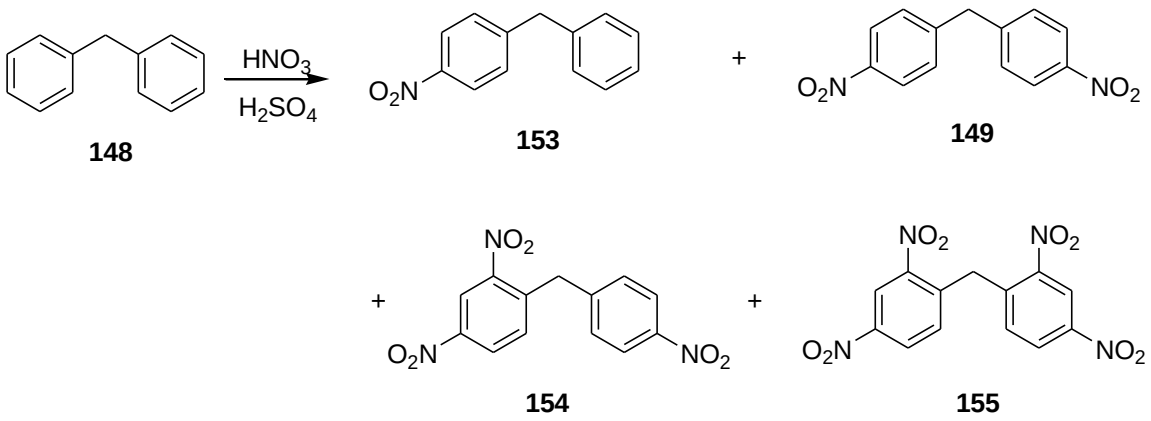

Scheme 40. The side reaction with the nitric acid

6.1.3 Bromination on the two benzene rings

The substitution of hydrogen on the two benzene ring structure **149** was performed with iodine or iron as the catalyst, and bromine as the reagent. Monobromine substituted product **157** has been separated from the reaction crude, further bromination was required to form **156** under similar reaction conditions as in section 6.1.2 (Scheme 41). Based on the results of the bromination, iron used as the catalyst gave the higher yield. However, the monohalide was the primary product as determined by ^{1}H-NMR of the crude product. The difficulty in the double halogenation may be due to the deactivating effects of the two nitro groups.

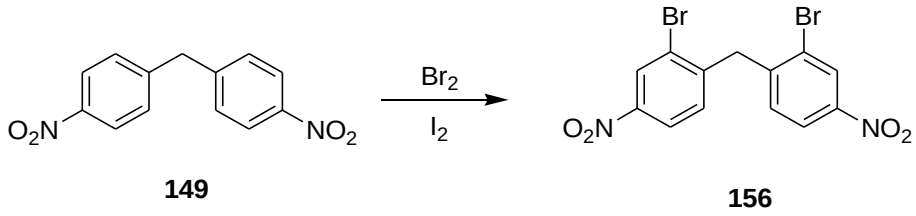

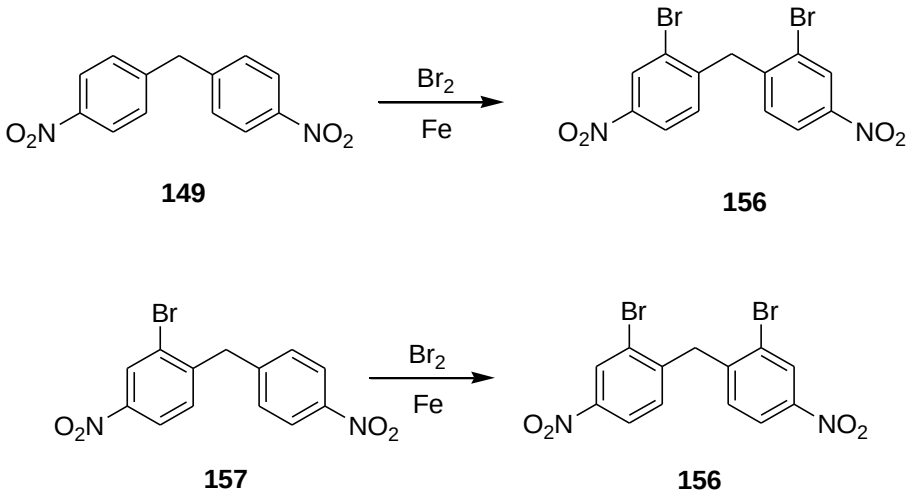

Scheme 41. The introduction of bromine at the ortho positions of the benzene ring

6.1.4 Suzuki coupling

The Suzuki coupling reaction was performed starting from **155** and p-bromophenylboronic acid to form **151**. Boronic acids always exist in equilibrium with their trimer structures. However, only starting material was identified in the ^{1}H-NMR spectrum of the reaction crude. A potential problem is Suzuki coupling of the p-bromophenylboronic acid with itself, which interfered the Suzuki coupling reaction with the bromine intermediate **155**. (Scheme 42).

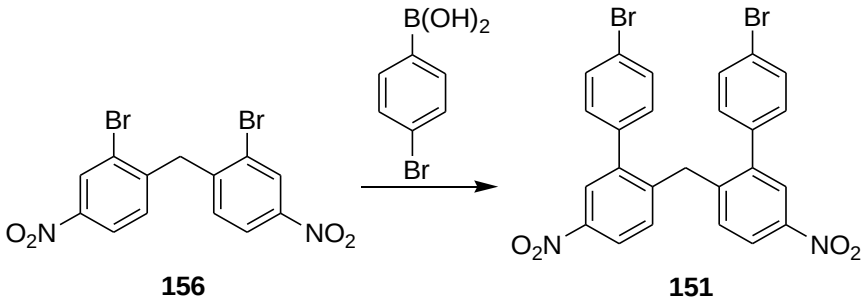

Scheme 42. The Suzuki coupling of the dibromine substituted benzene

6.1.5 Iodination on the two benzene rings

In order to improve the Suzuki coupling step, iodine instead of bromine was introduced in the second step, as aryl iodides are known to be more reactive than bromides in Suzuki coupling reactions. The iodination of **149** was performed with KIO_3 or KIO_4 as the oxidant, sulfuric acid as the catalyst, and I_2 or KI as the source of iodine. The desired product **150** was identified in the ^{1}H-NMR spectrum of the reaction crude. The highest yield was associated with the reaction with KI as the reagent, KIO_3 as the oxidant, and H_2SO_4 as the catalyst (Scheme 43).

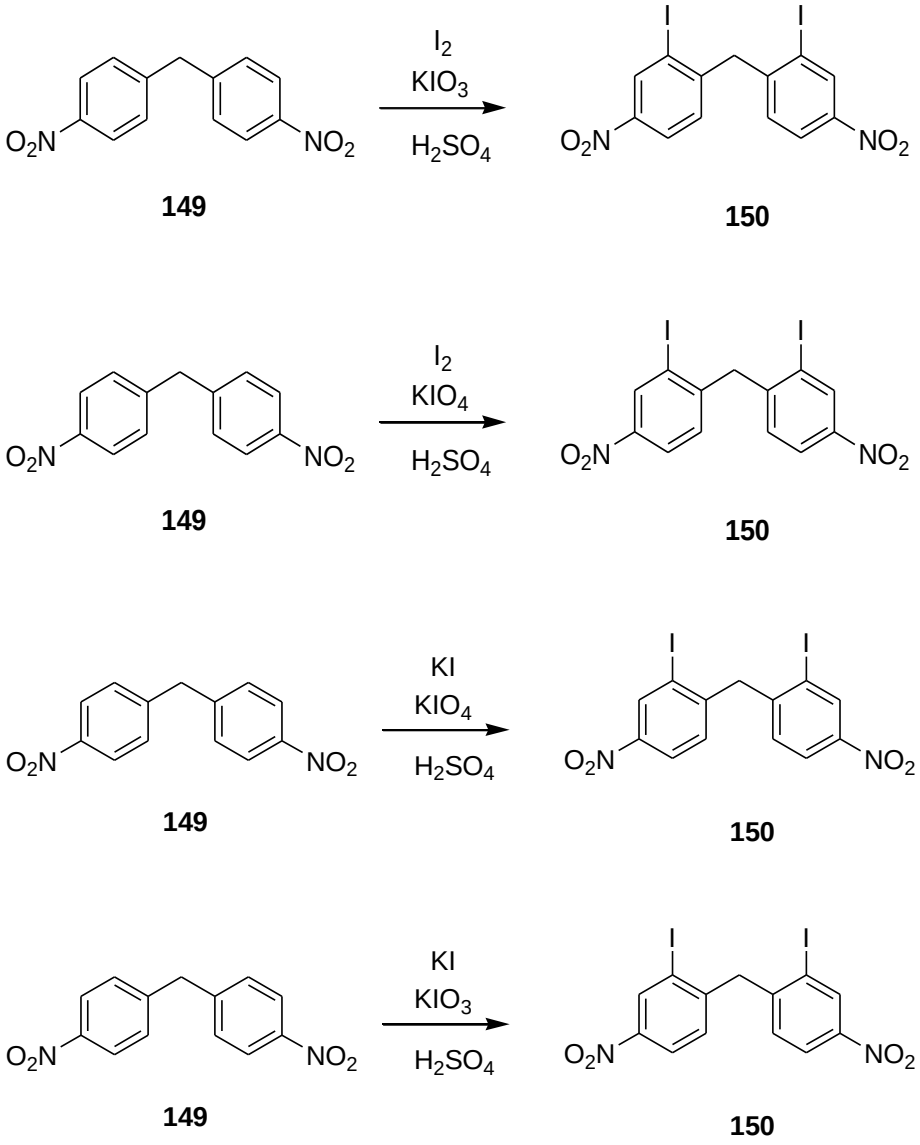

Scheme 43. The introduction of iodine at the ortho positions of the benzene rings

6.1.6 Alternative Suzuki coupling of boronic acid

An alternative Suzuki coupling of boronic acid and the iodine substituted intermediate **150** recovered only the starting materials. Due to the low yield of the introduction of iodine at the ortho positions of the benzene rings with the high electron withdrawing effects of the nitro substituents at the para positions, an alternative synthetic approach through an acyl substituted intermediate was pursued as shown in section 6.2 (Scheme 44).

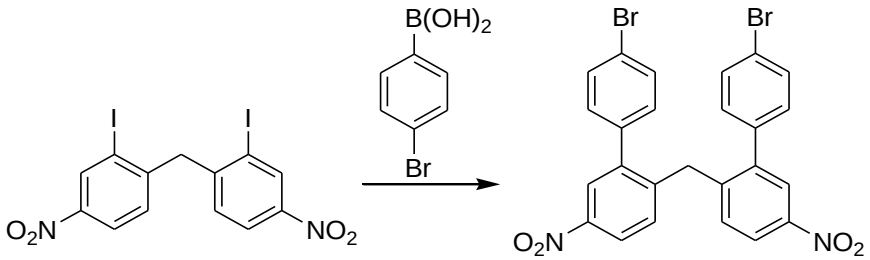

150 **151**

Scheme 44. The Suzuki coupling reaction starting from the dinitro substituted intermediate **150**

6.2 An alternative synthetic approach towards 172

The synthetic approach to **172** was undertaken as shown in Scheme 45. First the acylation at the para position of **148** was performed with aluminum chloride as the catalyst, and acetyl chloride as the source of the acetyl group to form **158**. Iodization with sulfuric acid as the catalyst and KI and KIO_3 as the source of iodine formed **159**. Next the Suzuki coupling was undertaken starting from the two iodine substituted intermediate **159** to form **160** (Scheme 45).

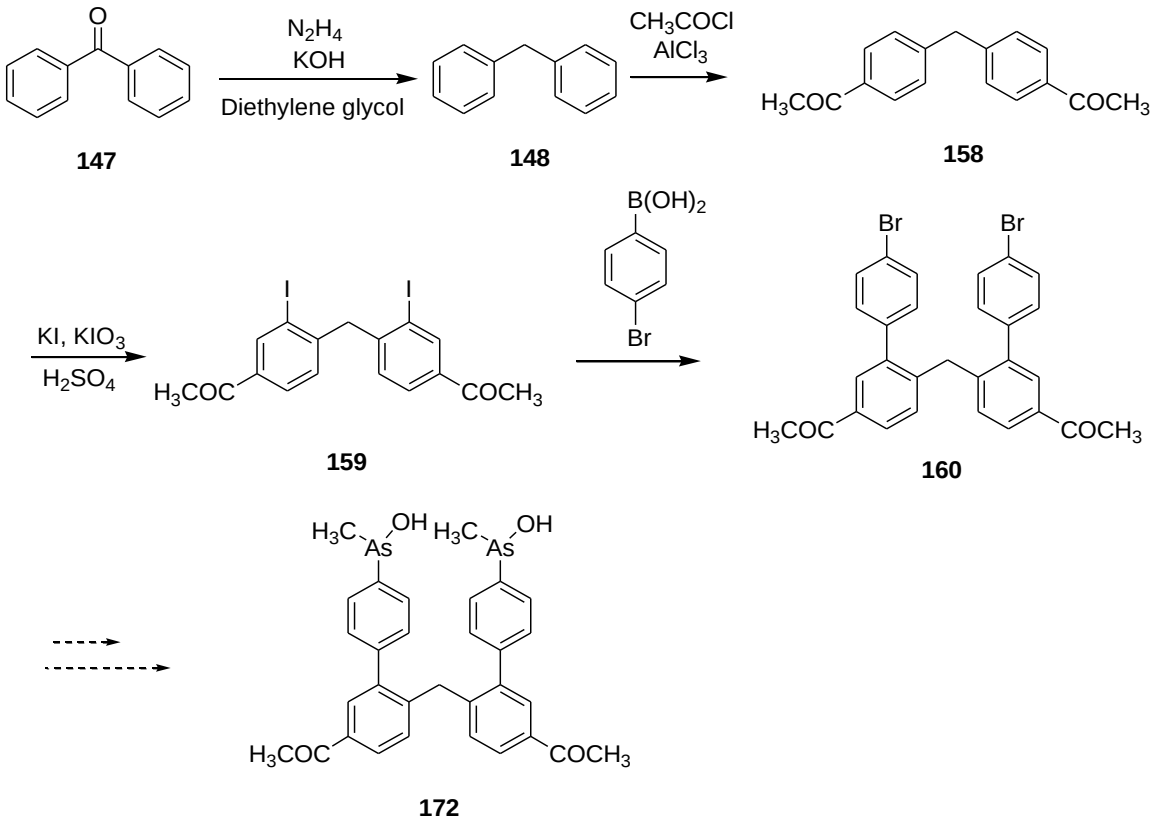

Scheme 45. The synthetic approach to probe **CAAC1o1-62**

6.2.1 Introduction of acetyl substituents at the para positions of the two benzene rings

As the nitro substituted intermediate gave low yield with the iodination, acetyl substituents were introduced at the para positions of the two benzene rings as shown in Scheme 45. The synthetic approach of **148** was performed by Friedel-Crafts alkylation, with the expectation to lower the electron withdrawing effects of the substituents. Next further acylation of the purified mono ketone intermediate **161** was undertaken as shown in Scheme 48 under similar conditions as in section 6.2. The purification of the desired product with two ketone substitutes was quite straightforward. Peaks were identified in the ^{1}H-NMR and TLC results (R_f = 0.3 in ethyl acetate:hexane=1:4) of the reaction crude (Scheme 46).

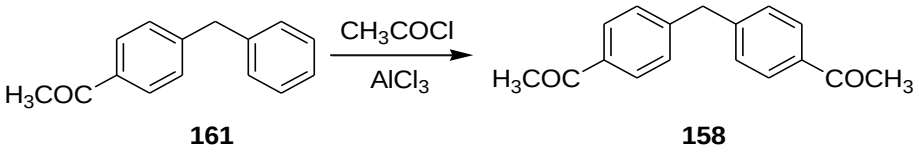

161 **158**

Scheme 46. The further alkylation at the para positions of the benzene ring

6.2.2 Iodination at the ortho positions of the two benzene rings

Iodination at the ortho positon was performed with aluminum trichloride as the catalyst, and iodine chloride as the source of iodine to form **159**. However, peaks were corresponding to the starting material **158** in the ^{1}H-NMR spectrum of the reaction crude (Scheme 47). Due to the failure of this reaction, an alternate iodination approach was developed as described in the earlier section 6.1.5.

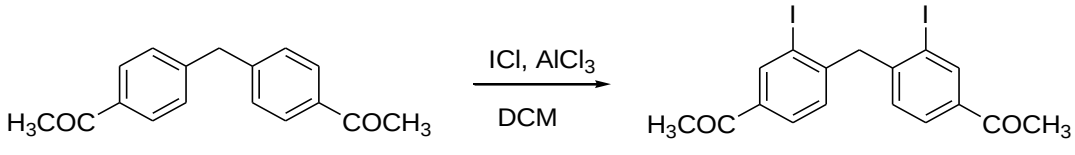

158 **159**

Scheme 47. Iodination at the ortho positions of **158**

6.2.3 Suzuki coupling reaction starting from iodine substituted intermediate

The Suzuki coupling reaction was performed starting from iodine substituted intermediate **159** and p-bromophenyl boronic acid with tetrakis(triphenylphosphine)palladium(0) or (1,1'Bis(diphenylphosphino)ferrocene)palladium(II) dichloride as the catalyst, and potassium phosphate as the base to form **160.** The desired product **160** was identified in the TLC and NMR results with relatively low yield (less than 10%), which might due to coupling of boronic acid with itself (Scheme 48).

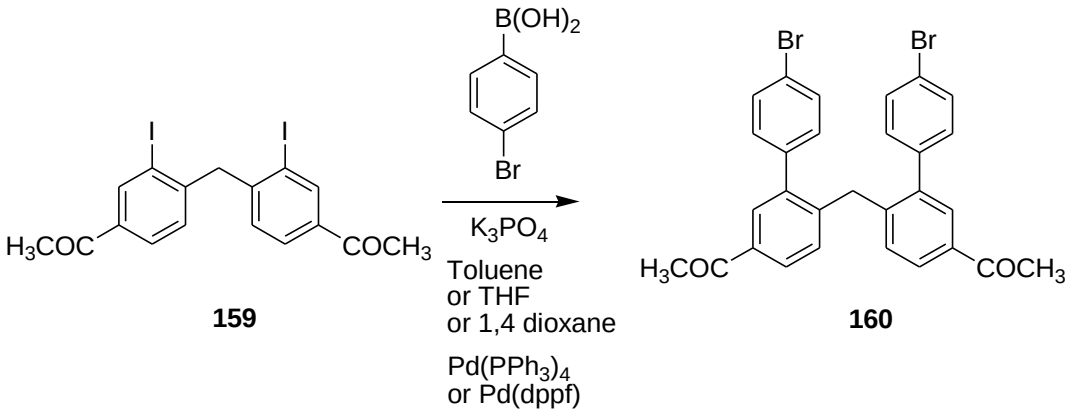

Scheme 48. The Suzuki coupling reaction of the iodine intermediate

6.2.4 Conversion of bromine atoms to boronic acid substituents

The synthetic approach to boronic acid was performed starting from dibromine intermediate **160** with 2 eq of *n*BuLi as the base followed by conversion to boronic acid **162** with trimethoxylborane **163** as the source of boron. However, no desired product **162** was identified in the NMR and TLC results of the reaction crude. Efforts to solve this problem were further pursued by the coupling reaction with 4,4,5,5-tetramethyl-1,3,2-dioxaborolane **164** or bis(pinacolato)diboron **166** as the source of boron, (1,1'Bis(diphenylphosphino)ferrocene)palladium(II) dichloride as the catalyst, and TEA or potassium acetate as the base (Scheme 49) to form **165**. However, no desired product has been recovered from the product crude.

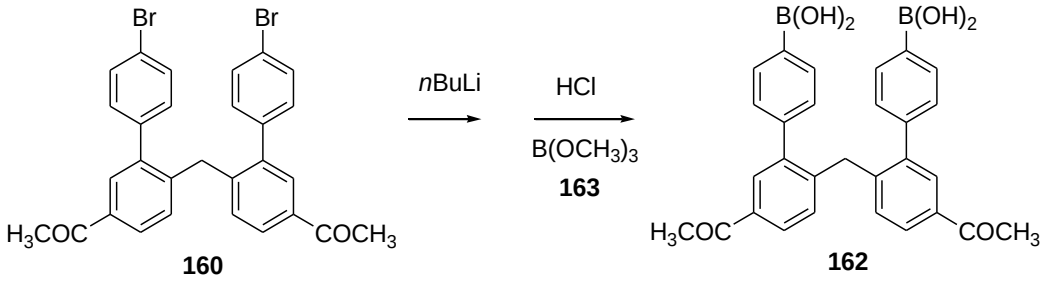

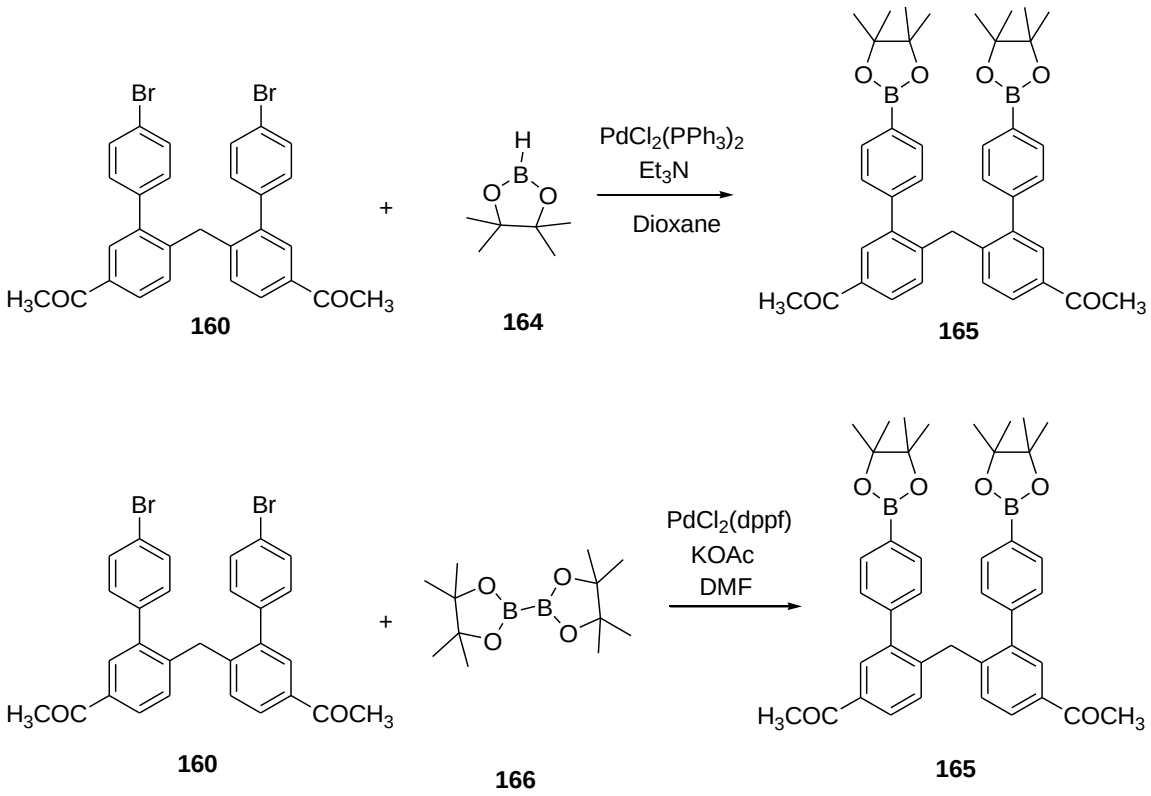

Scheme 49. The conversion to the boronic acid

6.2.5 Summary of the synthetic approach to 172

The bromine intermediate **160** has been successfully synthesized by Suzuki coupling reaction in section 6.2.3. Next boronic acid would be introduced at the positions of bromine of **160** to form the intermediate **162** as shown in section 6.2.4. The last step is coupling with arsenic dibromide to form **172** referring to the arsenic carbon bond formation in section 3.5 (Scheme 50).

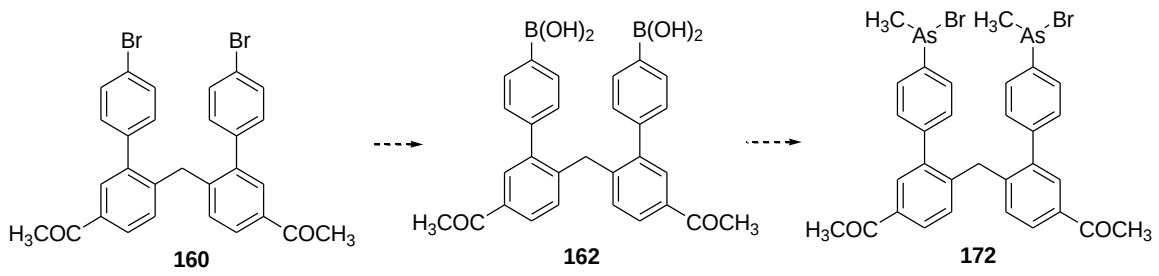

Scheme 50. The proposed synthetic approach to **172**

7 Experimental

The chemicals were purchased from Sigma-Aldrich, Fisher Scientific, and VWR International, and used as received. Dichloromethane was distilled prior to use from calcium hydride under nitrogen. Tetrahydrofuran was distilled from sodium and benzophenone. Other solvents were dried with molecular sieves. [55] 3 A˚ and 5 A˚ molecular sieves were obtained from commercial suppliers and were preheated at 300 ℃ for 24 h immediately before use. Solvents were dried by allowing them to stand over the desiccant under nitrogen. Table 6 shows the water content in DCM after drying with 3 A˚ molecular sieves.

Solvents acetone and heptane used in chromatography and glassware washing were purified by distillation as published by our group. [56] Automated combiflash machine used acetone−heptane gradients, with primary detection at 210 nm. In purifying compounds exhibiting UV absorbance, eluent not detected at 210 nm was sent directly to waste. The eluent not collected in fractions, discarded fractions, and solvent collected from rotary evaporation of saved fractions were combined for solvent recovery. The recovered solvent mixture was distilled using an automated commercial solvent recycling unit that performs fractional distillation in 19 L batches with a claimed efficiency of 10 theoretical plates. For acetone−heptane mixtures, the solvent distilling from 55 ℃ to 77 ℃ was collected as the acetone fraction and the solvent distilling from 77 ℃ to 120 ℃ was collected as the heptane fraction. For recycling of acetone from glassware washing, the liquid distilling from 50 ℃ to 80 ℃ was collected. Samples from before and after recycling were analyzed by ^{1}H-NMR in $CDCl_3$. Ratios of acetone to heptane were determined by comparing integration of the acetone peak to both the methylene multiplet and the methyl signal of heptane and were converted to mass percentage. ^{1}H-NMR analysis of a 1:1 heptane−acetone mixture was used to confirm the accuracy of this quantitation method under standard spectral acquisition parameters.[56]

ITC experiments. ITC experiments were performed on a Model CSC 4200 microcalorimeter (Calorimetry Sciences Corp.) at 25 ℃ with stirring at 297 rpm. The cell (1.3 mL) contained a 0.5 mM solution of phenyl methyl arsenic hydroxyl compound **94** in 5 mM potassium phosphate buffer pH 7.0 containing 2% DMSO. A solution of 2–mercaptoethanol (6.0 mM) in the same buffer with 2% DMSO was added in 23 injections of 10 μL each, with 300 s between injections. Data was processed using BindWorks 3.0 software.

NMR thiol-exchange experiment. The ^{1}H-NMR spectrum was taken of a solution of thiol adduct **95** (9 μmol) in D_2O (1 mL). A solution of cysteine hydrochloride in D_2O (27 μl, 1 M, 27 μmol) was added and the spectrum was taken immediately and again after 30 minutes. Both spectra showed formation of equal amounts of free the mercaptoethanol S-CH_2 triplet at δ 2.55.

Titration of *n*butyl lithium. A solution of 1 M *sec*-butyl alcohol in dry ether in a dry flask under nitrogen was prepared. About 1 to 2 mg of 1,10-phenanthroline (the exact quantity is not critical) and an appropriate size magnetic stir bar was placed in a 50 mL round bottom flask. The flask was connected to a vacuum line and evacuated the flask with vacuum for about 10 minutes, and next the flask was refilled with dry nitrogen via the vacuum manifold. About 10 mL of dry ether solvent was transferred to the flask via syringe. Magnetic stir was used to dissolve the indicator and continued stirring through the remaining steps of the procedure. The flask was cooled in a dry ice bath while the flask was still connected to a dry nitrogen inlet. *N*BuLi (2 mL, 2 M) solution was transferred to the flask. 2 mL or more of the titrant solution from step 1 was filled in a syringe and recorded the volume in the syringe. Addition was stopped immediately when the solution became colorless and recorded the remaining volume in the syringe[32].

1,6-Dibromo-2-methoxy-naphthalene (5). To a solution of 1,6-dibromo-2-naphthol (2.00 g, 6.60 mmol) in anhydrous DMF (2 mL) was added cesium carbonate (3.26 g, 10.00 mmol) while stirring, forming a light red suspension. Iodomethane (1.90 g, 13.20 mmol) was added all at once, and the reaction crude was stirred overnight at room temperature. The mixture was portioned between H_2O and CH_2Cl_2 (20 mL each), and the aqueous layer was further extracted with CH_2Cl_2 (2 × 20 mL). The combined organic layers were dried over $MgSO_4$ and concentrated in vacuum to give **5** (2.00 g, 96% yield).

Alternatively, 1,6-dibromo-2-naphthol (2.00 g, 6.60 mmol) was dissolved in anhydrous DMF (10 mL), and potassium carbonate (2.28 g, 16.60 mmol) was added while stirring, forming a light red suspension. Iodomethane (1.90 g, 13.20 mmol) was added in one portion and the reaction crude was stirred overnight

at room temperature. The mixture was partitioned between H_2O and CH_2Cl_2 (20 mL each), and the aqueous layer was further extracted with CH_2Cl_2 (2 × 20 mL). The combined organic layers were dried over $MgSO_4$ and concentrated in vacuum to give the desired product as red oil (2.00 g, 96% yield). NMR data was in agreement with literature values, ^{1}H-NMR ($CDCl_3$) δ 4.02 (s, 3H), 7.58 (d, 1H), 7.61 (d, 1H), 7.92 (d, 1H), 8.00 (s, 1H), 8.07 (d, 1H).[34] (Figure 41)

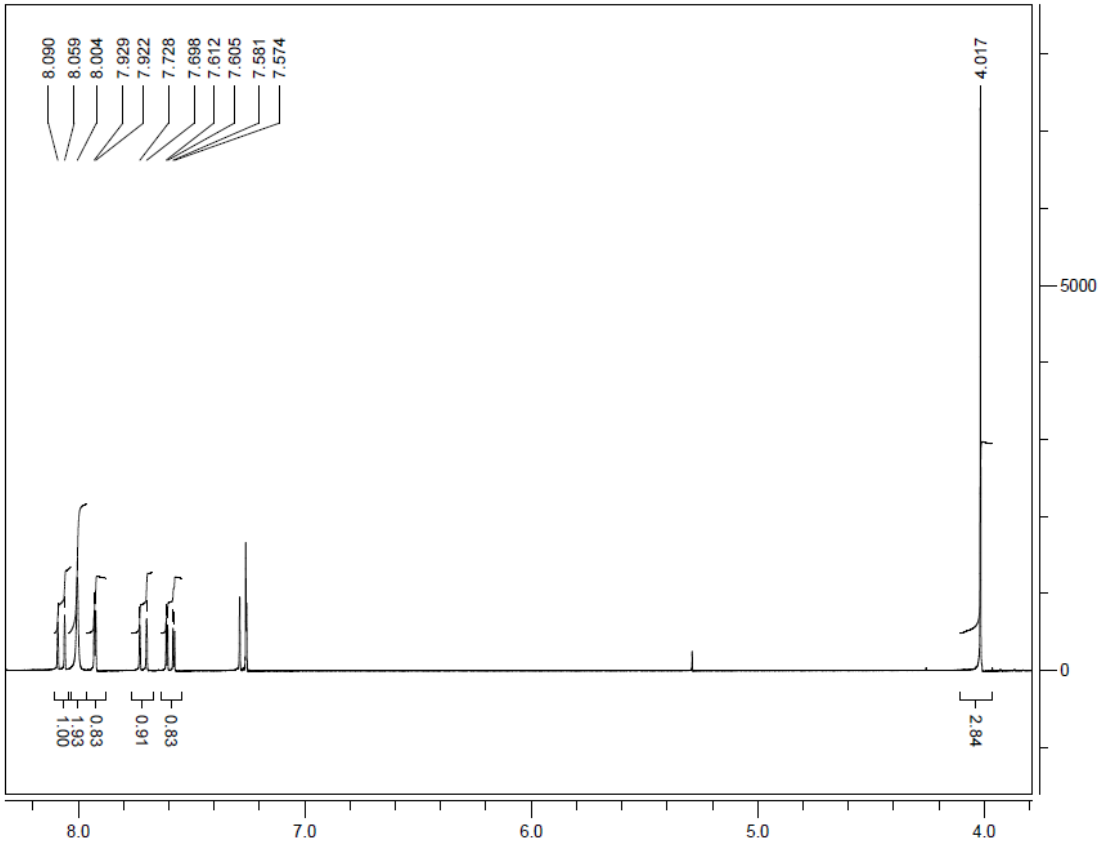

Figure 41. NMR for 1,6-Dibromo-2-methoxy-naphthalene

1,6-Dialdehyde-2-methoxy-naphthalene (6). To a solution of 1,6-Dibromo-2-methoxy-naphthalene (0.75 g, 2.37 mmol) in ether (35 mL) under nitrogen atmosphere was added *n*-butyl lithium (4.00 mL, 6.40 mmol) dropwise using syringe, dry ice was used for cooling, and green color appeared in the reaction mixture. TLC was used to monitor the reaction while stirring, R_f of the reaction crude (added saturated aq. NH_4Cl solution) was compared with 2-bromo-6-methoxynaphthalene and 2-methoxynaphthalene (R_f = 0.9 in hexane: ethyl acetate=1:1). When the spot of 2-bromo-6-methoxynaphthalene disappeared completely, dimethyl formamide (0.40 mL, 4.40 mmol) was added at -20 ℃. The reaction solution was left to warm slowly to room temperature. Saturated aq. NH_4Cl solution (7 mL) was added, and organic layer was separated. The aqueous layer was extracted with ether (2 × 7

mL). The original ether layer and the separation ether layers were combined together, dried over $MgSO_4$, and concentrated in vacuum. Several spots were identified in TLC results (R_f = 0.9, 0.7, 0.6 in hexane: ethyl acetate = 1:1), and the ^{1}H-NMR spectrum was corresponding to this result. The nonselectivity of bromine at positions one and six would contribute to the side reaction[35].

Alternatively, Tetramethylethylenediamine (TMEDA) was added to the solution of the starting material dissolved in diethyl ether at 0 ℃ under nitrogen atmosphere. *n*-butyllithium was added dropwise over five minutes. The mixture was stirred at room temperature for 12 hours. DMF was added to the mixture on ice and the reaction was stirred for 30 minutes. Then the reaction solution was warmed to room temperature, aq. HCl solution (7 mL, 3.00 M) was added. The organic layer was separated, and the aqueous layer was extracted with ether (3 × 15 mL). The organic layer was dried over $MgSO_4$. No desired product was identified in TLC results (hexane: ethyl acetate = 1:1, $R_{f\ (s.m)}$: $R_{f\ (product)}$ = 1:1). The product mixture was purified by combiflash (eluting solution started with 5% acetone in heptane, increase for 35% acetone in heptane) and NMR spectrum of each component was shown below.

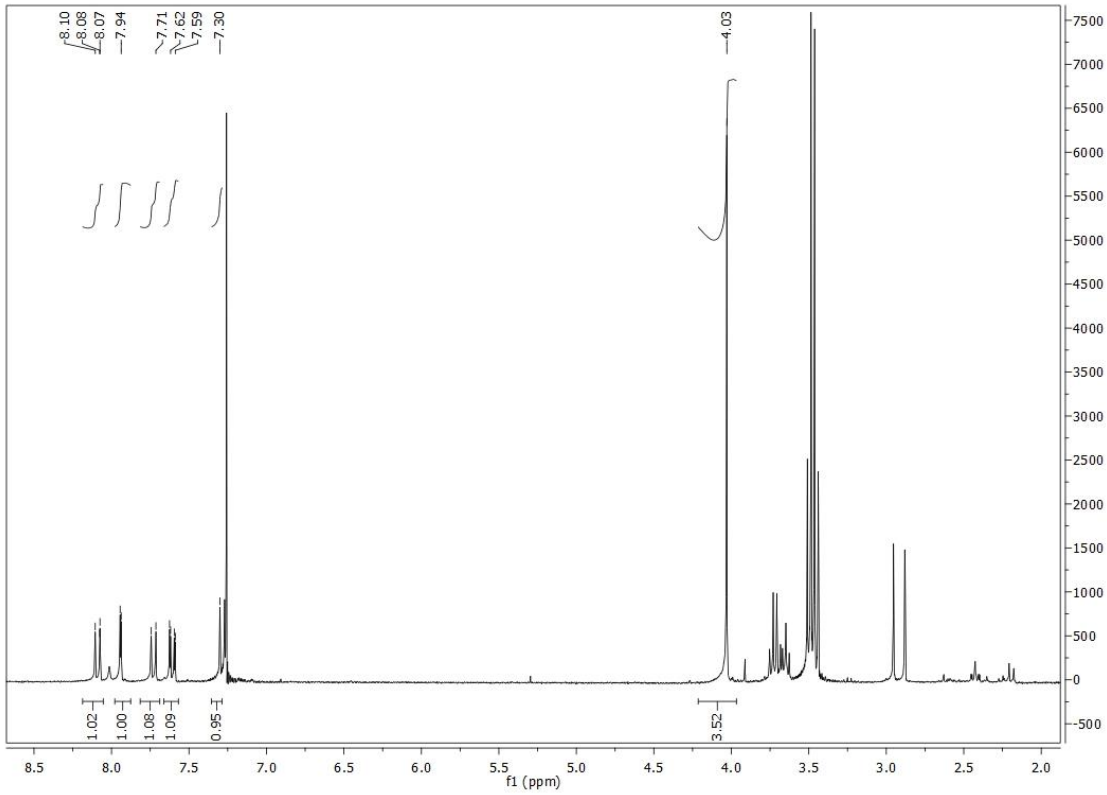

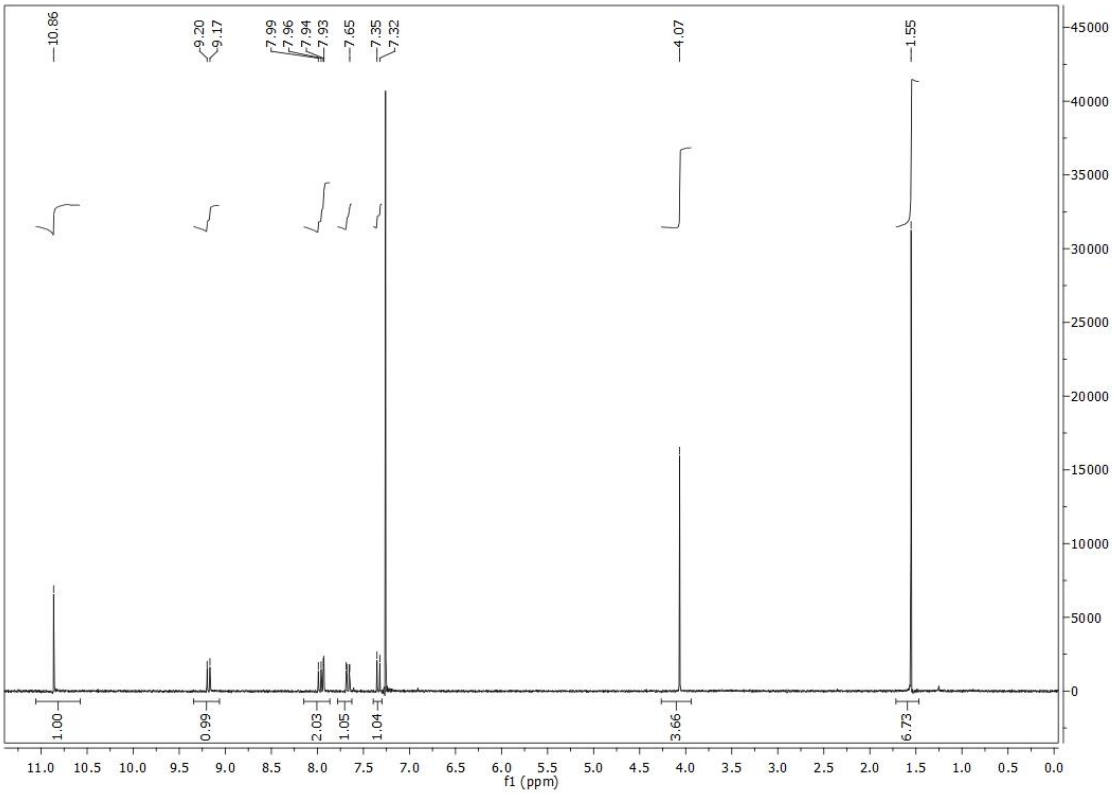
10.86
9.20
9.17
7.99
7.96
7.94
7.93
7.65
7.35
7.32
4.07
1.55
1.00
0.99
2.03
1.05
1.04
3.66
6.73
f1 (ppm)

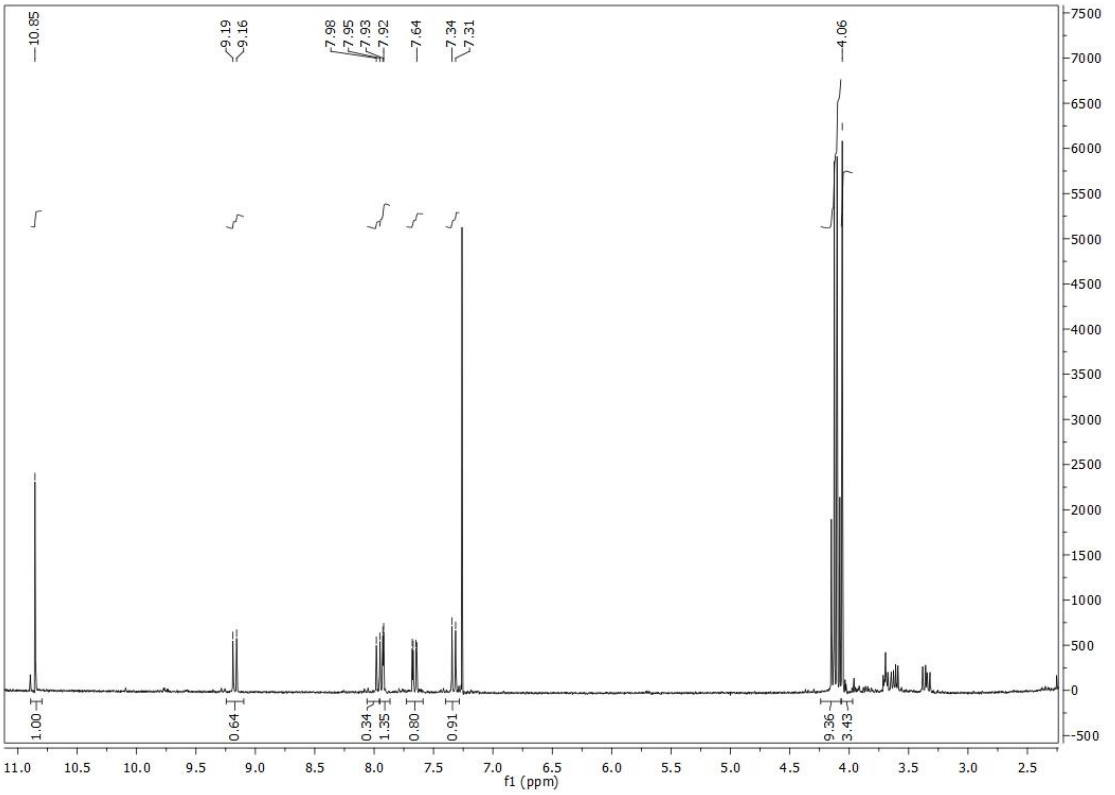
10.85
9.19
9.16
7.98
7.95
7.93
7.92
7.64
7.34
7.31
4.06
1.00
0.64
0.34
1.35
0.80
0.91
9.36
3.43
f1 (ppm)

Figure 42. NMR for each component of *n*BuLi reaction crude

(2-Methoxy-1,6-dimethanol)naphthene (7). To a solution of 1,6-dialdehyde-2-methoxy-naphthalene product mixture (0.56 g, 1.00 mmol) in methanol (10 mL) was added $NaBH_4$ (0.38 g, 1.00 mmol) with ice cooling. The mixture was stirred at room temperature for 1.0 h and concentrated. The residue was partitioned between ethyl acetate and water and the organic layer was separated, dried over $MgSO_4$ and concentrated. However, no desired product was identified in the NMR results of the reaction crude.[36]

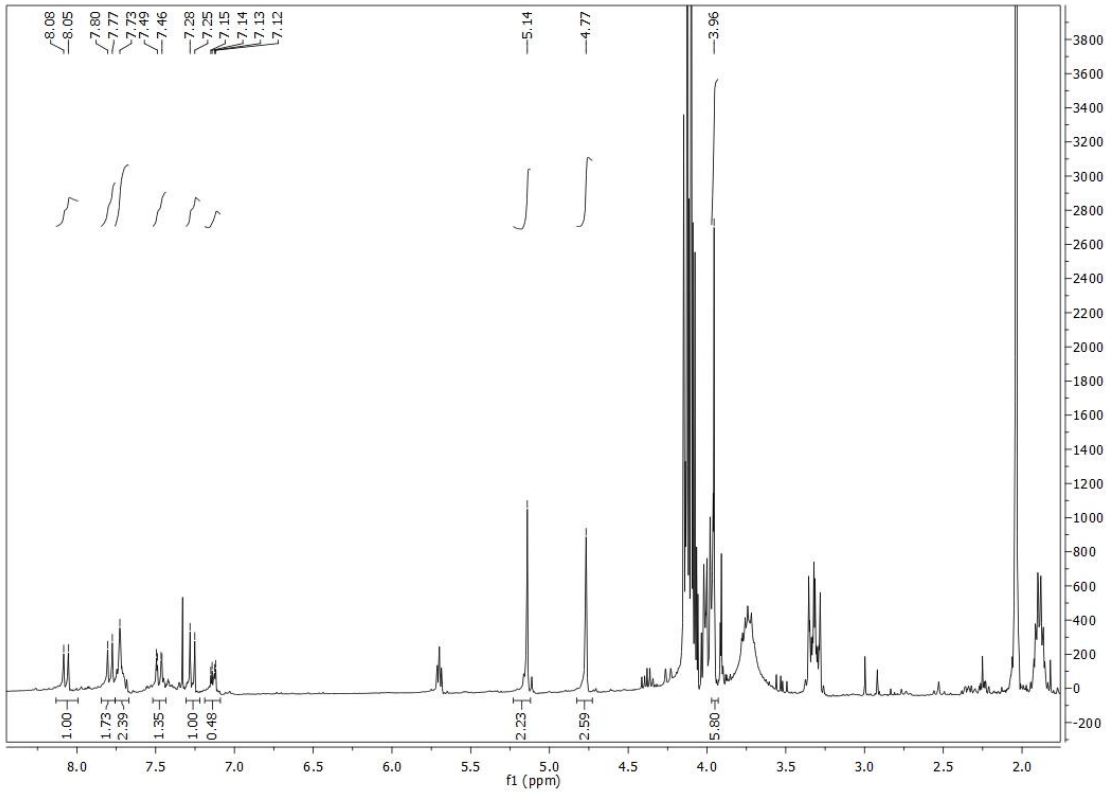

Figure 43. NMR for reaction crude **7**

6-Bromo -2-methoxy-naphthalene-1-carboxaldehyde (9). To a solution of 1,6-dibromo-2-methoxy-naphthalene (0.32 g, 1.00 mmol) in ether (17 mL) under nitrogen atmosphere was added *n*-butyl lithium (1.00 mL, 1.00 mmol) dropwise using syringe while cooling in dry ice. TLC was used to monitor the reaction crude while stirring (R_f s.m. = 0.8, R_f p = 0.5 in hexane: ethyl acetate = 1:1). After 3 hours dimethyl formamide (0.50 mL, 3.00 mmol) was added to the reaction solution. The reaction was allowed to warm to room temperature slowly, and stirred overnight, then saturated aq. NH_4Cl solution (10 mL) was added. The organic layer was separated, and the aqueous layer was extracted with ether (2 × 10 mL), combined with the original ether layer, and dried over $MgSO_4$. Only starting material was

identified in the NMR and TLC results (hexane: ethyl acetate = 1:1).

(6-Bromo-2-methoxy-1-naphthyl)methanol (10). To a solution of 6-bromo-2-methoxy-naphthalene-1-carboxaldehyde mixture (0.28 g, 0.50 mmol) in methanol (5 mL) was added $NaBH_4$ (0.19 g, 0.50 mmol) with ice cooling. The mixture was stirred at room temperature for 1.0 h and concentrated. The reaction crude was partitioned between ethyl acetate and water, and the organic layer was separated, dried over $MgSO_4$ and concentrated under vacuum. ^{1}H-NMR spectrum of the product was too messy to identify the desire product, due to the nonselectivity of positions one and six on the naphthalene ring.

Synthesis of compound 14 by a radical reaction. A solution of 3,4'-dimethyldiphenyl (0.99 g, 5.00 mmol) in ether was added *n*-bromosuccinimide (1.87 g, 10.60 mmol), and benzoyl peroxide (0.01 g, 0.04 mmol) dissolved in CCl_4 (75 mL), and heated reflux at 70 ℃ for 8 h. The reaction crude was cooling to room temperature, and the excess succinimide was precipitated and removed by filtration. The solvent was removed by evaporation. The product mixture was monitored by TLC overnight, which showed multiple spots in TLC results. R_f (s.m) = 0.69, R_f of the product mixture at 4 h was 0.62, 0.56, 0.67 (hexane: ethyl acetate = 3:1), and the ^{1}H-NMR spectrum was corresponding to this result.

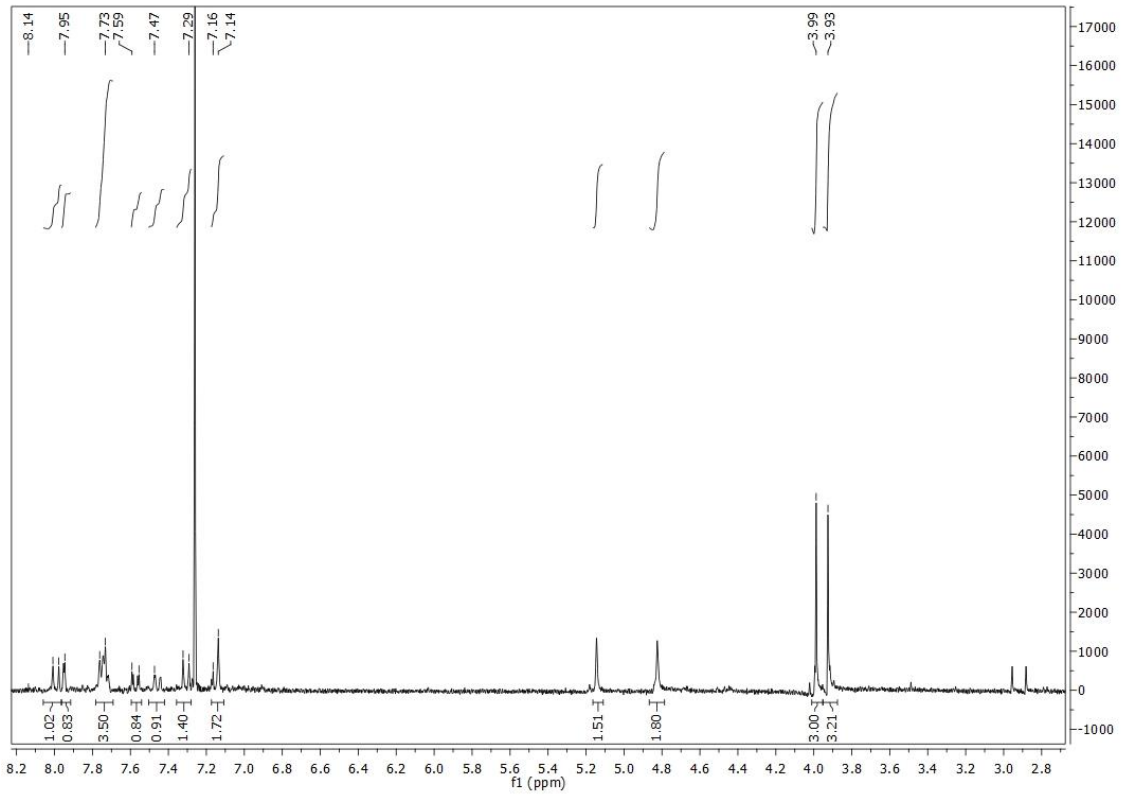

Figure 44. NMR for the radical reaction crude

Alternative synthesis of compound 14 by a radical reaction. A solution of 3,4'-dimethyldiphenyl ether (0.99 g, 5.00 mmol) in CCl_4 (75 mL) was added N-bromosuccinimide (1.87 g, 10.50 mmol), and azobisisobutyronitrile (0.05 g, 0.30 mmol). Bright light was used to irritate the radical reaction. TLC was used to monitor the reaction crude starting from reaction time 0.5 hour, which was compared to the R_f of the product with 1 eq and 0.5 eq NBS separately. The two methyl substituted product was formed after about 3 hours with R_f = 0.56 in 25% ethyl acetate to hexane. ^{1}H-NMR data was in agreement with literature values, ^{1}H-NMR ($CDCl_3$) δ 4.52 (s, 2H), 4.59 (s, 2H), 7.04 (d, 2H), 7.06 (s, 1H), 7.14 (s, 1H), 7.24 (s, 1H), 7.34 (s, 1H), 7.45 (d, 2H).

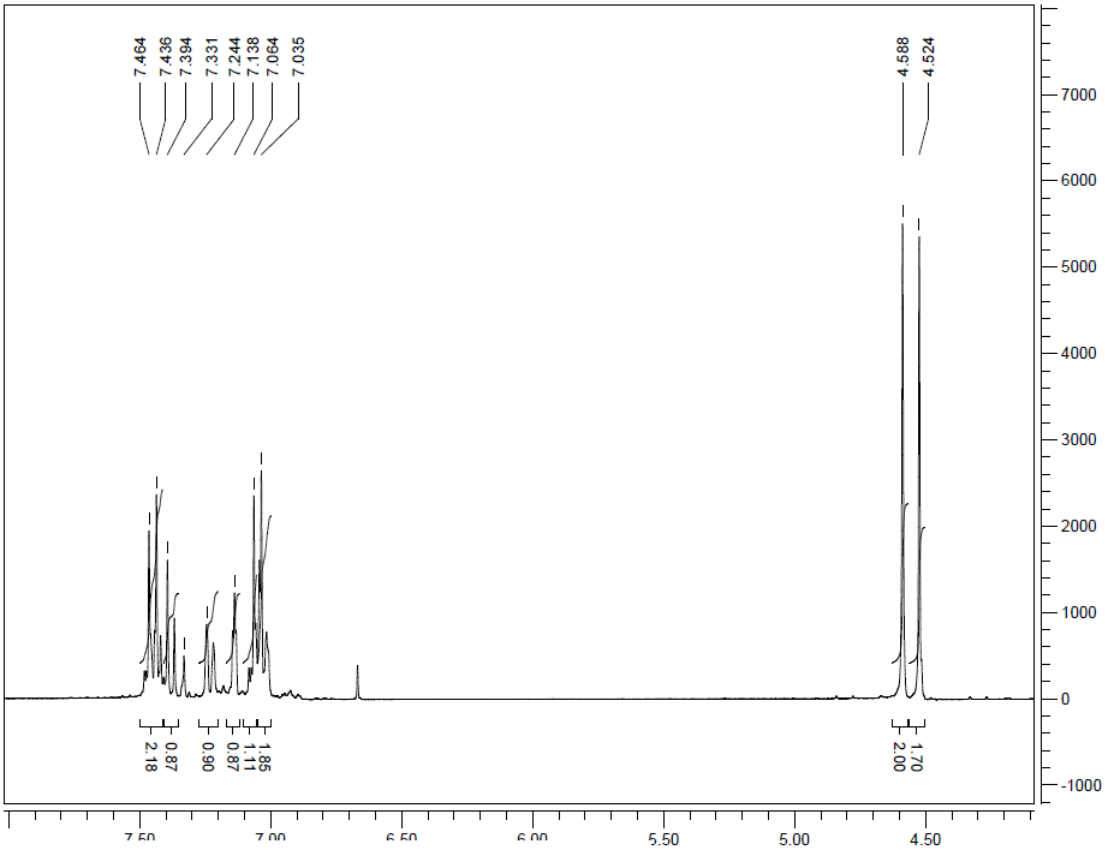

Figure 45. NMR for {3-[4-(hydroxymethyl)phenoxy]phenyl}methanol

Synthesis of compound 18 by a coupling reaction. **(**4-Bromophenyl)methanol (0.19 g, 1.00 mmol), 3-(hydroxymethyl)phenol (0.17 g, 1.4 mmol), copper(I)trifluoromethanesulfonate benzene complex (0.012 g, 0.025 mmol), and cesium carbonate (0.46 g, 1.40 mmol) were placed in a 25 mL flask. The flask was evacuated and refilled with nitrogen. Ethyl acetate (4.88 mL, 0.05 mmol) and toluene (0.80 mL) were added to the flask, and heated to 110 ℃ under nitrogen atmosphere. TLC was used to monitor the reaction residue until the reagent aryl halide had been consumed completely. The reaction crude was

cooled to room temperature, diluted with ether, and washed sequentially with 5% aqueous NaOH, water, and brine. The organic layer was dried over $MgSO_4$ and concentrated under vacuum to give the crude product, but the NMR spectrum was too messy to identify the desired product.

Alternately, **(**4-Bromophenyl)methanol (0.19 g, 1.00 mmol), 3-(hydroxymethyl)phenol (0.17 g, 1.40 mmol), copper(I)trifluoromethanesulfonate benzene complex (0.012 g, 0.025 mmol), cesium carbonate (0.46 g, 1.4 mmol), and 1-naphthoic acid (0.24 g, 1.40 mmol) were placed in a 25 mL flask under an inert atmosphere of nitrogen. Ethyl acetate (4.88 mL, 0.05 mmol) and toluene (0.80 mL) were added, and the reaction was heated at 110 ℃ under nitrogen. The reaction was cooled to room temperature, diluted with ether and washed sequentially with 5% aqueous NaOH, water, and brine. The organic layer was dried over $MgSO_4$ and concentrated under vacuum to give the crude product, but the NMR spectrum was too messy to identify the desired product.[37]

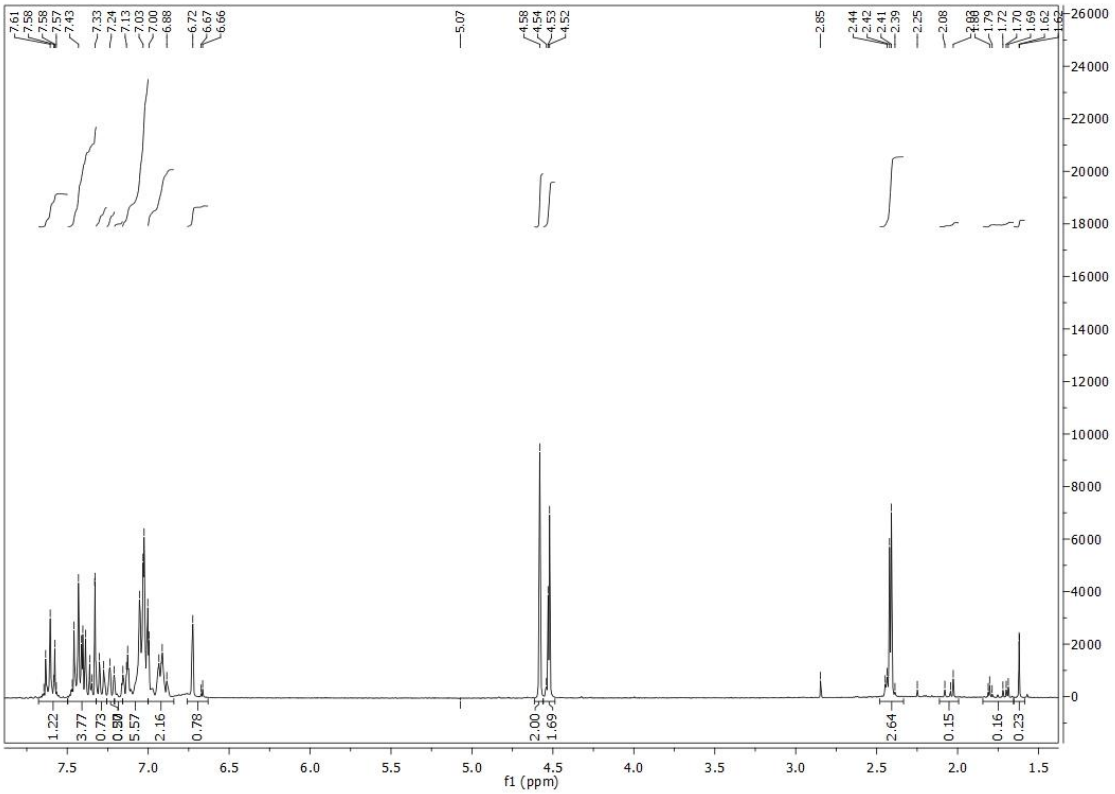

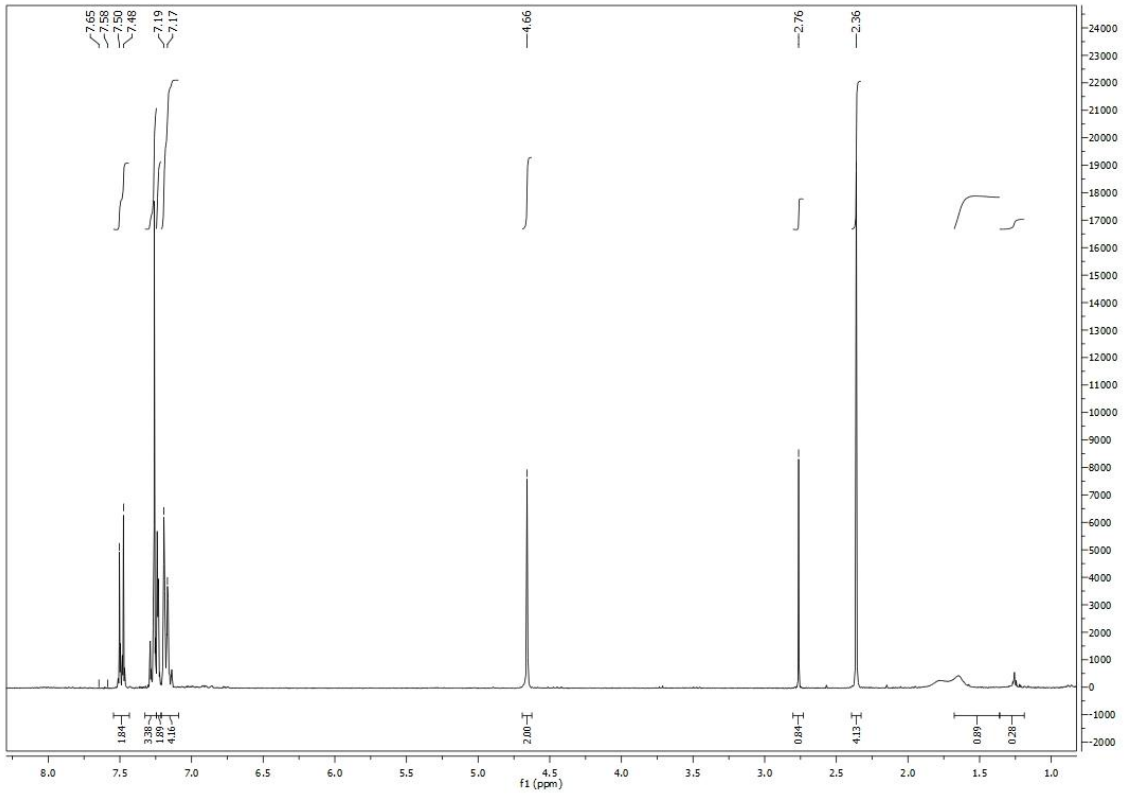

Figure 46. NMR for the bonded reaction

Another coupling reaction (24). **(**4-Bromophenyl)methanol (0.19 g, 1.00 mmol), 4-bromobenzoic acid (0.28 g, 1.40 mmol), copper(I)trifluoromethanesulfonate benzene complex (0.012 g, 0.025 mmol), cesium carbonate (0.46 g, 1.40 mmol), and 1-naphoic acid (0.24 g, 1.40 mmol) were placed in a 25 mL round bottom flask. The flask was evacuated and refilled with nitrogen. Ethyl acetate (4.88 mL, 0.05 mmol) and toluene (0.80 mL) were added to the reaction crude, and the reaction was heated at 110 ℃ under nitrogen. The reaction crude was cooled to room temperature, diluted with ether, and washed sequentially with 5% aqueous NaOH, water, and brine. The organic layer was dried over $MgSO_4$ and concentrated under vacuum to give the crude product. However, the side reaction product was identified in the ^{1}H-NMR spectrum of the reaction crude together with the desired product showing similar polarities.

1,6-Dibromonaphthalene (27). To an ice-cooled solution of triphenylphosphine (3.28 g, 12.50 mmol) in acetonitrile (6.00 mL) was added bromine (0.64 mL, 12.50 mmol) dropwise. Naphthalene-1,6-diol (1.00 g, 6.25 mmol) was added, and the reaction mixture was heated for 2 hours at 80 ℃. The solvent was evaporated under reduced pressure and the reaction crude was heated on sand at 240 ℃ for 10

minutes. The residue was dissolved in ethanol (10.0 mL) and heated until boiling for 30 minutes, followed by hot and cold filtration, the filtrate was evaporated under reduced pressure, and then the product mixture was purified by chromatography on silica gel (hexane: ethyl acetate= 9:1). The purified product was corresponding to the starting material triphenylphosphine in the ^{1}H-NMR spectrum and TLC (R_f =0.1 in hexane: ethyl acetate = 9:1) result, ^{1}H-NMR ($CDCl_3$) δ 7.71 (multiple, 6H), 7.64-7.27 (multiple, 9H).[31]

Benzaldehyde (33). Bromobenzene (0.58 g, 5.50 mmol) was dissolved in ether (35 mL) under nitrogen. The reaction crude was cooled in dry ice bath. *n*-butyl lithium (2.75 mL, 5.50 mmol) was added dropwise using syringe, and the reaction crude was stirred for 15 minutes. Dimethyl formamide (0.50 mL, 5.50 mmol) was added to the reaction, and kept stirring for 15 minutes. The reaction was warmed slowly to room temperature, and saturated aq. NH_4Cl solution (15 mL) was added. The aqueous layer was extracted with ether (2 × 20 mL), the combined organic layers were dried over $MgSO_4$, and the organic solution was evaporated under reduced pressure. [33] Only the starting material was identified in the NMR results.

1,6-naphthyl bis(trifluoromethanesulfonate) (35). To a solution of naphthalene-1,6-diol (0.45 g, 2.80 mmol) in dry CH_2Cl_2 (18 mL) was added pyridine (0.80 mL) followed by addition of triflic anhydride (1.00 mL, 6.00 mmol) dropwise at 0 ℃. The reaction residue was stirred at room temperature for 6h. Then the solvent was removed, and the left residue was diluted with EtOAc (10 mL), washed with 5% aq. HCl (3 mL), saturated aq. $NaHCO_3$ (3 mL) and brine (3 mL). The organic layer was dried over anhydrous sodium sulfate, concentrated under vacuum, and passed through a silica gel plug (hexane: ethyl acetate = 9:1) to give the desired product (0.55 g, 46% yield). ^{1}H-NMR data was in agreement with literature values, ^{1}H-NMR ($CDCl_3$) δ 7.54 (d, 1H), 7.57 (s, 1H), 7.62 (t, 1H), 7.85 (d, 1H), 7.91 (d, 1H), 8.18 (d, 1H).[38]

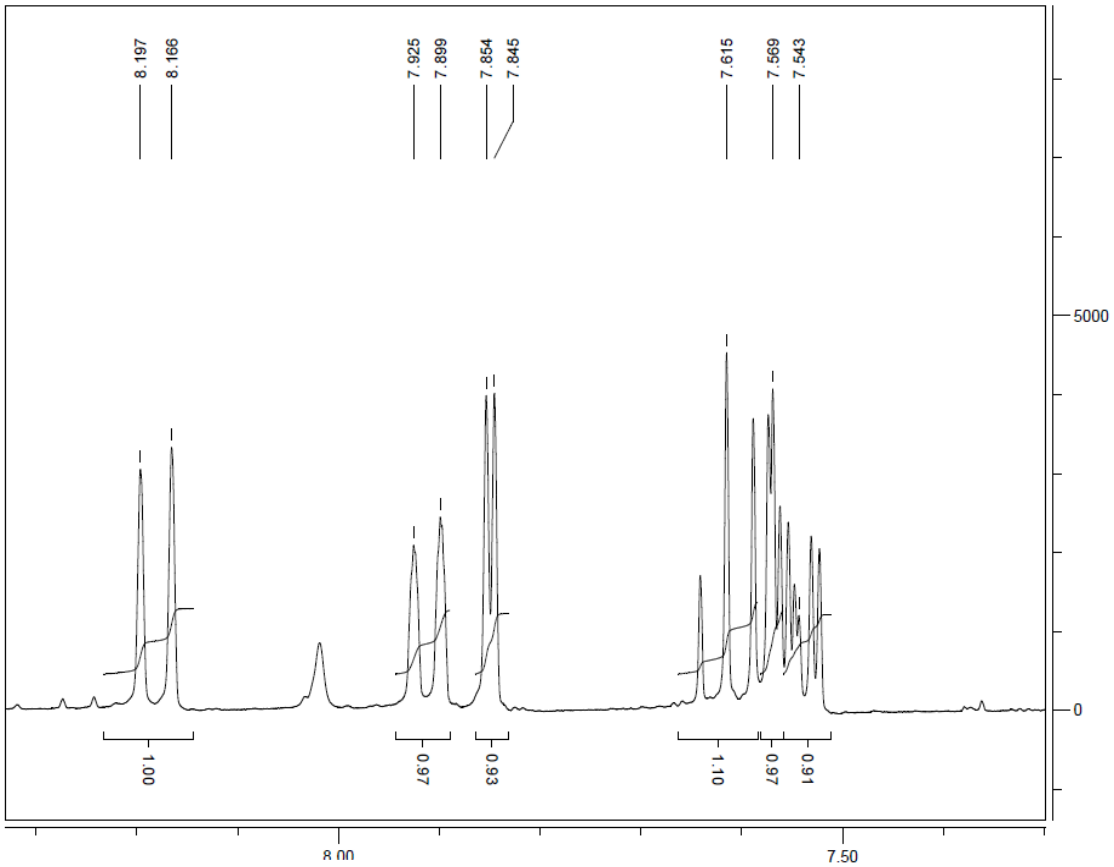

Figure 47. NMR for 1,6-naphthyl-bis(trifluoromethanesulfonate)

1,6-dimethyl-naphthalene (36). To a solution of 1,6-naphthyl-bis(trifluoromethanesulfonate) (0.30 g, 0.70 mmol) and $NiCl_2(PPh_3)_2$ (0.031 g, 0.05 mmol) in anhydrous Et_2O (3 mL) under nitrogen, MeMgBr (0.93 mL, 2.80 mmol) was added dropwise. During the addition of the Grignard reagent, the reaction mixture was warmed to room temperature spontaneously while the solvent was boiling vigorously. The reaction crude was cooled in a water-ice bath. After stirring for 1 h, the solution was diluted with Et_2O, washed with 5% aqueous HCl and brine, and then dried over anhydrous Na_2SO_4. The solvent was evaporated under vacuum, and the residue was purified by column chromatography (ethyl acetate: hexane= 1:9) affording 1,6-dimethyl-naphthalene (0.09 g, 72% yield), R_f = 0.81 in 10% ethyl acetate of hexane. ^{1}H-NMR data was in agreement with literature values, ^{1}H-NMR ($CDCl_3$) δ 2.53 (s, 3H), 2.68 (s, 3H), 7.35 (d, 1H), 7.37 (d, 1H), 7.38 (t, 1H), 7.61 (d, 1H), 7.62 (s, 1H), 7.90 (d, 1H).[39]

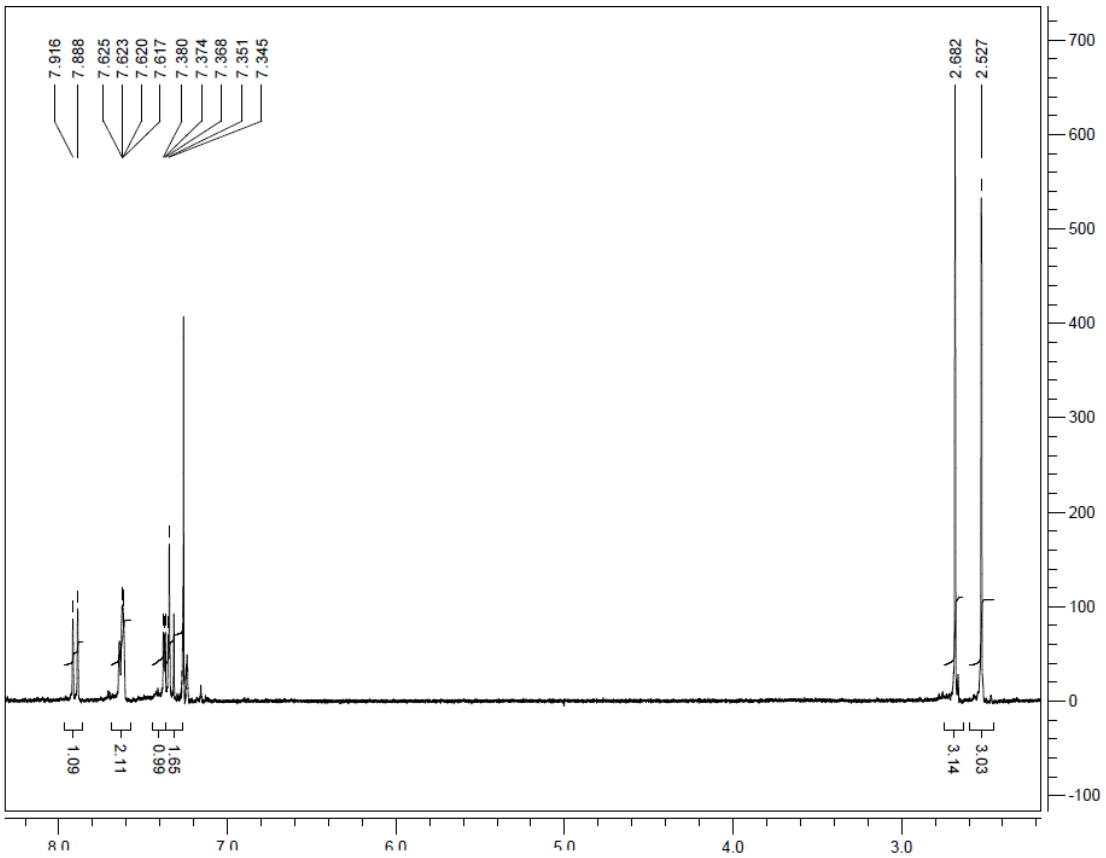

Figure 48. NMR for 1,6-dimethyl-naphthalene

1,6-dilithium-1,6-dimethyl-naphthalene (37). 1,6-dimethyl-naphthalene (0.6 g, 0.4 mmol) was placed in a 25 mL round bottom flask. The flask was evacuated and then refilled with nitrogen. TMEDA (0.12 mL, 0.8 mmol) and *n*BuLi (0.5 mL, 0.8 mmol) were added to the reaction in ice bath. The reaction solution was then heated for 10 h, and left to stir at room temperature overnight. The reaction solution was used for the subsequent reaction without further purification.

Synthesis of compound 3. CH_3AsBr_2 (0.5 g, 2.0 mmol) was added to the 1,6-dilithium-1,6-dimethyl-naphthalene **37** solution, and stirred for 3 h. 2-mercaptoethanol (1.6 g, 20.4 mmol) and TEA (0.8 ml, 5.7 mmol) were added to the reaction, and left stirring at r.t. overnight. The solution was washed with 5% aqueous HCl and brine, and then dried over anhydrous Na_2SO_4. The solvent was evaporated under vacuum, but only 1,6-dimethyl-naphthalene **36** was identified in the NMR results.

Phenylarsenic dichloride (41). Phenyl arsenic acid (6.00 g, 30.00 mmol) was placed in a 100 mL graduated cylinder with a stir bar. A small amount of iodine (crushed) and concentrated aq. HCl (48

mL) were added into the reaction, and the solution was kept stirring until fully dissolved. A plastic bubbler was inserted to near bottom of graduated cylinder with the top somewhat sealed with a rubber septum. The bubbler was connected via tygon tubing to an empty trap connected to a vacuum connector, which was attached to a 100 mL round bottom flask containing sodium bisulfite (32.00 g, 307.69 mmol). To the top of the vacuum connector, an additional funnel containing concentrated aq. HCl (20 mL) was inserted. The graduate cylinder was placed in an 800 mL beaker with 45 ℃ water bath. Aq. HCl from the addition funnel was added very slowly over the course of about 4 hours to the flask containing sodium bisulfite. After an additional two hours the graduated cylinder was removed from the water bath, the bubbler was removed, and the top of the cylinder was sealed with a rubber septum. The cylinder and its contents were left at room temperature overnight. The contents were transferred to a separatory funnel and extracted with CH_2Cl_2 (2×25 mL). The combined CH_2Cl_2 layers were dried over $MgSO_4$, filtered, evaporated under vacuum, and the desired product was recovered (5.6 g, 84%, unstable in water and air exposure). ^{1}H-NMR ($CDCl_3$) δ 7.53 (t, 3H) (J=6Hz), 7.87 (q, 2H) (J=9Hz).

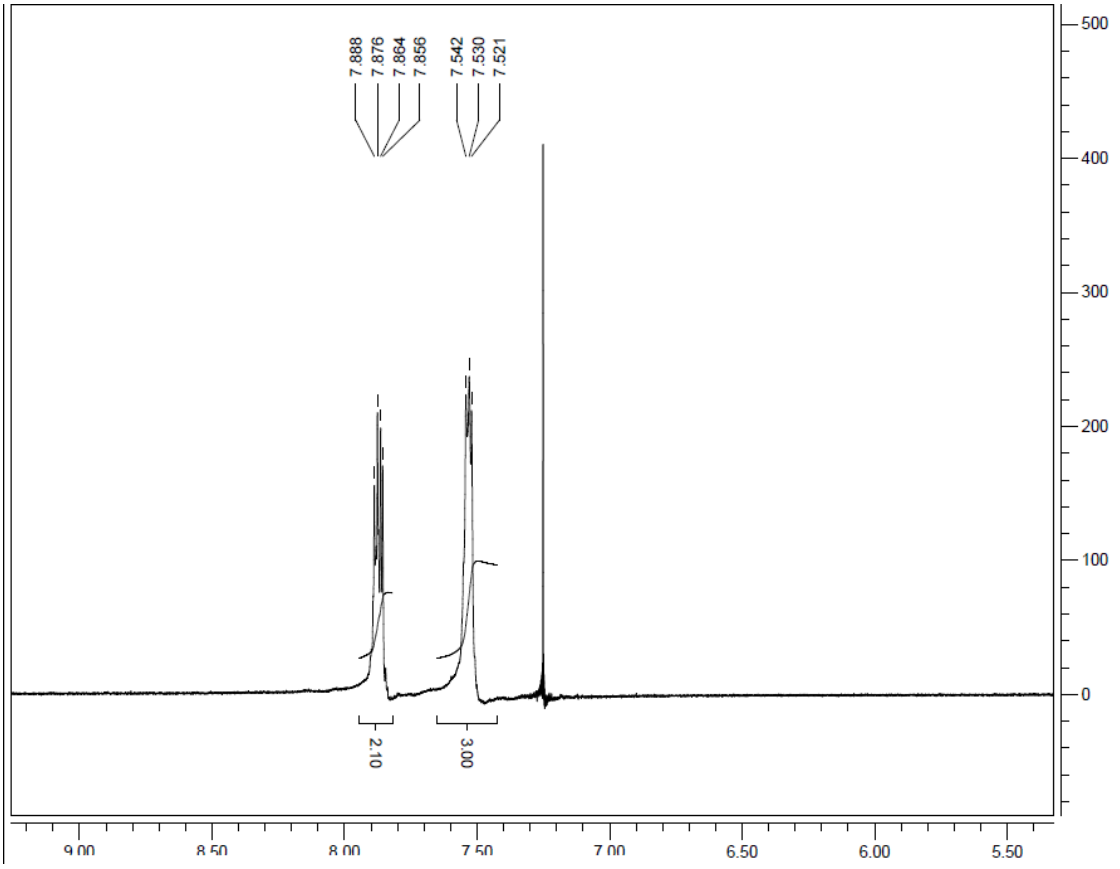

Figure 49. NMR for phenylarsenic dichloride

Alternatively, phenylarsonic acid (2.00 g, 10.00 mmol) placed in a 25 mL round bottom flask was added concentrated aq. HCl (5 mL) at room temperature, the reaction residue was stirred to dissolve. While stirring, aq. hypophosphorous acid (1.3 mL, 50%) was added. A rubber stopper was inserted and vented to a bubbler. The reaction crude was heated in a 40-45 ℃ water bath for about two hours. Saturated aq. NaCl solution (3 mL) and water (3 mL) were added after the reaction crude was cooled to room temperature, and extracted with CH_2Cl_2 (2 × 15 mL). The combined CH_2Cl_2 layers were dried over $MgSO_4$, evaporated under vacuum, and the desired product (1.00 g, 45%) was recovered.

Dimethylchloroarsine (43). Cacodylic acid (1.38 g, 10.00 mmol) was placed in a 25 ml round bottom flask at room temperature, concentrated aq. HCl (3 mL) was added, and the reaction residue was stirred to dissolve. While stirring, aq. hypophosphorous acid (1.30 mL, 50%) was added. A rubber stopper was inserted in the flask and vented to a bubbler. The reaction crude was heated in a 40-45 ℃ water bath for about two hours. Saturated aq. NaCl solution (3 mL) and water (3 mL) were added after cooling to room temperature, and extracted with CH_2Cl_2 (2 × 15 mL). The combined CH_2Cl_2 layers were dried over $MgSO_4$, evaporated under vacuum, and the desired product (1.72 g) was recovered. ^{1}H-NMR ($CDCl_3$) δ 1.68 (s, 6H).

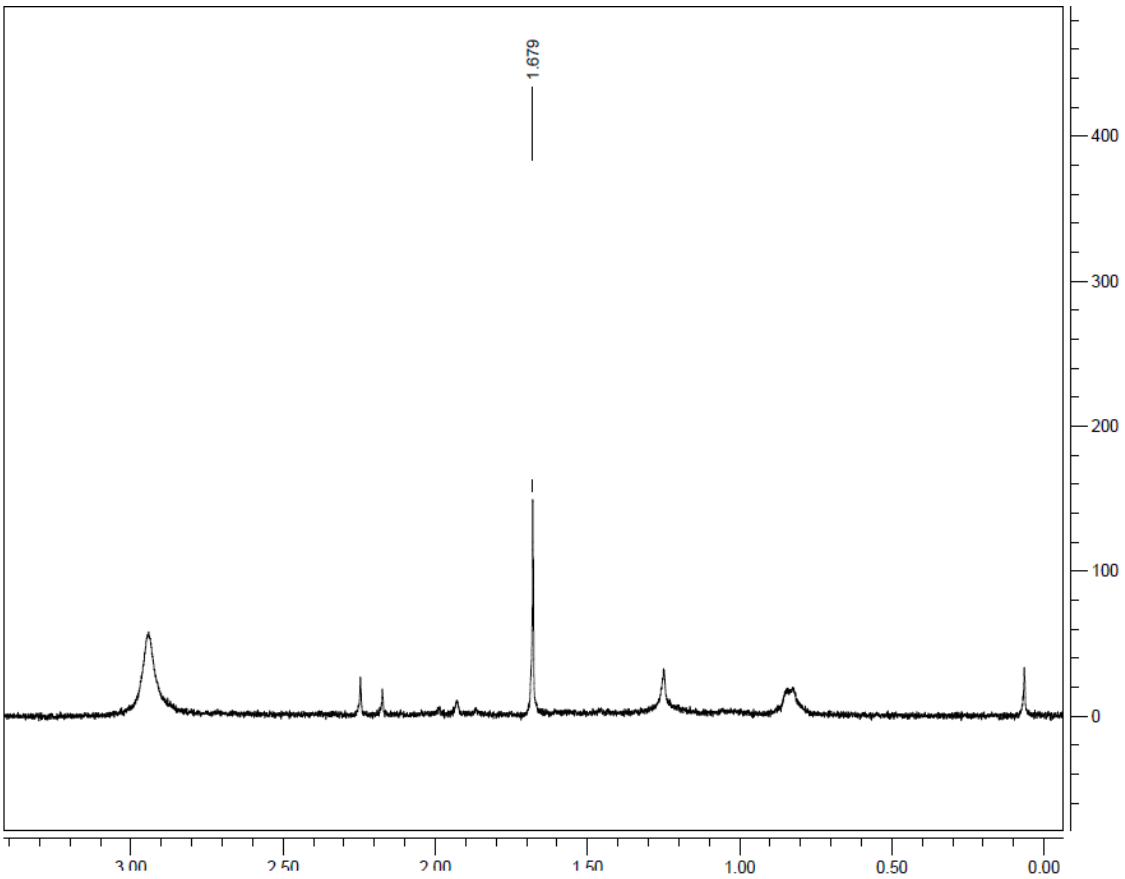

Figure 50. NMR for dimethylchloroarsine

Benzylchloro(phenyl)arsine (45). To a solution of $PhAsCl_2$ (0.20g, 1.00 mmol) in dry THF (5 mL) was added benzylmagnesium chloride (1.00 mmol in 0.50 mL THF) dropwise with vigorous stirring at -78 °C over a period of 3 h under an atmosphere of nitrogen. The reaction was left to stir at room temperature overnight. The reaction mixture was filtered and the filtrate was diluted with water. The aqueous layer was extracted with THF (3×5 mL), and concentrated under vacuum, but only the starting material was identified in the ^{1}H-NMR spectrum.[40]

Chloro(methyl)(phenyl)arsine(48). To a stirred dry THF (5 mL) solution of $PhAsCl_2$ **41** (0.20g, 1.00 mmol) was added a THF solution of CH_3MgCl (0.30 mL, 1.00 mmol) dropwise with vigorous stirring at -78 °C over a period of 3 h under an atmosphere of nitrogen. The reaction solution was kept stirring overnight at room temperature. The reaction mixture was filtered and diluted with water, and the aqueous layer was extracted with THF (3×5 mL), concentrated by rotary evaporator. However, the ^{1}H-NMR spectrum of the reaction crude corresponded to only starting material **41**.

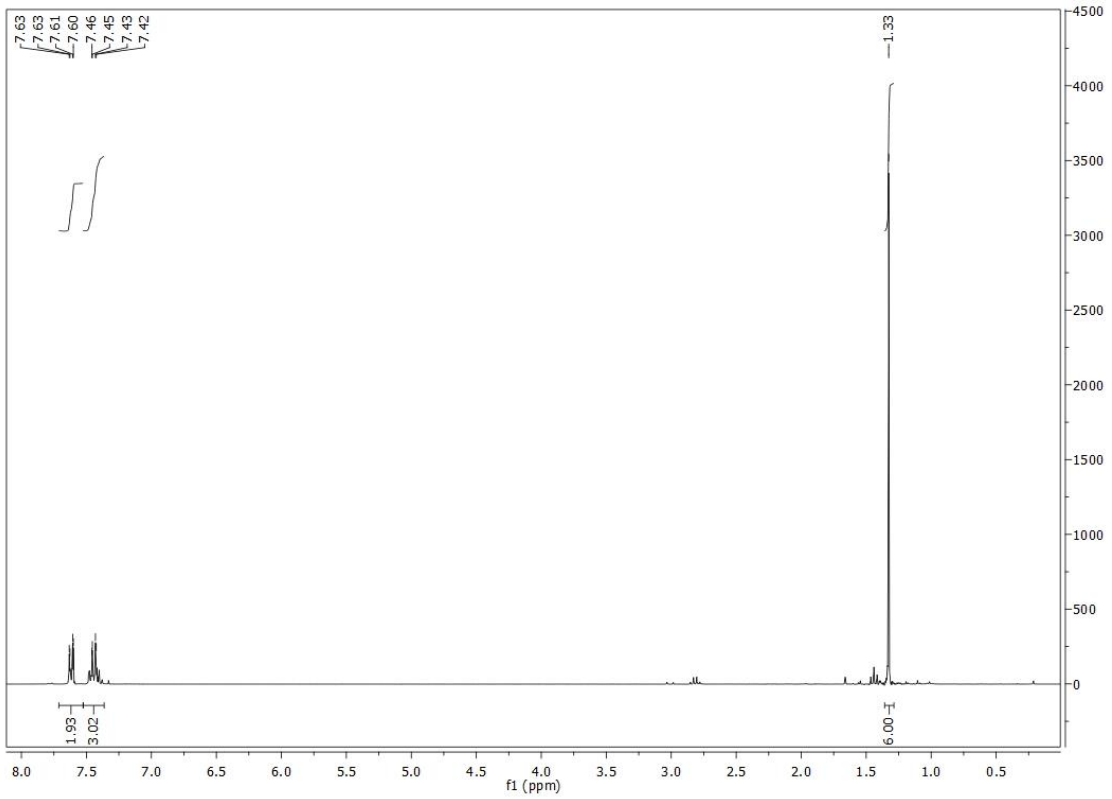

Figure 8. ^{1}H-NMR spectrum for the reaction crude of **48**

Diethyl phenylarsonodithioite (50). $PhAsCl_2$ **41** (1.20 g, 5.00 mmol) placed in a 50 mL round bottom flask was dissolved in dry ether (20 mL), and cooled in ice bath, ethanethiol (0.31 g, 5.00 mmol) and triethylamine (1.50 mL, 211.00 mmol) were added. Gravity filtration was performed after the reaction was allowed to warm to room temperature, the solid was washed with ether (2×25 mL), and the combined organic layers were evaporated by rotovap. The reaction residue was redissolved in a small volume of CH_2Cl_2, and purified by Combiflash (eluting solution: heptane and acetone). However, the NMR result of the product was too messy to identify the desired product.

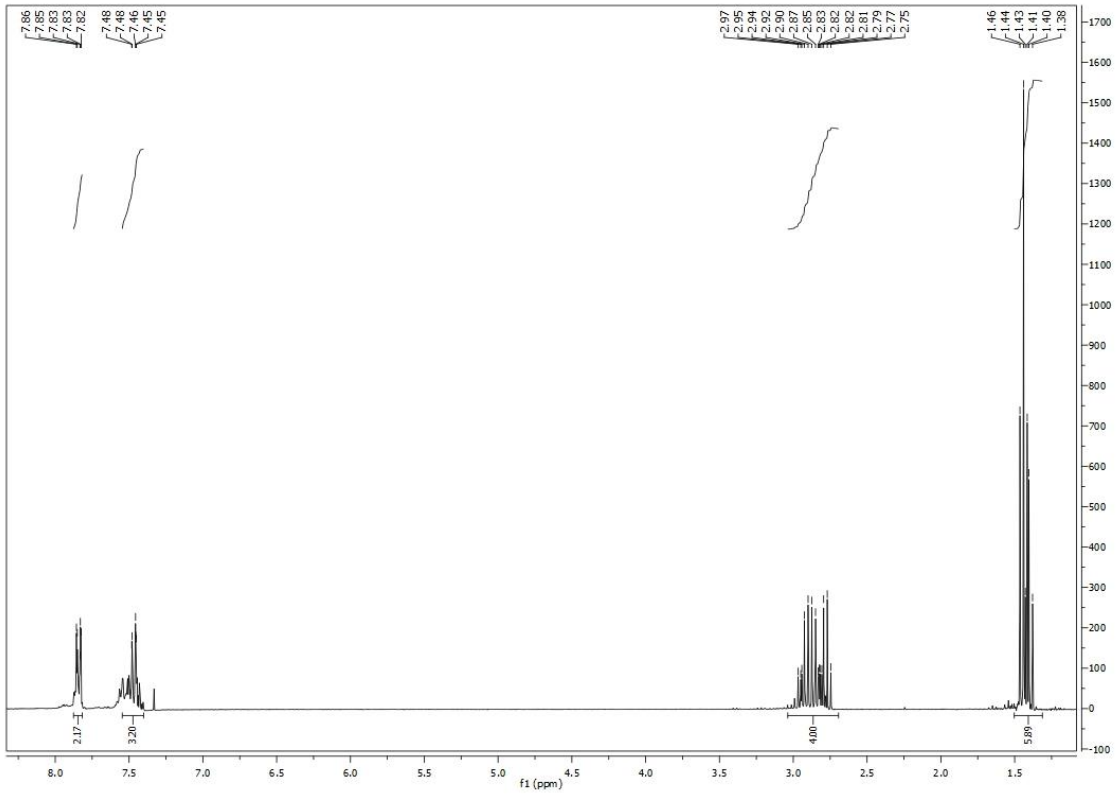

Figure 52. NMR for the reaction crude of **50**

Bis(2-aminoethyl) phenylarsonodithioite (51). $PhAsCl_2$ **41** (1.20 g, 5.00 mmol) placed in a 50 mL round bottom flask was dissolved in dry THF (20 mL), and cooled in ice bath, 2-aminoethanethiol (0.38 g, 5.00 mmol) and triethylamine (1.50 mL, 211.00 mmol) were added. The precipitate was filtered away from the reaction crude. The reaction crude was allowed to warm to room temperature slowly, after gravity filtration, the solid was washed with cold THF (2×25 mL), and the combined organic layers were evaporated and purified by Combiflash (eluting solution: heptane and acetone). However, the NMR spectrum of the product was too messy to identify the desired product.

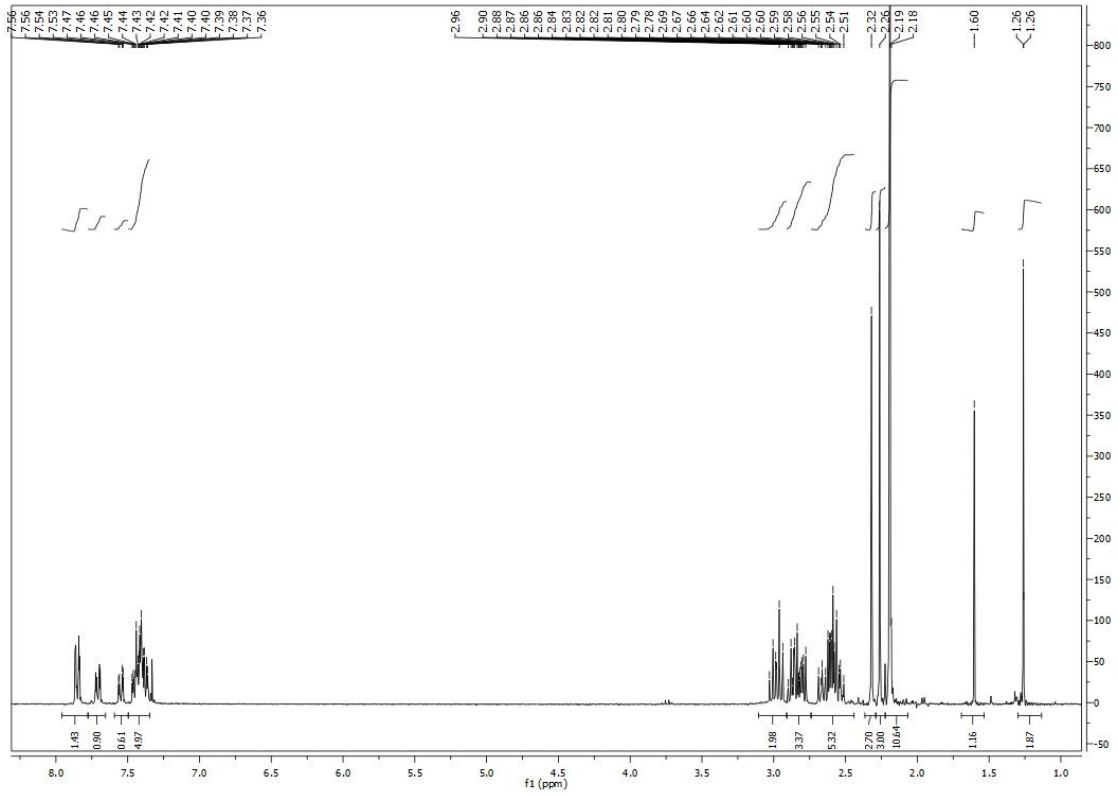

Figure 53. NMR for the reaction crude of **51**

2-phenyl-1,3,2-oxathiarsolane (52). $PhAsCl_2$ (1.20 g, 5.00 mmol) placed in a 50 mL round bottom flask was added dry ether (20 mL), and cooled in ice bath, 2-mercaptoethanol (0.39 g, 5.00 mmol) and triethylamine (1.50 mL, 211.00 mmol) were added. The reaction crude was allowed to warm to room temperature slowly, after gravity filtration, the solid was washed with ether (2×25 mL). The combined organic layers were evaporated by rotovap. The reaction residue was redissolved in a small volume of CH_2Cl_2, purified by Combiflash. (The washing procedure stated from 10% ethyl acetate in hexane at 2 min to 20% ethyl acetate in hexane at 9 min. The washing solution was held at 20% ethyl acetate in hexane for 1 min. The desired product was eluted at 2-3 min.)

2-phenyl-1,3,2-oxathiarsolan-5-one(53). $PhAsCl_2$ (1.20 g, 5.00 mmol) placed in a 50 mL round bottom flask was dissolved in dry ether (20 mL). While cooling in ice bath, 2-mercaptoacetic acid (0.46 g, 5.00 mmol) and triethylamine (1.5 mL, 211.0 mmol) were added. The reaction solution was allowed to warm to room temperature slowly, the reaction residue was diluted with ether (15 mL), and washed with aq. NaH_2PO_4 solution (10 mL) and saturated aq. NaCl solution (5 mL). The organic layer was dried over Na_2SO_4, and evaporated under vacuum, no desired product was identified in the ^{1}H-NMR spectrum.

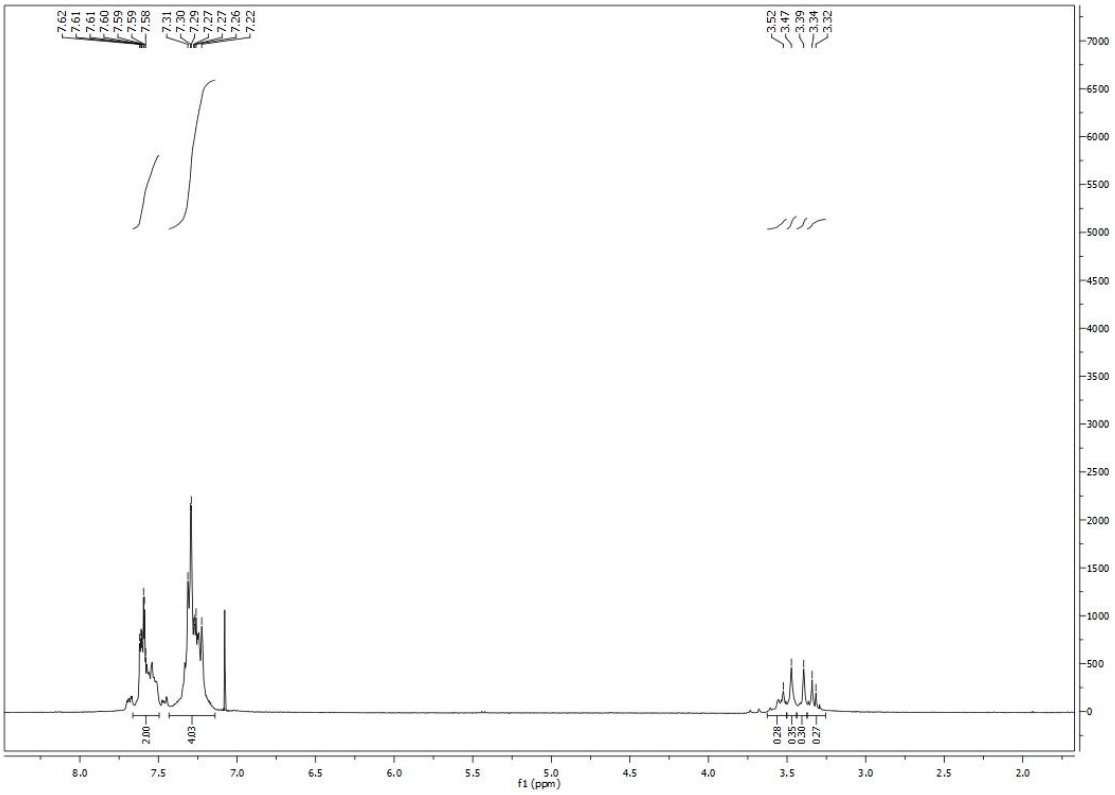

Figure 54. NMR of the reaction crude of **53**

Ethylthio(methyl)(phenyl)arsine (54). Diethyl phenylarsonodithioite (0.36 g, 1.00 mmol) was placed in a 25 ml round bottom flask with a stir bar. The flask was evacuated and refilled with nitrogen. Dry THF (5 mL) was added to the reaction crude, while cooling in liquid nitrogen and ethyl acetate (or on ice). MeMgCl solution (0.3 mL, 1.00 mmol) was added dropwise, and the reaction solution was kept in liquid nitrogen and ethyl acetate bath (or on ice). The reaction mixture was filtered, the filtrate was diluted with water, and the aqueous layer was extracted with THF (3×5 mL), and the combined organic layers were concentrated by rotary evaporator. However, the NMR spectrum of the reaction crude corresponded to the byproduct **41**.

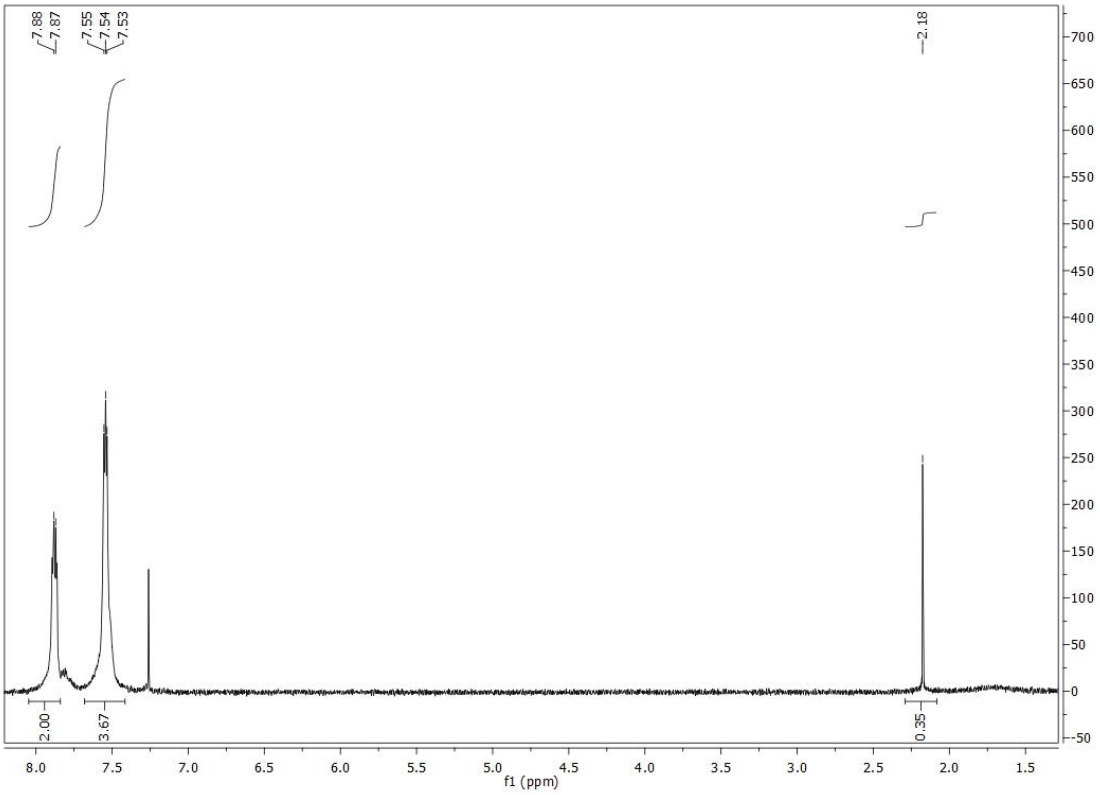

Figure 55. NMR for the reaction crude of **54**

2-[benzyl(phenyl)arsinothio]ethanamine (55). Bis(2-aminoethyl)phenylarsonodithioite (0.30 g, 1.00 mmol) was placed in a 25 mL round bottom flask with a stir bar. The flask was evacuated and refilled with nitrogen. Dry THF (5 mL) was added, and the reaction was cooled in liquid nitrogen and ethyl acetate (or on ice). Benzyl magnesium chloride solution (0.3 mL, 1.00 mmol) was added dropwise over 30 minutes. R_f (starting material) = 0.36, R_f (desired product) = 0.46, R_f ($PhAsMe_2$) = 0.61. (5% Et_3N and 10% methanol in ethyl acetate). The reaction mixture was filtered, the filtrate was diluted with water, and the aqueous layer was extracted with THF (3×5 mL), and the combined organic layers were concentrated by rotary evaporator. However, the NMR spectrum of the reaction crude corresponded to only starting material.

2-[methyl(phenyl)arsinothio]ethanamine (56). Bis(2-aminoethyl)phenylarsonodithioite (0.30 g, 1.00 mmol) was placed in a 25 mL round bottom flask with a stir bar, pumped for 5 min, and refilled with nitrogen. Dry THF (5 mL) was added, and the reaction was cooled in liquid nitrogen and ethyl acetate (or on ice). MeMgCl solution (0.3 mL, 1.00 mmol) was added dropwise over 30 minutes. The reaction mixture was filtered and diluted with water, and the aqueous layer was extracted with THF (3×5 mL).

The combined organic layers were concentrated by rotary evaporator. However, the NMR spectrum of the reaction crude corresponded to only starting material.

Lithium(2-aminoethylthio)(phenyl)arsenide (57). Bis(2-aminoethyl) phenylarsonodithioite (0.30 g, 1.00 mmol) was placed in a 25 mL round bottom flask with a stir bar, pumped for 5 min, and refilled with nitrogen. Dry THF (5 mL) was added, and the reaction was cooled in liquid nitrogen and ethyl acetate (or on ice). *n*-BuLi solution (0.60 mL, 1.00 mmol) was added dropwise, followed by TMEDA solution (0.24 g, 2.00 mmol). The reaction mixture was diluted with saturated aqueous NH_4Cl, and the aqueous layer was extracted with THF (3×5 mL), and the combined organic layers were concentrated by rotary evaporator. No desired product was identified.

2-{[methyl(phenyl)arsino]thio}ethanol(58). 2-phenyl-1,3,2-oxathiarsolane (0.46 g, 2.00 mmol) was placed in a 25 mL round bottom flask with a stir bar, pumped for 5 min, and refilled with nitrogen. Dry THF (10 mL) was added, and the reaction residue was cooled in liquid nitrogen and ethyl acetate (or on ice). MeMgCl solution (0.60 mL, 2.00 mmol) was added dropwise over 5 minutes. The reaction crude was diluted with ether (25 mL), and transferred to a separatory funnel. Saturated aq. $NaHCO_3$ solution (2.5 mL) and water (10 mL) were added, and the aqueous layer was extracted with ether (2×15 mL). The ether layers were combined and dried over Na_2SO_4, filtered and evaporated under vacuum. The NMR spectrum corresponded to the starting material.

Sodium ethanethiolate ionic solution (59). Sodium hydride (0.51 g, 20.00 mmol) was placed in a 100 mL round bottom flask, pumped for 5 min, and then refilled with nitrogen, and the procedure was repeated 3 times. Dry THF solvent (40 mL) was added to the reaction crude in ice bath, then ethanethiol (1.5 mL, 20.00 mmol) was added, and stirred for 1 h. The solution was used in the subsequent step without further purification.

Chloro(ethylthio)(phenyl)arsine (60). $PhAsCl_2$ (1.20 g, 5.00 mmol) was placed in a 50 mL round bottom flask, pumped for 5 min, then refilled with nitrogen, and the procedure was repeated 3 times. Dry THF solvent (5 mL) was added, and the reaction was cooled in ice bath. Sodium ethanethiolate ionic solution (10.00 mL, 5.00 mmol) was added, and a small amount of sample was removed with syringe every one hour, evaporated under vacuum and analyzed by NMR, and the desired product was identified in the ^{1}H-NMR spectrum of the reaction crude. ^{1}H-NMR δ (300 MHz: $CDCl_3$) 1.46 (3 H, t, J=15 Hz), 3.05 (2 H, q, J=24 Hz), 7.46 (3 H, m, J = 9 Hz), 7.79 (2 H, m, J = 9 Hz).

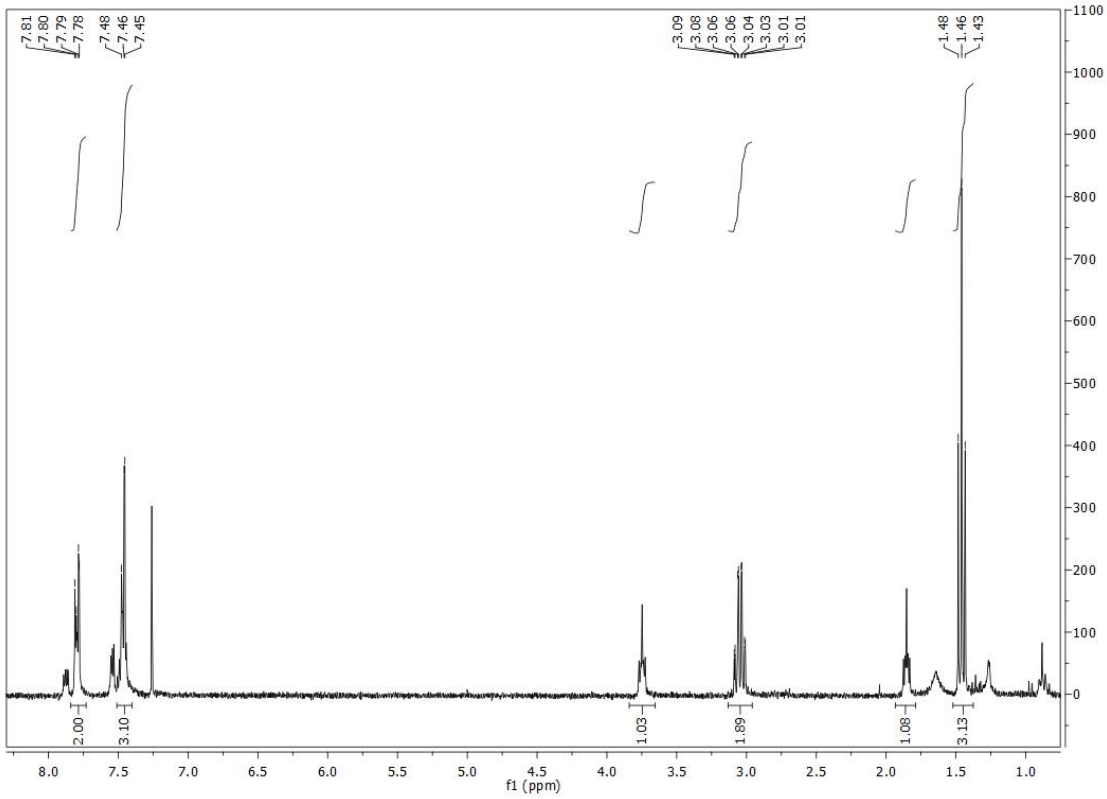

Figure 56. NMR for the reaction crude of **60**

(Ethylthio)(methyl)(phenyl)arsine (54). The above chloro(ethylthio)(phenyl)arsine was dissolved in dry THF (10 mL), and the reaction was cooled in liquid nitrogen and ethyl acetate. A THF solution of MeMgCl (1.60 mL, 5.00 mmol) was added dropwise. The reaction was warmed to room temperature, left to react overnight, evaporated under vacuum, and characterized by ^{1}H-NMR. However, no desired product was identified in the NMR spectrum.

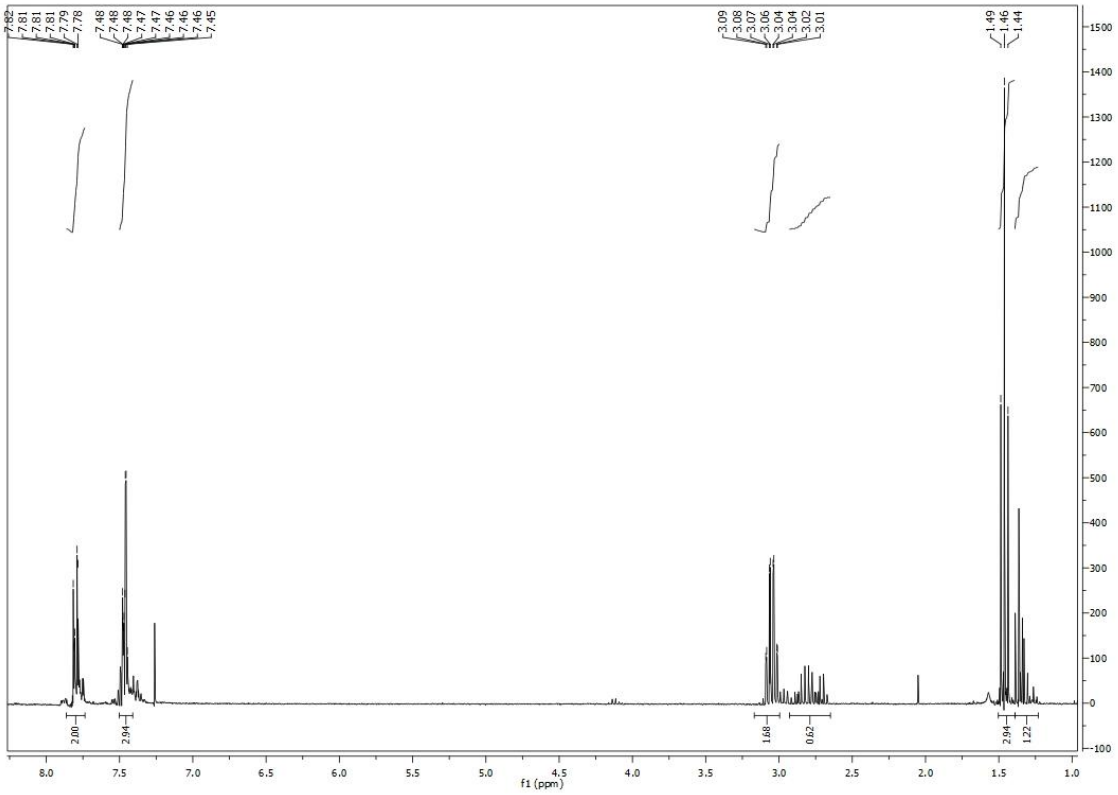

Figure 57. NMR for the reaction crude of **54**

It was attempted to separate chloro(ethylthio)(phenyl)arsine from the product mixture. The column was washed by hexane, and the separated components were analyzed by ^{1}H-NMR. However, the purification of the desired product was not successful.

Sodium 2-(dimethylamino)ethanethiolate ionic solution (61). Sodium hydride (0.51 g, 20.00 mmol) was placed in a 100 mL round bottom flask. The flask was evacuated for 5 min, then refilled with nitrogen, and the procedure was repeated 3 times. Dry THF (20 mL) was added, the solution was cooled in an ice bath, then 2-(dimethylamino)ethanethiol.HCl (1.42 g, 10.00 mmol) was added, and stirred for 1 h. The solution was used in the subsequent reaction without further purification.

2-{[chloro(phenyl)arsino]thio}-N,N-dimethylethanamine (62). $PhAsCl_2$ (1.20 g, 5.00 mmol) was placed in a 50 mL round bottom flask. The flask was evacuated for 5 min, then refilled with nitrogen, and the procedure was repeated 3 times. Dry THF (5 mL) was added, and the reaction was cooled in an ice bath. The newly synthesized sodium 2-(dimethylamino)ethanethiolate ionic solution (10.00 mL,

5.00 mmol) was added to the reaction. After 1 h the reaction crude was removed with syringe and evaporated under vacuum. The product was used in the subsequent reaction without further purification.

N,N-dimethyl-2{[methyl(phenyl)arsino]thio}ethanamine (63). The above 2-{[chloro(phenyl)arsino]thio}-N,N-dimethylethanamine solution was diluted in dry THF (10 mL). The reaction was cooled in liquid nitrogen and ethyl acetate. MeMgCl solution (1.60 ml, 5.00 mmol) was added dropwise, and then the reaction was warmed to room temperature, and left to react overnight. The reaction crude was evaporated under vacuum. However, 2-{[chloro(phenyl)arsino]thio}-N,N-dimethylethanamine **62** was separated by Combiflash. The column washing solutions were hexane, hexane: ethyl acetate = 1:1, and hexane: ethyl acetate = 3:7 sequentially.

Lithium diethylamine ionic solution. A 50 mL round bottom flask was evacuated for 5 min, then refilled with nitrogen, the procedure was repeated 3 times. Dry THF (20 mL) was added, and the reaction was kept in an ice bath. Diethylamine (0.36 g, 5.00 mmol) was added, followed by *n*-BuLi (3.10 mL, 5.00 mmol), and stirred for 1 h. The solution was used in the subsequent reaction without further purification.

1-chloro-N,N-diethyl-1-phenylarsinamine(64). $PhAsCl_2$ (0.60 g, 2.50 mmol) was placed in a 25 mL round bottom flask, evacuated for 5 min, then refilled with nitrogen, and the procedure was repeated 3 times. Anhydrous ether (3 mL) was added to the solution. The above lithium diethylamide ionic solution (10.00 mL, 2.50 mmol) was added to the reaction solution dropwise. The reaction was cooled in an ice-water bath. Vigorous stirring was maintained throughout the course of the addition. The reaction was monitored by ^{1}H-NMR. However, the NMR spectrum of the reaction crude corresponded to the byproduct N,N,N',N'-tetraethyl-1-phenylarsinediamine **70**.

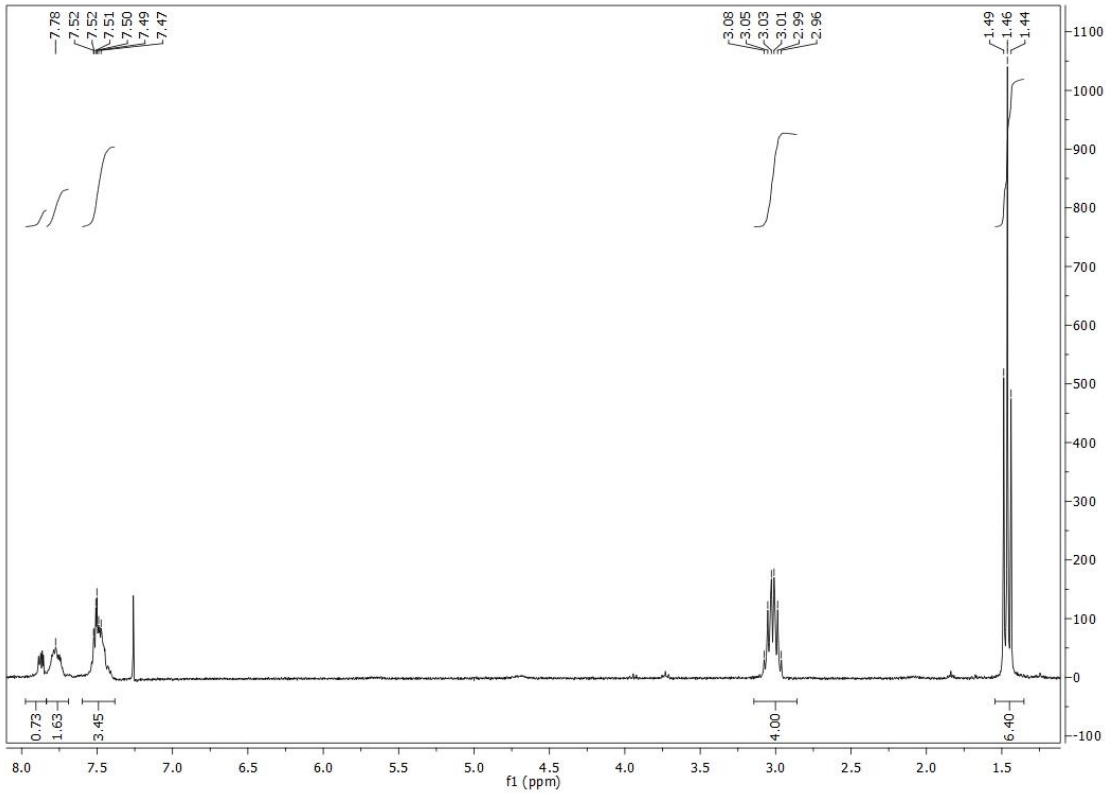

Figure 58. NMR for the reaction crude of **64**

N,N-diethyl-1-methyl-1-phenylarsinamine (65). A THF solution of MeMgCl (0.80 mL, 2.50 mmol) was added dropwise to the above 1-chloro-N,N-diethyl-1-phenylarsinamine solution, the reaction was cooled in ice bath, stirred for 2 h.[42] The reaction mixture was diluted with saturated aqueous NH_4Cl, and the aqueous layer was extracted with THF (3×5 mL) and the combined organic layers were concentrated by rotary evaporator. However, the NMR spectrum of the reaction crude corresponded to the byproduct N,N,N',N'-tetraethyl-1-phenylarsinediamine **70**.

Lithium piperidin-1-ide ionic solution (67). A 50 mL round bottom flask was evacuated for 5 min, then refilled with nitrogen, and the procedure was repeated 3 times. Dry THF (20 mL) was added, and the reaction was kept in an ice bath. Piperidine (0.43 g, 5.00 mmol), and a THF solution of *n*-BuLi (3.10 mL, 5.00 mmol) were added, and the reaction was stirred for 1 h. The solution was used in the subsequent reaction without further purification.

1-[chloro(phenyl)arsino]piperidine (68). $PhAsCl_2$ (0.60 g, 2.50 mmol) was placed in a 25 mL round bottom flask, evacuated for 5 min, then refilled with nitrogen, and the procedure was repeated 3 times.

Anhydrous THF (3 mL) and the above lithium piperidin-1-ide ionic solution (10.00 mL, 2.50 mmol) were added dropwise. The reaction was cooled in an ice-water bath. Vigorous stirring was maintained throughout the course of the addition. The reaction solution was used in the subsequent reaction without further purification.

1-[methyl(phenyl)arsino]piperidine (69). A THF solution of MeMgCl (0.80 ml, 2.50 mmol) was added dropwise to the above 1-[chloro(phenyl)arsino]piperidine solution. The reaction was cooled in ice bath and stirred for 1 h. The reaction crude was diluted with saturated aqueous NH_4Cl (10 mL) and extracted with THF (3×10 mL). However, 1-[chloro(phenyl)arsino]piperidine **68** was separated from the product mixture by Combiflash (eluting solution: heptane and acetone).

N,N,N',N'-tetraethyl-1-phenylarsinediamine (70). To a solution of diethylamine (0.73 g, 10.00 mmol) in anhydrous ether (3 mL) placed in a 25 mL round bottom flask, $PhAsCl_2$ (0.60 g, 2.50 mmol) was added dropwise over 15 minutes. The reaction was cooled in an ice-water bath. Vigorous stirring was maintained throughout the course of the addition. Voluminous amounts of diethylamide hydrochloride precipitated from the reaction crude. The reaction crude was then filtered into a specially constructed filtration apparatus under an atmosphere of nitrogen, which permitted the separation of amine hydrochloride from the ethereal N,N,N',N'-tetraethyl-1-phenylarsinediamine solution under the oxygen free and anhydrous condition. The reaction crude was analyzed by ^{1}H-NMR. However, the NMR spectrum of the reaction crude corresponded to the byproduct N,N,N',N'-tetraethyl-1-phenylarsinediamine **70**.

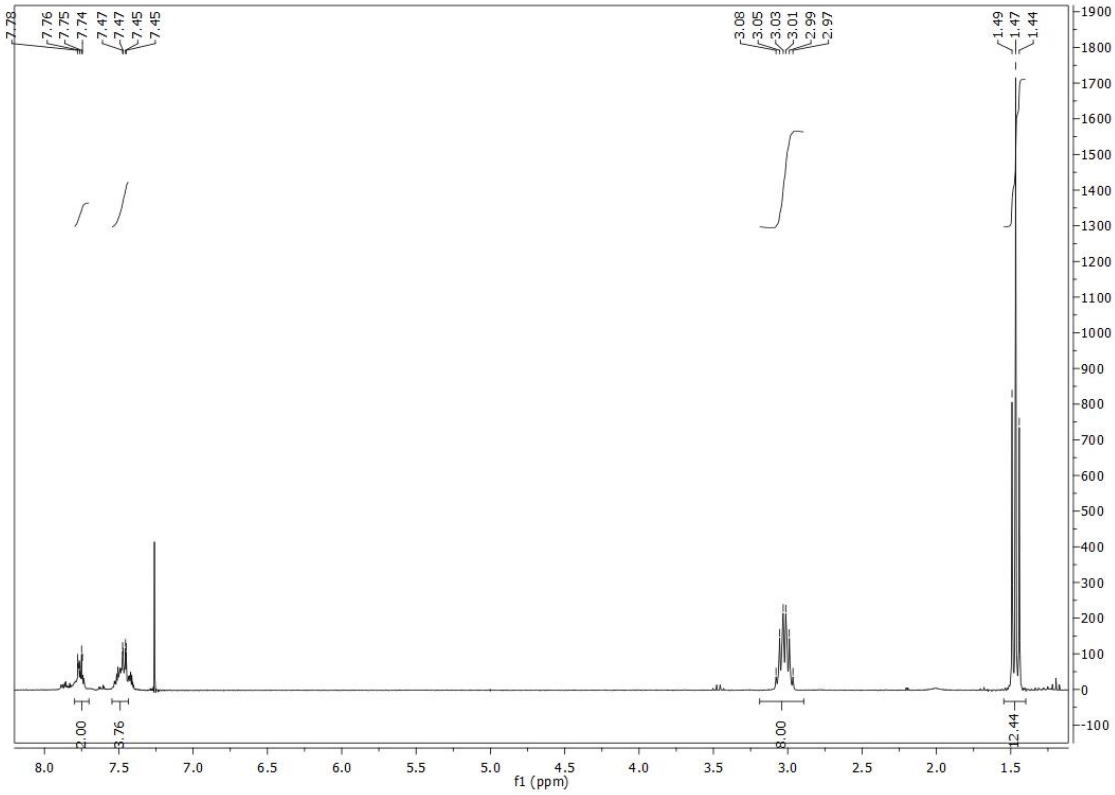

Figure 59. NMR for the reaction crude of **70**

1-chloro-N,N-diethyl-1-phenylarsinamine (64). $PhAsCl_2$ (0.60 g, 2.50 mmol) was placed in a 25 mL round bottom flask, evacuated for 5 min, then refilled with nitrogen, and the procedure was repeated 3 times. Anhydrous ether (3 mL) and diethylamine (0.35 g, 5.00 mmol) were added dropwise. The reaction was cooled in an ice-water bath. Vigorous stirring was maintained throughout the course of the addition. Voluminous amounts of diethylamine hydrochloride precipitated from the reaction crude. The reaction mixture was then filtered into a specially constructed filtration apparatus under an atmosphere of nitrogen, which permitted the separation of amine hydrochloride from the ethereal 1-chloro-N,N-diethyl-1-phenylarsinamine solution under oxygen free and anhydrous conditions. The reaction crude was analyzed by NMR spectrum and separated by Combiflsh (eluting solution: heptane and acetone). Two different substituted products were appeared in the reaction crude together with the starting material.

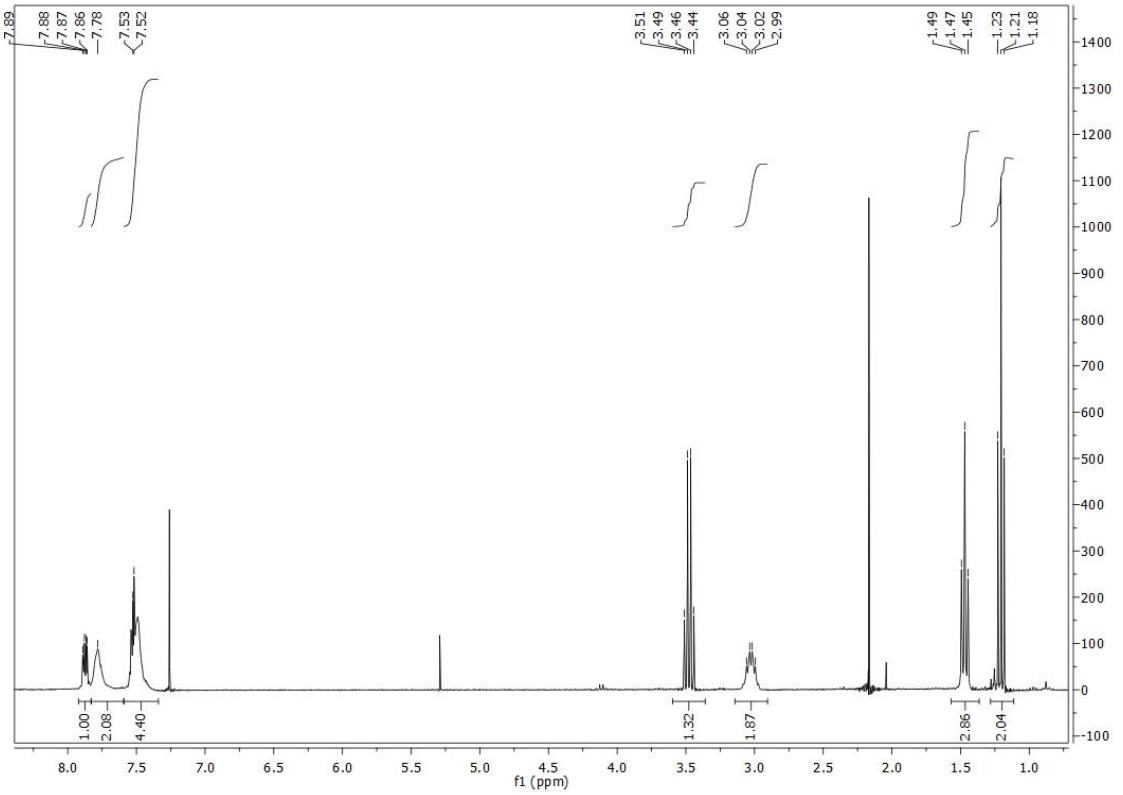
7.89
7.88
7.87
7.86
7.78
7.53
7.52
3.51
3.49
3.46
3.44
3.06
3.04
3.02
2.99
1.49
1.47
1.45
1.23
1.21
1.18
1.00
2.08
4.40
1.32
1.87
2.86
2.04
f1 (ppm)

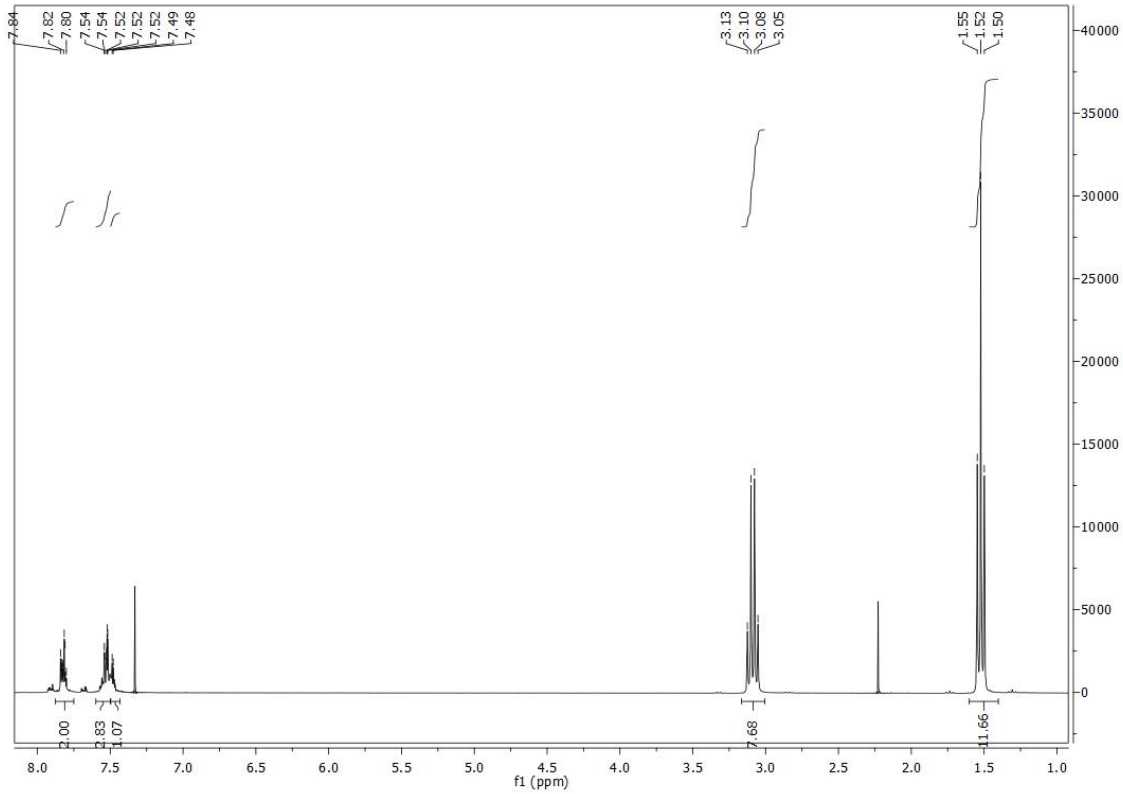
7.84
7.82
7.80
7.54
7.54
7.52
7.52
7.52
7.49
7.48
3.13
3.10
3.08
3.05
1.55
1.52
1.50
2.00
2.83
1.07
7.68
11.66
f1 (ppm)

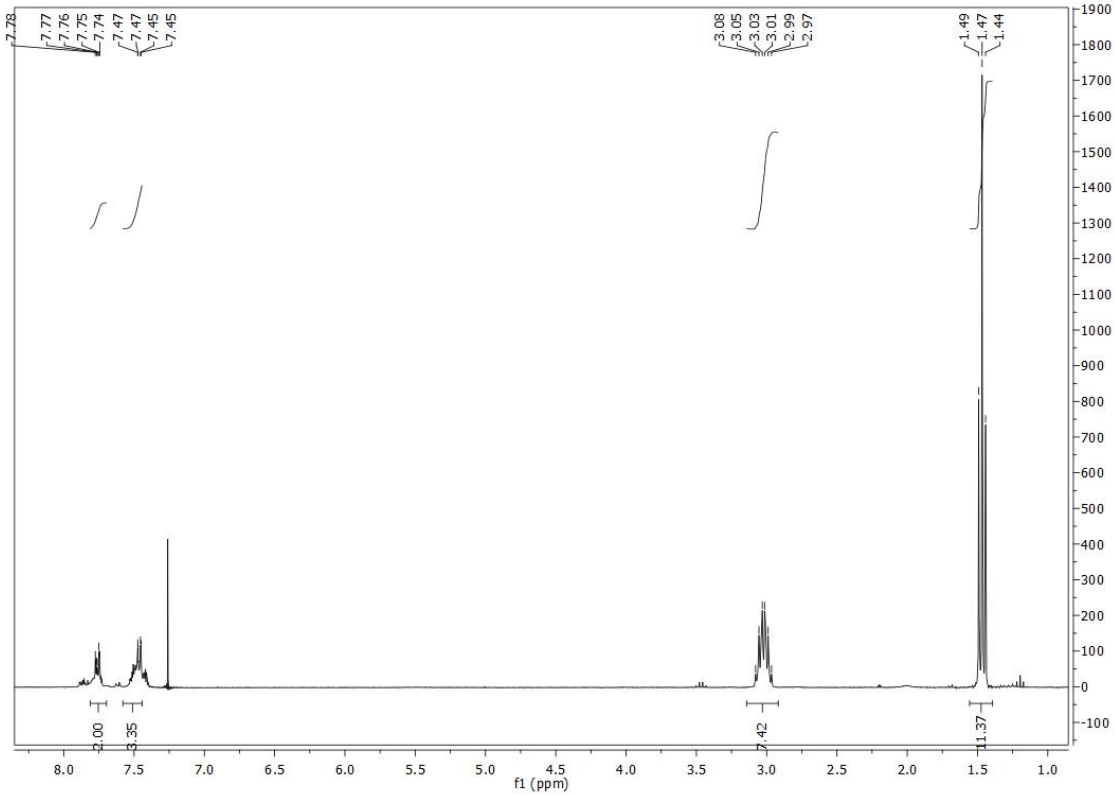

Figure 60. NMR for the reaction crude of **64**

Alternative amine introduction reaction. The above reaction was performed with 1 eq. $HNEt_2$. However, both mono and bisubstituted products, together with the starting material were identified in the NMR spectrum.

1-chloro-N,N-diethyl-1-phenylarsinamine (64). $PhAsCl_2$ (0.60 g, 2.50 mmol) was placed in a 25 mL round bottom flask, evacuated for 5 min, then refilled with nitrogen, the procedure was repeated 3 times. Anhydrous ether (3 mL), diethylamine (0.18 g, 2.50 mmol), and triethylamine (0.25 g, 2.50 mmol) were added dropwise. The reaction was cooled in an ice-water bath. Vigorous stirring was maintained throughout the course of the addition. Voluminous amounts of diethylamide hydrochloride precipitated from the reaction solution. The reaction mixture was then filtered into a specially constructed filtration apparatus under an atmosphere of nitrogen, which permitted the separation of amine hydrochloride from the ethereal 1-chloro-N,N-diethyl-1-phenylarsinamine solution under the oxygen free and anhydrous condition. The reaction crude was analyzed by NMR spectrum. ^{1}H-NMR δ (300 MHz: $CDCl_3$) 1.25 (3 H, t, J=21 Hz), 3.72 (2 H, q, J=21 Hz), 7.46 (3 H, m, J = 21 Hz), 7.75 (2 H, m, J = 9 Hz).

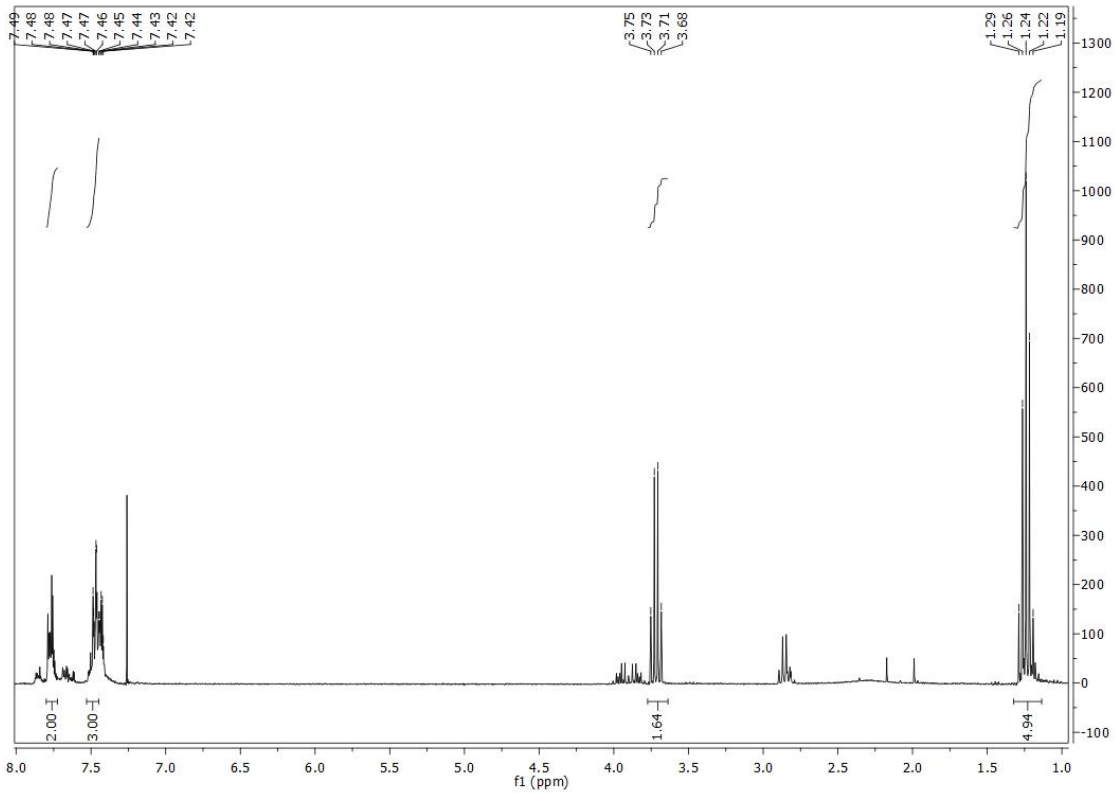
7.49
7.48
7.48
7.47
7.47
7.46
7.45
7.44
7.43
7.42
7.42
3.75
3.73
3.71
3.68
1.29
1.26
1.24
1.22
1.19
2.00
3.00
1.64
4.94
f1 (ppm)

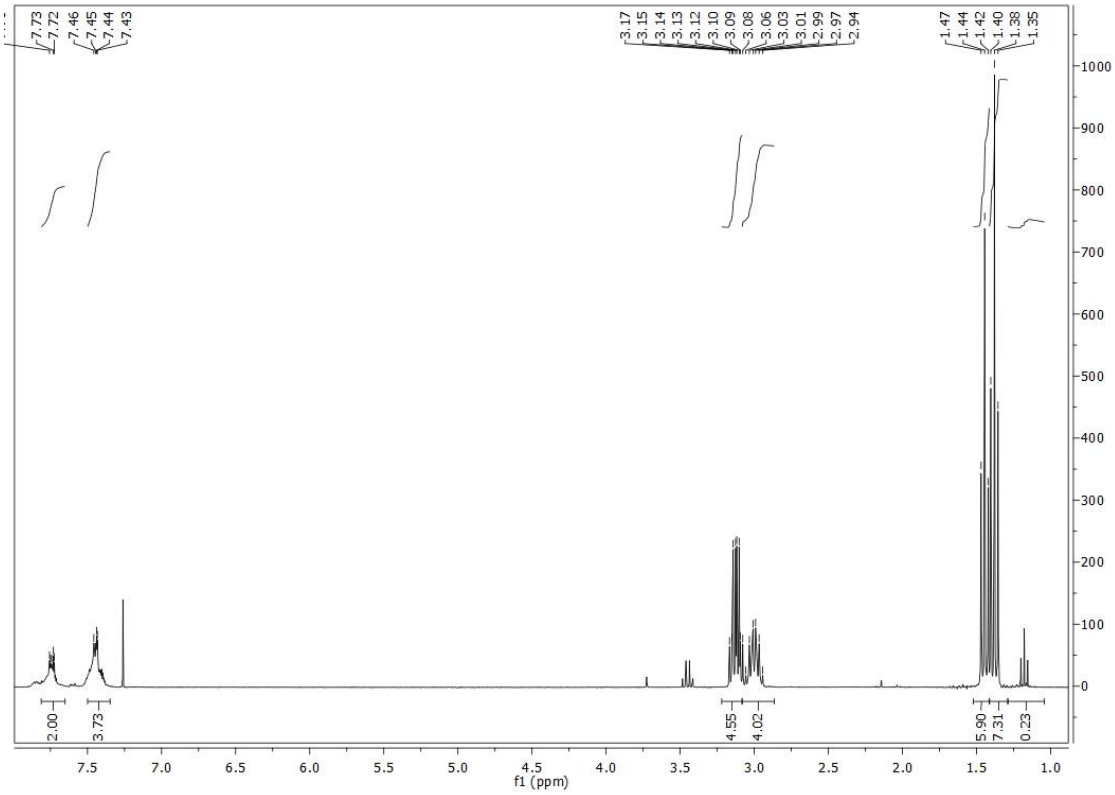
7.73
7.72
7.46
7.45
7.44
7.43
3.17
3.15
3.14
3.13
3.12
3.10
3.09
3.08
3.06
3.03
3.01
2.99
2.97
2.94
1.47
1.44
1.42
1.40
1.38
1.35
2.00
3.73
4.55
4.02
5.90
7.31
0.23
f1 (ppm)

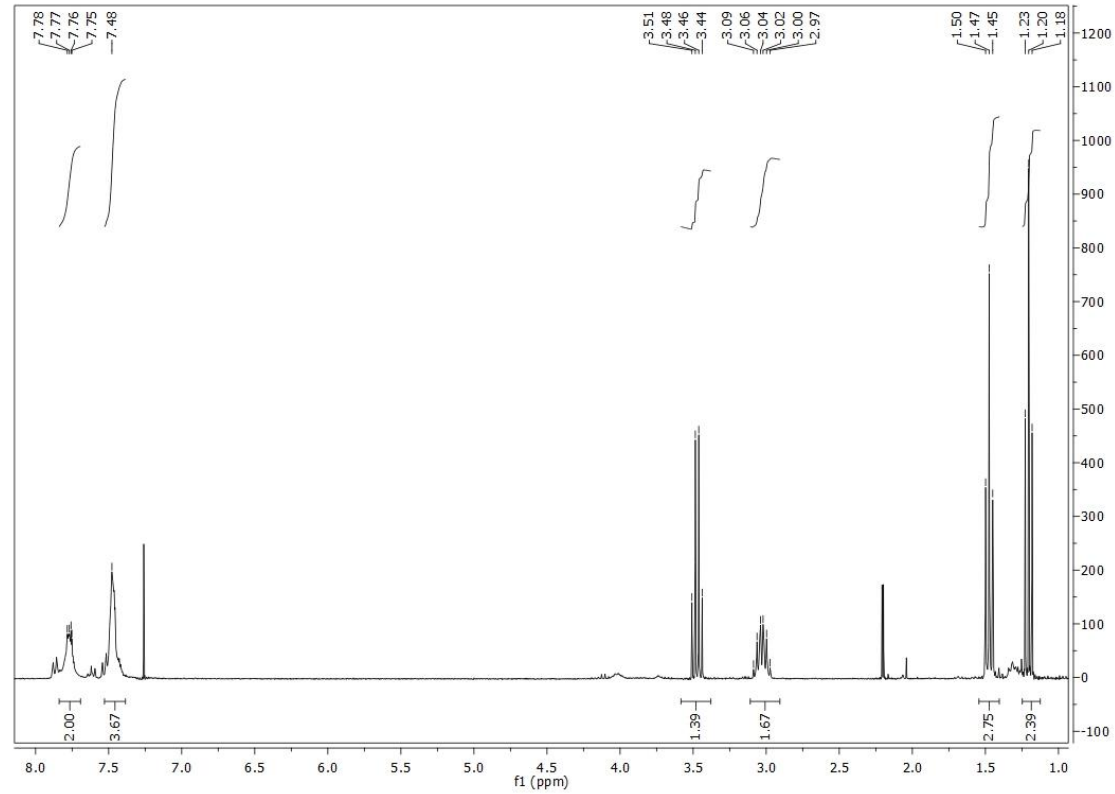
7.78
7.77
7.76
7.75
7.48
3.51
3.48
3.46
3.44
3.09
3.06
3.04
3.02
3.00
2.97
1.50
1.47
1.45
1.23
1.20
1.18
2.00
3.67
1.39
1.67
2.75
2.39
f1 (ppm)

Figure 61. NMR for the components of the reaction crude of **64**

N,N-diethyl-1,1-dimethylarsinamine (72). $(CH_3)_2AsCl$ (0.20 g, 1.50 mmol) was placed in a 25 mL round bottom flask. The flask was evacuated for 5 min, then refilled with nitrogen, and the procedure was repeated 3 times. Anhydrous ether (3 mL) or dry THF, and diethylamine (0.21 g, 3.00 mmol) were added dropwise. The reaction was cooled in an ice-water bath. Vigorous stirring was maintained throughout the course of the addition. No diethylamine hydrochloride precipitation had been recognized during the reaction. The reaction crude was analyzed by ^{1}H-NMR, but no desired product was identified.

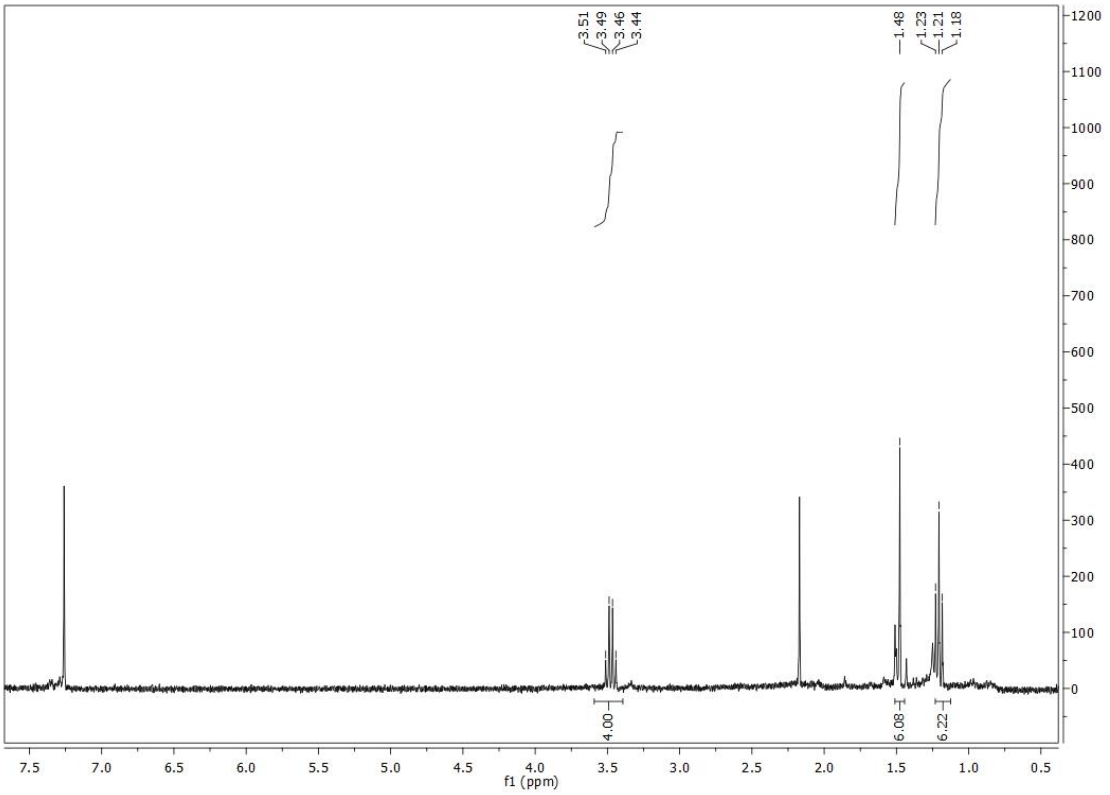

Figure 9. NMR for the reaction crude of **72**

Dibromo(methyl)arsine (73). To a suspension of cacodylic acid (2.00 g, 14.5 mmol) placed in a 25 mL round bottom flask with a stir bar was added concentrated aq. HBr (13.00 mL, 115.00 mmol, 48%). A reflux condenser was inserted and heated at 120 ℃ for about 7 h. The reaction crude was allowed to cool to room temperature overnight, extracted with CH_2Cl_2 (3 × 12 mL). Densities of the two layers were very similar, and the more colored layer is probably the aqueous layer. The combined organic layers were dried over anhydrous magnesium sulfate, filtered and evaporated under vacuum. The water

bath on the rotary evaporator was kept at room temperature to avoid evaporation of the product. The product was used in the subsequent reaction without further purification.

N-(bromo(methyl)arsino)-N-methylmethanamine(75). To a solution of CH_3AsBr_2 (0.5 g, 2.0 mmol) in THF (10 mL) was added dimethyl amine (1.4 mL, 13.5 mmol) while stirring. After several hours, precipitate of Me_2NH_2Br was allowed to settle, and filtered away. The solvent THF was evaporated by rotovap without heating. The remaining material was transferred to a smaller round bottom flask for distillation. Vacuum distillation with pump was used to purify the product. No desired product was identified in the NMR spectrum.

N-(bromo(methyl)arsino)-N-ethylethanamine (76). CH_3AsBr_2 (0.5 g, 2.0 mmol) was placed in a round bottom flask, cooled in ice bath. THF (10 mL) and diethylamine (1.4 mL, 13.5 mmol distilled before use) were added into the reaction with stirring. After 3 h stirring, and the reaction was allowed ppt. of Et_2NH_2Br to settle. The product mixture was filtered under nitrogen, and used without further purification in the subsequent reaction.

N-ethyl-N-(methyl(phenyl)arsino)ethanamine (77). The early filtrated solution was kept in an ice bath, and a THF solution of phenylmagnismchloride (2.0 M, 0.5 mL) was added while stirring. After one hour, the product mixture was removed by syringe, evaporated under vacuum, redisolved in $CDCl_3$, and analyzed by the NMR spectrum. Then a THF solution of phenylmagnesiumchloride (2.0 M in THF, 0.5 mL) was added into the reaction solution. No desired product was identified in the NMR spectrum.

N-(bromo(methyl)arsino)-N-ethylethanamine (76). To a solution of CH_3AsBr_2 (0.5 g, 2.0 mmol) and potassium carbonate (1.4 g, 2.9 mmol) placed in a round bottom flask was dissolved in ether (10 mL). Diethylamine (0.7 mL, 6.8 mmol, distilled before use) was added with stirring. The stirring was stopped after two hours, and ppt. of Et_2NH_2Br was allowed to settle, and the reaction was filtered under nitrogen. The filtered solution was achieved without evaporation, which was used in the subsequent reaction without further purification.

N-(butyl(methyl)arsino)-N-ethylethanamine (79). The above filtrated solution was kept in an ice bath, and a THF solution of *n*-butylmagnesiumchloride (1.5-2.5 M, 0.7 mL) was added while stirring for two hours. The product was removed by syringe, which was used in the subsequent reaction without further purification.

2-(butyl(methyl)arsinothio)ethanol (81). The above reaction solution was evaporated, and methanol (20 mL) was added. 2-mercaptoethanol (1.4 g, 17.9 mmol) was added while stirring for two hours. Saturated aq. ammonium chloride solution was used to dilute the product mixture, and extracted with ether. The product mixture was filtered, and used in the subsequent reaction without further purification.

N-(benzyl(methyl)arsino-N-ethylethanamine (84). Toluene (1.06 mL, 1.0 mmol) placed in a 25 mL round bottom flask was cooled in an ice bath, and ether (9 mL) was added with stirring, then *n*-butyl lithium (0.62 mL, 1.00 mmol) was added into the reaction. After one hour the filtrated solution **83** was added into the reaction in ice bath. The reaction was stirred at r.t. overnight. However, the NMR spectrum of the product crude was too messy to identify the desired product.

Synthesis of compound 88 by a coupling reaction. To a mixture of phenyl arsenic oxide (2.0 mmol) and BnCl (2.0 mmol) in H_2O (5 mL), Zn powder (2.0 mmol), $CdCl_2$ (1.0 mmol), and $InCl_3$ (0.1 mmol) were added. The reaction was stirred at r.t. for 15 h. Then the aqueous layer was extracted with EtOAc (3×10 mL) and dried over $MgSO_4$. Only starting material was recovered after evaporation.

To a mixture of dibromomethylarsenic (2.0 mmol) and BnCl (2.0 mmol) in H_2O (5 mL), Zn powder (2.0 mmol), $CdCl_2$ (1.0 mmol), and $InCl_3$ (0.1 mmol) were added. The reaction was stirred at r.t. for 15 h. Then the mixture was extracted with EtOAc (3×10 mL) and dried over $MgSO_4$. However, the NMR spectrum corresponded to only starting material.

To a well stirred solution of phenyl arsenic oxide (1.5 mmol), benzyl bromide (1.5 mmol) and $CuCl_2.2H_2O$ (4.0 mmol) in THF (10 mL) was added Mg turnings (4.0 mmol). The reaction was stirred at r.t. for 15 h. The reaction was then treated successively with water (5 mL) and EtOAc (10 mL), stirred for 10 min more and then filtered. The filtrate was treated with 2% aqueous HCl to dissolve a little amount of suspended particles. The organic layer was recovered. The aqueous layer was extracted with EtOAc. The combined organic layers were extracted with water, brine and then dried over $MgSO_4$. Only starting material was identified after evaporation.

Bromo(butyl)(methyl)arsine (89). Dibromo(methyl)arsine (0.5 g, 2.0 mmol) was dissolved in ether (10 mL) under N_2. The reaction was cooled in an ice bath, and stirred for 3 h. The reaction solution was used in the subsequent reaction without further purification.

2-(butyl(methyl)arsinothio)ethanol (90). 2-mercaptoethanol (1.6 g, 20.5 mmol) and TEA (3.0 mL, 21.5 mmol) were added into the bromo(butyl)(methyl)arsine solution under N_2. The reaction was stirred for three hours, diluted by saturated aqueous NH_4Cl (5 mL), and extracted by THF (3×10 mL). Only starting material was recovered after evaporation.

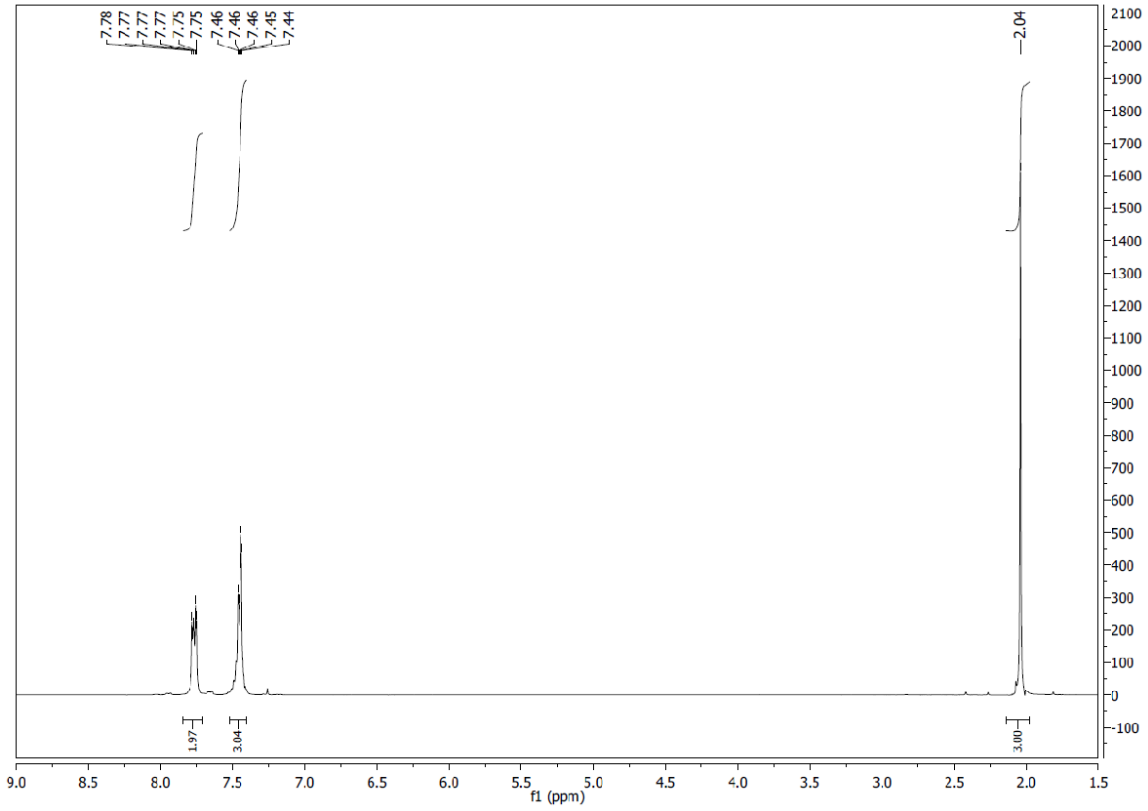

Figure 63. NMR for Bromo(methyl)(phenyl)arsine **91**

Mercuric acetate derivative of p-cresol (93). To a solution of p-cresol (4.32 g, 40 mmol) in methanol (180 mL) at room temperature was added acetic acid (2 mL) and mercuric acetate (12.8 g, 40 mmol). The reaction was heated at 70 ℃ for 24 h, and then allowed to cool to room temperature. The suspension was filtered to remove the insoluble solid, which corresponded to the 2,6-bis-mercurated product in the ^{1}H-NMR spectrum (aromatic singlet at δ 6.94 in DMSO-d_6). The filtrate was evaporated to about 10 mL, 40 mL water was added, and the mixture was cooled to 4 ℃ for 40 minutes. The resulting suspension was vacuum filtered to recover the solid product. About 20% unreacted p-cresol along with the desired monomercurated product were identified in the NMR spectrum. ^{1}H-NMR δ (300 MHz: DMSOd_6) 2.02 (3 H, s, OAc), 2.20 (3 H, s, Ar-CH_3), 6.73 (1 H, d, J = 8 Hz), 6.93 (1 H, dd, J = 2, 8 Hz),

7.01 (1 H, d, J = 2 Hz). This crude product was stable at room temperature, and was used in the subsequent step without further purification.

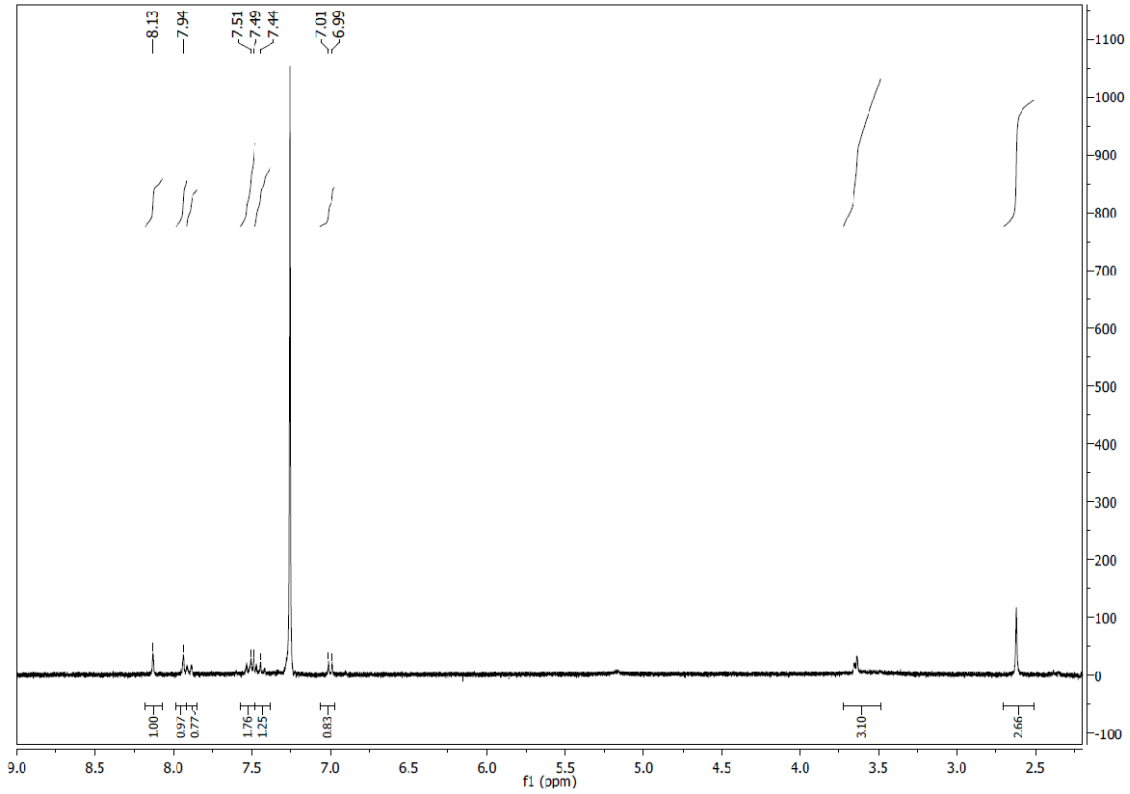

Figure 64. NMR for the mercury compound **93**

2-(bromo(methyl)arsino)-4-methylphenol(94). To a solution of the starting material (0.72 g, 2.0 mmol) in THF (15 mL) was added DIPEA (0.5 mL, 2.0 mmol), CH_3AsBr_2 (0.5 g, 2.0 mmol), and $Pd(OAc)_2$ (0.6 g, 2.0 mmol). The reaction was heated at 50 ℃ for 2 h, then cooled to r.t., and stirred at r.t. overnight. The reaction crude was poured into acetone/aqueous phosphate buffer (1:1, 0.5 M, K_2HPO_4, pH 7, 100 mL) containing ethanedithiol (3 mL). After 30 minutes of stirring, $CHCl_3$ (50 mL) was added, and the mixture was stirred for another 30 minutes. The aqueous layer was extracted with chloroform (3 × 30 mL), and the organic layers were combined. The product was used in the subsequent reaction without further purification.

2-((2-hydroxyethylthio)(methyl)arsino)-4-methylphenol(95). To a 100 mL round bottom flask containing the crude mercuric acetate derivative of p-cresol **(93)** (0.54 g, 1.47 mmol) and palladium(II) acetate trimer (8 mg, 0.036 mmol Pd) was added a THF solution of methylarsenic dibromide (1.30 g,

5.0 mmol, 17 mL) under N_2. Diisopropylethylamine (1.20 mL, 7.5 mmol) was added into the reaction and stirred at room temperature for 18 h. The reaction crude was poured into a solution of 2-mercaptoethanol (0.80 mL, 0.89 g, 11.4 mmol) in aq. sodium phosphate (70 mL, 0.25 M, pH 7.0) and acetone (70 mL). The mixture was stirred at room temperature for 1 h and extracted with ether (3 × 50 mL). The combined organic layers were dried over $MgSO_4$, evaporated under vacuum, and purified by chromatography on silica gel (25 to 65% acetone in heptane) to recover the desired product as white powder (0.23 g, 0.84 mmol, 57%). ^{1}H-NMR data was in agreement with literature values, ^{1}H-NMR δ H (300 MHz: $CDCl_3$) 1.62 (3 H, s, As-CH_3) 2.28 (3 H, s, Ar-CH_3) 2.92 (2 H, t, J = Hz, S-CH_2) 3.79 (2 H, m, CH_2-OH) 6.75 (1 H, d, J = 8.1 Hz) 7.05 (1 H, dd, J = 2, 8.1 Hz) 7.20 (1 H, d, J = 2 Hz). ^{13}C-NMR (75 MHz, $CDCl_3$): δ =11.80 (CH_3As) 20.50 (CH_2S) 34.96 (Ar-CH_3) 62.87 (CH_2O) 116.29 (CH) 124.88 (C) 130.30(CH) 31.78 (C) 132.24 (CH) 156.46 (C); HRMS (ESI): m/z calculated for $C_{10}H_{15}AsO_2S$ [M-H]$^-$: 272.9936; found: 272.9939.

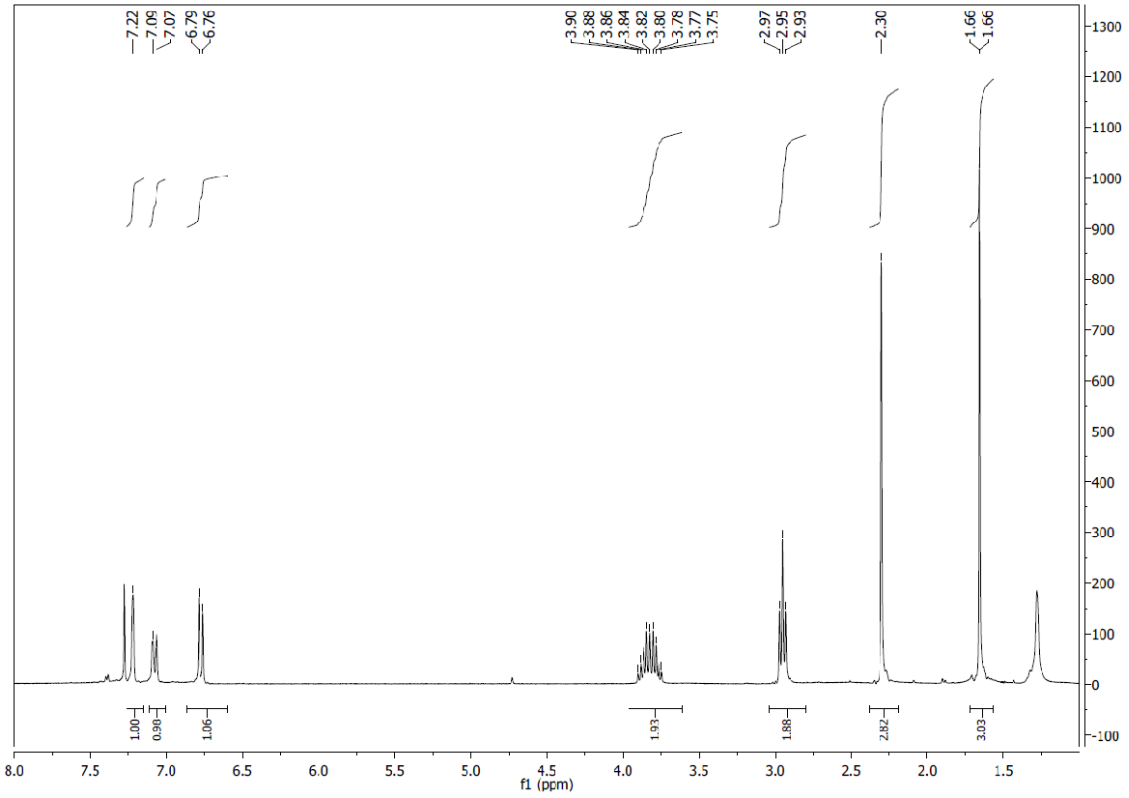

Figure 65. NMR for 2-((2-hydroxyethylthio)(methyl)arsino)-4-methylphenol **95**

2-(hydroxy(methyl)arsino)-4-methylphenol (96). Compound **95** (0.0079 g, 28.5 μmol) was dissolved in 8 drops methanol in a test tube, and then a solution of silver nitrate in methanol (1.25 mL, 0.025 M,

31.25 μmol) was added with immediate formation of a light yellow precipitate. After 30 minutes, a solution of lithium chloride in methanol (50 μL, 0.2 M, 10 μmol) was added. After 10 minutes the suspension was filtered through a cotton plug, the filtrate was evaporated, and the residue was dissolved in DMSO-d_6 (0.7 mL). ^{1}H-NMR δ H (300 MHz: DMSO-d_6) 1.46 (3 H, s, As-CH_3) 2.20 (3 H, s, Ar-CH_3), 6.68 (1 H, d, J = 8 Hz) 6.99 (1 H, dd, J = 2, 8 Hz) 7.26 (1 H, d, J = 2 Hz). 0.1 mL of the solution was mixed with 0.5 mL D_2O and 0.1 mL of a 0.021 M solution of pinacol in D_2O and the concentration of the desired product in the NMR sample was determined to be 0.026 M by relative integration of the ^{1}H-NMR signals of the desired product and the methyl singlet of pinacol at δ 1.05. This corresponded to a total yield of desired product of 18.5 μmol (59%).

Ethyl-3,5-dihydroxy-2-naphthoate (105). To a solution of 3,5-dihydroxy-2-naphthoic acid (1.00 g, 4.90 mmol) in EtOH (20 mL) was carefully added concentrated aq. H_2SO_4 (1.0 mL). The reaction mixture was heated under reflux for 6 h, and poured into water (250 ml) after cooling to room temperature. Saturated aq. $NaHCO_3$ (100 mL) was added and the mixture was extracted with CH_2Cl_2 (3× 50 mL). NMR data was in agreement with literature values, ^{1}H-NMR ($CDCl_3$) δ 1.47 (t, 3H) (J=12Hz) 4.52 (q, 2H) (J=21Hz) 7.70 (s, 2H) 7.96 (s, 1H) 8.04 (d, 1H) (J=6Hz) 8.74 (s, 1H).

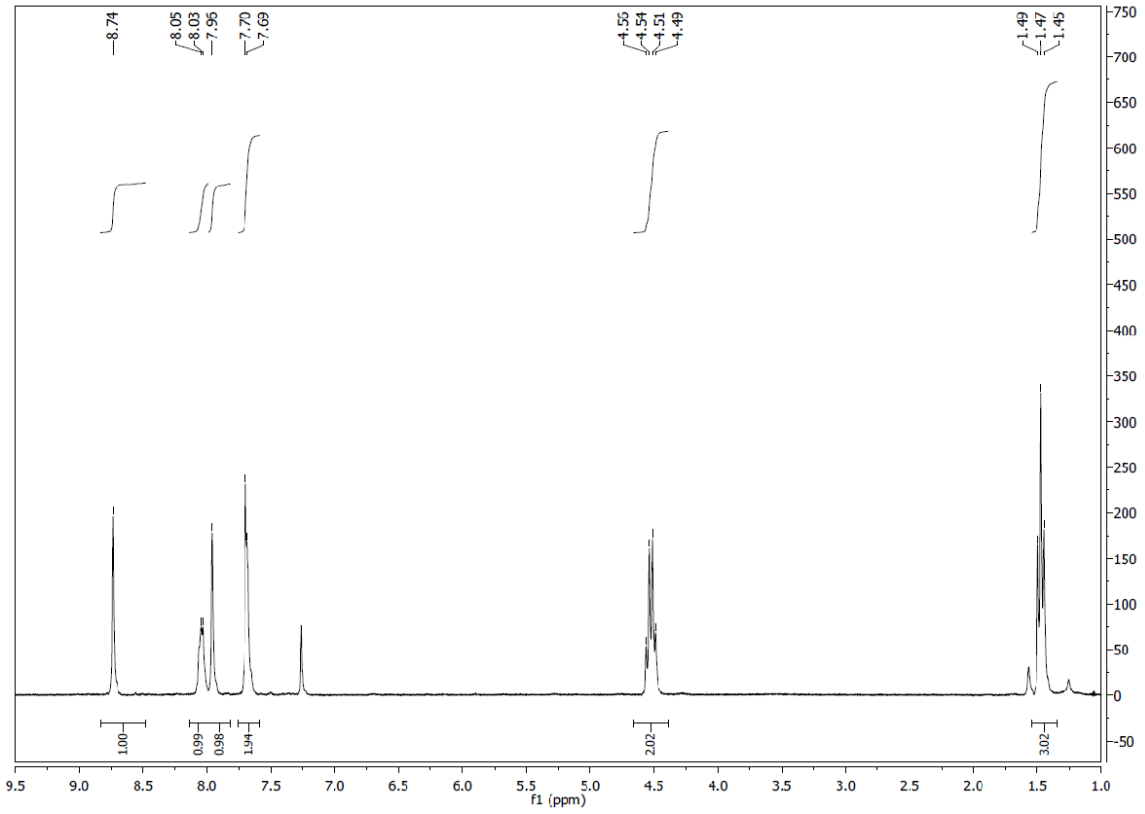

Figure 66. NMR for ethyl-3,5-dihydroxy-2-naphthoate **105**

Ethyl-3,5-bis(trifluoromethylsulfonyloxy) (106). To a solution of ethyl-3,5-dihydroxy-2-naphthoate (1.50 g, 6.40 mmol) in CH_2Cl_2 was added pyridine (2.00 mL, 25.80 mmol), and the solution was stirred at r.t. for 10 min under N_2, then Tf_2O (2.60 mL, 15.30 mmol) was added at -78 ℃, and the reaction was allowed to warm to r.t. and stirred for 14 h. The reaction mixture was filtered and the filtrate was concentrated under vacuum. ^{1}H-NMR data was in agreement with literature values, ^{1}H-NMR ($CDCl_3$) δ 1.51 (t, 3H) (J=15Hz) 4.52 (q, 2H) (J=24Hz) 7.30 (t, 1H) 7.49 (m, 2H) (J=6Hz) 7.81 (d, 1H) (J=9Hz) 8.53 (s, 1H)

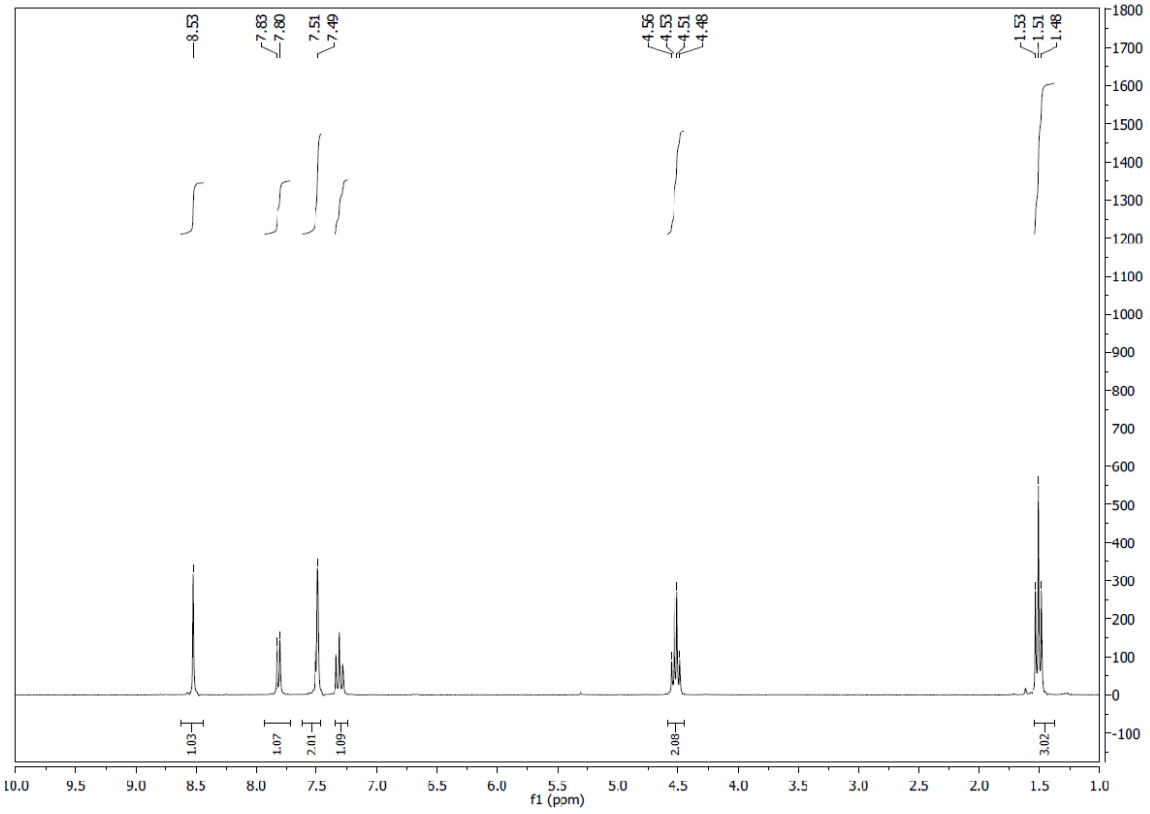

Figure 67. NMR for Ethyl-3,5-bis(trifluoromethylsulfonyloxy) **106**

Ethyl-3,5-bis(4-methoxy-3-methylphenyl)-2-naphthoate (107). A suspension of bitriflate (0.10 g, 0.20 mmol), K_3PO_4 (1.50 mmol per cross-coupling step), $Pd(PPh_3)_4$ (3 mol% per cross-coupling step), and arylboronic acid (1.0-1.2 equiv per cross-coupling step) in dioxane (4 mL) was stirred at 108 ℃ for 8-12 h, water (25 mL) and CH_2Cl_2 (25 mL) were added to the reaction solution at 20 ℃. The organic and aqueous layers were separated and the latter was extracted with CH_2Cl_2 (2×25 mL). The combined organic layers were dried over magnesium sulfate, filtered, and the filtrate was concentrated under vacuum. The residue was purified by column chromatography (eluting solution: heptane and acetone) and identified by NMR spectrum. ^{1}H-NMR ($CDCl_3$) δ 1.14 (t, 3H) (J=12Hz) 2.25 (s, 3H) 2.31 (s, 3H) 3.87 (s, 3H) 3.92 (s, 3H) 4.22 (q, 2H) (J=12Hz) 6.86 (d, 1H) 6.96 (m, 1H) 7.14 (s, 1H) 7.28 (m, 1H) 7.54 (m, 2H) 7.92 (m, 1H) (J=9Hz) 8.06 (s, 1H) 8.38 (d, 1H).

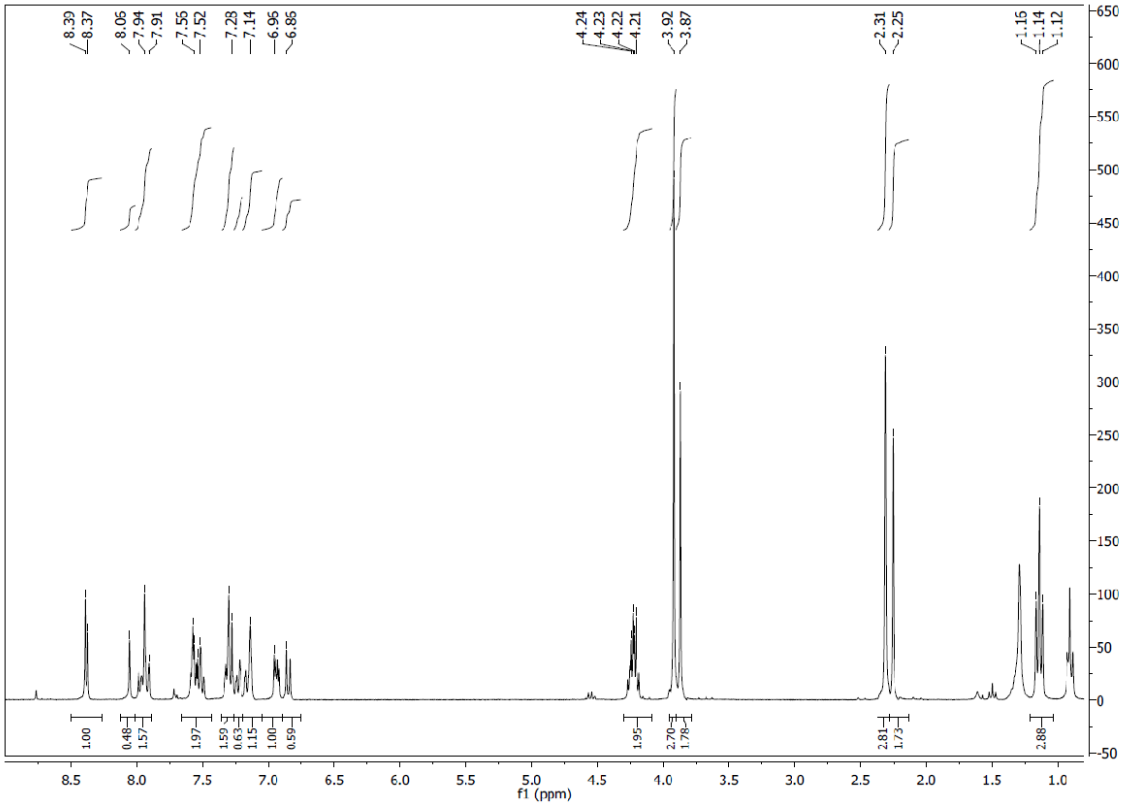

Figure 68. NMR for Ethyl-3,5-bis(4-methoxy-3-methylphenyl)-2-naphthoate **107**

Ethyl-3,5-bis(4-hydroxy-3-methylphenyl)-2-naphthoate (108). The starting material (0.28 g, 0.60 mmol) was dissolved in DMF (4 mL), and iodocyclohexane (1.30 ml, 10.00 mmol) was added dropwise. The reaction solution was heated up to 150 ℃ and stirred overnight. The reaction solution was poured into water (20 mL) after cooling to room temperature. Ethyl acetate (3×20 mL) was used to extract the aqueous layer, washed by $NaHCO_3$ and brine. The combined organic layers were dried over magnesium sulfate, filtrated, evaporated under vacuum, and identified by NMR. ^{1}H-NMR ($CDCl_3$) δ 1.16 (t, 3H) (J=12Hz) 2.24 (s, 3H) 2.32 (s, 3H) 4.24 (q, 2H) (J=21Hz) 6.75 (d, 1H) (J=6Hz) 6.86 (d, 1H) (J=6Hz) 7.02 (d, 1H) 7.10 (s, 1H) 7.21 (m, 1H) 7.28 (m, 1H) (J=9Hz) 7.50 (m, 2H) 7.91 (s, 1H) 8.39 (s, 1H).

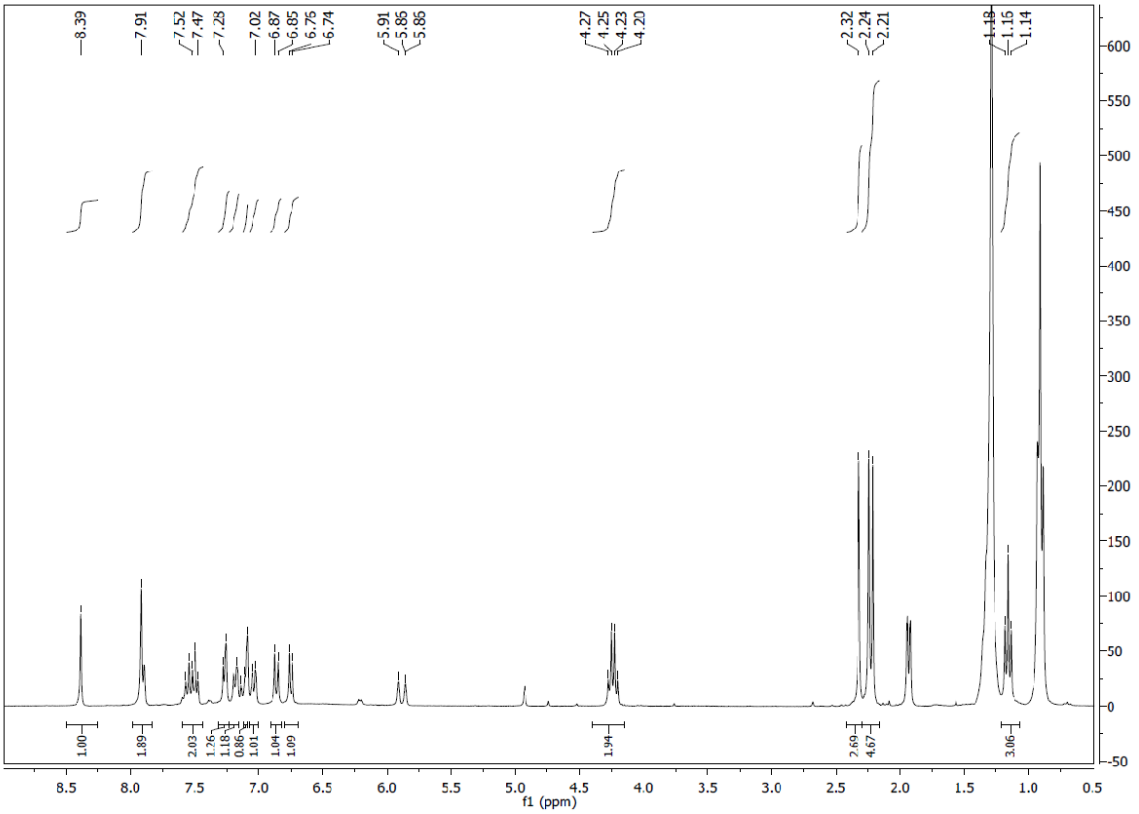

Figure 69. NMR for Ethyl-3,5-bis(4-hydroxy-3-methylphenyl)-2-naphthoate **108**

The mercury material (109). To a solution of ethyl-3,5-bis(4-hydroxy-3-methylphenyl)-2-naphthoate (0.41 g, 1.00 mmol) in methanol (10 mL) was added mercuric acetate (0.64 g, 2.0 mmol). The reaction was heated to 80 ℃, then decreased to 65 ℃, and white precipitate was formed while heating. The precipitate was removed by vacuum filtration, concentrated to about 2.0 mL, more solid was formed from the reaction solution. Vacuum filtration was used to isolate the filtrate, filtrate volume was reduced to about 1.0 mL. Then 2.0 mL water was added to the filtrate, kept in refrigerator for 4 h, solid was isolated by vacuum filtration. The solid was left dry in open air overnight, and identified by NMR. However, the NMR spectrum was too messy to identify the desired product.

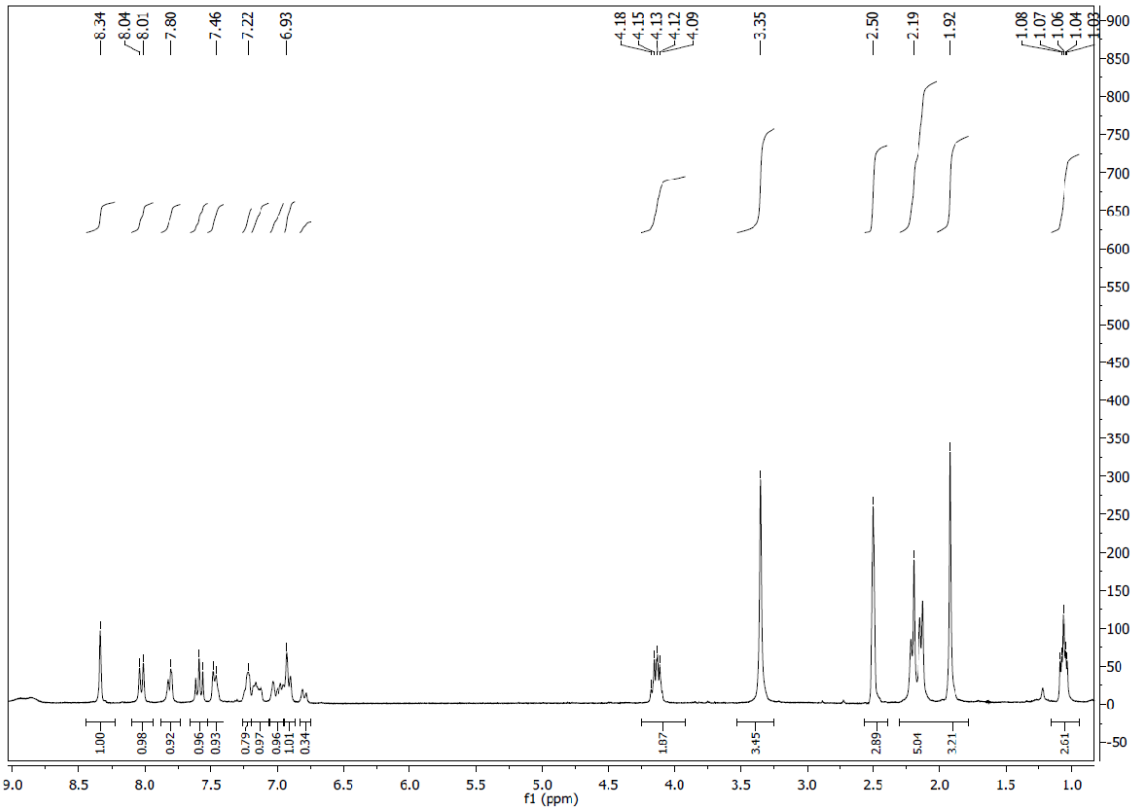
8.34
8.04
8.01
7.80
7.46
7.22
6.93
4.18
4.15
4.13
4.12
4.09
3.35
2.50
2.19
1.92
1.08
1.07
1.06
1.04
1.03
1.00
0.98
0.92
0.96
0.93
0.79
0.97
0.96
1.01
0.34
1.87
3.45
2.89
5.04
3.21
2.61
f1 (ppm)

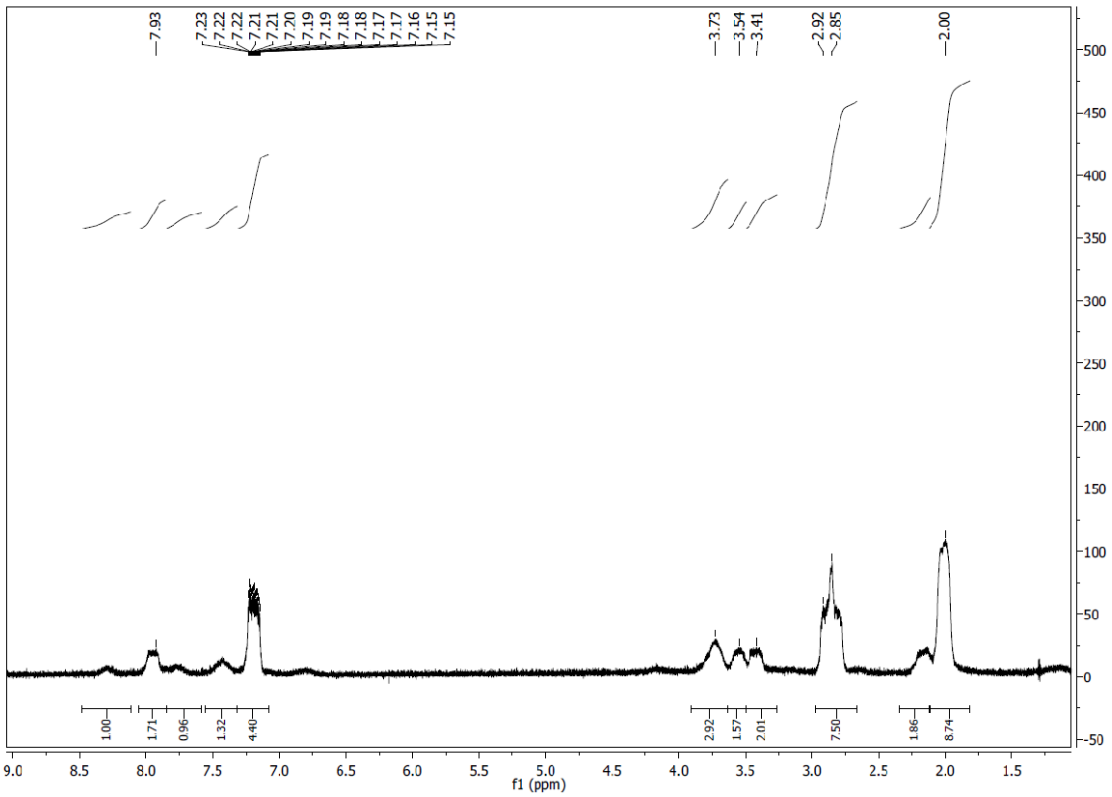

Figure 70. NMR for the mercury compound **109**

i, i+4 probe (102). To a solution of the starting material (0.93 g, 1.00 mmol) in THF (15 mL) was added DIPEA (0.50 mL, 2.00 mmol), CH_3AsBr_2 (0.50 g, 2.00 mmol), and $Pd(OAc)_2$ (0.60 g, 2.00 mmol). The reaction was heated at 50 ℃ for 2 h, and cooled to r.t., and left stirring at r.t. overnight. The reaction mixture was poured into acetone/aqueous phosphate buffer (1:1, 0.5 M, K_2HPO_4, pH 7, 100 mL) containing ethanedithiol (3 mL). After 30 min of stirring, $CHCl_3$ (50 mL) was added, and the reaction residue was stirred for another 30 min. The organic layer was separated, and the aqueous layer was extracted with chloroform (3 × 30 mL). The combined organic layers were dried over magnesium sulfate, filtrated, and evaporated under vacuum. No desired product was identified in the NMR spectrum.

1,7-dimethoxynaphthalene(115): To a freshly prepared solution of 1,7-dihydroxynaphthalene **(114)** (1.0 g, 6.25 mmol) in 10% aqueous solution of potassium hydroxide (0.77 g, 13.7 mmol), was added dimethyl sulfate (1.81 g, 14.4mmol) portion-wise with stirring. The reaction was heated for 2 hours in a water-bath, and then potassium hydroxide (0.2 g, 3.6 mmol) was added, followed by one equivalent amount of dimethyl sulfate (0.34 mL, 0.45 g, 3.6 mmol). After cooling and basification with more potassium hydroxide, the reaction crude was extracted with ether, the ether layer was dried over

magnesium sulfate, and the solvent was removed by rotovap to recover the desired product as pale yellow oil (0.67g, 60%). ^{1}H-NMR data was in agreement with literature values, ^{1}H-NMR: δ 3.95 (s, 3H) 4.01 (s, 3H) 6.82 (d, 1H) (J=7.8Hz) 7.16 (dd, 1H) (J=9Hz) 7.24 (d, 1H) (J=7.8Hz) 7.38 (d, 1H) (J=7.8Hz) 7.55 (d, 1H) (J=2.4) 7.71 (d, 1H) (J=9Hz).

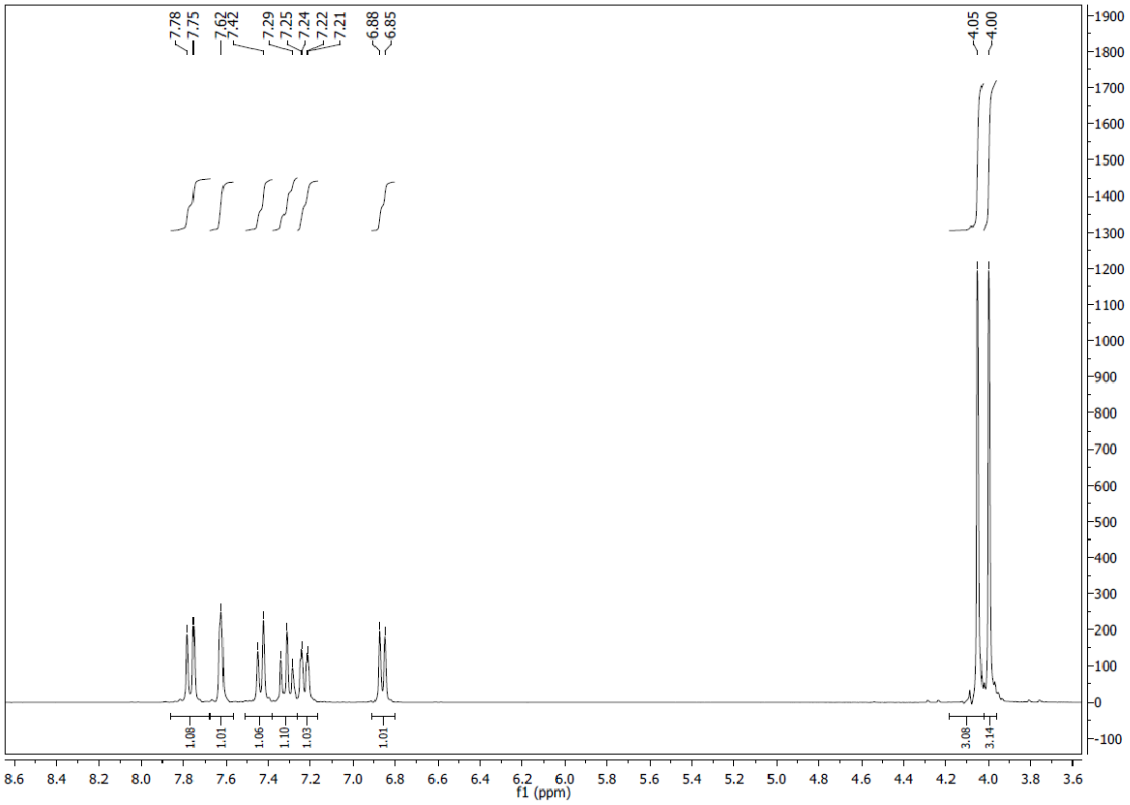

Figure 71. NMR for 1,7-dimethoxynaphthalene **115**

4,6-dimethoxy-1-naphthaldehyde(116): A mixture of 1,7-dimethoxynaphthalene (0.5 g, 2.66 mmol), dimethylformamide (0.25 g, 0.26 mL, 3.42 mmol), and phosphorus oxychloride (0.47 g, 0.28 mL, 3.00 mmol) were reacted for 5 hours. A saturated aqueous solution of sodium acetate (10 mL) was added, and the mixture was refluxed for 30 minutes; after cooling, the reaction product was taken up in ethyl acetate (10 mL), and the organic layer was extracted with dilute aqueous hydrochloric acid (10 mL), water (2×10 mL), dried over magnesium sulfate. After evaporation of solvent yellowish needle crystal (0.46 g, 80%) was recovered. ^{1}H-NMR data was in agreement with literature values, ^{1}H-NMR ($CDCl_3$) δ 3.95 (s, 3H) 4.10 (s, 3H) 6.93 (d, 1H) (J=8.1) 7.36 (dd, 1H) (J=9.3Hz J=3Hz) 7.61 (d, 1H) (J=3Hz) 7.79 (d, 1H) (J=7.8Hz) 9.23 (d, 1H) (J=8.7) 10.15 (s, 1H).

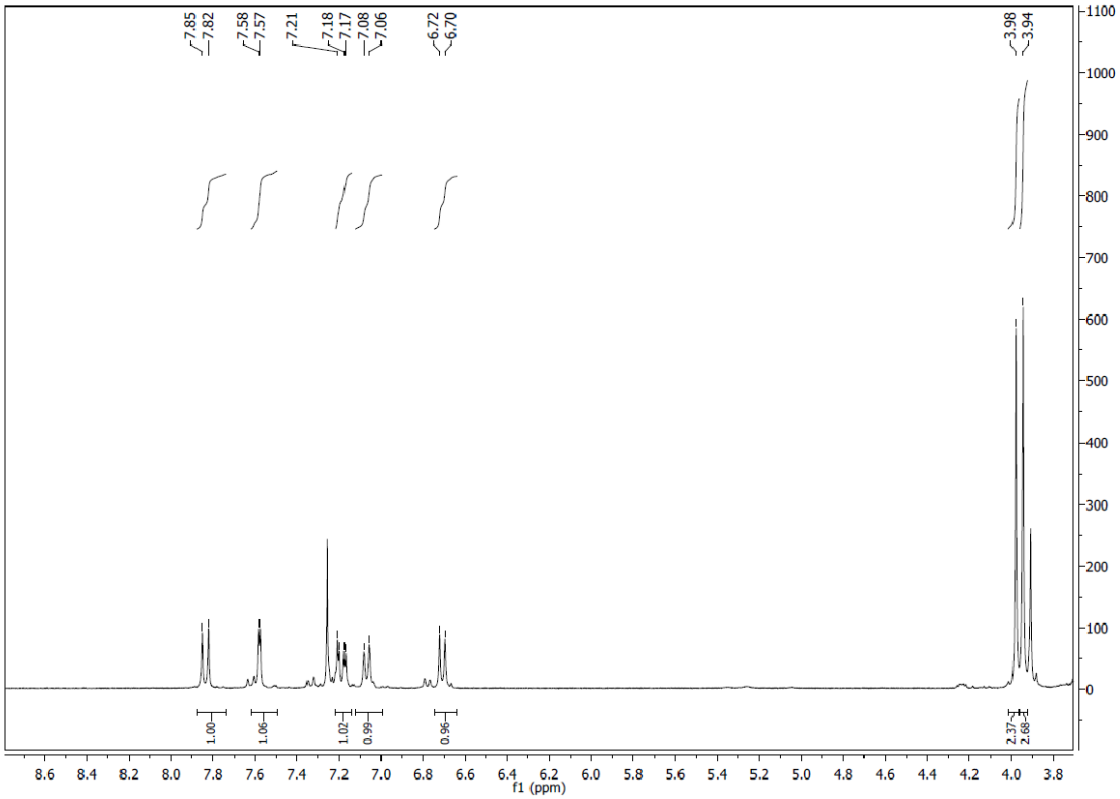

Figure 72. NMR for 4,6-dimethoxy-1-naphthaldehyde **116**

4,6-dimethoxy-1-methylnaphthalene(117): To a solution of 4,6-dimethoxy-1-naphthaldehyde (0.22 g , 1.00 mmol), and 98% hydrazine (0.19 mL, 6.00 mmol) in diethylene glycol (5 mL), KOH (0.80 g, 14.26 mmol) was added, and heated until fully dissolved. The reaction residue was boiled to reflux for 15h. After cooling, water (5 mL) was added and the reduction product was extracted by ethyl acetate (10 mL). The organic layer was extracted with dilute aq. HCl (10 mL) and water (2 × 10 mL). The organic layer was dried over sodium sulfate and evaporated to give a yellowish solid (0.14g, 68.1%). ^{1}H-NMR data was in agreement with the literature values, ^{1}H-NMR ($CDCl_3$) δ 2.58 (s, 3H) 3.95 (s, 3H) 3.98 (s, 3H) 6.71 (d, 1H) (J=8.1Hz) 7.07 (d, 1H) (J=7.5Hz) 7.20 (dd, 1H) (J=9Hz J=2.7Hz) 7.57 (s, 1H) 7.83 (d, 1H) (J=9.3Hz).

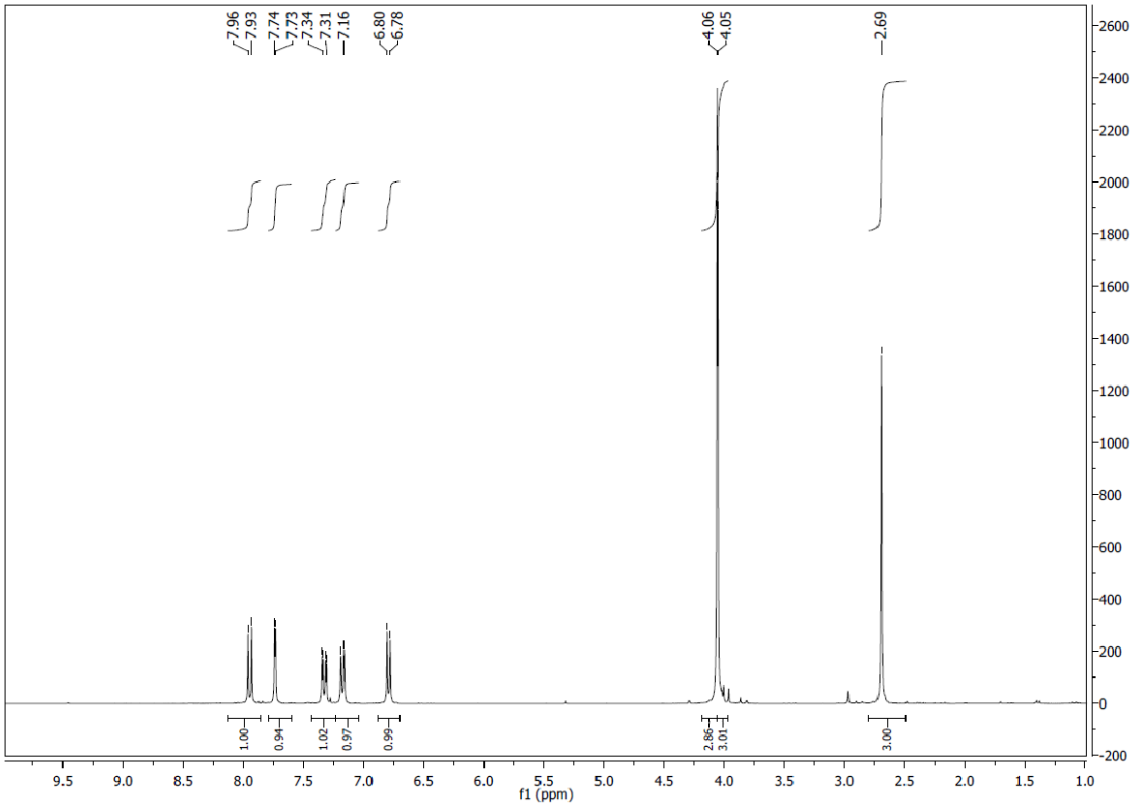

Figure 73. NMR for 4,6-dimethoxy-1-methylnaphthalene **117**

2,8-dimethoxyl-5-methyl-1-naphthaldehyde (118). A mixture of 4,6-dimethoxy-1-methylnaphthalene (0.45 g, 2.22 mmol), dimethylformamide (0.60 mL, 7.70 mmol), and phosphorus oxychloride (0.60 mL, 6.33 mmol) was dissolved in toluene (1.20 mL), and heated for 15h at 105 ℃, and the reaction mixture was worked up same as compound **116,** and the organic layer was dried over sodium sulfate and evaporated to give a colorless solid (0.42g, 88%). ^{1}H-NMR data was in agreement with literature values, ^{1}H-NMR ($CDCl_3$) δ 2.59 (s, 3H) 3.90 (s, 3H) 3.94 (s, 3H) 6.76 (d, 1H) (J=8.1Hz) 7.12 (d, 1H) (J=8.1Hz) 7.32 (d, 1H) (J=9.9Hz) 8.00 (d, 1H) (J=9.6Hz) 10.72 (s, 1H).

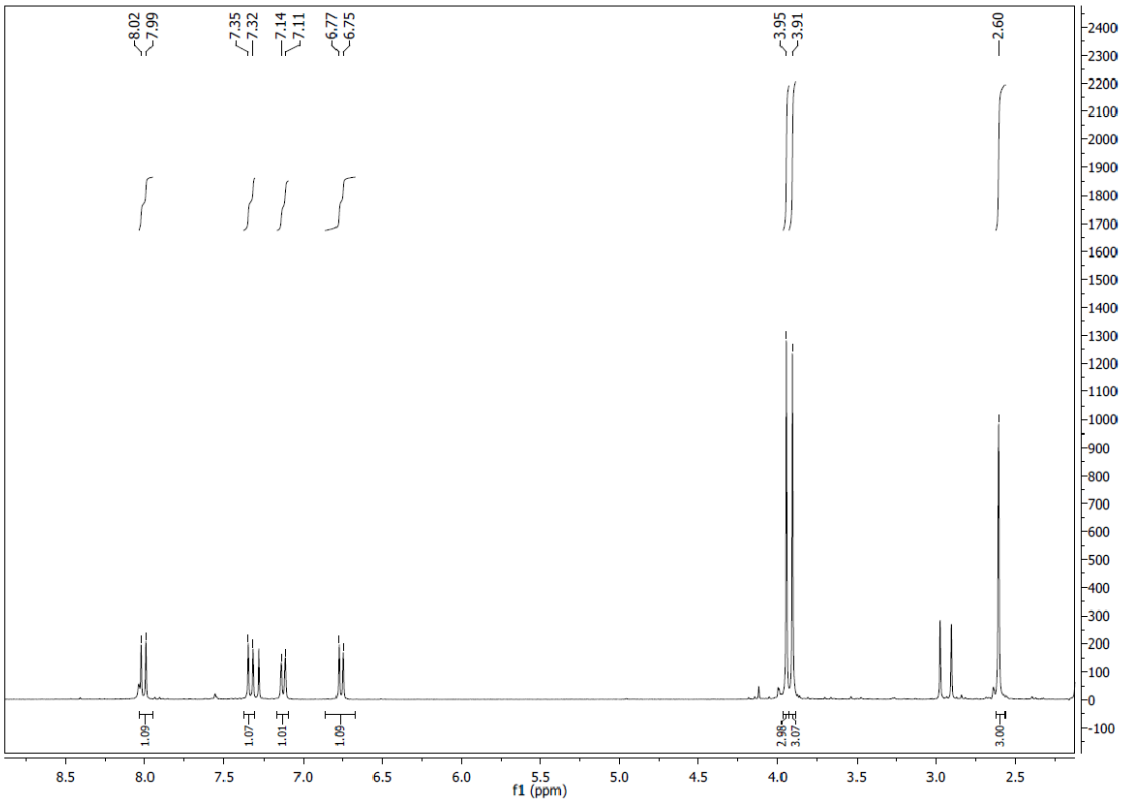

Figure 74. NMR for 2,8-dimethoxyl-5-methyl-1-naphthaldehyde **118**

1,7-dimethoxy-4,8-dimethylnaphthalene (**119**). A solution of 2,8-dimethoxy-5-methyl-1-naphthaldehyde (0.45 g, 2.00 mmol) and hydrazine hydrate (0.37mL, 12.00 mmol) in diethylene glycol (4 mL) was added potassium hydroxide (0.80 g, 14.26 mmol), which followed the same procedure as the synthesis of **117**. The reaction was quenched by water after 15h, the product was extracted by ethyl acetate (15 mL) and washed with 5% aq. HCl (10 mL) and water (10 mL), and the organic layer was dried over sodium sulfate and evaporated to give a colorless solid (0.33 g, 78%). ^{1}H-NMR data was in agreement with literature values, ^{1}H-NMR ($CDCl_3$) δ 2.56 (s, 3H) 2.79 (s, 3H) 3.88 (s, 3H) 3.92 (s, 3H) 6.69 (d, 1H) (J=8.1Hz) 7.06 (d, 1H) (J=6.9Hz) 7.29 (d, 1H) (J=10.2Hz) 7.77 (d, 1H) (J=9Hz).

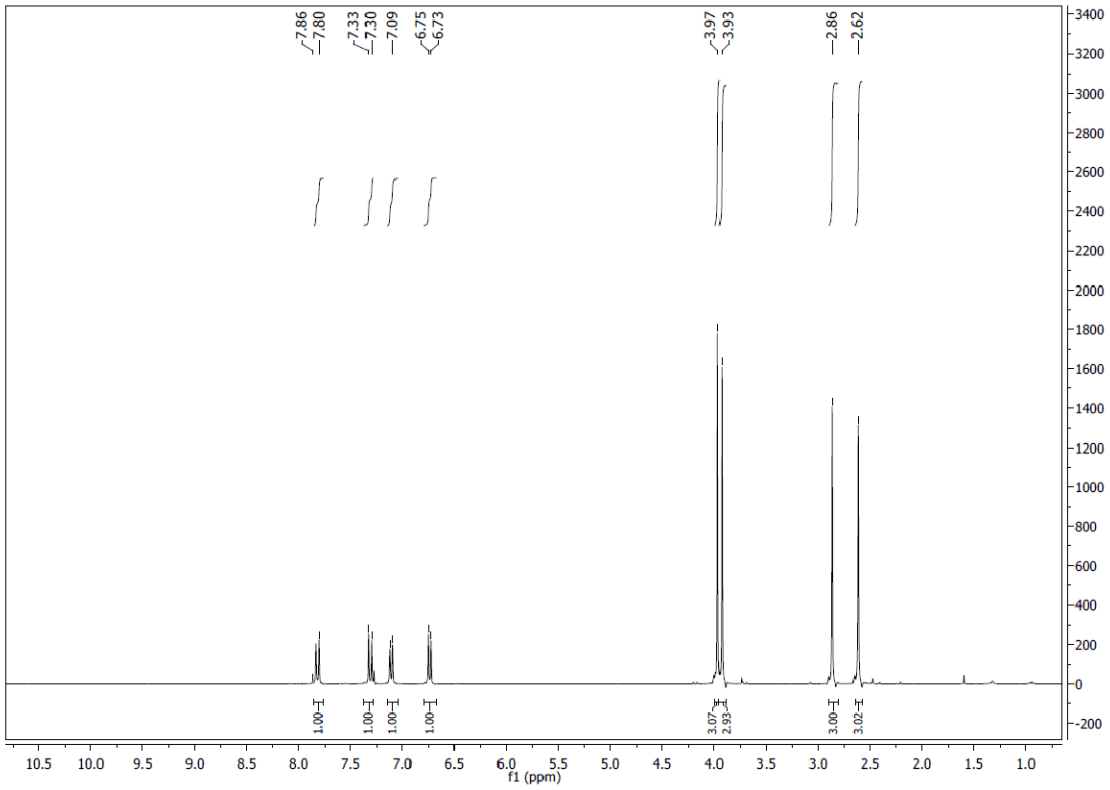

Figure 75. NMR for 1,7-dimethoxy-4,8-dimethylnaphthalene **119**

1,7-dihydroxy-4,8-dimethylnaphthalene(120). To a solution of 1,7-dimethoxy-4,8-dimethylnaphthalene (0.33 g, 1.53 mmol) dissolved in dry CH_2Cl_2 (24 mL) was slowly added a solution of BBr_3 (1.00 mL, 10.00 mmol) at -78 ℃ under nitrogen. The reaction mixture was stirred at room temperature for 20h, and quenched carefully with 10% aq. HCl (20 mL) at 0^0C. The aqueous layer was then extracted by ethyl acetate (10 mL), and the organic layer was dried over anhydrous $MgSO_4$. After evaporation under reduced pressure, the product mixture was separated by Combiflash (heptane: acetone = 4:1) to give a yellowish crystal (0.14 g, 50%). ^{1}H-NMR data was in agreement with literature values, ^{1}H-NMR ($CDCl_3$) δ 2.54 (s, 3H) 2.83 (s, 3H) 4.85 (s, 1H) 4.99 (s, 1H) 6.61 (d, 1H) (J=7.5Hz) 6.96 (d, 1H) (J=7.2Hz) 7.09 (d, 1H) (J=9.3Hz) 7.69 (d, 1H) (J=9.3Hz).

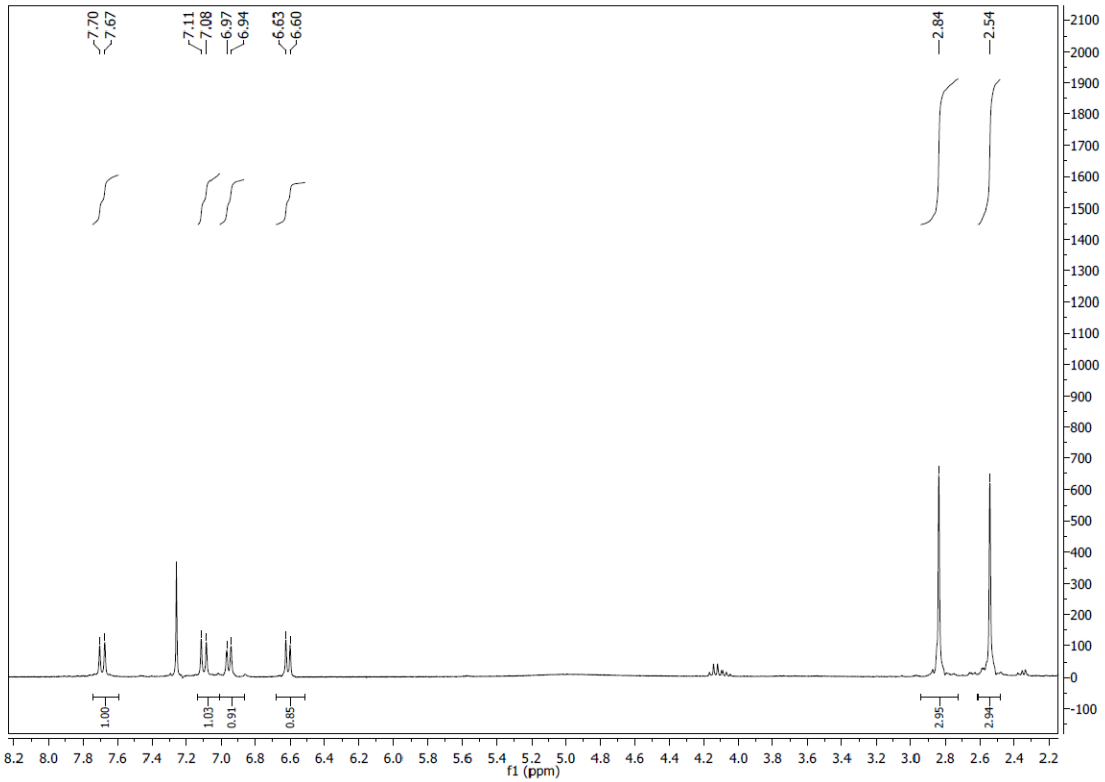

Figure 76. NMR for 1,7-dihydroxy-4,8-dimethylnaphthalene **120**

1,5-dimethyl-2,8-bis(((trifluoromethyl)sulfonyl)methyl)naphthalene (121). To a solution of 1,7-dihydroxy-4,8-dimethylnaphthalene (0.14 g, 0.70 mmol) in 2 mL of dry CH_2Cl_2 was added pyridine (0.50 mL), followed by dropwise addition of triflic anhydride (0.30 mL, 1.80 mmol) at 0 ℃. The mixture was stirred at r.t. for 24h, after the removal of solvent, the residue was diluted with ethyl acetate (10 mL) and then extracted with 5% aqueous HCl (10 mL), saturated $NaHCO_3$ (10 mL) and brine (10 mL). The organic layer was dried over anhydrous sodium sulfate, concentrated and passed through a silica gel plug to give a yellowish solid (0.10g, 30%). ^{1}H-NMR data was in agreement with literature values, ^{1}H-NMR ($CDCl_3$) δ 2.72 (s, 3H) 2.87 (s, 3H) 7.40 (d, 1H) (J=7.5Hz) 7.50 (m, 2H) (J=9.6Hz J=6Hz) 7.99 (d, 1H) (J=9.9Hz).

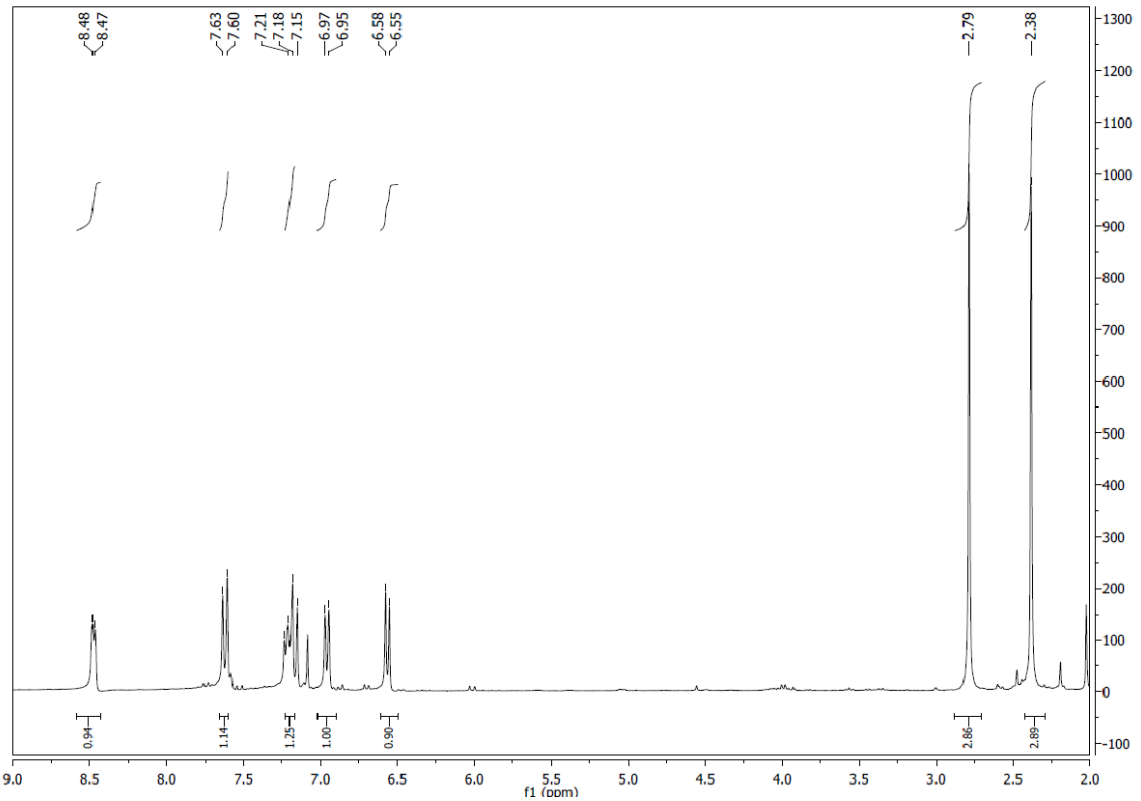

Figure 77. NMR for 1,5-dimethyl-2,8-bis(((trifluoromethyl)sulfonyl)methyl)naphthalene **121**

2,8-bis(2-methoxy-5-methylphenyl)-1,5-dimethylnaphthalene (122). A suspension of bitriflate (0.094 g, 0.20 mmol), K_3PO_4 (1.50 mmol per cross-coupling step), $Pd(PPh_3)_4$ (3 mol% per cross-coupling step), and arylboronic acid (1.0-1.2 equiv per cross-coupling step) in dioxane (4 ml) was stirred at 108 ℃ for 8-12 h, and the amount of the boronic acid was increased by sequence. For the work up of the reaction mixture water (25 ml) and CH_2Cl_2 (25 ml) were added at 20 ℃. The organic and aqueous layers were separated and the latter was extracted with CH_2Cl_2 (2×25 ml). The combined organic layers were dried, filtered, and concentrated under vacuum. The residue was purified by column chromatography (eluting solution: heptane and acetone). ^{1}H-NMR data was in agreement with literature values, ^{1}H-NMR ($CDCl_3$) δ 2.29 (s, 3H) 2.31 (s, 3H) 2.34 (s, 3H) 2.73 (s, 3H) 3.65 (s, 3H) 3.75 (s, 3H) 6.82 (t, 1H) (J=9Hz) 6.85 (d, 1H) (J=3Hz) 7.03 (s, 1H) 7.13 (t, 2H) (J=9.9Hz) 7.13 (d, 1H) 7.30 (s, 1H) 7.38 (d, 1H) (J=6Hz) 7.40 (s, 1H) 8.01 (d, 1H) (J=9Hz).

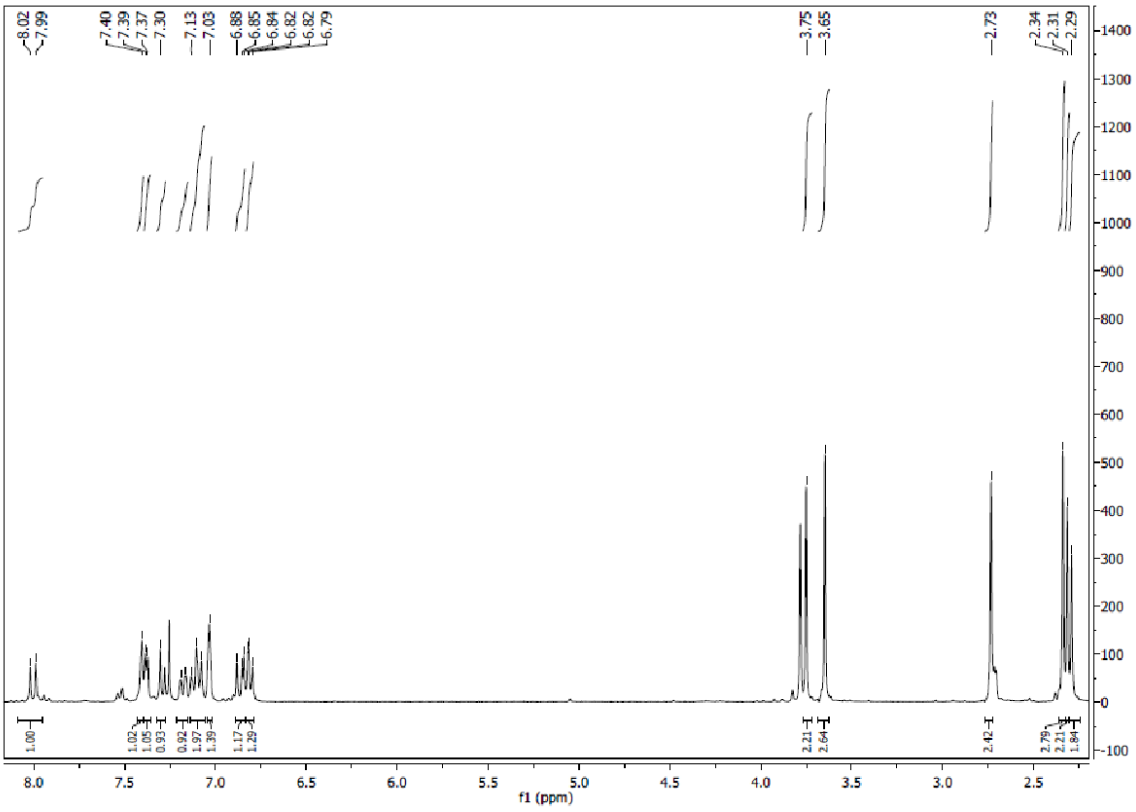

Figure 78. NMR for 2,8-bis(2-methoxy-5-methylphenyl)-1,5-dimethylnaphthalene **122**

2-(8-(2-hydroxy-5-methylphenyl)-1,5-dimethylnaphthalen-2-yl)-4-methylphenol (123). A suspension of the starting material (0.04 g, 0.97 mmol) was dissolved in CH_2Cl_2 (15.0 mL), the reaction was kept in liquid nitrogen bath for a while. Borane tribromide (0.28 ml, 3.0 mmol) was added dropwise. The reaction solution was left stirring at r.t. overnight, 10% aq. HCl was added in ice bath. The aqueous layer was extracted by ethyl acetate, washed by aq. $NaHCO_3$, and brine. The desired product was recovered by evaporation under vacuum and identified by NMR. ^{1}H-NMR data was in agreement with literature values, ^{1}H-NMR ($CDCl_3$) δ 2.35 (t, 3H) (J=6Hz) 2.55 (m, 6H) (J=3Hz) 2.84 (m, 3H) (J=3Hz) 6.62 (d, 1H) (J=6Hz) 6.93 (m, 2H) 7.05 (d, 1H) 7.11 (d, 2H) 7.46 (s, 1H) 7.64 (s, 1H) 7.79 (d, 1H) 7.82 (d, 1H).

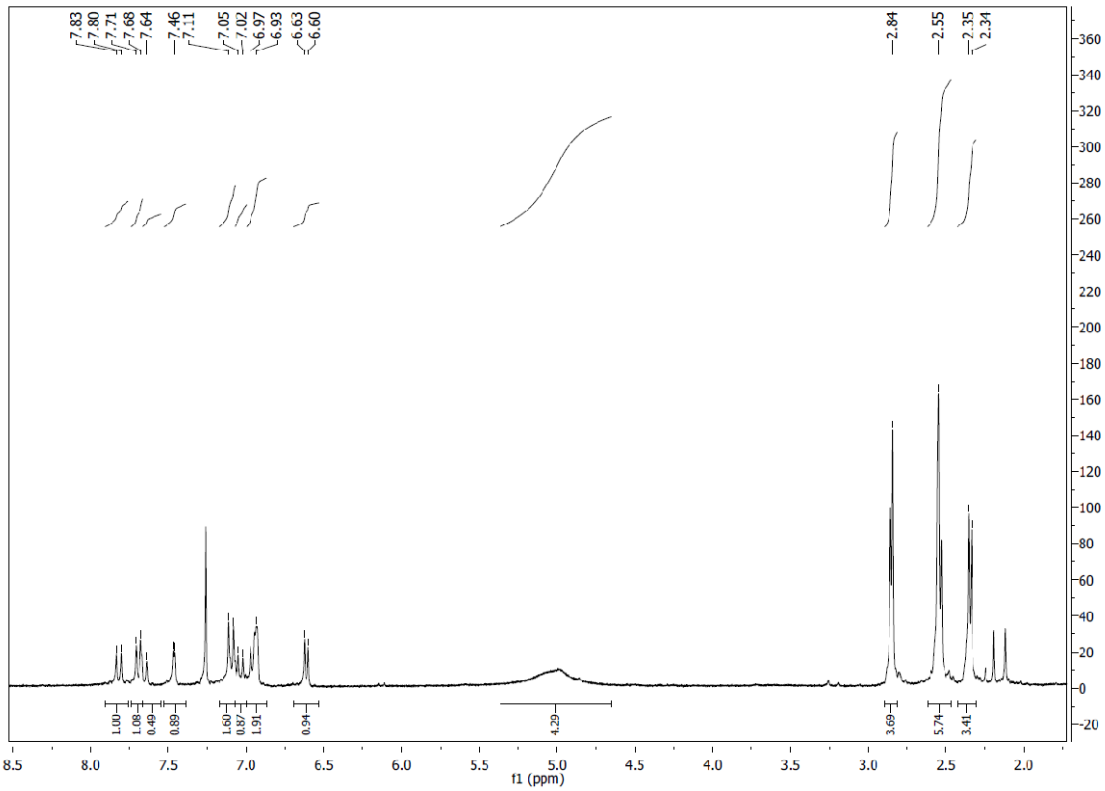

Figure 79. NMR for 2-(8-(2-hydroxy-5-methylphenyl)-1,5-dimethylnaphthalen-2-yl)-4-methylphenol **123**

Bromo(4-methoxyphenyl)(methyl)arsine(125). To a solution of (4-methoxyphenyl)boronic acid (0.15 g, 1.0 mmol) and anhydrous cesium carbonate (1.6 g, 5.0 mmol) in anhydrous toluene (5 mL) under nitrogen was added tetrakis(triphenylphosphine) palladium(0) (0.5 M), followed by CH_3AsBr_2 (0.25 g, 1.0 mmol). The reaction was heated at 100 ℃ for 16 hours and diluted with ethyl acetate (20 mL). The reaction crude was washed successively with water, a saturated solution of sodium bicarbonate, and brine, dried over sodium sulfate and concentrated under vacuum. No desired product was identified in the NMR spectrum.

Alternatively, to a solution of (4-methoxyphenyl)boronic acid (0.15 g, 1.0 mmol) and anhydrous potassium phosphate (1.0 g, 5.0 mmol) in anhydrous toluene (5 mL) under nitrogen was added tetrakis(triphenylphosphine) palladium(0) (0.5 M), followed by CH_3AsBr_2 (0.25 g, 1.0 mmol). The reaction mixture was heated at 110 ℃ for 16 hours and diluted with ethyl acetate (20 mL). The reaction crude was washed successively with water, a saturated solution of sodium bicarbonate, and brine, dried over sodium sulfate and concentrated under vacuum. The desired product was recovered and identified

by NMR spectrum, ^{1}H-NMR ($CDCl_3$) δ 1.59 (s, 3H) 7.65 (d, 2H) (J=6Hz) 8.06 (d, 2H) (J=9Hz). MS (ESI): *m/z* $C_8H_{10}AsBrO$ $[M-H]^-$: 274.9.

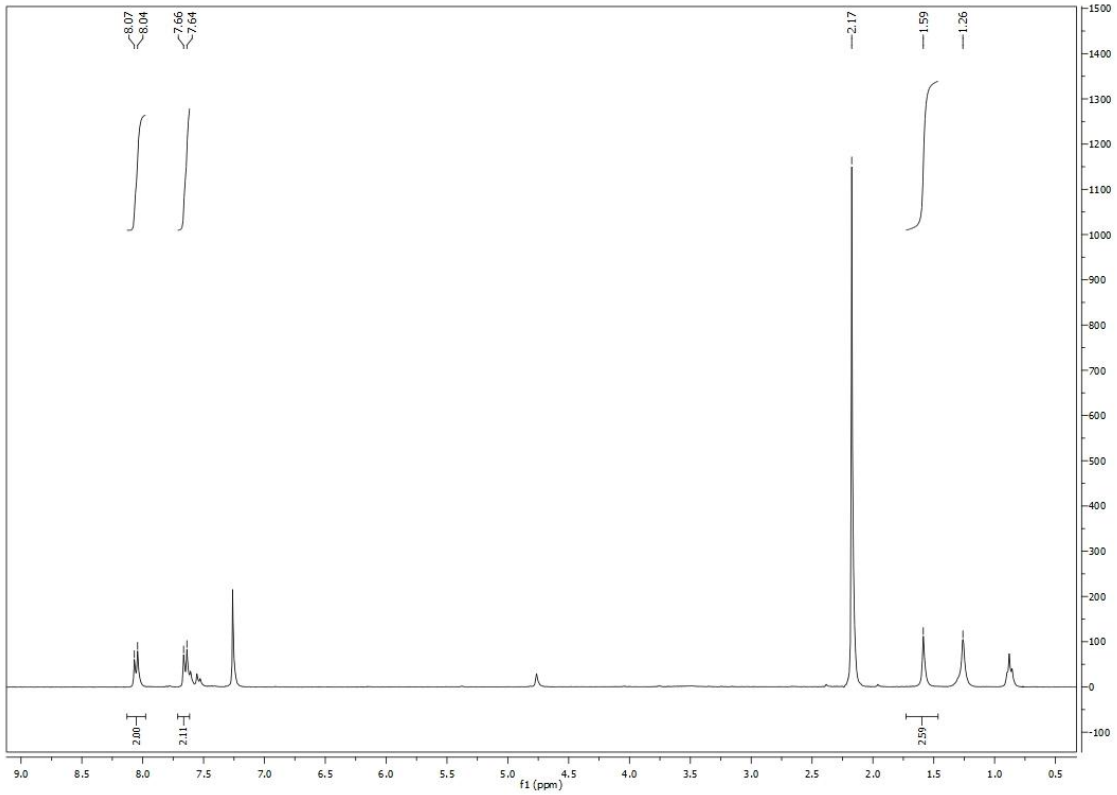

Figure 80. NMR for bromo(4-methoxyphenyl)(methyl)arsine **125**

3-(bromo(methyl)arsino)benzoic acid(127). To a solution of 3-boronobenzoic acid (0.166 g, 1.0 mmol) and anhydrous potassium phosphate (1.0 g, 5.0 mmol) in anhydrous toluene (5 mL) under nitrogen was added tetrakis(triphenylphosphine)palladium(0) (0.5 M), followed by CH_3AsBr_2 (0.25 g, 1.0 mmol). The reaction was heated at 110 ℃ for 16 hours and diluted with ethyl acetate (20 mL). The reaction crude was washed successively with water, a saturated solution of sodium bicarbonate, and brine, dried over sodium sulfate and concentrated under vacuum. The desired product was recovered and identified by NMR spectrum, ^{1}H-NMR ($CDCl_3$) δ 2.04 (s, 3H) 7.56 (t, 1H) (J=18Hz) 8.00 (d, 1H) (J=9Hz) 8.15 (d, 1H) (J=6Hz) 8.45 (s, 1H). MS (ESI): *m/z* $C_8H_8AsBrO_2$ $[M-H]^+$: 290.89.

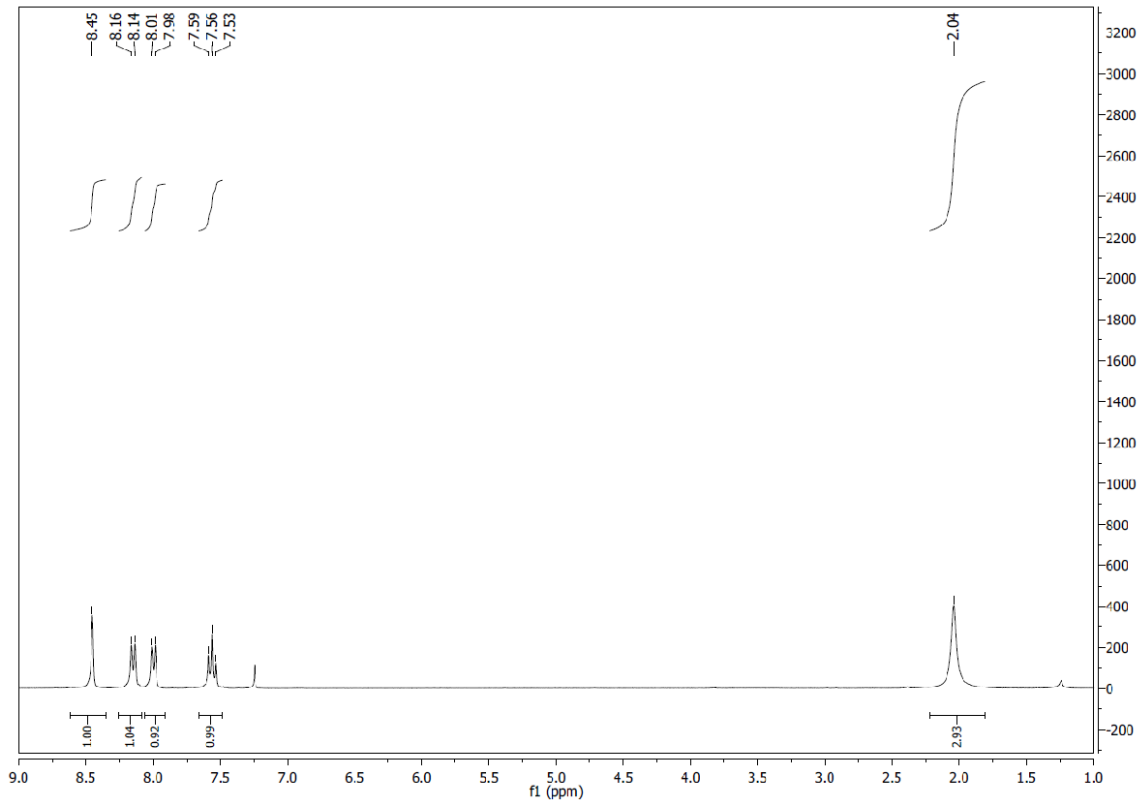

Figure 80. NMR for 3-(bromo(methyl)arsino)benzoic acid **127**

Bromo(3-bromophenyl)(methyl)arsine (129). To a solution of 3-bromophenylboronic acid (0.20 g, 1.0 mmol) and anhydrous potassium phosphate (1.0 g, 5.0 mmol) in anhydrous toluene (5 mL) under nitrogen was added tetrakis(triphenylphosphine)palladium(0) (0.5 M), followed by CH_3AsBr_2 (0.25 g, 1.0 mmol). The reaction mixture was heated at 110 ℃ for 16 hours and diluted with ethyl acetate (20 mL). The reaction crude was washed successively with water, a saturated solution of sodium bicarbonate, and brine. The organic layer was dried over sodium sulfate and concentrated under vacuum. The desired product was recovered and identified by NMR spectrum, ^{1}H-NMR ($CDCl_3$) δ 1.56 (s, 3H) 7.16 (d, 1H) (J=9Hz) 7.25 (s, 1H) 8.12 (d, 1H) (J=9Hz) 8.51 (s, 1H).

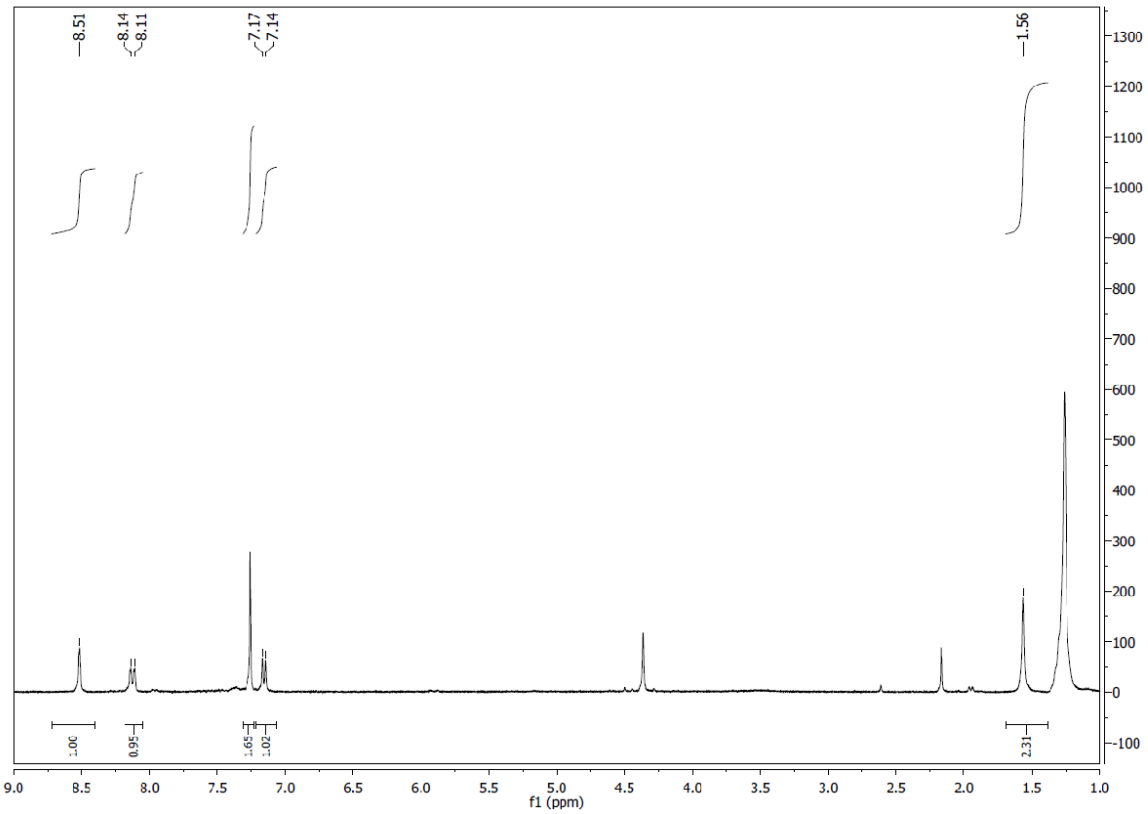

Figure 81. NMR for Bromo(3-bromophenyl)(methyl)arsine **129**

Bromo(2,3-dimethylphenyl)(methyl)arsine(131). To a solution of 2,3-dimethylphenylboronic acid (0.15 g, 1.0 mmol) and anhydrous potassium phosphate (1.0 g, 5.0 mmol) in anhydrous toluene (5 mL) under nitrogen was added tetrakis(triphenylphosphine)palladium(0) (0.5 M), followed by CH_3AsBr_2 (0.25 g, 1.0 mmol). The reaction was heated at 110 ℃ for 16 hours and diluted with ethyl acetate (20 mL). The reaction crude was washed successively with water, a saturated solution of sodium bicarbonate, and brine. The organic layer was dried over sodium sulfate and concentrated under vacuum. The desired product was recovered and identified by the NMR spectrum, ^{1}H-NMR ($CDCl_3$) δ 2.02 (s, 3H) 6.88 (d, 1H) (J=9Hz) 7.51 (m, 1H) 7.58 (d, 1H) (J=3Hz). MS (ESI): *m/z* $C_9H_{12}AsBr$ $[M-H]^-$: 274.93 $[M-H]^+$: 272.93.

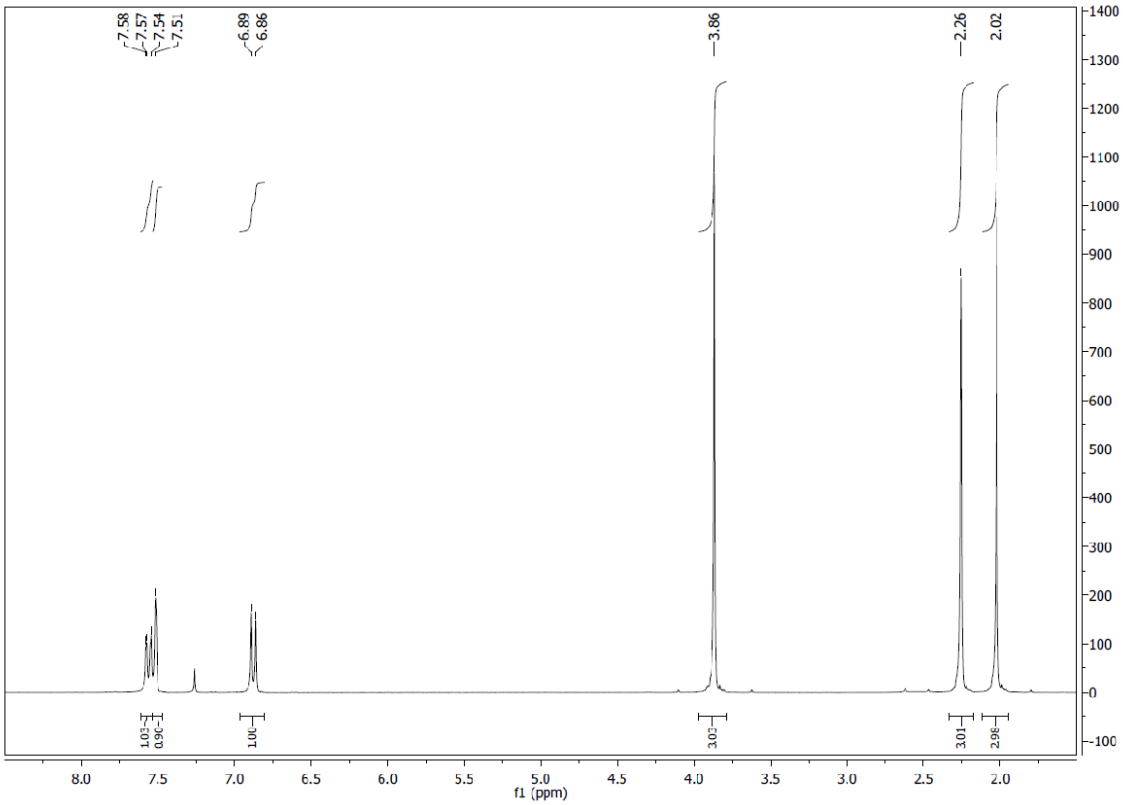

Figure 82. NMR for Bromo(2,3-dimethylphenyl)(methyl)arsine **131**

Synthesis of compound 133. To a solution of dibenzo[b,d]thiophene-4-yl-boronic acid (0.23 g, 1.0 mmol) and anhydrous potassium phosphate (1.0 g, 5.0 mmol) in anhydrous toluene (5 mL) under nitrogen was added tetrakis(triphenylphosphine)palladium(0) (0.5 M), followed by CH_3AsBr_2 (0.25 g, 1.0 mmol). The reaction was heated at 110 ℃ for 16 hours and diluted with ethyl acetate (20 mL). The reaction crude was washed successively with water, a saturated solution of sodium bicarbonate, and brine. The organic layer was dried over sodium sulfate and concentrated under vacuum. The desired product was recovered and identified by NMR spectrum, ^{1}H-NMR ($CDCl_3$) δ 2.19 (s, 3H) 7.48 (d, 1H) (J=6Hz) 7.50 (t, 1H) (J=6Hz) 7.54 (m, 1H) 7.77 (dd, 1H) (J=6Hz) 7.90 (d, 2H) (J=3Hz) 8.14 (d, 1H) (J=3Hz) 8.17 (d, 1H) (J=6Hz).

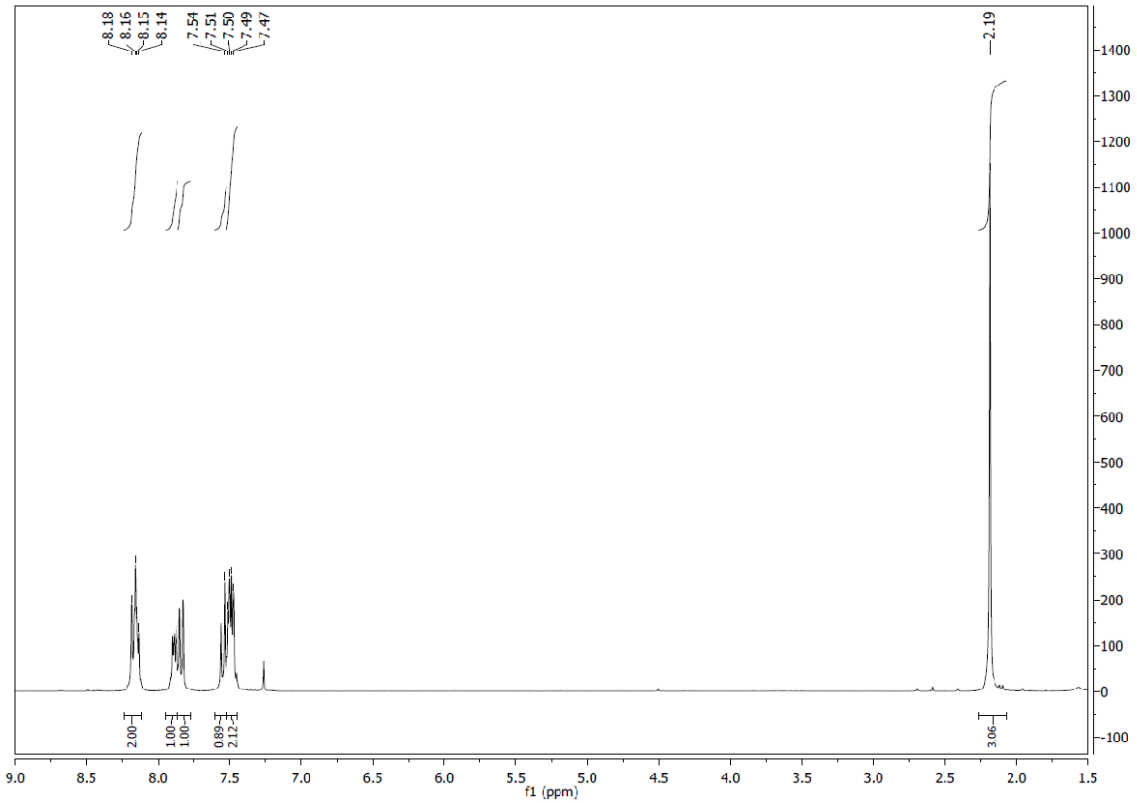

Figure 83. NMR for compound **133**

Synthesis of compound **135.** To a solution of 4-dibenzofuranylboronic acid (0.21 g, 1.0 mmol) and anhydrous potassium phosphate (1.0 g, 5.0 mmol) in anhydrous toluene (5 mL) under nitrogen was added tetrakis(triphenylphosphine) palladium(0) (0.5 M), followed by CH_3AsBr_2 (0.25 g, 1.0 mmol). The reaction was heated at 110 ℃ for 16 hours and diluted with ethyl acetate (20 mL). The reaction crude was washed successively with water, a saturated solution of sodium bicarbonate, and brine. The organic layer was dried over sodium sulfate and concentrated under vacuum. The desired product was recovered and identified by NMR spectrum, ^{1}H-NMR ($CDCl_3$) δ 2.23 (s, 3H) 7.37 (t, 1H) (J=15Hz) 7.45 (dd, 1H) (J=12Hz) 7.50 (d, 1H) (J=6Hz) 7.62 (d, 1H) (J=6Hz) 7.82 (d, 2H) (J=6Hz) 7.96 (d, 1H) (J=6Hz) 8.00 (d, 1H) (J=9Hz).

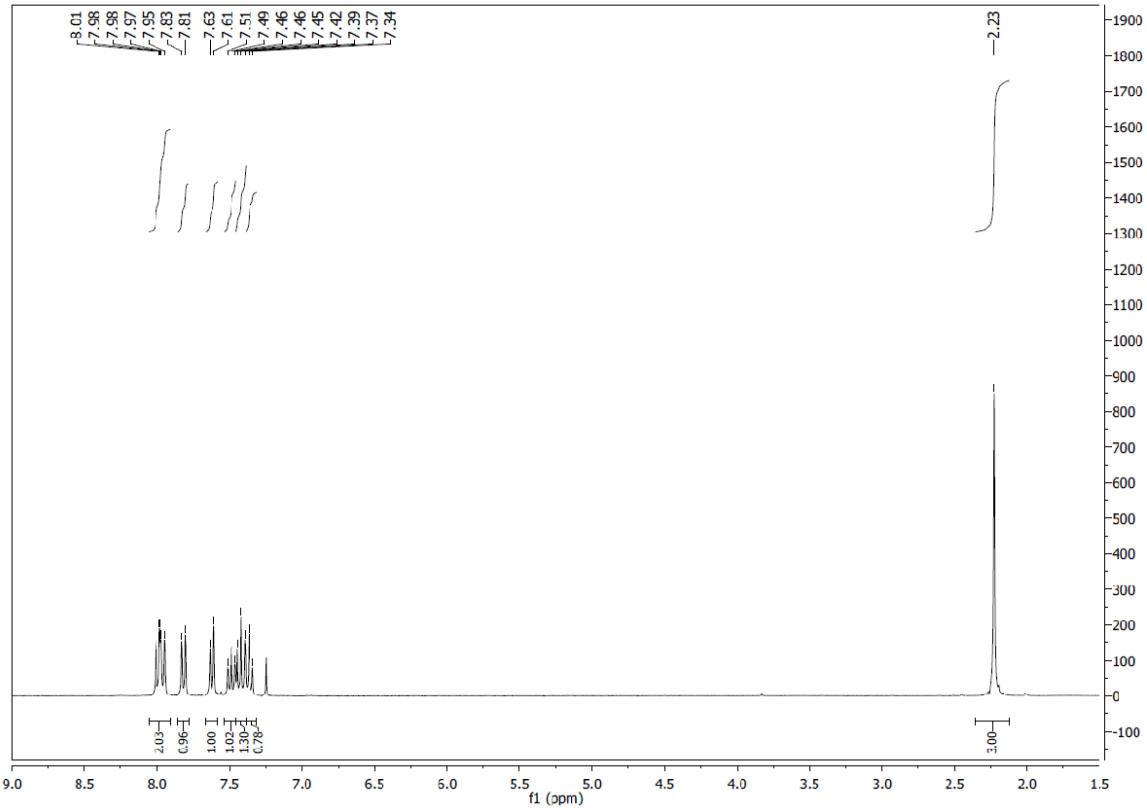

Figure 84. NMR for compound **135**

(4-*tert*-butylphenyl)magnesium bromide (139). Magnesium (0.115 g, 4.73 mmol) was stirred for 3 h under nitrogen gas in a round bottom flask. A THF solution of 1-bromo-4-tert-butylbenzene (5 mL, 0.49 g, 2.3 mmol) was added to the reaction. After half an hour iodine (0.63 g, 5.0 mmol) was added to the reaction. Hair dryer was used to heat the reaction. Dark pink color disappeared while heating. Then the reaction was left stirring for another 1 h, dark black color formed. The THF solution of (4-*tert*-butylphenyl)magnesium bromide was used in the subsequent reaction without further purification.

(4-*tert*-butylphenyl)lithium (140). 1-bromo-4-*tert*-butylbenzene (0.21 g, 1.0 mmol) was disolved in THF (0.11 mL) and hexane (1.2 mL) under nitrogen. *n*-butyl lithium (0.8 mL, 1.3 mmol) was added to the reaction solution while kept on ice, and stirred for another 1 h. The lithium reagent dissolved in THF and hexane solution was used in the subsequent reaction without further purification.

2-(4-*tert*-butylphenyl)propan-2-ol (141). 1-bromo-4-tert-butylbenzene (0.21 g, 1.0 mmol) was dissolved in THF (4 mL) under nitrogen. *n*-butyl lithium (0.8 mL, 1.3 mmol) was added to the reaction in an ice bath, and stirred at room temperature for another 1 h. Then acetone (15 mL) was added to the

reaction. The reaction was stirred at r.t. overnight and quenched by water (15 mL). The aqueous layer was extracted by DCM (3×20 mL). The combined organic layers were evaporated under vacuum. The NMR spectrum of the product corresponded to the desired product, ^{1}H-NMR ($CDCl_3$) δ 1.34 (s, 9H) 1.54 (s, 6H) 7.41 (m, 4H) (J=24Hz).

Chloro(4-methoxyphenyl)(phenyl)arsine (142). To a solution of 4-methoxyphenylboronic acid (0.15 g, 1.0 mmol) and anhydrous potassium phosphate (1.0 g, 5.0 mmol) in anhydrous toluene (5 mL) under nitrogen was added tetrakis(triphenylphosphine)palladium(0) (0.5 M), followed by dichloro(phenyl)arsine (0.22 g, 1.0 mmol). The reaction was heated at 110 ℃ for 16 hours and diluted with ethyl acetate (20 mL). The reaction crude was washed subsequently with water, a saturated solution of sodium bicarbonate, and brine. The organic layer was dried over sodium sulfate and concentrated under vacuum. The product was used in the subsequent reaction without further purification.

To a solution of 4-methoxyphenylboronic acid (0.15 g, 1.0 mmol) and anhydrous cesium carbonate (1.6 g, 5.0 mmol) in anhydrous toluene (5 mL) under nitrogen was added bis(diphenylphosphino)ferrocene]palladium(II) dichloride (3% M), followed by dichloro(phenyl)arsine (0.22 g, 1.0 mmol). The reaction was heated at 110 ℃ for 16 hours and diluted with ethyl acetate (20 mL). The reaction crude was washed sequentially with water, a saturated solution of sodium bicarbonate, and brine. The organic layer was dried over sodium sulfate and concentrated under vacuum. The product was used in the subsequent reaction without further purification.

4-bromo-*N*,*N*-dimethylbenzenamine (145). 4-bromo-*N*,*N*-dimethylaniline (0.1 g, 0.5 mmol) placed in a 25 mL round bottom flask was degassed and refilled with nitrogen two times, and then the starting material was dissolved in hexane (4 mL) and THF (0.5 mL). While cooling in an ice bath, *n*-BuLi (0.5 mL, 1.6 M in hexane) was added dropwise, stirred for three hours, then acetone (2 mL) was added. The reaction was quenched by water, and extracted by dichloromethane. The lithium solution **145** was used in the subsequent reaction without further purification.

(4-*tert*-butylphenyl)(4-methoxyphenyl)(phenyl)arsino (143). The newly synthesized lithium reagent **145** was added to the solution of the starting material. The reaction was stirred at room temperature overnight, and purified by Combiflash (eluting solution: heptane and acetone). However, the NMR spectrum of the product was too messy to identify the desired product.

Diphenylmethane (148). In a 50 mL three-necked flask fitted with a stopper, a reflux condenser, and a 250 mL dropping funnel were placed, amalgamated zinc (1.5 g) and concentrated aq. hydrochloric acid

(0.8 mL) were added. The flask is heated to cause gentle refluxing to occur. A solution of benzophenone (0.188 g, 1.0 mmol) in 95% ethanol (0.450 mL) and concentrated aq. hydrochloric acid (1.5 mL) were added dropwise through the dropping funnel over an 8-hour period. After the addition of the vanillin was complete, the mixture was refluxed for 30 minutes more.

Iodine (1.00 g, 4.00 mmol) and acetic acid (50 mL) were stirred together under N_2 in a flask fitted with a condenser and a dropping funnel. 50% aq. hypophosphorous acid (2 mL, 19.3 mmol) was added and the mixture was heated to reflux. A solution of 4-bromobenzophenone (3.18 g, 12.0 mmol) in acetic acid (15 mL) was added over a period of 1–2 h. The mixture was then stirred and refluxed for an additional 24 h, after cooling down the reaction crude was diluted with water and extracted with hexane. The hexane layer was dried over $MgSO_4$.

A solution of benzophenone (2.00 mmol) and hydrazine hydrate (0.37 mL, 12.00 mmol) in diethylene glycol (4 mL) was treated with potassium hydroxide (0.8 g). The reaction was quenched by water after 15h, the product was extracted into ethyl acetate (15 mL) and washed with 5% aq. HCl (10 mL) and water (10 mL). The desired product was recovered by evaporation, and identified by NMR spectrum. ^{1}H-NMR data was in agreement with literature values, ^{1}H-NMR ($CDCl_3$) δ 4.10 (s, 2H) 7.31 (m, 6H) 7.42 (m, 4H).

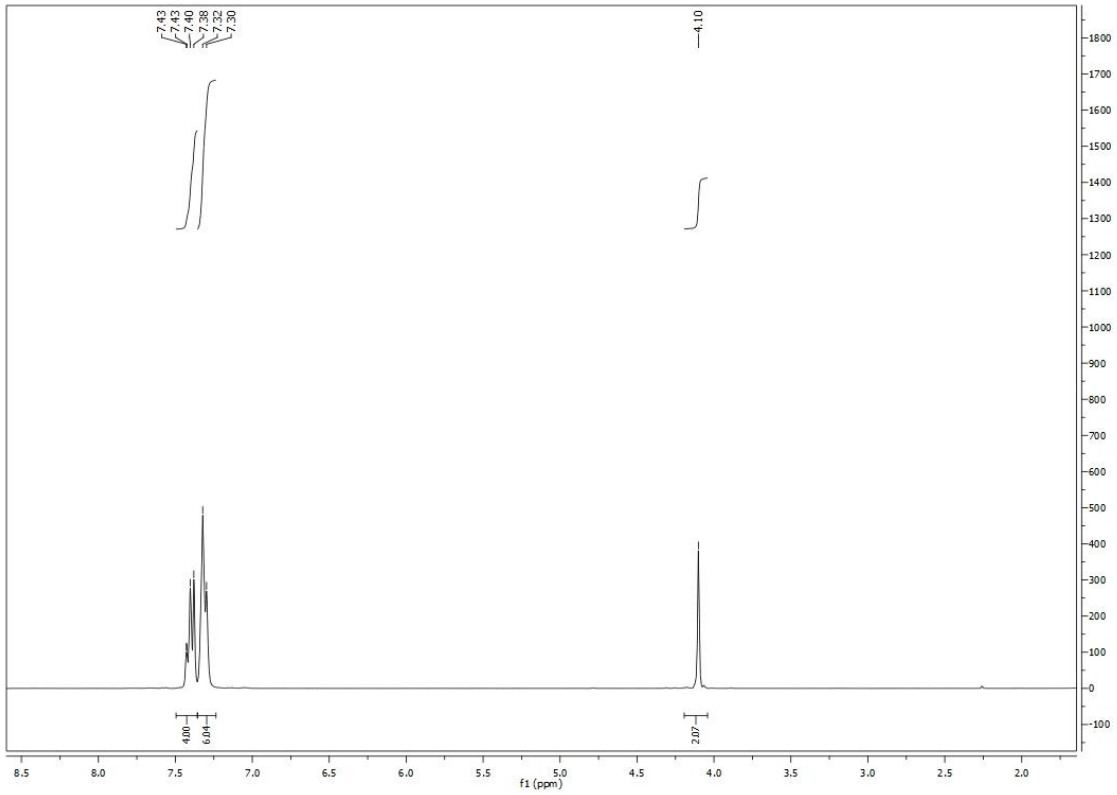

Figure 85. NMR for diphenylmethane **148**

Bis(4-nitrophenyl)methane (149). Diphenylmethane (0.08 g, 0.48 mmol) was dissolved in 70% aq. HNO_3 (20 mL) in an ice bath, stirred for 20 min. Water (100 mL) was added slowly, the aqueous layer was extracted by CH_2Cl_2, and purified by Combiflash. ^{1}H-NMR data was in agreement with literature values, ^{1}H-NMR ($CDCl_3$) δ 4.19 (s, 2H) 7.33 (d, 4H) (J=9Hz) 8.18 (d, 4H) (J=9Hz).

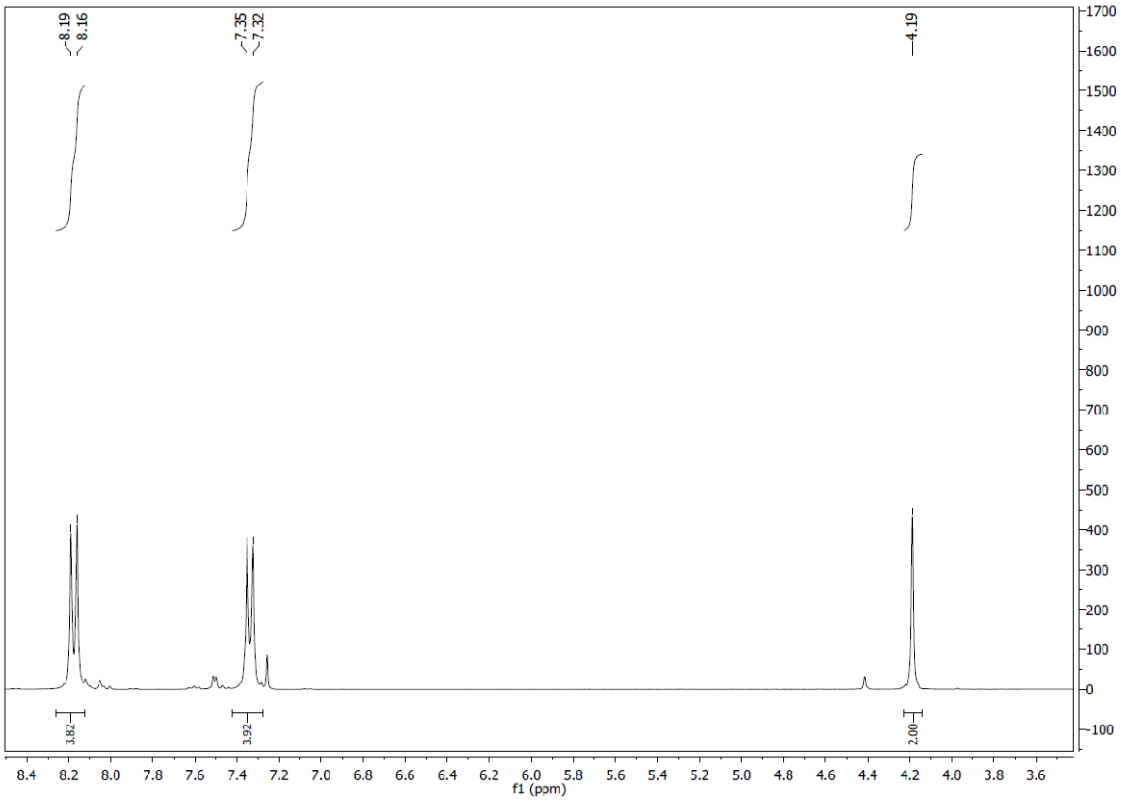

Figure 86. NMR for Bis(4-nitrophenyl)methane **149**

Bis(2-bromo-4-nitrophenyl)methane (150). A mixture of bis(4-nitrophenyl)methane (5.00 mg, 0.02 mmol) and iodine (0.50 g, 3.93 mmol) were cooled in an ice bath. Bromine (2.00 g, 2 mmol) was added dropwise while cooling in the ice bath for twelve hours. Subsequently, the very viscous reaction-product was poured into water and the resulting highly colored, heavy oil was extracted with ether. The ethereal solution was washed with sodium hydroxide and then treated with aq. $NaHCO_3$ to remove the iodine, dried over magnesium sulfate, and purified by pipet column, but only the starting material was recovered. ^{1}H-NMR ($CDCl_3$) δ 4.37 (s, 2H) 7.16 (d, 2H) (J=9Hz) 8.16 (d, 2H) (J=9Hz) 8.52 (s, 2H).

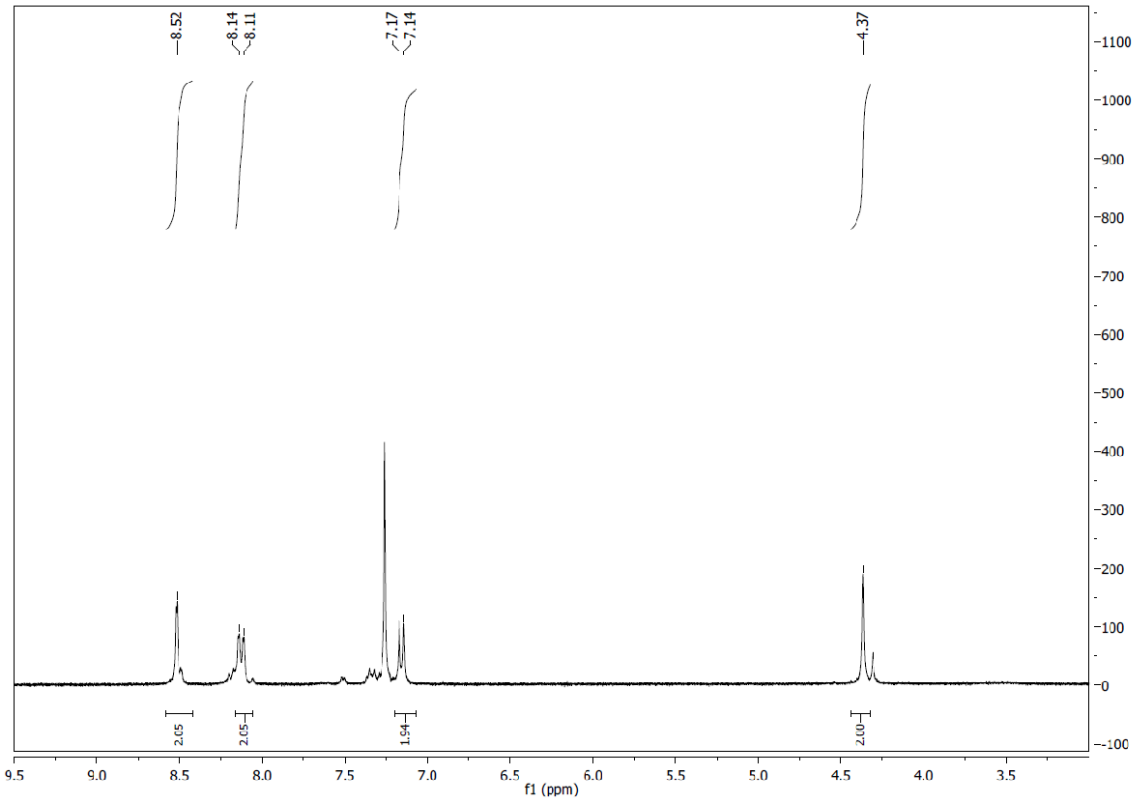

Figure 87. NMR for bis(2-bromo-4-nitrophenyl)methane **150**

Bis(2-bromo-4-nitrophenyl)methane (155). To a mixture of bis(4-nitrophenyl)methane (0.035 g, 0.13 mmol) and iron (0.50 g, 9.00 mmol) placed in a 50 mL round bottom flask was added bromine (15 mL, 0.30 mmol) slowly, stirred at r.t. for 12 h. The reaction mixture was poured into ice water. 3M aq. NaOH was added into the reaction crude, extracted by CH_2Cl_2, and washed by aq. HCl, and saturated aq. $NaHCO_3$. The desired product was recovered by evaporation and identified by NMR spectrum. ^{1}H-NMR ($CDCl_3$) δ 4.29 (s, 2H) 7.07 (d, 2H) (J=9Hz) 8.17 (d, 2H) (J=9Hz) 8.78 (s, 2H).

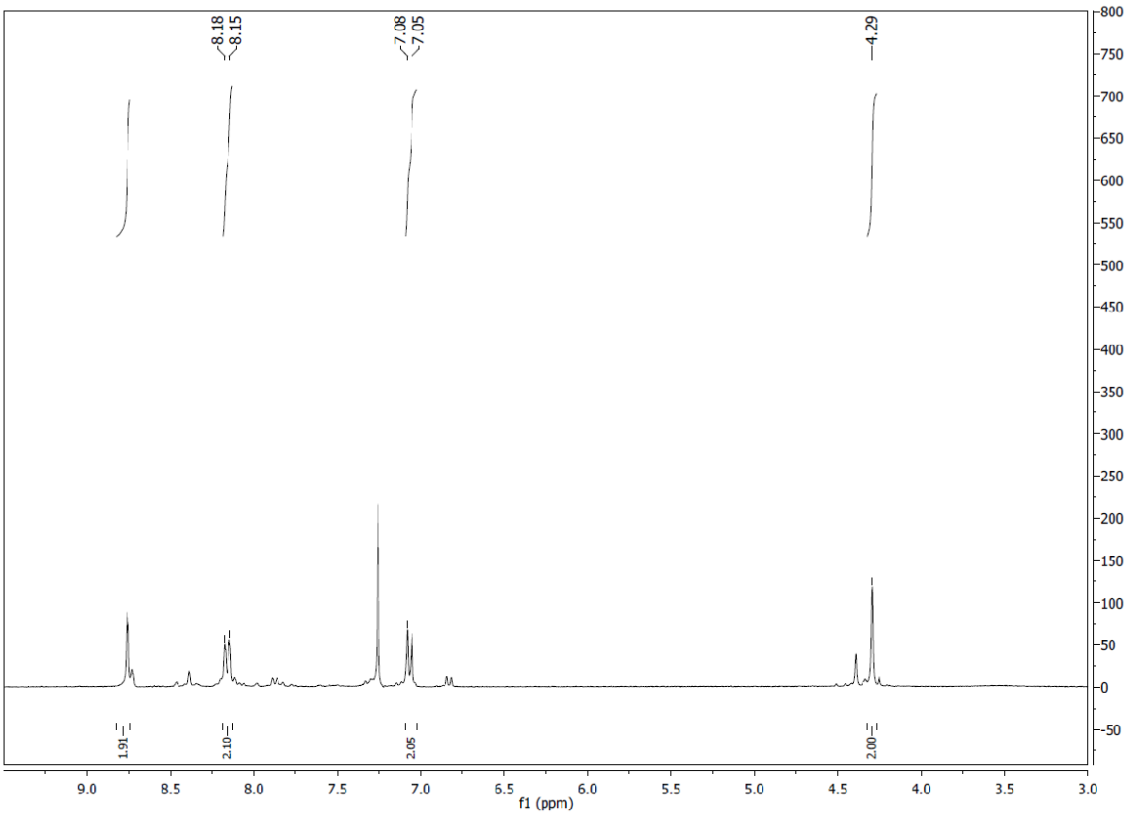

Figure 88. NMR for Bis(2-iodo-4-nitrophenyl)methane **155**

Synthesis of compound **158** by alkylation reaction. Aluminum trichloride (0.30 g, 2.10 mmol) was dissolved in DCM (7 mL) under nitrogen in an ice bath. CH_3COCl (0.17 g, 2.2 mmol, dissolved in DCM 5 mL) was added dropwise through dropping funnel, and then diphenylmethane (0.17 g, 1.00 mmol, dissolved in DCM 5 mL) was added dropwise, and stirred at room temperature for 15 min. The reaction was quenched by concentrated aq. hydrochloride (8 mL) and ice water (20 g), extracted by CH_2Cl_2, and evaporated under vacuum. The NMR spectrum corresponded to the literature values. ^{1}H-NMR ($CDCl_3$) δ 2.58 (t, 6H) 4.09 (s, 2H) 7.28 (d, 4H) (J=9Hz) 7.91 (d, 4H) (J=9Hz). ^{13}C NMR (75 MHz, CDCl3): δ = 26.59 (CH_3), 41.83 (CH_2), 128.79 (CH-benzene-CH_2), 129.75 (CH-benzene-CO), 135.56 (C-benzene-CO), 145.63 (C-benzene-CH_2), 197.69(CO).

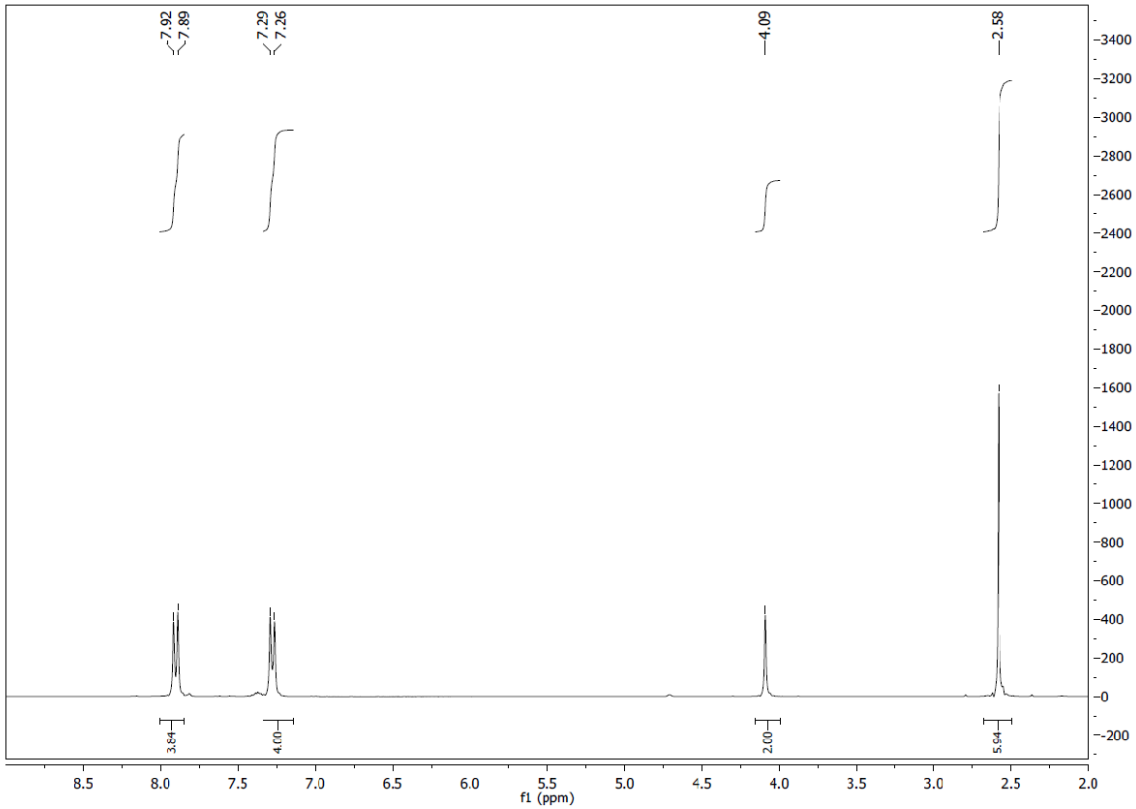
7.92
7.89
7.29
7.26
4.09
2.58
3.64
4.00
2.00
5.54
f1 (ppm)

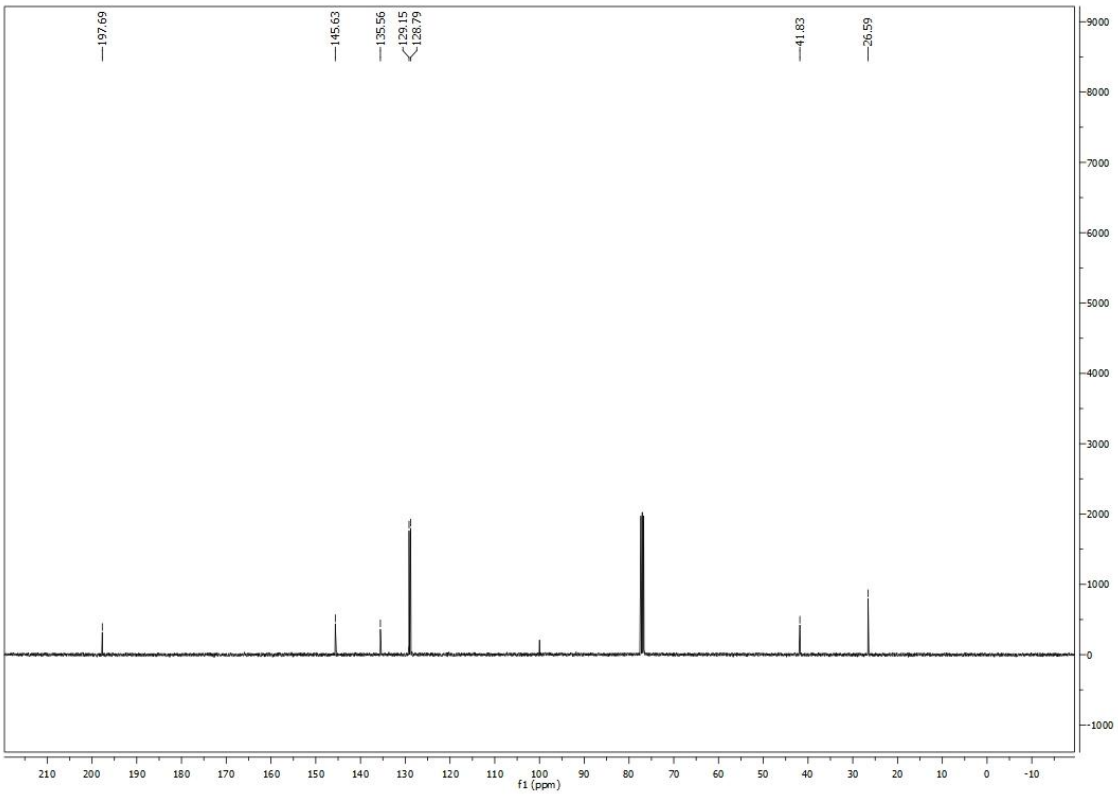
197.69
145.63
135.56
129.15
128.79
41.83
26.59
f1 (ppm)

Figure 89. NMR for alkylation molecule **158**

Diiodoalkylation compound (159). The alkylation compound **153** (0.18 g, 0.72 mmol), potassium iodide (0.24 g, 1.5 mmol), and potassium iodate (0.15 g, 0.72 mmol) placed in a 50 mL round bottom flask was added concentrated aq. sulfuric acid (6 mL) on ice. DCM (5 mL) was added into the reaction crude after 30 min. The reaction was stirred at room temperature at dark overnight. The reaction crude was poured into ice water, extracted by DCM. The desired product was recovered by evaporation and analyzed by the NMR spectrum, which corresponded to the literature values. ^{1}H-NMR ($CDCl_3$) δ 2.58 (t, 6H) 4.21 (s, 2H) 6.99 (d, 2H) (J=6Hz) 7.84 (d, 4H) (J=6Hz) 8.46 (s, 2H).

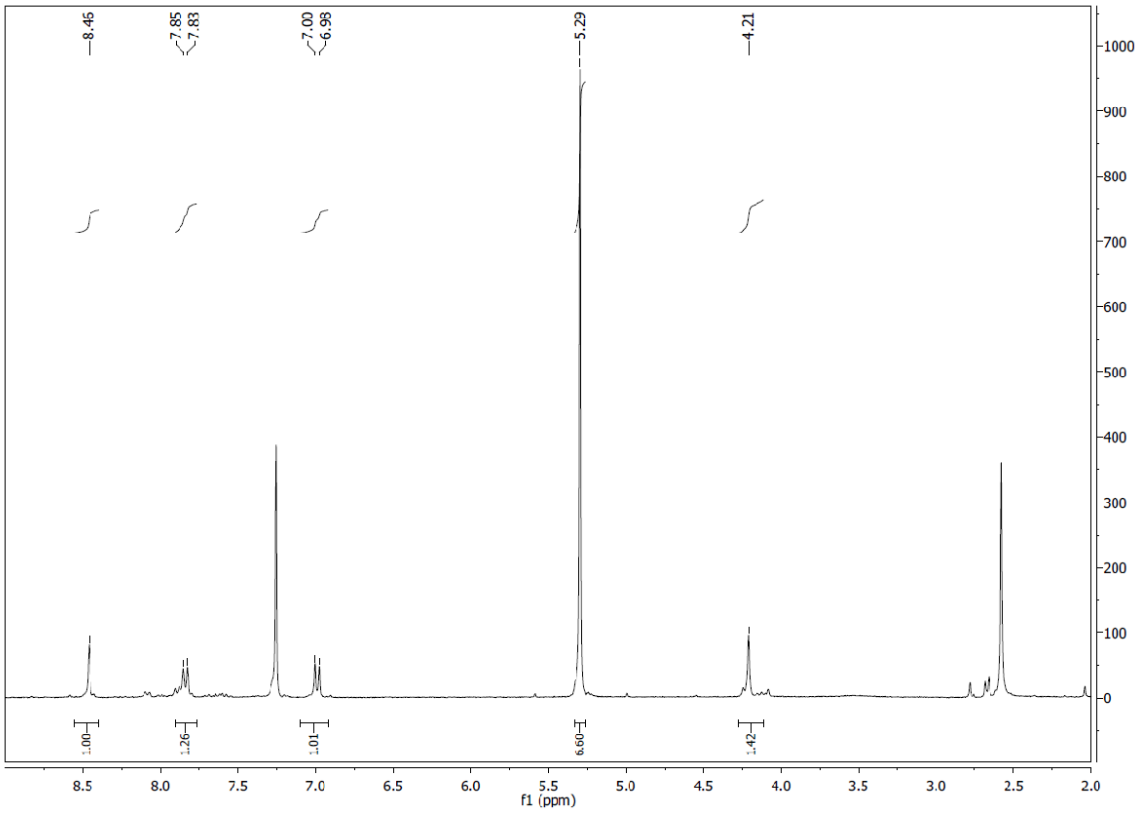

Figure 90. NMR for diiodoalkylation molecule **159**

Synthesis of compound **160.** A suspension of diiodoalkylation compound **159** (0.06 g, 0.12 mmol), K_3PO_4 (1.5 mmol per cross-coupling step), $Pd(PPh_3)_4$ (3 mol% per cross-coupling step), and arylboronic acid (1.0-1.2 equiv per cross-coupling step) in dioxane (4 mL) was stirred at 108 ℃ for 8-12 h. To the reaction water (25 mL) and CH_2Cl_2 (25 mL) were added at 20 ℃. The organic and aqueous layer were separated and the latter was extracted with CH_2Cl_2 (2× 25 mL). The combined organic layers were dried,

filtered, and the filtrate was concentrated under vacuum. The desire product was purified by column chromatography, and analyzed by NMR spectrum, which corresponded to the literature values. ^{1}H-NMR ($CDCl_3$) δ 2.58 (t, 6H) 4.21 (s, 2H) 7.01 (d, 2H) (J=9Hz) 7.38 (m, 2H) 7.43 (m, 2H) 7.57 (m, 2H) 7.61 (m, 2H) 7.84 (d, 4H) (J=6Hz) 8.46 (s, 2H).

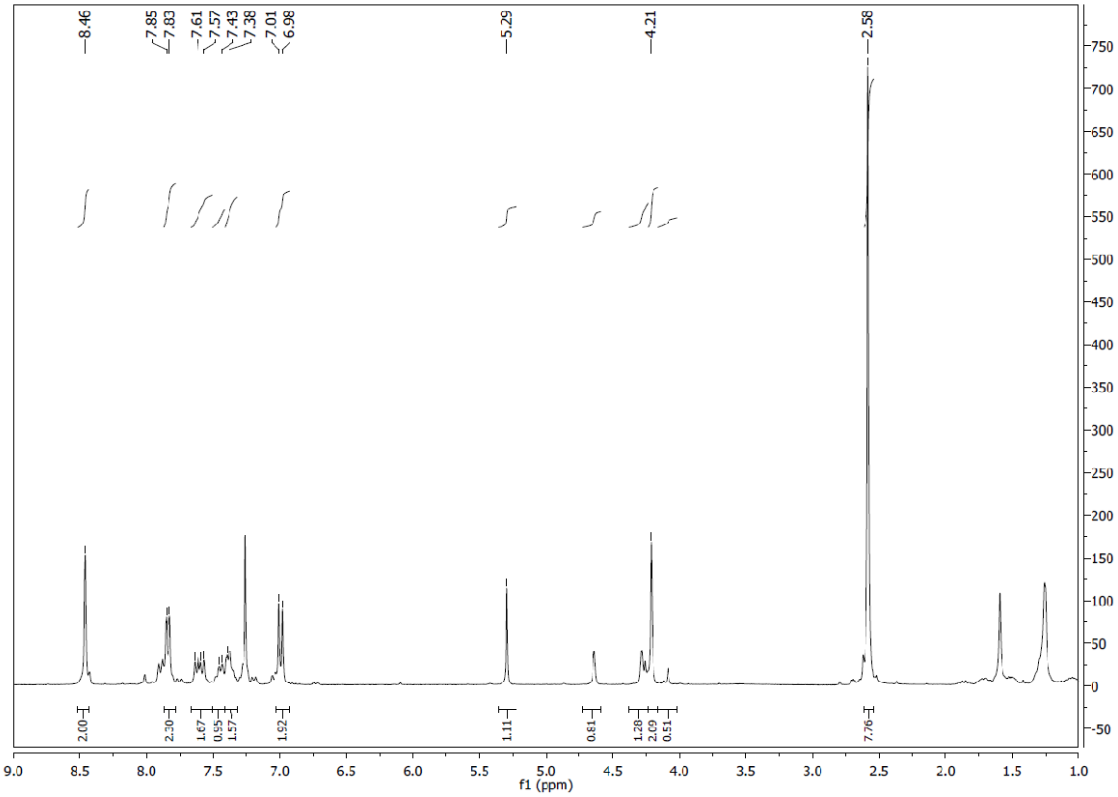

Figure 91. NMR for compound **160**

4-Bromophenylboronic acid (165). To a flame-dried 100 mL flask under nitrogen was added 1,4-dibromobenzene (0.78 g, 3.3 mmol), followed by anhydrous diethyl ether (17 mL). The solution was cooled to –78 ℃, and *n*-BuLi (1.6 M, 2.3 mL, 3.7 mmol) was added dropwise over 15 min. The reaction was stirred at –78 ℃ for 1 h then allowed to warm to r.t. over the course of 1 h, then rechilled to –78 ℃. Trimethoxyl borate (0.56 mL, 5.0 mmol) was added and the reaction was stirred for a further 15 min and allowed to warm to r.t., precipitate formed during that time. The reaction was cooled to 0 ℃, quenched with aq. hydrochloric acid (1 M, 50 mL) and diluted with 50 mL diethyl ether (precipitate dissolved). The two phases were separated and the organic phase was washed with water (2 × 30 mL) and brine (20 mL). The resulting aqueous phase was extracted with ether (2 × 30 mL) and the combined

organic layers were dried over sodium sulfate, filtered and concentrated under vacuum. Purification and identification of the product were not successful yet.

2-(4-bromophenyl)-4,4,5,5-tetramethyl-1,3,2-dioxaborolane (168). To a solution of 1,4-dibromo-benzene (0.47 g, 2.0 mmol) and bis(triphenylphosphine)palladium(II) dichloride (3% M) in anhydrous dioxane (8 mL) under nitrogen was added TEA (1.2 mL, 8 mmol) and 4,4,5,5-tetramethyl-1,3,2-dioxaborolane (0.9 mL, 6 mmol) dropwise. The reaction mixture was heated at 120 ℃ for 16 hours and quenched with water (20 mL). The solution was extracted by DCM (3×20 mL), dried over sodium sulfate and concentrated under vacuum. Purification and identification of the product was not successful yet.

2-(4-*tert*-butylphenyl)-4,4,5,5-tetramethyl-1,3,2-dioxaborolane (169). To a solution of 1-bromo-4-*tert*-butylbenzene (0.3 g, 2 mmol) and bis(triphenylphosphine)palladium(II) dichloride (3% M) in anhydrous dioxane (4 mL) under nitrogen was added TEA (1.2 mL, 8 mmol) and 4,4,5,5-tetramethyl-1,3,2-dioxaborolane (0.9 mL, 6 mmol) dropwise. The reaction mixture was heated at 120 ℃ for 16 hours and quenched with water (20 mL). The solution was extracted by DCM (3×20 mL), dried over sodium sulfate and concentrated under vacuum. Purification and identification of the product was not successful yet.

To a solution of 1-bromo-4-tert-butylbenzene (0.15 g, 0.7 mmol), potassium acetate (0.2 g, 2 mmol) and bis(diphenylphosphino)ferrocene]palladium(II) dichloride (3% M) in anhydrous DMF (4 mL) under nitrogen was added 4,4,5,5-tetramethyl-(4,4,5,5-tetramethyl-1,3,2-dioxaborolan-2-yl)-1,3,2-dioxaborolane (0.2 g, 0.79 mmol) dropwise. The reaction mixture was heated at 150 ℃ for 16 hours and quenched with water (20 mL). The aqueous layer was extracted by DCM (3×20 mL), dried over sodium sulfate and concentrated under vacuum. Purification and identification of the product was not successful yet.

8 Discussion

We are going to finish the following synthetic approach to arrive at the diarsenical probe **i, i+4**. Our synthetic goal is to attach arsenic to the scaffold structure by reaction of boronic acid intermediate with $RAsX_2$, with one X group displaced by water. First Wolff-Kishner reduction at the ketone group was straightforward with high yield to form **143**. Next for the iodization reaction at the two ortho positions of the CH_2 groups connecting the two benzene rings were deactivated by the electronic withdrawing

effects of the alkyl groups at the para positions of **153**, several iodization conditions have been tried to increase the yield of the reaction. Suzuki coupling reaction starting from boronic acids was coupling at two iodine atoms positions of **154**, which might due to the steric hindrance and electronegative effects of the monocoupling product (Scheme 51).

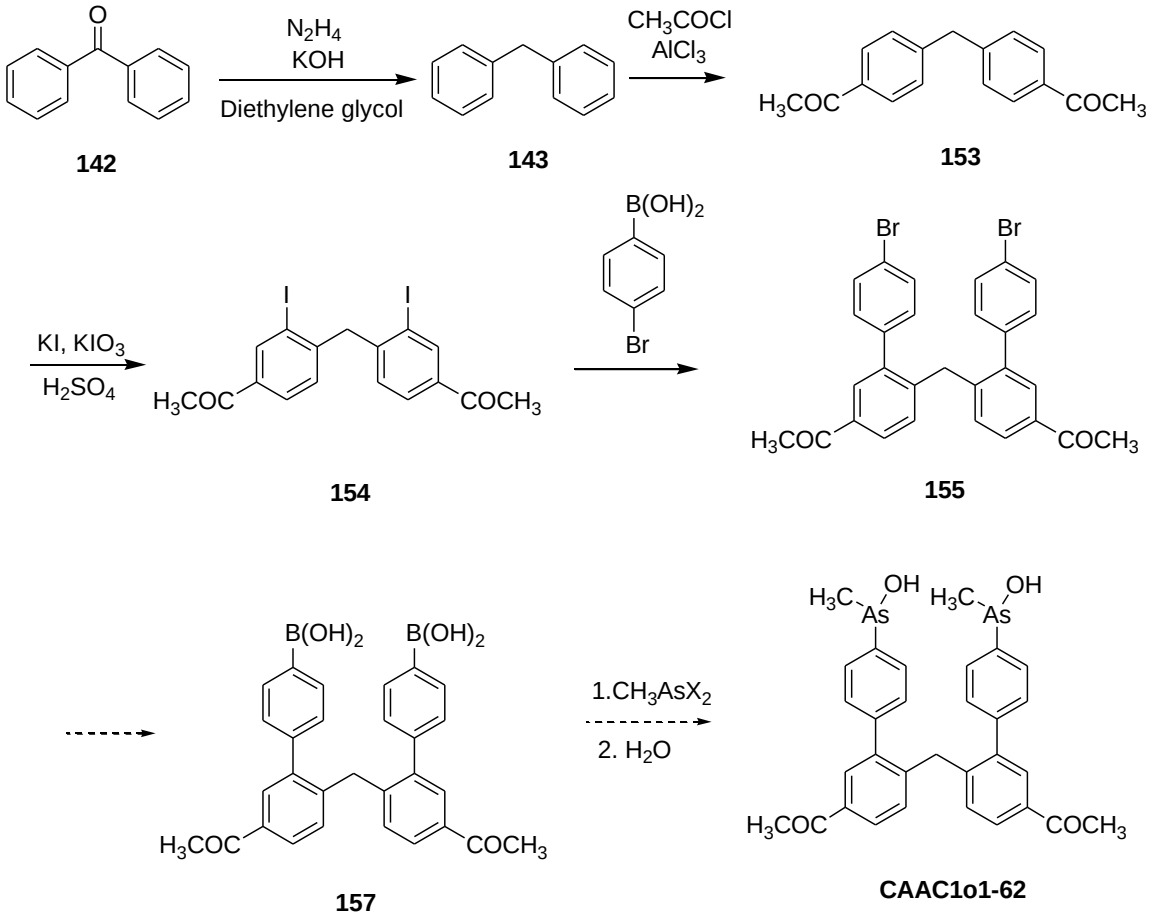

Scheme 51. The synthetic approach of **probe i, i+4**

The synthetic approach of compounds **1**-**3** was abandoned, since the benzylic group connected with arsenic was very easy to be oxidized when dealt with base, and the introduction of two lithium atoms at the same time to form **1** and **3** was not successful with *n*BuLi as the base, the radical reaction at the two methyl positions to form **2** was associated with low yield, and the coupling reaction of phenol and halide to form **2** was not selective.

Most available arsenic compounds are associated with the As(V) oxidation state, thus formation of an As(III) organoarsenic dihalide requires a reduction reaction. Reduction of phenylarsonic acid and methylarsonic acid was performed with aq. HCl and HBr as both the reagents and solvents to form dihalide (chloride and bromine) substituted arsenic atom, however, arsenic halide bond cannot be selectively broken, more stable bonds were introduced on the arsenic atom, such as nitrogen, sulfur and oxygen bonds. But the more stable substituents have not increased the selectivity of the breakage of the arsenic halide bonds. One halide atom and one other stable substituent on the arsenic center was an alternative approach for the formation of arsenic carbon bond selectively. X-As-N, X-As-S, and X-As-O models have been built up to increase the selectivity of arsenic carbon bond formation, however, byproduct bialkyl substituted arsenic was formed even reacted with one equivalent of Grignard reagent or lithium reagent.

Mercuration at the ortho position of phenol-OH was come up as a new method to form the arsenic carbon bond through the further arsenic mercury exchange reaction, however, both **99** and **102** required ortho mercuration at both ortho postions on the benzene rings, which were hard to be recovered and identified in the NMR spectrum and TLC results.

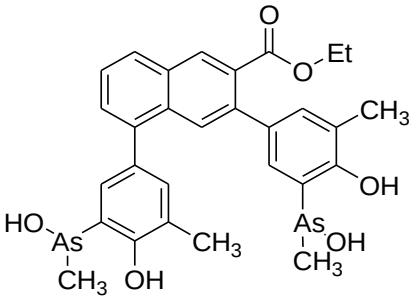

99

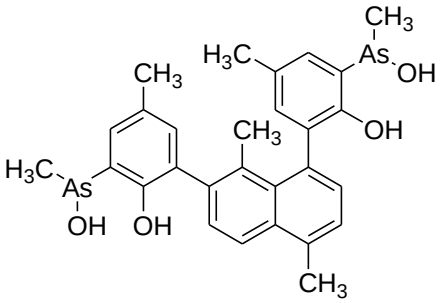

102

An alternative synthetic approach of arsenic carbon bond was performed with boronic acid as the starting material and arsenic dihalide as the source of arsenic. The similar Suzuki coupling reaction was undertaken in basic conditions performing highly selective coupling on one arsenic halide bond. The three aromatic rings substituted on the same arsenic center would be an interesting application of the method of forming arsenic carbon bond with boronic acids.

9 Conclusion

For the following two biarsenical probes calculated from Hostdesigner, problems still exist with the synthesis of the moieties on the naphthalene ring and the phenol ether. For **1**, the nonselectivity of positions 1 and 6 would prevent the concurrent forming of two aryl-arsenic bonds, and CH_2 groups on the naphthalene ring are very easy to be oxidized when reacted with arsenic. For **2**, it is problematic due to the low yield of radical substitution on the two methyl groups of the 1,6-dimethyl-2-methoxy-naphthalene and the nonselectivity of the bonding reaction to form ether between phenol and the aryl halide.

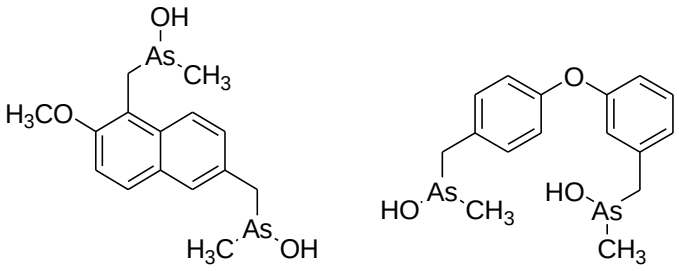

1 **2**

Figure 92. Chemical structures of compound **1** and **2**

For the synthesis of **3**, we have already synthesized the 1,6-dimethyl naphthalene with good yield. However, problems still existed in the bonding between the naphthalene substrate and arsenic atoms, due to the properties of oxidization of the CH_2 groups connected on the naphthalene ring.

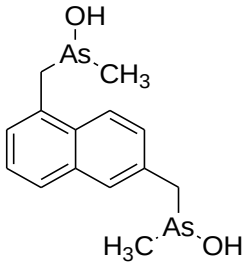

Figure 93. Chemical structure of compound **3**

Finally, the following two compounds might be promising probes for the synthesis, the scaffold structure of which were searched in HostDesigner and strained energy was calculated in Gaussian software.

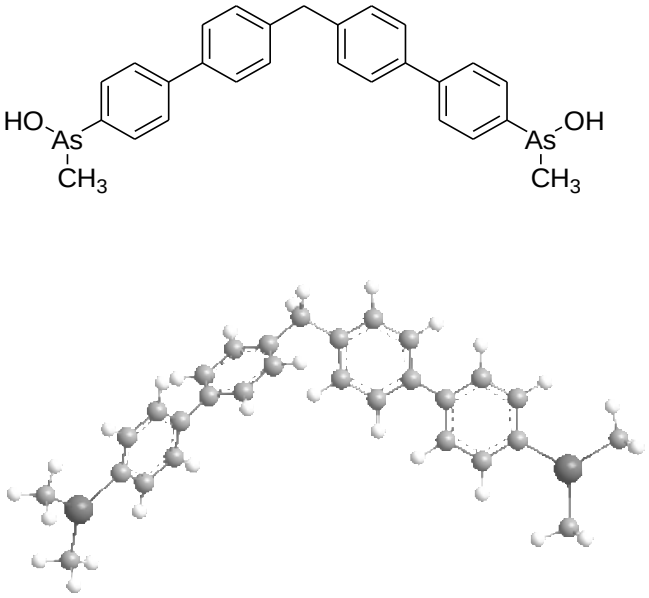

Probe i,i+7

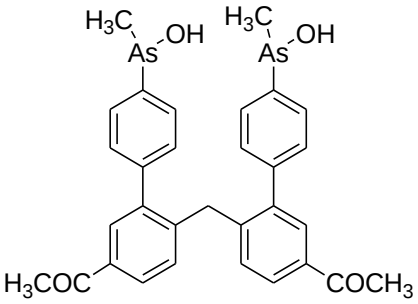

Probe i,i+4

Figure 94. Chemical structure of the other two probes

Reference

1

1. Huang, J. W.; Poynton, C. Y.; Kochian, L. V.; Elless, M. P., Phytofiltration of Arsenic from Drinking Water Using Arsenic-Hyperaccumulating Ferns. *Environmental Science & Technology* **2004,** *38* (12), 3412-3417.

2. Meharg, A. A.; Rahman, M. M., Arsenic Contamination of Bangladesh Paddy Field Soils: Implications for Rice Contribution to Arsenic Consumption. *Environmental Science & Technology* **2003,** *37* (2), 229-234.

3. Sele, V.; Amlund, H.; Berntssen, M. G.; Berntsen, J.; Skov, K.; Sloth, J., Detection of arsenic-containing hydrocarbons in a range of commercial fish oils by GC-ICPMS analysis. *Anal Bioanal Chem* **2013,** *405* (15), 5179-5190.

4. Park, S.-G.; Butcher, D. J., Investigation of the interaction between arsenic species and thiols via electrospray ionization tandem mass spectrometry. *Microchemical Journal* **2010,** *95* (1), 57-66.

5. Calderón, J.; Navarro, M. E.; Jimenez-Capdeville, M. E.; Santos-Diaz, M. A.; Golden, A.; Rodriguez-Leyva, I.; Borja-Aburto, V., Exposure to Arsenic and Lead and Neuropsychological Development in Mexican Children. *Environmental Research* **2001,** *85* (2), 69-76.

6. Ralph, S. J., Arsenic-Based Antineoplastic Drugs and Their Mechanisms of Action. *Metal-Based Drugs* **2008,** *2008*.

7. Lin, S.; Cullen, W. R.; Thomas, D. J., Methylarsenicals and Arsinothiols Are Potent Inhibitors of Mouse Liver Thioredoxin Reductase. *Chemical Research in Toxicology* **1999,** *12* (10), 924-930.

8. Bhattacharyya, K.; Danon, A.; K.Vijayan, B.; Gray, K. A.; Stair, P. C.; Weitz, E., Role of the Surface Lewis Acid and Base Sites in the Adsorption of CO2 on Titania Nanotubes and Platinized Titania Nanotubes: An in Situ FT-IR Study. *The Journal of Physical Chemistry C* **2013,** *117* (24), 12661-12678.

9. Shen, S.; Li, X.-F.; Cullen, W. R.; Weinfeld, M.; Le, X. C., Arsenic Binding to Proteins. *Chemical Reviews* **2013,** *113* (10), 7769-7792.

10. Spuches, A. M.; Kruszyna, H. G.; Rich, A. M.; Wilcox, D. E., Thermodynamics of the As(III)-thiol interaction: Arsenite and monomethylarsenite complexes with glutathione, dihydrolipoic acid, and other thiol ligands. *Inorg. Chem.* **2005,** *44* (8), 2964-2972.

11. Petrick, J. S.; Jagadish, B.; Mash, E. A.; Aposhian, H. V., Monomethylarsonous Acid (MMAIII) and Arsenite: LD50 in Hamsters and In Vitro Inhibition of Pyruvate Dehydrogenase. *Chemical Research in Toxicology* **2001,** *14* (6), 651-656.

12. Miller, L. W.; Cornish, V. W., Selective chemical labeling of proteins in living cells. *Current Opinion in Chemical Biology* **2005,** *9* (1), 56-61.

13. Danna, E. A.; Nolan, G. P., Transcending the biomarker mindset: deciphering disease mechanisms at the single cell level. *Current Opinion in Chemical Biology* **2006,** *10* (1), 20-27.

14. Saghatelian, A.; Cravatt, B. F., Corrigendum: Assignment of protein function in the postgenomic era. *Nat Chem Biol* **2005,** *1* (4), 233-233.

15. Xie, J.; Schultz, P. G., A chemical toolkit for proteins an expanded genetic code. *Nat Rev Mol Cell Biol* **2006,** *7* (10), 775-782.

16. Nguyen, T.; Joshi, N. S.; Francis, M. B., An Affinity-Based Method for the Purification of Fluorescently-Labeled Biomolecules. *Bioconjugate Chemistry* **2006,** *17* (4), 869-872.

17. Johnson, I., *The Molecular Probes Handbook: A Guide to Fluorescent Probes and Labeling Technologies, 11th Edition*. Life Technologies Corporation: 2010.

18. Waggoner, A., Fluorescent labels for proteomics and genomics. *Current Opinion in Chemical Biology* **2006,** *10* (1), 62-66.

19. Deerinck, T. J., The Application of Fluorescent Quantum Dots to Confocal, Multiphoton, and Electron Microscopic Imaging. *Toxicologic pathology* **2008,** *36* (1), 112-116.

20. Pisanic, T. R.; Zhang, Y.; Wang, T. H., Quantum Dots in Diagnostics and Detection: Principles and Paradigms. *The Analyst* **2014,** *139* (12), 2968-2981.

21. Bohunicky, B.; Mousa, S. A., Biosensors: the new wave in cancer diagnosis. *Nanotechnology, Science and Applications* **2011,** *4*, 1-10.

22. Shaner, N. C.; Steinbach, P. A.; Tsien, R. Y., A guide to choosing fluorescent proteins. *Nat Meth* **2005,** *2* (12), 905-909.

23. Chalfie, M.; Tu, Y.; Euskirchen, G.; Ward, W.; Prasher, D., Green fluorescent protein as a marker for gene expression. *Science* **1994,** *263* (5148), 802-805.

24. Ormö, M.; Cubitt, A. B.; Kallio, K.; Gross, L. A.; Tsien, R. Y.; Remington, S. J., Crystal Structure of the Aequorea victoria Green Fluorescent Protein. *Science* **1996,** *273* (5280), 1392-1395.

25. Stryer, L., Fluorescence energy transfer as a spectroscopic ruler. *Annual review of biochemistry* **1978,** *47* (1), 819-846.

26. Chin, J. W.; Cropp, T. A.; Anderson, J. C.; Mukherji, M.; Zhang, Z.; Schultz, P. G., An Expanded Eukaryotic Genetic Code. *Science* **2003,** *301* (5635), 964-967.

27. (a) Jares-Erijman, E. A.; Jovin, T. M., FRET imaging. *Nature Biotechnology* **2003,** *21* (11), 1387-1395; (b) Giepmans, B. N.; Adams, S. R.; Ellisman, M. H.; Tsien, R. Y., The fluorescent toolbox for assessing protein location and function. *Science* **2006,** *312* (5771), 217-224.

28. Wiedenmann, J.; Oswald, F.; Nienhaus, G. U., Fluorescent proteins for live cell imaging: Opportunities, limitations, and challenges. *IUBMB Life* **2009,** *61* (11), 1029-1042.

29. Sarquis, M., Arsenic and old myths. *Journal of Chemical Education* **1979,** *56* (12), 815.

30. Chen-Yu, X.; Ying, G.; Wang-Heng, H.; Yu-Qiong, Q.; Shuang-Guan, G.; Cheng, T.; Ning-Shao, X., Tetracysteine as a reporter for gene therapy. *Biomedical and Environmental Sciences* **2009,** *22* (6), 496-501.

31. Marks, K. M.; Nolan, G. P., Chemical labeling strategies for cell biology. *Nature Meth* **2006,** *3* (8), 591-596.

32. Adams, S. R.; Tsien, R. Y., Preparation of the membrane-permeant biarsenicals, FlAsH-EDT(2) and ReAsH-EDT(2) for fluorescent labeling of tetracysteine-tagged proteins. *Nature Protocols* **2008,** *3* (9), 1527-1534.

33. Balbi, A.; Anzaldi, M.; Macciò, C.; Aiello, C.; Mazzei, M.; Gangemi, R.; Castagnola, P.; Miele, M.; Rosano, C.; Viale, M., Synthesis and biological evaluation of novel pyrazole derivatives with anticancer activity. *European Journal of Medicinal Chemistry* **2011,** *46* (11), 5293-5309.

34. Scheck, R. A.; Schepartz, A., Surveying protein structure and function using bis-arsenical small molecules. *Accounts of Chemical Research* **2011,** *44* (9), 654-665.

35. Kalef, E.; Walfish, P.; Gitler, C., Arsenical-based affinity chromatography of vicinal dithiol-containing proteins: purification of L1210 leukemia cytoplasmic proteins and the recombinant rat c-erb Aβ 1 T 3 receptor. *Analytical biochemistry* **1993,** *212* (2), 325-334.

36. Taber, D. F.; Neubert, T. D.; Rheingold, A. L., Synthesis of (−)-Morphine. *Journal of the American Chemical Society* **2002,** *124* (42), 12416-12417.

37. Kuhnert, N.; Burzlaff, N.; Patel, C.; Lopez-Periago, A., Tuning the size of macrocyclic cavities in trianglimine macrocycles. *Organic & Biomolecular Chemistry* **2005,** *3* (10), 1911-1921.

38. Matsunaga, N.; Kaku, T.; Ojida, A.; Tanaka, T.; Hara, T.; Yamaoka, M.; Kusaka, M.; Tasaka, A., C17,20-lyase inhibitors. Part 2: Design, synthesis and structure–activity relationships of (2-naphthylmethyl)-1H-imidazoles as novel C17,20-lyase inhibitors. *Bioorganic & Medicinal Chemistry* **2004,** *12* (16), 4313-4336.

39. Marcoux, J.-F.; Doye, S.; Buchwald, S. L., A general copper-catalyzed synthesis of diaryl ethers. *Journal of the American Chemical Society* **1997,** *119* (43), 10539-10540.

40. Mendieta, M. A. P.-B.; Negri, M.; Jagusch, C.; Hille, U. E.; Müller-Vieira, U.; Schmidt, D.; Hansen, K.; Hartmann, R. W., Synthesis, biological evaluation and molecular modelling studies of novel ACD-and ABD-ring steroidomimetics as inhibitors of CYP17. *Bioorganic & medicinal chemistry letters* **2008,** *18* (1), 267-273.

41. Pinto-Bazurco Mendieta, M. A. E.; Negri, M.; Jagusch, C.; Hille, U. E.; Müller-Vieira, U.; Schmidt, D.; Hansen, K.; Hartmann, R. W., Synthesis, biological evaluation and molecular modelling studies of novel ACD- and ABD-ring steroidomimetics as inhibitors of CYP17. *Bioorganic & Medicinal Chemistry Letters* **2008,** *18* (1), 267-273.

42. Xiao, D.; Zhang, Z.; Zhang, X., Synthesis of a Novel Chiral Binaphthyl Phospholane and Its Application in the Highly Enantioselective Hydrogenation of Enamides. *Organic Letters* **1999,** *1* (10), 1679-1681.

43. Mecca, T.; Superchi, S.; Giorgio, E.; Rosini, C., 1,1′ -Binaphthylazepine-based ligands for asymmetric catalysis. Part 1: Preparation and characterization of some new aminoalcohols and diamines. *Tetrahedron: Asymmetry* **2001,** *12* (8), 1225-1233.

44. Phadnis, P. P.; Jain, V. K.; Klein, A.; Weber, M.; Kaim, W., Configurational selectivity in benzyldimethylarsine complexes of palladium(II) and platinum(II): synthesis, spectroscopy and structures. *Inorganica Chimica Acta* **2003,** *346* (0), 119-128.

45. Zhou, C.; Wang, Z., Cadmium-Mediated Carbonyl Benzylation in Tap Water. *Synthesis* **2005,** *2005* (10), 1649-1655.

46. Cline, D. J.; Thorpe, C.; Schneider, J. P., Effects of As(III) Binding on α-Helical Structure. *Journal of the American Chemical Society* **2003,** *125* (10), 2923-2929.

47. Liang, X.; Drueckhammer, D. G., Arsinous acid as a thiol binding group: potential cysteine peptide tagging functionality that binds a single thiol. *New Journal of Chemistry* **2014,** *38* (4), 1368-1371.

48. Whitmore, F. C.; Thorpe, M. A., The Reaction of Iodine Monochloride with Certain Organic Mercury Compounds. *Journal of the American Chemical Society* **1933,** *55* (2), 782-786.

49. Urawa, Y.; Ogura, K., A convenient method for preparing aromatic ketones from acyl chlorides and arylboronic acids via Suzuki–Miyaura type coupling reaction. *Tetrahedron Letters* **2003,** *44* (2), 271-273.

50. Drueckhammer, D., Scaffold Design Using Computational Chemistry. In *Chemosensors*, John Wiley & Sons, Inc.: 2011; pp 69-85.

51. Hay, B. P.; Firman, T. K., HostDesigner: A Program for the de Novo Structure-Based Design of Molecular Receptors with Binding Sites that Complement Metal Ion Guests. *Inorganic Chemistry* **2002,** *41* (21), 5502-5512.

52. Motherwell, W.; Nutley, C., The role of zinc carbenoids in organic synthesis. *Contemporary Organic Synthesis* **1994,** *1* (4), 219-241.

53. Hicks, L. D.; Han, J. K.; Fry, A. J., Hypophosphorous acid–iodine: a novel reducing system.: Part 1: Reduction of diaryl ketones to diaryl methylene derivatives. *Tetrahedron Letters* **2000,** *41* (41), 7817-7820.

54. Hutchins, R.; Hutchins, M. K.; Trost, B., Reduction of C= X to CH2 by Wolff-Kishner and Other Hydrazone Methods. *Comprehensive organic synthesis* **1991,** *8*, 327.

55. Williams, D. B. G.; Lawton, M., Drying of Organic Solvents: Quantitative Evaluation of the Efficiency of Several Desiccants. *The Journal of Organic Chemistry* **2010,** *75* (24), 8351-8354.

56. Drueckhammer, D. G.; Gao, S. Q.; Liang, X.; Liao, J., Acetone–Heptane as a Solvent System for Combining Chromatography on Silica Gel with Solvent Recycling. *ACS Sustainable Chemistry & Engineering* **2013,** *1* (1), 87-90.